Laboratory Medicine

May 2022 Vol 53 No 3 Pgs 223–329

labmedicine.com

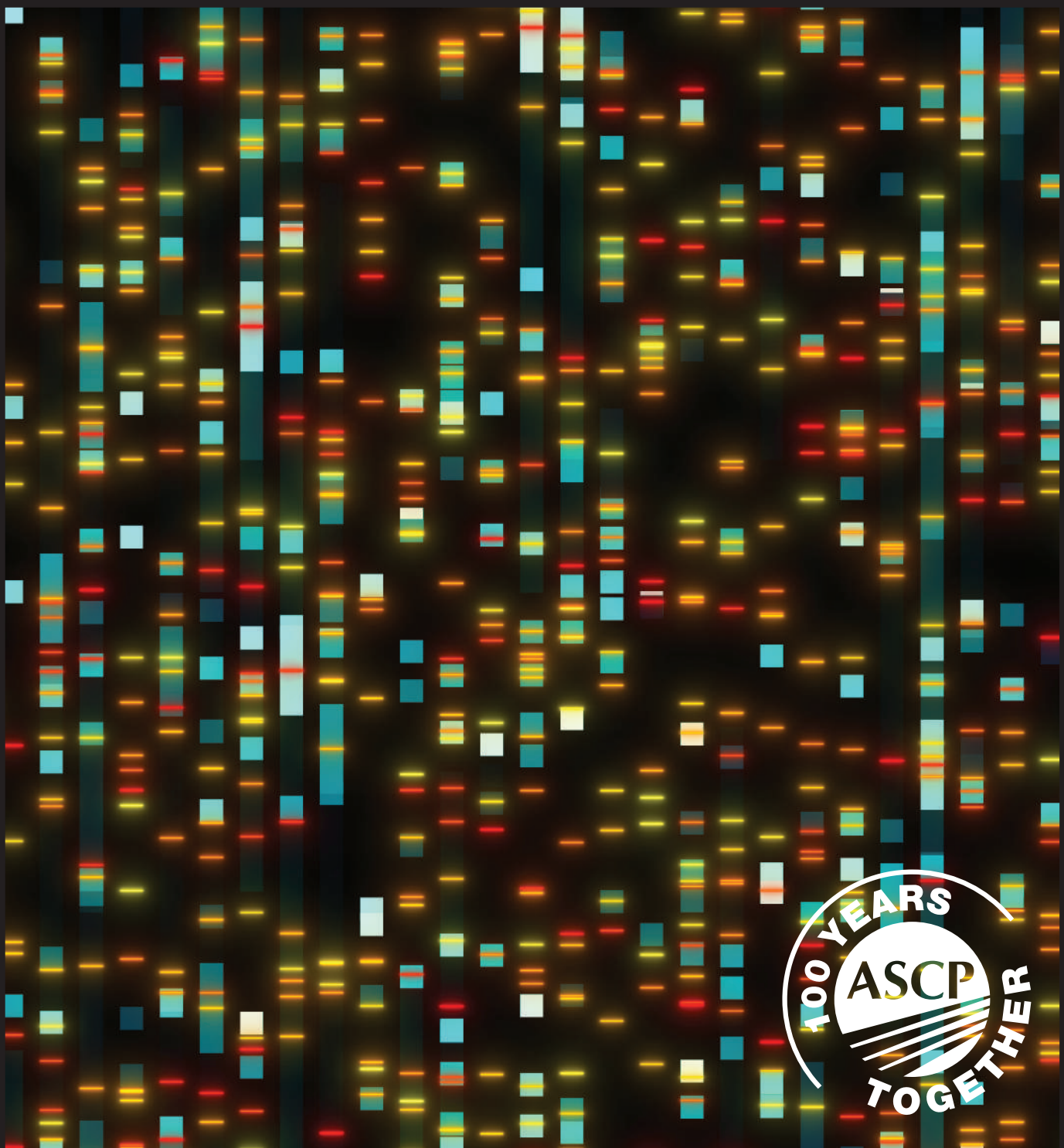

Laboratory Medicine (ISSN 0007-5027), is published 6 times per year (bimonthly). Periodicals Postage paid at Chicago, IL and additional mailing offices. POSTMASTER: Send address changes to *Laboratory Medicine*, Journals Customer Service Department, Oxford University Press, 2001 Evans Road, Cary, NC 27513-2009.

SUBSCRIPTION INFORMATION: Annually for North America, $173 (electronic) or $225 (electronic and print); single issues for individuals are $29 and for institutions $64. Annually for Rest of World, £112/€159 (electronic) or £144/€206 (electronic and print); single issues for individuals are £19/€27 and for institutions £40/€57. All inquiries about subscriptions should be sent to Journals Customer Service Department, Oxford Journals, Great Clarendon Street, Oxford OX2 6DP, UK, Tel: +44 (0) 1865-35-3907, e-mail: jnls.cust.serv@oup.com. In the Americas, please contact Journals Customer Service Department, Oxford Journals, 2001 Evans Road, Cary, NC 27513. Tel: 800-852-7323 (toll-free in USA/Canada) or 919-677-0977, e-mail: jnlorders@oup.com.

MEMBERSHIP INFORMATION: The ASCP membership fees for pathologists are as follows: fellow membership is $349; fellow membership plus 1-year unlimited online CE is $519; 2-year fellow membership is $675; and 2-year fellow membership plus 2-year unlimited online CE is $1,015. The ASCP membership fees for laboratory professionals are as follows: newly certified membership is $49; annual membership is $99; annual membership plus 1-year unlimited online CE is $129; 3-year membership is $349. All inquiries about membership should be sent to American Society for Clinical Pathology, 33 West Monroe Street, Suite 1600, Chicago, IL 60603, Tel: 312-541-4999, e-mail: ascp@ascp.org.

CLAIMS: Publisher must be notified of claims within four months of dispatch/ order date (whichever is later). Subscriptions in the EEC may be subject to European VAT. Claims should be made to Laboratory Medicine, Journals Customer Service Department, Oxford University Press, 2001 Evans Road, Cary, NC 27513, Tel: 800-852-7323 (toll-free in USA/Canada) or 919-677-0977, e-mail: jnlorders@oup.com.

Laboratory Medicine is published bimonthly by Oxford University Press (OUP), on behalf of the ASCP, a not-for-profit corporation organized exclusively for educational, scientific, and charitable purposes. Devoted to the continuing education of laboratory professionals, *Laboratory Medicine* features articles on the scientific, technical, managerial, and educational aspects ofthe clinical laboratory. Publication of an article, column, or other item does not constitute an endorsement by the ASCP of the thoughts expressed or the techniques, organizations, or products described therein. *Laboratory Medicine* is indexed in the following: MEDLINE/PubMed, Science Citation Index, Current Contents—Clinical Medicine, and the Cumulative Index to Nursing and Allied Health Literature.

Printed in the USA

ASCP
Laboratory Medicine
33 West Monroe Street, Suite 1600
Chicago, IL 60603

T: 312-541-4999
F: 312-541-4750

LaboratoryMedicine

May 2022
Vol 53, No 3
p. 223-329

SCIENCE

CASE STUDY

The following are online-only papers that are available as part of Issue 53(3) online.

ON THE COVER: First described in 1977, Frederick Sanger's eponymous DNA sequencing method involves chain termination with radioactively or fluorescently labeled nucleotides, and subsequent separation of the labeled fragments by electrophoresis (an example of capillary electrophoresis with fluorescent labels is shown). The Sanger method was the principal tool used to sequence the human genome, the ambitious billion dollar project that began in 1990 and was completed in 2003. Next-generation sequencing technologies have since improved the throughput and reduced the cost of DNA sequencing. However, inconsistencies exist among nomenclature standards for describing DNA variants, despite recommendations from the Human Genome Variation Society for a standardized system. In this issue of *Laboratory Medicine* pp 242–245, Kyoung-Jin Park and Jong-Ho Park report significant discordance between two commonly used sequence annotation tools when both are applied to the Human Genome Mutation Database of nearly 220,000 clinical variants.

SCIENCE

Quantitative Detection of Anti-SARS-CoV-2 Antibodies Using Indirect ELISA

Shuhong Luo,[1,2,a] Jianhua Xu,[3,a] Chih Yun Cho,[2,a] Siwei Zhu,[1] Kelly C. Whittaker,[2] Xingqi Wang,[2] Jie Feng,[2] Meng Wang,[2] Shehuo Xie,[1] Jianmin Fang,[1,2] Andy S. Huang,[2] Xuedong Song,[1] Ruo-Pan Huang[1,2,4,]*

[1]RayBiotech, Guangzhou, China; [2]RayBiotech Life, Peachtree Corners, Georgia, US; [3]Department of Laboratory Science, Shunde Hospital of Guangzhou University of Chinese Medicine, Guangzhou, China; [4]South China Biochip Research Center, Guangzhou, China; *To whom correspondence should be addressed. rhuang@raybiotech.com; [a]Contributed equally to this work.

Keywords: COVID-19, SARS-CoV-2, iELISA, S1 RBD, nucleocapsid protein, serum/plasma, dried blood

Abbreviations: ELISA, enzyme-linked immunosorbent assay; RT-qPCR, reverse transcription-quantitative polymerase chain reaction; iELISA, indirect enzyme-linked immunosorbent assay; S protein, spike protein; N protein, nucleocapsid protein; RBD, receptor binding domain; HEK, human embryonic kidney; SDS-PAGE, sodium docetyl sulfate-polyacrylamide gel electrophoresis; PBS, phosphate buffered saline; PVDF, polyvinylidene fluoride; TBST, tris-buffered saline with Tween-20; HRP, horseradish peroxidase; PBST, phosphate buffered saline with Tween-20.

Laboratory Medicine 2022;53:225–234; https://doi.org/10.1093/labmed/lmab085

Objective: Real-time reverse transcription-polymerase chain reaction is the gold standard for the diagnosis of COVID-19, but it is necessary to utilize other tests to determine the burden of the disease and the spread of the outbreak such as IgG-, IgM-, and IgA-based antibody detection using enzyme-linked immunosorbent assay (ELISA).

Materials and Methods: We developed an indirect ELISA assay to quantitatively measure the amount of COVID-19 IgG, IgM, and IgA antibodies present in patient serum, dried blood, and plasma.

Results: The population cutoff values for positivity were determined by receiver operating characteristic curves to be 1.23 U/mL, 23.09 U/mL, and 6.36 U/mL for IgG, IgM, and IgA, respectively. After albumin subtraction, the specificity remained >98% and the sensitivity was 95.72%, 83.47%, and 82.60%, respectively, for IgG, IgM, and IgA antibodies to the combined spike subunit 1 receptor binding domain and N proteins in serum. Plasma and dried blood spot specimens were also validated on this assay.

Conclusion: This assay may be used for determining the seroprevalence of SARS-CoV-2 in a population exposed to the virus or in vaccinated individuals.

In December 2019, the novel coronavirus SARS-CoV-2 emerged in Wuhan, China, and has led to a global pandemic, with the COVID-19 disease affecting >61 million individuals worldwide and accounting for nearly 300,000 deaths in the United States to date.[1,2] The transmissibility and disease severity are much higher compared to the original SARS virus, and effective control over the disease is still lacking. The fight against SARS-CoV-2 has been focused on the prevention of infection, detection of cases of infection, and diagnosis and monitoring of the disease. Prevention of infection is predominantly accomplished through vaccination, social distancing, hand hygiene, and masking. Unfortunately, a recommended, global therapy is still not currently available, although the US Food and Drug Administration had approved one treatment (remdesivir) as of November 2020 and has issued emergency use authorizations for several other treatments.[3] Molecular tests have been the gold standard for the detection and diagnosis for cases of infection; however, large-scale, continued implementation has been hindered because of cost, feasibility, speed, and reagent availability. Analytical issues with reverse transcription-quantitative polymerase chain reaction (RT-qPCR) assays have been well documented and include high false-positive and false-negative rates because of contamination, specimen integrity, or cross-reactivity issues.[4-6] To develop diagnostics, therapeutics, and vaccines against SARS-CoV-2, a better understanding of the immunogenicity and pathobiology of SARS-CoV-2 infections is needed. Immunological assays have become a good alternative in this regard.

An indirect enzyme-linked immunosorbent assay (iELISA) is a common biochemical technique that is most suitable for determining total antibody concentrations in a specimen. This method is commonly utilized to diagnose infection and to quantify antibodies against an invading antigen rather than to detect a virus itself. Infection with the SARS-CoV-2 virus elicits the development of IgM- and IgG-specific antibodies, which are the most available antibodies for assessing response, whereas less is known about the response of IgA in the blood. Previous studies have shown variable isotype responses to SARS-CoV-2, with 1 study noting that 92.7% of patients tested positive for anti-SARS-CoV-2 nuclear capsid IgA, whereas only 85.4% had IgM and only 77.9% tested positive for IgG.[7] Current testing for the SARS-CoV-2 virus is limited, and compared to RT-qPCR, ELISA is a less complex procedure that uses more affordable and available equipment. Similarly, antigens and antibodies are considerably more stable than RNA, which reduces the potential of false-negative results. The ability to collect specimens from many places in the body (and not being restricted to nasal swabs)

improves testing accuracy as well. Although iELISA is not ideal for early diagnosis, it has been used to (1) diagnose patients who are more than 1 week post-symptom onset, (2) determine potential immunity and risk of infection, (3) advance contact tracing, and (4) understand the extent of COVID-19 spread and immunity in communities through epidemiological studies that are particularly important for fighting COVID-19 while minimizing economic impact.[8,9] Similarly, with the many different antibody serology tests commercially available, a number of studies assessing their performance have been conducted suggesting that the antibody isotype and timing should be carefully considered to optimize the diagnostic accuracy and usefulness of the assay.[9-17]

The SARS-CoV-2 virus contains approximately 27 proteins, including 4 structural proteins: the spike proteins (S protein), membrane proteins, envelope proteins, and nucleocapsid proteins (N protein). The S protein, through the receptor-binding domain (RBD) of the S1 subunit, is understood to be the viral faction that binds with the host cell receptors and facilitates viral entry into the cell.[18] The N protein is the most abundant viral protein and was characterized first after emergence of the virus.[9] Thus, the S1 RBD and N proteins are of the most interest as candidates for diagnosis and antibody determination. Here, we report the development of the recombinant SARS-CoV-2 antigen that is used in production and iELISAs to the N protein, the S1 RBD protein, and the combination of both the N and S1 RBD proteins. The determination of the sensitivity and specificity, dynamics, and magnitude of IgG, IgM, and IgA antibody responses in patients with COVID-19 are presented and the antibody responses in a variety of biological specimens including serum, plasma, and dried blood spot are discussed.

Materials and Methods

Cloning and DNA Preparation

We cloned cDNA fragments encoding the S1 RBD protein (GenBank accession number QHD43416, Arg319-Phe541) and the full-length N protein (GenBank accession number QHD43423, Met1-Ala419) of SARS-CoV-2 (Wuhan-Hu-1 strain) into a mammalian cell expression vector, pExpR10, with an *N*-terminal signaling peptide to direct the secretion of the recombinant proteins into the cell culture medium and a *C*-terminal His-tag for protein affinity purification. The recombinant expression constructs were confirmed by DNA sequencing. A large amount of endotoxin-free cell transfection-grade plasmid DNA was extracted using the Thermo Invitrogen GigaPrep plasmid preparation kits according to the manufacturer's protocol (Thermo Fisher Scientific, New York, NY).

Gene Expression

Large-scale, transient cell transfection of human embryonic kidney (HEK) 293 suspension cells was performed using the VWR DNA Transfection Reagent following the manufacturer's protocol (VWR, Philadelphia, PA). The cell culture was collected 72 hours post transfection and was centrifuged at 3000*g* for 20 minutes at 4°C; the culture supernatants were further clarified by passing through a 0.45 μm membrane filter.

Protein Purification

His-tagged recombinant S1 RBD and N proteins were purified using immobilized metal affinity chromatography. Briefly, the clarified culture supernatant was diluted with an equal amount of 2× binding buffer (40 mM sodium phosphate buffer, pH 7.4) and loaded onto a 5 mL-Ni sepharose high performance nickel-charged column (GE Healthcare, Chicago, IL) with the flow rate at 5 mL/min, pre-equilibrated with 1× binding buffer (20 mM sodium phosphate buffer, pH 7.4). After specimen loading, the column was sequentially washed with 1× binding buffer (10 column volumes) and then 1× washing buffer (20 mM sodium phosphate buffer, pH 7.4, containing 40 mM imidazole; 10 column volumes). The Ni-column-bound proteins were eluted with a 1× elution buffer (20 mM sodium phosphate buffer, pH 7.4, containing 750 mM imidazole). All fractions were collected and analyzed by sodium dodecyl sulfate-polyacrylamide gel electrophoresis (SDS-PAGE) with Coomassie blue staining. Appropriate fractions were then pooled and concentrated using a Millipore Amicon Ultra-4 Centrifugal Filter Unit (MilliporeSigma, St Louis, MO). The final purified protein was thoroughly desalted by dialysis against 1× phosphate buffered saline (PBS; pH 7.4) at 4°C overnight with 2 buffer changes. The protein concentration was determined with a Thermo Pierce bicinchoninic acid assay kit using bovine serum albumin as the protein standard (Thermo Fisher Scientific). The final protein products were aliquoted and stored at −80°C until use.

Western Blot Analysis

Purified protein was mixed with a 5× SDS protein loading buffer and boiled for 10 minutes. For each individual specimen, 0.5 μg of purified S1 RBD or N protein was loaded per lane on a 10% SDS-PAGE. Proteins were electrotransferred to polyvinylidene fluoride (PVDF) membranes at a constant 100 V for 60 minutes. The PVDF membranes were blocked with 5% nonfat milk for 2 hours at room temperature and incubated with primary antibody (catalog numbers 130–10808, 130–10807, RayBiotech, Peachtree Corners, GA) at a 1:1000 dilution overnight at 4°C, according to the manufacturer's protocol. The membranes were washed with tris-buffered saline with Tween-20 (TBST) 5 times for 5 minutes per wash and incubated with horseradish peroxidase (HRP)–conjugated goat anti-mouse IgG antibody (catalog number 115–035–003, Jackson ImmunoResearch, West Grove, PA) at a 1:5000 dilution for 1 hour at room temperature. The membranes were washed with TBST again and visualized using an enhanced chemiluminescence reagent (CHMI-0300–2C, Surmodics, Eden Prairie, MN) and scanned using UVP Bioimaging systems (Wazobia Enterprise, Houston, TX).

Indirect ELISA

Indirect ELISA for the determination of IgG, IgM, and IgA antibodies to the S1 RBD and N protein in serum, plasma, and dried blood was developed. A 96-well microplate (Greiner Bio-One, Monroe, NC) was coated with 1.5 μg/mL of recombinant S1 RBD protein and/or 1 μg/mL N protein in 100 μL of 0.1 M Na_2HPO_4 buffer (pH 9.0) and incubated overnight at 4°C. Plates were washed 5 times with PBS and 1% Tween-20 (PBST) and then blocked by adding 120 μL of blocking buffer per well (Rockland, PA). The plates were incubated for 1.5 hours at room temperature. The blocking buffer was then discarded and 100 μL of the specimen was added into the wells and incubated for 1 hour at room temperature. Serum and plasma specimens were diluted at 1:1500 for IgG and 1:500 for IgM and IgA. Dried blood specimens were eluted at a 1:10 ratio in elution buffer and diluted with specimen diluent at a 1:10 ratio for IgG and a 1:100 ratio for IgM and IgA analysis. The wells were washed 5 times with PBST, and 100 μL of antihuman biotinylated IgG, IgM, or IgA was added (Jackson ImmunoResearch; Southern Biotech, Birmingham, AL) to each well and incubated for 30 minutes. After washing 5 times with PBST, 100 μL of HRP-streptavidin solution was added to each

well and incubated for another 30 minutes. The wells were washed another 5 times, and 100 μL of TMB substrate (Surmodics, Eden Prairie, MN) was added to each well and incubated for 15 minutes. The enzymatic reaction was stopped by adding 50 uL of 0.2 M sulfuric acid to each well. The absorbance of each specimen was measured at 450 nm using an ELISA plate reader (BioTek, Winooski, VT).

Patient Specimens

Serum specimens from patients with COVID-19 were commercially sourced: Bioresource Technology (57 specimens; Weston, FL), Cantor Bioconnect (54 specimens; Santee, CA), Texas Direct Diagnostics (79 specimens; Irving, TX), and PanoHealth (41 specimens; Peachtree Corners, GA). Thirty-one and 27 specimens collected by PanoHealth had matched plasma and dried blood specimens, respectively. Another set of 20 specimens was collected in the Shunde Hospital at Guangzhou University of Chinese Medicine (Guangzhou, China). Patient COVID-19 status was determined with RT-PCR using nasopharyngeal or oropharyngeal swab specimens to detect SARS-CoV-2 nucleic acid, and specimens were at least 10 days post-symptom onset. Pre-COVID-19 serum specimens collected prior to 2019 and negative for COVID-19 were obtained from BioIVT (15 specimens; Westbury, NY) and RayBiotech Life (249 specimens). The serum specimens were separated after centrifugation at 1000 rpm for 10 minutes, and COVID-19-positive specimens were then inactivated with 0.5% Triton X-100 for 1.5 hours. All specimens were stored at −80°C until further use. Overall, 515 serum specimens (251 COVID-19-positive, 264 COVID-19-negative) were included for assay validation. Assay cross-reactivity was determined with 72 COVID-19 negative serum specimens from patients who were RT-PCR-positive for adenovirus, antinuclear antibodies of autoimmune disease, cytomegalovirus, hepatitis B virus, hepatitis C virus, human parainfluenza viruses, influenza B, MP virus, or respiratory syncytial virus. These pathogens were chosen based on the US Food and Drug Administration recommendations for validation studies to be conducted for SARS-CoV-2 serology tests related to the tested specimen types. A summary of the specimens used in this study are noted in **TABLE 1**. This study was approved by the institutional review board (number 8291-BZhang), and the Institutional Human Ethics Committee of the Shunde Hospital of Guangzhou University of Chinese Medicine approved this study (approval number KY-2020001).

Statistical Analysis

The concentrations of antibodies against the SARS-CoV-2 S1 RBD and N proteins were summarized as the mean ± standard deviation by COVID-19 diagnosis and the interval between the specimen collection after the onset of COVID-19 symptoms. We conducted receiver operating characteristic analysis[19] on the antibody concentration measured using iELISA to assess its diagnostic performance, with SARS-CoV-2 RT-PCR results as the reference standard. The cutoff with the best performance was selected based on the sensitivity and specificity; ie, the true positive rate among PCR-confirmed positive specimens and the true negative rate among pre-COVID-19 negative control specimens. The correlation of iELISA results among different specimen types (serum, plasma, and dried blood specimens) from the same individual were evaluated with Pearson's correlation coefficient. The antibody concentrations in patients who were PCR-confirmed positive were plotted against time after symptom onset, with a smoothed line predicted by local weighted regression (loess)[20] to reflect the trend of time-course shifting. All statistical analyses were implemented using R (version 3.6.3).[21]

TABLE 1. Sample Information

Positive Specimens	COVID-19, PCR Confirmed	251
Prepandemic specimens (collected before 2019)	Adenovirus infected	7
	Antinuclear antibodies infected	5
	Cytomegalovirus infected	5
	Hepatitis B virus infected	13
	Hepatitis C virus infected	15
	Human parainfluenza viruses infected	6
	Influenza B infected	5
	MP virus infected	6
	Respiratory syncytial virus infected	10
	Healthy control sample	179
Total		515

PCR, polymerase chain reaction.

Results

Production of Recombinant SARS-Cov-2 S1 RBD and N Proteins in Mammalian Cells

At 3 days post-transfection, recombinant S1 RBD and N proteins were successfully secreted into the serum-free HEK293 cell culture medium. The expressed and secreted recombinant proteins were further affinity-purified with the *C*-terminal-fused His-tag. The final desalted S1 RBD protein (RayBiotech; catalog number 230–30162) migrated as an approximately 30 kDa protein band on SDS-PAGE under dithiothreitol, beta-mercaptoethanol reducing conditions (**FIGURE 1A**), which was larger than the expected size of 25 kDa. The purified N protein (RayBiotech; catalog number 230–30164; **FIGURE 1B**) had 1 major band at approximately 55 kDa, which was larger than the expected size of 47 kDa. To investigate these differences, the N and S1 RBD proteins were deglycosylated using an enzyme mixture. After cleaving the glycans, major bands at the expected size were present, indicating that the untreated recombinant proteins were glycosylated (data not shown). The purified recombinant proteins were confirmed by Western blot using a mouse monoclonal antibody, anti-SARS-CoV-2 S1RBD (130–10808) and anti-N protein (130–10817) (**FIGURE 1C** and **1D**).

Production and Comparison of S1 RBD and N Protein iELISAs

The iELISAs measuring the IgG, IgM, and IgA antibodies to the S1 RBD and N proteins of SARS-CoV-2 were developed for the serology testing of the patient specimens. Pre-COVID-19 (collected before 2019) negative control specimens and PCR-confirmed positive specimens were incubated on the S1 RBD and N protein coated plates. The anti-S1 RBD protein antibodies or anti-N protein antibodies present in the patient specimens were bound to the plate and unbound antibodies were removed. The specific, bound antibodies were detected with anti-human IgG, anti-human IgM, or anti-human IgA. To quantitatively measure the relative titer of patient antibodies, we selected a pool of 10 PCR-confirmed positive specimens with high titers (optical density [OD] > 1.0) of the IgG, IgM, and IgA antibodies and defined a certain dilution as an arbitrary unit. Then, we used a serial dilution of this positive

FIGURE 1. 12% SDS-PAGE analysis of purified recombinant S1 RBD and N proteins. Purified S1 RBD (A) and N protein (B) were run at 10% SDS-PAGE and probed with mouse monoclonal anti-SARS-CoV-2 S1 RBD antibody (130–10808) (C) and anti-SARS-CoV-2 N protein antibody (130–10817) (D). Lane 1 is purified *Escherichia coli*-derived N protein and Lane 2 is HEK293-purified N protein. HEK, human embryonic kidney; N protein, nucleocapsid protein; RBD, receptor binding domain; S1, spike subunit 1 protein; SDS-PAGE, sodium docetyl sulfate-polyacrylamide gel electrophoresis.

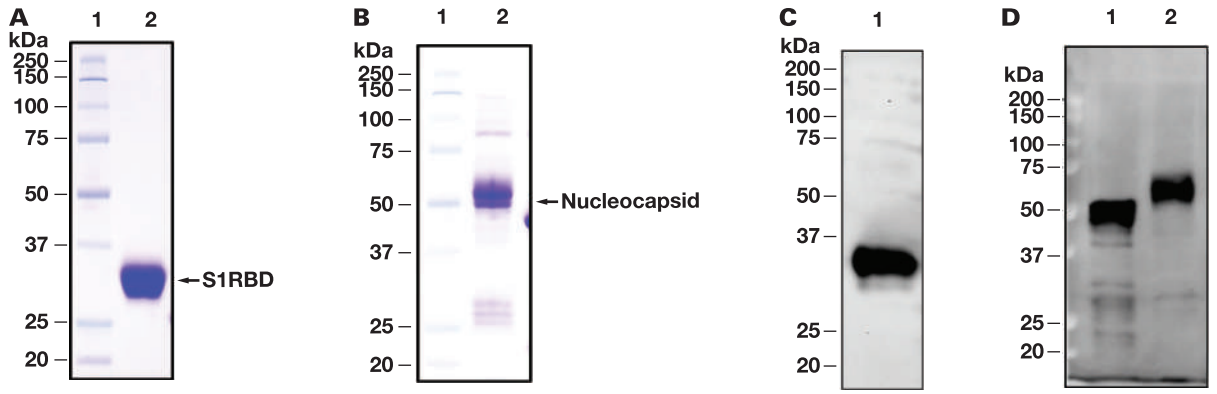

control to determine the quantitative units of antibodies present in each unknown specimen tested.

The IgG antibodies to the N protein were determined in 246 pre-COVID-19 negative control serum specimens and 81 PCR-confirmed positive serum specimens, and the IgM and IgA antibodies were determined in 56 pre-COVID-19 negative control serum specimens and 10 PCR-confirmed positive serum specimens. The IgG antibodies to the S1 RBD protein were determined in 264 pre-COVID-19 negative control serum specimens and 114 PCR-confirmed positive serum specimens, and the IgM and IgA antibodies were determined in 264 pre-COVID-19 negative control serum specimens and 115 PCR-confirmed positive serum specimens. The positivity cutoff values for the serum IgG antibodies to the S1 RBD and N proteins were determined to be 23.84 U/mL and 22.81 U/mL, respectively. The positivity cutoff values for the serum IgM antibodies to the S1 RBD and N proteins were 507.06 U/mL and 668.83 U/mL, respectively. Finally, the positivity cutoff values for the serum IgA antibodies to the S1 RBD and N proteins were 329.93 U/mL and 33.72 U/mL, respectively. The specificity and sensitivity for each protein and each antibody are shown in **TABLE 2**. The specificity for the IgG, IgM, and IgA antibodies to both proteins was >98%, whereas the sensitivity ranged, with IgG antibodies being the highest at 76% for both proteins. The sensitivity of IgM to the S1 RBD was only 66% and the sensitivity to the N protein was only 10%. The sensitivity of IgA was 80% to the N protein but was only 26% to the S1 RBD protein.

Interestingly, most of the pre-COVID-19 negative control specimens and PCR-confirmed positive specimens were accurately identified for IgG antibodies to both the N and S1 RBD proteins; however, a subset of specimens was inaccurately identified as either a false negative or a false positive. All the false-positive specimens for each IgG, IgM, and IgA antibody were different between the S1 RBD and N protein assays. Of the larger number of false-negative specimens, only 1 IgG and IgM specimen and 2 IgA specimens were the same for both the S1 RBD and N protein assays. These data strongly suggest that a subset of individual specimens will react differently to the S1 RBD or N proteins. Given these data, we decided to combine both the S1 RBD and N proteins together on a plate to increase the sensitivity and minimize the rate of false negatives for each specimen.

Comparison of the Combined S1 RBD and N Protein iELISA

To test whether the specificity and sensitivity could be enhanced by using a combination of the S1 RBD and N proteins, the 2 proteins were first mixed, and then the mixture of proteins was coated into 96-well plates. The IgG antibodies to the combined S1 RBD and N proteins were measured in 260 pre-COVID-19 negative control serum specimens and 117 PCR-confirmed positive serum specimens; the IgM and IgA antibodies to the combined S1 RBD and N proteins were measured in 264 pre-COVID-19 negative control serum specimens and 115 PCR-confirmed positive serum specimens. The positivity cutoff values for the serum IgG, IgM, and IgA antibodies to the combined S1 RBD and N proteins were 6.13 U/mL, 146.97 U/mL, and 68.32 U/mL, respectively. The data showed that the specificity remained >98% for all antibodies and the sensitivity increased for IgG from 76% up to 94.87%. The sensitivity for IgM was 62.60%, which was decreased slightly from 66.09% compared to the S1 RBD protein–alone assay but significantly increased from 10% compared to the N protein–alone assay. The sensitivity for IgA was 51.30%, which was significantly increased from 26.08% compared to the S1 RBD protein–alone assay and was decreased from 80% compared to the N protein–alone assay (**TABLE 3**). Although we found that this approach minimized the number of false negatives/positives, we noticed a significant level of background in the pre-COVID-19 negative control specimens that was decreasing the sensitivity and specificity of the assay. To overcome this issue, we included an albumin-coated plate. The same 264 pre-COVID-19 negative control serum specimens and 115 PCR-confirmed positive serum specimens were incubated on both the combined S1 RBD and N protein coated plates and an albumin-coated plate, and the assay was run simultaneously. The resulting ODs for each specimen on the albumin plate were subtracted from the ODs of the respective specimens on the S1 RBD and N protein-coated plates before we

TABLE 2. Comparison Sensitivity and Specificity of S1 RBD and N Protein iELISAs for IgG, IgM, and IgA Antibodies

	Target	Specificity	False Positives	Sensitivity	False Negatives
S1 RBD	IgG	98.48%	4	76.31%	27
N	IgG	98.37%	4	76.54%	19
S1 RBD	IgM	98.10%	5	66.09%	39
N	IgM	98.21%	1	10.00%	9
S1 RBD	IgA	98.10%	5	26.08%	85
N	IgA	98.21%	1	80.00%	2

RBD, receptor binding domain; S1, spike subunit 1 protein.

TABLE 3. Sensitivity and Specificity of the Combined S1 RBD and N Protein iELISA for IgG, IgM, and IgA Antibodies

Target	Specificity	False Positives	Sensitivity	False Negatives
IgG	98.07%	5	94.87%	6
IgM	98.11%	5	62.60%	43
IgA	98.11%	5	51.30%	56

degermined the quantitative units of antibodies present. After albumin subtraction, the specificity remained >98% and the sensitivity was significantly increased to 95.72%, 83.47%, and 82.60%, respectively for the IgG, IgM, and IgA antibodies (**TABLE 4**). A population cutoff for positivity was determined for each antibody to be 1.23 U/mL, 23.09 U/mL, and 6.36 U/mL for IgG, IgM, and IgA, respectively. Thus, an unknown serum specimen above the respective U/mL cutoff was considered positive.

Detection of IgG, IgM, and IgA Antibodies in Different Specimen Matrices

Analysis of COVID-19 in several different specimen types provide a few advantages. Dried blood specimens in particular have a minimally invasive specimen collection, minimal specimen processing requirements, low cost, long-term stability in shipping or storage, and increased feasibility for remote sampling, which makes it an ideal specimen type for large-scale serological profiling of patients with COVID-19. To test whether this quantitative approach can be used to effectively measure antibodies present in specimen types other than serum, we also tested plasma and dried blood specimens. The amount of IgG, IgM, and IgA antibodies present in the combined S1 RBD and N proteins using albumin-subtracted ELISA in 31 matched, PCR-confirmed positive serum and plasma specimens and 27 matched, PCR-confirmed positive serum and dried blood specimens was moderately correlated between all 3 specimen types (**FIGURE 2** and **FIGURE 3**). These data suggest that this approach is well suited and can be easily adapted to different specimen types.

Cross-Reactivity and Double-Blind Validation of the Combined S1 RBD and N Proteins Using Albumin-Subtracted Assay

In addition to validating this assay's use in multiple specimen types, we wanted to validate the assay for lack of cross-reactivity to other viruses and autoimmune diseases. We examined the IgG, IgM, and IgA antibody levels to the SARS-CoV-2 S1 RBD and N proteins using albumin-subtracted iELISA in serum specimens from 72 patients with confirmed virus infection, including those with adenovirus, antinuclear antibodies of autoimmune disease, cytomegalovirus, hepatitis B virus, hepatitis C virus, human parainfluenza viruses, influenza B, MP virus, and respiratory syncytial virus. As shown in **TABLE 5**, among the 72 specimens, none cross-reacted for IgG, and only 2 specimens, a hepatitis C virus–infected specimen and a respiratory syncytial virus–infected specimen, cross-reacted for IgM. Only 1 specimen, a respiratory syncytial virus–infected specimen, cross-reacted for IgA. These data show low cross-reactivity of this assay with several common viruses.

We also performed a double-blinded study with a unique specimen set of 30 serum specimens, containing 10 pre-COVID-19 negative control specimens and 20 PCR-confirmed positive specimens each. The established cutoffs of 1.23 U/mL, 23.09 U/mL, and 6.36 U/mL for IgG, IgM, and IgA, respectively, were used for assessment of positivity. The specificities of both double-blinded studies were >90% for all antibodies and the sensitivities were 90.00%, 75.00%, and 70.00% for IgG, IgM, and IgA, respectively. These data were similar, despite the small sample size, to the original specimen set used to establish the cutoffs (**TABLE 6**). Taken together, these data show the robustness of the assay in accurately determining the SARS-CoV-2 antibodies present in a patient specimen.

TABLE 4. Sensitivity and Specificity of the Combined S1 RBD and N Protein and Albumin Subtracted iELISA for IgG, IgM, and IgA Antibodies

	IgG	IgM	IgA
AUC	0.9839	0.9606	0.9441
Specificity	98.07%	98.48%	98.10%
Sensitivity	95.72%	83.47%	82.60%
Accuracy	96.34%	93.93%	93.40%
Population positivity cutoff	1.23 U/mL	23.09 U/mL	6.36 U/mL
Kappa	0.95	0.9	0.89

AUC, area under the curve.

Time Course of Antibody Response During COVID-19

The quantitative nature of the developed assay allowed for the determination of the time course of the antibody response while a patient has COVID-19 disease. We assessed the IgG, IgM, and IgA antibody response in 251 PCR-confirmed positive serum specimens: 50 specimens were 1 to 7 days post-symptom onset, 30 specimens were 8 to 14 days post-symptom onset, 41 specimens were 15 to 25 days post-symptom onset, 103 specimens were 26 to 40 days post-symptom onset, 16 specimens were 41 to 60 days post-symptom onset, and 11 specimens were >60 days post-symptom onset. The levels of IgG, IgM, and IgA antibodies to the combined S1 RBD and N proteins using albumin-subtracted assay are shown in **FIGURE 4** and **FIGURE 5**. These data show that most specimens have a similar response for IgG, IgM, and IgA antibodies, in terms of peak response and particularly after 10 days post-symptom onset.

Correlation of Antibody Responses Against S1 RBD and N Proteins

To have a better understanding of the correlation of the immune response between the S1 RBD and N proteins, we analyzed 135 PCR-confirmed positive specimens for IgG and 12 PCR-confirmed positive specimens for IgM and IgA using a scatterplot. As shown in **FIGURE 6**, the anti-S1 RBD protein IgG, IgM, and IgA response correlations with the anti-N protein IgG, IgM, and IgA antibody response were r^2 = .3045, .5264, and .5185, respectively (P <.05). Overall, the S1 RBD protein–specific IgM and IgA responses were well correlated with the N protein–specific IgM and IgA responses, whereas the S1 RBD protein–specific IgG response was weakly correlated with the N protein–specific IgG response.

Discussion

Here, we have established a comprehensive approach to measure antibodies against SARS-CoV-2. We have developed a quantitative immunoassay to detect IgG, IgM, and IgA antibodies to SARS-CoV-2

FIGURE 2. Correlations between serum and plasma. We analyzed 31 positive specimens using a scatterplot; each blue dot represents a specimen. The *x* axis represents U/mL for serum and the *y* axis represents U/mL for plasma. Correlations for IgG (A), IgM (B), and IgA (C) between serum and plasma, respectively.

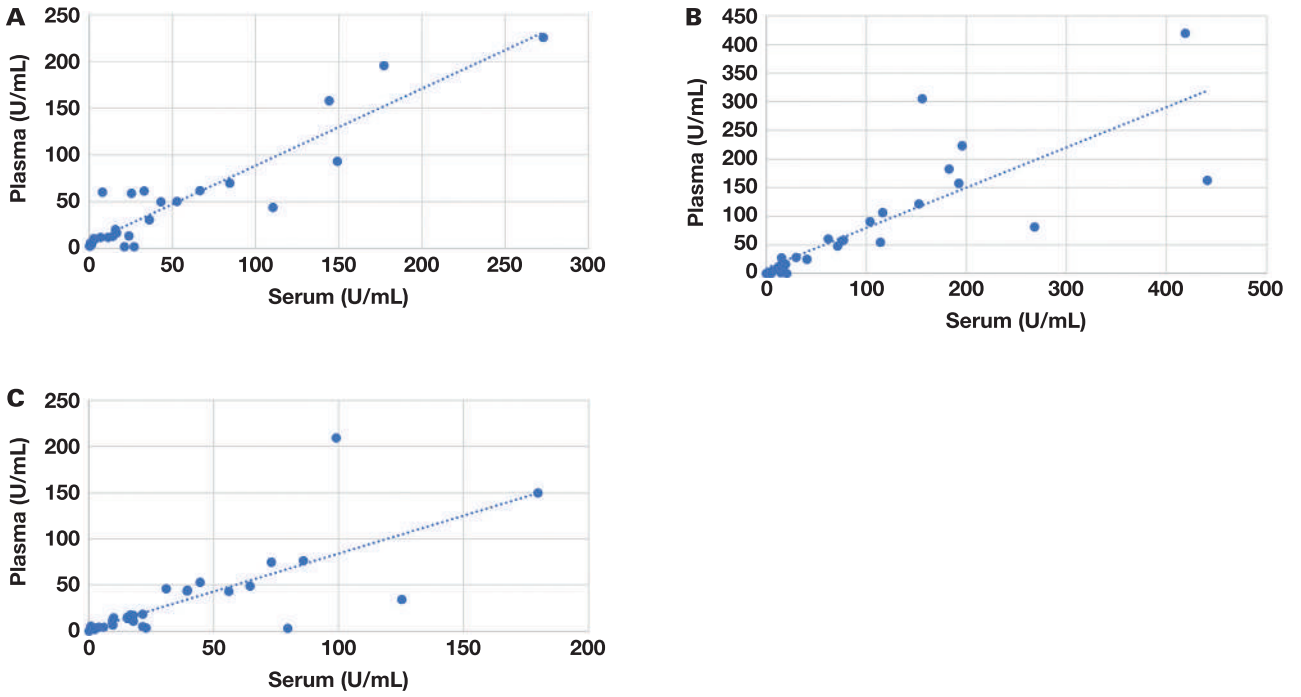

FIGURE 3. Correlations between serum and DBS. We analyzed 27 positive specimens using a scatterplot; each blue dot represents a sample. The *x* axis represents U/mL for serum and the *y* axis represents U/mL for DBS. Correlations for IgG (A), IgM (B), and IgA (C) between serum and DBS, respectively. DBS, dried blood specimen.

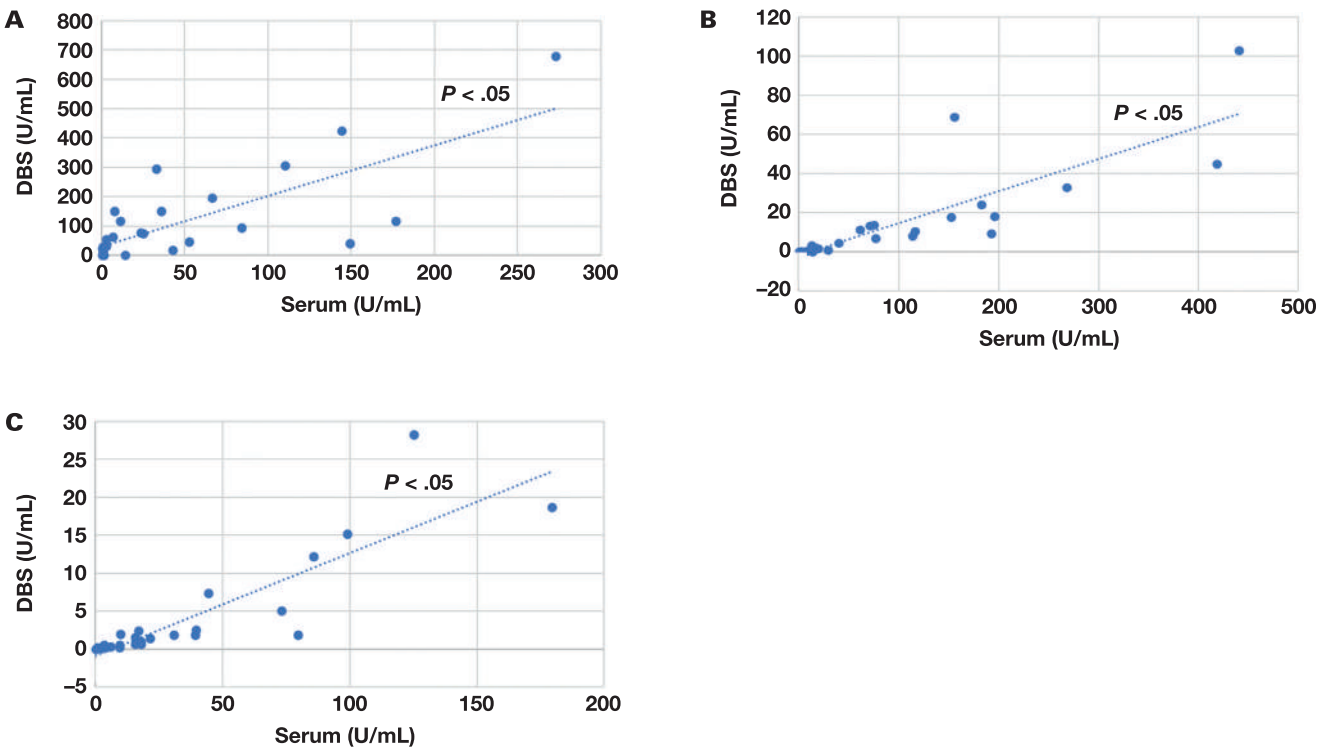

with high specificity and sensitivity and low cross-reactivity to several common viruses. This novel approach features a mixture of both the S1 RBD and N proteins and an albumin-coated plate that allows for the capture of a broad antibody response and at the same time a reduction of the nonspecific background. We were also able to confirm the suitability of this assay in several specimen types, including serum, plasma, and dried blood specimens, which broadens the scope of its potential use.

TABLE 5. Cross-Reactivity of the Combined S1 RBD and N Protein and Albumin Subtracted iELISA for IgG, IgM, and IgA Antibodies with Several Common Viruses

Virus	Numbers of Specimens	Cross-Reactivity result (positive/negative)		
		IgG	IgM	IgA
Adenovirus	7	0/7	0/7	0/7
Antinuclear antibodies	5	0/5	0/5	0/5
Cytomegalovirus	5	0/5	0/5	0/5
Hepatitis B virus	13	0/13	0/13	0/13
Hepatitis C virus	15	0/15	1/14	0/15
Human parainfluenza viruses	6	0/6	0/6	0/6
Influenza B	5	0/5	0/5	0/5
MP virus	6	0/6	0/6	0/6
Respiratory syncytial virus	10	0/10	1/9	1/9

TABLE 6. Double-Blind Test Results of the Combined S1 RBD and N Protein and Albumin Subtracted iELISA for IgG, IgM, and IgA Antibodies

Target	Specificity	False Positives	Sensitivity	False Negatives
IgG	90.00%	1	90.00%	2
IgM	100.00%	0	75.00%	5
IgA	100.00%	0	70.00%	6

In this assay, after albumin subtraction, the specificity remained >98% and the sensitivity was significantly increased to 95.72%, 83.47%, and 82.60%, respectively, for IgG, IgM, and IgA antibodies to the combined S1 RBD and N proteins. Several immunoassays targeting IgG, IgM, or IgA antibodies have been developed with varying degrees of accuracy. Some of this variation results from the use of different antigens and protocols or from measuring different antibodies. Those different approaches may have different applications: eg, S1 RBD antibody detection can be used to indicate potential neutralization activity. In this study, we found differences in the response of some specimens to the S1 RBD protein vs the N protein and between the antibody isotypes. A previous study testing the performance of several chemiluminescence immunoassays showed that when using the S1 RBD protein, the responses of IgM and IgA were higher compared to the use of the N protein antigen.[22] Liu et al[23] showed varying sensitivities and specificities of IgG and IgM antibodies, with the S protein having higher sensitivity and an earlier antibody response compared to the N protein. Another study also confirmed differing antibody responses in the same specimen along with differing assay sensitivity and specificity.[13] By combining different SARS-CoV-2 antigens, we were able to detect a broader antibody response. Based on these data, we expected that the combined detection of both the S1 RBD and the N proteins may improve the detection of the antibody response.

Cai et al[10] showed that combining IgM and IgG isotypes improved the positivity of the assay. Several studies examined the accuracy

FIGURE 4. Time course for IgG (A), IgM (B), and IgA (C). We analyzed 251 positive specimens. Each blue dot represents a specimen; the thick black line represents the median for each group and the thin black line is for error bars. The *x* axes represent days after symptoms; there are 6 groups: 1–7 days, 8–14 days, 15–25 days, 26–40 days, 41–60 days, and >60 days. The *y* axes represent concentration (U/mL) for IgG, IgM, and IgA, respectively.

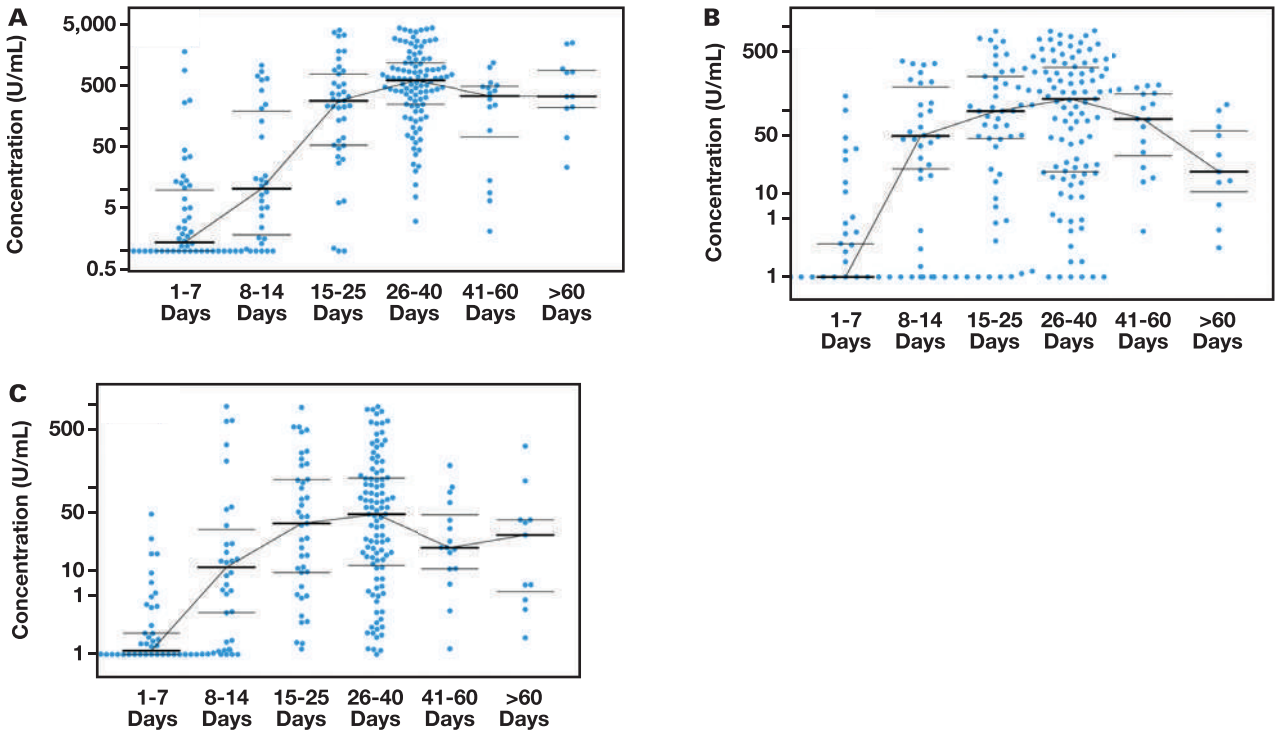

FIGURE 5. Time course for IgG (A), IgM (B), and IgA (C). We analyzed 223 positive specimens. Each black dot represents a specimen. The *x* axes represent days after symptoms. The *y* axes represent concentration (U/mL) for IgG, IgM, and IgA, respectively. The red dotted line indicates the cutoff value, and the blue smooth line indicates the median.

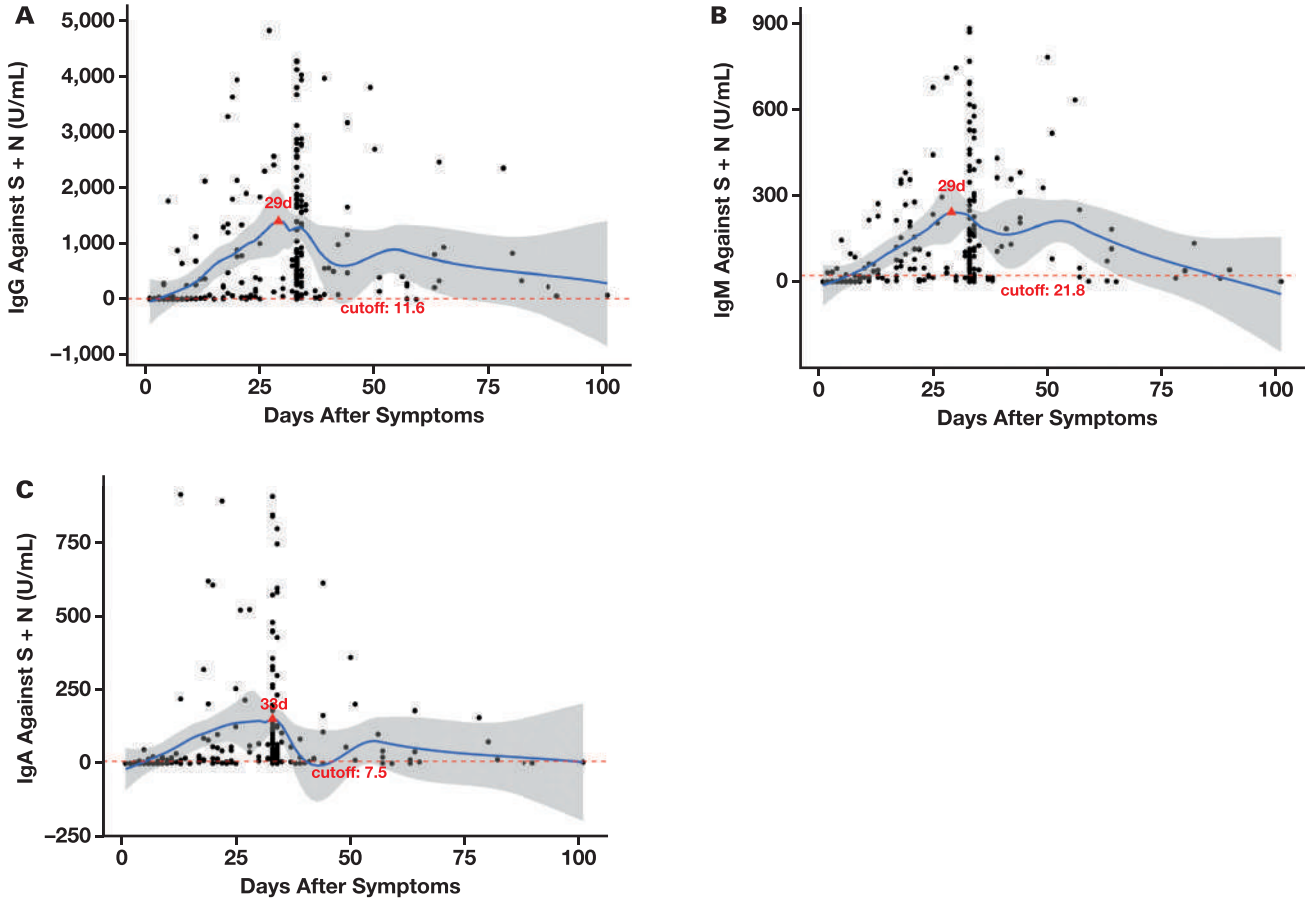

of different lateral-flow immunoassays and ELISAs and found the highest accuracy in detection to be with combined IgG, IgM, and IgA analyses.[11,12,14,15] A meta-analysis of the diagnostic performance of serology tests for COVID-19 showed that the combination of antigens—S, S1 RBD, and/or N proteins—also improved the accuracy of detection compared with any single antigen alone.[24] Krishnamurthy et al[25] also tested the IgG, IgM, and IgA antibody responses to the S1, S1 RBD, S2, and N antigens and found that the sensitivity varied among the tested antigens and antibodies and showed the highest sensitivity and specificity when combining all antigens and antibodies. Like the authors of these studies, we found that by combining the S1 RBD and N antigens and an albumin plate, we were able to improve the sensitivities of each antibody isotype in this assay.

The quantitative nature of the assay also allowed the determination of the time course of the antibody response while a patient has COVID-19 disease. Because most serological tests have tested specimens or groups of specimens collected at different time points, it is difficult to access the correct timeline for antibody responses against SARS-CoV-2 infection. We tested 251 PCR-confirmed positive serum specimens: 50 specimens were 1 to 7 days post-symptom onset, 30 specimens were 8 to 14 days post-symptom onset, 41 specimens were 15 to 25 days post-symptom onset, 103 specimens were 26 to 40 days post-symptom onset, 16 specimens were 41 to 60 days post-symptom onset, and 11 specimens were >60 days post-symptom onset; we found similar responses for IgG, IgM, and IgA antibodies in terms of peak response and particularly after 10 days post-symptom onset. Previous studies suggested that the sensitivity of antibody tests within the first week of disease is not ideal. However, sensitivity vastly increases in the second week.[9,16,17] Similar to these and our results, Hu et al[26] also observed a maximum antibody response on days 19 to 21, with the highest IgM response to be at days 16 to 18 and the highest IgG response to be at days 19 to 21 post-symptom onset. However, it is not yet clear how long the SARS-CoV-2–specific antibodies remain within a patient, or if the presence of those antibodies is an indicator of protection against COVID-19 disease. Because the likely path out of the current pandemic is through pharmaceutical means, it is essential to know the immune response for appropriate planning of vaccine strategies and protocols.

The antibody response at the site of infection or circulating systemically has not been well characterized. Thus, the ideal specimen type for use in serological analysis remains unknown. In this study, we confirmed the suitability of this assay in several specimen types, including serum, plasma, and dried blood specimens, which broadens the scope of its potential use. We found that the IgG, IgM, and IgA antibody responses were well correlated among tested specimen types. Krishnamurthy et al[25] also compared clinically paired dried blood and serum specimens and found >90% correlation. Plasma has also been used successfully to measure antibody responses in patients with COVID-19.[7,27,28]

FIGURE 6. Correlation of antibody response between the S1 RBD and N proteins. (A) IgG: We analyzed 135 positive specimens. Each blue dot represents a specimen. The *x* axis represents the anti-S1 RBD protein IgG concentration (U/mL). The *y* axis represents the anti-N protein IgG concentration (U/mL). (B) IgM: We analyzed 12 positive specimens. Each blue dot represents a specimen. The *x* axis represents the anti-S1 RBD protein IgM concentration (U/mL). The *y* axis represents the anti-N protein IgM concentration (U/mL). (C) IgA: We analyzed 12 positive specimens. Each blue dot represents a specimen. The *x* axis represents the anti-S1 RBD protein IgA concentration (U/mL). The *y* axis represents the anti-N protein IgA concentration (U/mL). N protein, nucleocapsid protein; RBD, receptor binding domain; S1, spike subunit 1 protein.

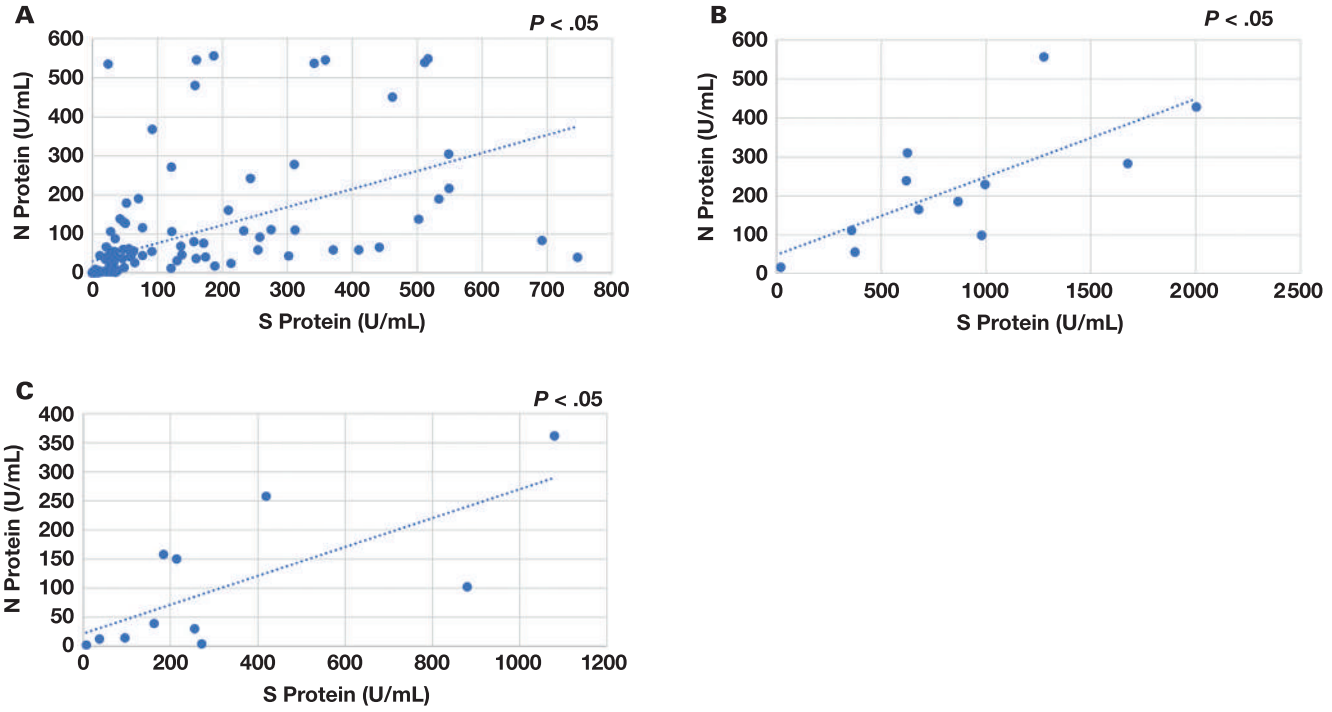

Our data indicate that the IgM and IgA responses to both the S1 RBD and N proteins have a significant and moderately strong correlation (r^2 = .5264 and .5185; P <.05), whereas a weak correlation was seen in the IgG response to both the S1 RBD and N proteins (r^2 = 0.3045, P <.05). This finding was consistent with previous studies.[29,30] In contrast, Chen et al[31] found a weak correlation of the IgM response between the S1 RBD and N proteins (r = .2928, corrected; P <.0001), whereas the IgG response between the S1 RBD and N proteins was significantly correlated (r = .5549, corrected; P <.001). Differences could be caused by specimen collection biases, the small number of specimens tested, or the different time frames of expression of each of the antibodies post-infection.

Conclusion

We have shown the quantitative detection of SARS-CoV-2 IgG, IgM, and IgA antibodies to the combined N and S1 RBD proteins with an albumin signal subtracted at a high sensitivity and specificity in serum, plasma, and dried blood specimens. We were also able to determine the temporal dynamics and magnitude of IgG, IgM, and IgA antibody responses in patients with COVID-19. Future studies that assess additional specimen types such as saliva or other oral specimens will be beneficial. Further analyses into the potential of these detected antibodies to be neutralizing can increase therapeutic and vaccine strategies in the future.

Acknowledgments

This research was funded by the RayBiotech Life innovative research fund, the Guangzhou Innovation Leadership Team (CXLJTD-201602), and The Science and Technology Innovation Project of Foshan Municipality, China (2020001000431).

Disclosure

Some authors (Shuhong Luo, Chih Yun Cho, Kelly C. Whittaker, Xingqi Wang, Jie Feng, Meng Wang, Jianmin Fang, and Ruo-Pan Huang) are employees of and have a financial stake in RayBiotech.

REFERENCES

1. Worldometer. Reported cases and deaths by country or territory. https://www.worldometers.info/coronavirus/#countries. Accessed September 13, 2021.
2. Centers for Disease Control and Prevention. COVID-19: data and surveillance. https://www.cdc.gov/coronavirus/2019-ncov/cases-updates/index.html. Accessed September 13, 2021.
3. U.S, Food & Drug Administration. *FDA combating COVID-19 with therapeutics*. https://www.fda.gov/media/136832/download. Accessed September 13, 2021.
4. Lippi G, Simundic AM, Plebani M. Potential preanalytical and analytical vulnerabilities in the laboratory diagnosis of coronavirus disease 2019 (COVID-19). *Clin Chem Lab Med*. 2020;58(7):1070–1076.

5. Tahamtan A, Ardebili A. Real-time RT-PCR in COVID-19 detection: issues affecting the results. *Expert Rev Mol Diagn.* 2020;20(5):453–454.
6. Pascarella G, Strumia A, Piliego C, et al. COVID-19 diagnosis and management: a comprehensive review. *J Intern Med.* 2020;288(2):192–206.
7. Guo L, Ren L, Yang S, et al. Profiling early humoral response to diagnose novel coronavirus disease (COVID-19). *Clin Infect Dis.* 2020;71(15):778–785.
8. Padoan A, Bonfante F, Pagliari M, et al. Analytical and clinical performances of five immunoassays for the detection of SARS-CoV-2 antibodies in comparison with neutralization activity. *EBioMedicine.* 2020;62:103101.
9. Ejazi SA, Ghosh S, Ali N. Antibody detection assays for COVID-19 diagnosis: an early overview. *Immunol Cell Biol.* 2021;99(1):21–33.
10. Cai XF, Chen J, Li Hu J, et al. A peptide-based magnetic chemiluminescence enzyme immunoassay for serological diagnosis of coronavirus disease 2019. *J Infect Dis.* 2020;222(2):189–193.
11. Espejo AP, Akgun Y, Al Mana AF, et al. Review of current advances in serologic testing for COVID-19. *Am J Clin Pathol.* 2020;154(3):293–304.
12. Ma H, Zeng W, He H, et al. COVID-19 diagnosis and study of serum SARS-CoV-2 specific IgA, IgM and IgG by chemiluminescence immunoanalysis. Preprint. Posted online April 30, 2020. *medRxiv*. https://doi.org/10.1101/2020.04.17.20064907.
13. Qian C, Zhou M, Cheng F, et al. Development and multicenter performance evaluation of fully automated SARS-CoV-2 IgM and IgG immunoassays. *Clin Chem Lab Med*. 2020;58(9):1601–1607.
14. Van Elslande J, Houben E, Depypere M, et al. Diagnostic performance of seven rapid IgG/IgM antibody tests and the Euroimmun IgA/IgG ELISA in COVID-19 patients. *Clin Microbiol Infect.* 2020;26(8):1082–1087.
15. Whitman JD, Hiatt J, Mowery CT, et al. Test performance evaluation of SARS-CoV-2 serological assays. Preprint. Posted online May 17, 2020. *medRxiv*. doi: 10.1101/2020.04.25.20074856.
16. To KK, Tsang OT, Leung WS, et al. Temporal profiles of viral load in posterior oropharyngeal saliva samples and serum antibody responses during infection by SARS-CoV-2: an observational cohort study. *Lancet Infect Dis.* 2020;20(5):565–574.
17. Xiao AT, Gao C, Zhang S. Profile of specific antibodies to SARS-CoV-2: the first report. *J Infect.* 2020;81(1):147–178.
18. Yoshimoto FK. The proteins of severe acute respiratory syndrome coronavirus-2 (SARS CoV-2 or n-COV19), the cause of COVID-19. *Protein J.* 2020;39(3):198–216.
19. Hanley JA, McNeil BJ. The meaning and use of the area under a receiver operating characteristic (ROC) curve. *Radiology.* 1982;143(1):29–36.
20. Cleveland WS. Robust locally weighted regression and smoothing scatterplots. *J Am Stat Assoc*. 1979;74(368):829–836.
21. R Core Team. 2017. *R: A Language and Environment for Statistical Computing*. Vienna, Austria: R Foundation for Statistical Computing.
22. Kumar S, Maurya VK, Prasad AK, Bhatt MLB, Saxena SK. Structural, glycosylation and antigenic variation between 2019 novel coronavirus (2019-nCoV) and SARS coronavirus (SARS-CoV). *Virusdisease.* 2020;31(1):13–21.
23. Liu W, Liu L, Kou G, et al. Evaluation of nucleocapsid and spike protein-based enzyme-linked immunosorbent assays for detecting antibodies against SARS-CoV-2. *J Clin Microbiol*. 2020;58(6):e00461-20.
24. Wang H, Ai J, Loeffelholz MJ, Tang YW, Zhang W. Meta-analysis of diagnostic performance of serology tests for COVID-19: impact of assay design and post-symptom-onset intervals. *Emerg Microbes Infect.* 2020;9(1):2200–2211.
25. Krishnamurthy HK, Jayaraman V, Krishna K, et al. Antibody profiling and prevalence in US patients during the SARS-CoV2 pandemic. *PLoS One.* 2020;15(11):e0242655.
26. Hu Q, Cui X, Liu X, et al. The production and clinical implications of SARS-CoV-2 antibodies. Preprint. Posted online April 24, 2020. *medRxiv*. doi: 10.1101/2020.04.20.20065953.
27. Wang Y, Zhang L, Sang L, et al. Kinetics of viral load and antibody response in relation to COVID-19 severity. *J Clin Invest.* 2020;130(10):5235–5244.
28. Ogata AF, Maley AM, Wu C, et al. Ultra-sensitive serial profiling of SARS-CoV-2 antigens and antibodies in plasma to understand disease progression in COVID-19 patients with severe disease. *Clin Chem.* 2020;66(12):1562–1572.
29. Algaissi A, Alfaleh MA, Hala S, et al. SARS-CoV-2 S1 and N-based serological assays reveal rapid seroconversion and induction of specific antibody response in COVID-19 patients. *Sci Rep.* 2020;10(1):16561.
30. Brochot E, Demey B, Touzé A, et al. Anti-spike, anti-nucleocapsid and neutralizing antibodies in SARS-CoV-2 inpatients and asymptomatic individuals. *Front Microbiol.* 2020;11:584251.
31. Chen Y, Tong X, Li Y, et al. A comprehensive, longitudinal analysis of humoral responses specific to four recombinant antigens of SARS-CoV-2 in severe and non-severe COVID-19 patients. *PLoS Pathog.* 2020;16(9):e1008796.

A Simplified Protocol for Microsatellite Instability Evaluation in Iranian Patients at Risk for Lynch Syndrome

Zeinab Abdollahi, MSc,[1] Mohammad Amin Tabatabaiefar, PhD,[1,2] Mahnaz Noruzi, PhD,[3] Paniz Miar, MSc,[1] Mohammad Kazemi, PhD,[1] Azar Naimi, MD,[4] Mohammad Hasan Emami, MD,[5] Mehrdad Zeinalian, MD, MPH, PhD[1,2,6,]*

[1]Department of Genetics and Molecular Biology, School of Medicine, Isfahan University of Medical Sciences, Isfahan, Iran; [2]Pediatric Inherited Disease Research Center, Research Institute for Primordial Prevention of Non-communicable Disease, Isfahan University of Medical Sciences, Isfahan, Iran; [3]Department of Biology, Faculty of Sciences, Shahid Chamran University, Ahvaz, Iran; [4]Department of Pathology, School of Medicine, Isfahan University of Medical Sciences, Isfahan, Iran; [5]Poursina Hakim Digestive Diseases Research Center, Isfahan, Iran, and; [6]Ala Cancer Prevention and Control Center, Isfahan, Iran; *To whom correspondence should be addressed. zeinalianmehrdad@gmail.com, m.zeinalian@med.mui.ac.ir

Keywords: Lynch syndrome, colorectal cancer, microsatellite instability, DNA mismatch repair, mononucleotide markers, BAT34c4

Abbreviations: CRC, colorectal cancer; LS, Lynch syndrome; HNPCC, hereditary nonpolyposis colorectal cancer; MMR, mismatch repair; MSI, microsatellite instability; STR, short tandem repeats; IHC, immunohistochemistry; MSS, microsatellite stable; MSI-H, MSI-high; NGS, next-generation sequencing; SNPs, single mononucleotide markers; ACSA, Ala Cancer Prevention and Control Center; FFPE, formalin-fixed-paraffin-embedded; MSI-L, MSI-low; PPVs, positive predictive values; FCCTX, familial colorectal cancer type X

Laboratory Medicine 2022;53:235–241; https://doi.org/10.1093/labmed/lmab064

ABSTRACT

Objective: The most important tumor characteristic of Lynch syndrome (LS) is microsatellite instability (MSI). In the current study, BAT34c4 and BAT26 mononucleotide markers were evaluated as part of efforts to test a cost-effective panel for MSI testing in Iranian patients, comparing it with the Promega kit.

Methods: Amsterdam II clinical criteria were used to identify patients at risk for LS. The MSI status of these patients was determined using BAT34c4 and BAT26 markers, as well as the Promega kit. The results of both methods were compared, and the sensitivity and specificity of new short tandem repeat (STR) markers were estimated using statistical formulas.

Results: Of the 37 patients we studied who were at risk for LS, 27% showed MSI-high results, via the Promega kit. The same results were achieved for BAT34c4 and BAT26 separately.

Conclusions: The novel 2-marker kit for MSI testing has similar accuracy as the Promega kit at a lower cost, due to fewer markers and a more economical labeling method.

The fourth most prevalent cancer leading to death in the United States is colorectal cancer (CRC).[1] According to the results of a recent study,[2] the incidence of CRC has been increased among Iranian people to greater than 80%, among all types of cancer diagnosed. Overall, there are 3 main forms of CRC: sporadic, familial, and hereditary. Approximately 70%–80% of CRC cases are classified in the sporadic category, with no evidence of genetic inheritance. Hereditary susceptibility is the most likely potential cause of cancer in the rest of the patients (20%–30%).[3]

Lynch syndrome (LS), which was previously known as hereditary nonpolyposis colorectal cancer (HNPCC), is caused by highly penetrant mutations in 1 of the 4 key mismatch repair (MMR) genes, including *MLH1*, *MSH2*, *MSH6*, and *PMS2*. This autosomal dominant hereditary syndrome includes 3%–5% of CRC cases.[4,5] Although these patients have a high risk for relapse, they could benefit from a better prognosis and longer survival rate at all stages of disease, with less spreading of cancerous nodes.[6]

Microsatellite instability (MSI) is defined as alteration in the length of short tandem repeats (STR) induced by MMR deficiency, the main molecular phenotype of LS. MSI has been observed in LS-associated cancers, such as stomach, small bowel, hepatobiliary system, upper urologic tract, glioblastoma, pancreas, breast, prostate, and adrenocortical tumors.[7] Moreover, approximately 15%–20% of sporadic colorectal tumors present as MSI due to somatic epigenetic silencing of the *MLH1* gene.[8]

Amsterdam I and II criteria and the Bethesda guideline are used to clinically differentiate LS from the sporadic type of CRC.[9] Molecular testing is also used in the next step, to confirm LS diagnosis at the molecular level.[3] Immunohistochemistry (IHC) is one of the available methods to detect MMR protein expression. Moreover, MSI phenotype can be

checked by a PCR-based method called MSI testing. These 2 procedures are currently used to identify MMR-deficient tumors.[7] A comprehensive testing strategy has been suggested by the Association of Molecular Pathology, including IHC and PCR-based methods to identify all new cases of LS.[10]

Meanwhile, there are some histopathologic differences between microsatellite stable (MSS) and MSI colorectal tumors; hence, mucinous histology, poor differentiation, and lymphocytic infiltration are the main characteristics of MSI-high (MSI-H) tumors. Moreover, these 2 tumor subgroups manifest different clinical behaviors.[11] For example, 5-fluorouracil chemotherapy has less of an effect on MSI-H tumors; the tumors are more sensitive to irinotecan and anti-PD1/PDL1 immunotherapy.[12] Currently, MSI testing is frequently used as a favorable prognostic and predictive marker in all CRC cases, particularly early-onset ones.[13]

In contrast, several new platforms have been recently developed in next-generation sequencing (NGS) technology to detect MSI status, which could be more reliable than previous methods through the evaluation of several markers.[14] Because in the NGS-based methods several markers are simultaneously checked for MSI testing, evaluating the sensitivity and specificity of new markers seems to be necessary.

Different panels have been suggested for MSI testing. The Bethesda panel was proposed by the National Cancer Institute collaborative group HNPCC (NCI/ICG-HNPCC) in 1997. It contains 5 markers, 2 mononucleotide repeats, and 3 dinucleotide repeats, to determine MSI status.[15] The results of another study[16] showed that mononucleotide markers were more sensitive than dinucleotide ones. Also, dinucleotide repeats showed polymorphism among individuals and were required to be matched with normal tissue, which can be laborious and costly. Therefore, the NCI-HNPCC suggested a new 5-mononucleotide panel to improve the accuracy of MSI testing.[17] Thereafter, the Promega Corporation developed a commercial MSI testing kit containing 5 quasimonomorphic mononucleotide markers—NR21, BAT25, MONO27, NR24, and BAT26—and 2 pentanucleotide repeats, Penta D, and PentaC (**TABLE 1**).

In using the Promega kit, which is currently one of the most widely used diagnostic kits worldwide, the comparison of tumor and adjacent normal tissue DNA is essential.[9] However, multimarker MSI testing is a labor-intensive and costly process, so efforts have been made to replace this method with simpler options that use fewer markers to detect MSI.[18] Numerous studies have been performed to evaluate the reliability and accuracy of single mononucleotide polymorphisms (SNPs) used as markers for MSI testing, to develop an easier, cost-effective, and quicker method without sensitivity and specificity concerns.[19–21]

In previous studies a 3-marker panel was evaluated in comparison with a 5-marker panel for MSI testing. The results showed that the sensitivity and specificity of the 3-marker panel was as high as that of the 5-marker panel.[22] Another study compared a single-marker panel with a 5-marker panel. The same results were obtained, and the single-marker panel showed high sensitivity.[23] The hypothesis was proposed that a single sensitive marker in a single population would be enough to evaluate MSI. It seems that the sensitivity and specificity of markers vary in different populations. MT1XT20, a mononucleotide marker located in the 3′-untranslated region of the *metallothionein 1X* gene, was evaluated in White patients and was introduced as a highly sensitive and specific marker for PCR-based MSI testing.[24] This marker is not sensitive in the Iranian population.[18]

Among the previously determined informative microsatellite loci in CRC, we selected 2 highly sensitive markers with short mononucleotide repeat units. The highest sensitivity for identification of MSI-H cancers has been reported for BAT-26, which is located on intron-5 of the *hMSH2* gene.[25,26] Moreover, some study reports have introduced BAT34c4, located in the 3′-untranslated region of exon 11 of the *P53* gene, as an appropriate detection marker. This marker has shown high sensitivity in determining MSI status after testing of the BAT26 marker.[27]

In this study, the sensitivity and specificity of BAT34c4 and BAT26 mononucleotide markers have been evaluated for MSI testing in patients with CRC, using the Amsterdam II criteria to evaluate the sensitivity and specificity of these markers among the Iranian population and to develop a simpler, less-expensive diagnostic kit (**TABLE 1**).

Methods

Population Study

Altogether, 685 patients with CRC were included from 2 well-known referral centers in Isfahan, central Iran—the Ala Cancer Prevention and Control Center (ACSA) and Poursina Hakim Gastrointestinal Clinic—between 2011 and 2018. Overall, 63 patients whose cases fit the Amsterdam II criteria were selected from a group of 210 patients with positive familial history. Finally, 37 patients were included based on patient-satisfaction feedback and availability of surgically obtained tumor specimen material. Written informed consent was obtained from all participants; this study was approved by the Ethical Committee of Isfahan University of Medical Sciences, Iran.

DNA Extraction and Multiplex PCR-Based MSI Testing

We extracted the genomic DNA from 37 colorectal tumors and their adjacent normal formalin-fixed-paraffin-embedded (FFPE) tissues, based on an available salting-out protocol described in the literature.[28] The Promega kit was used as the criterion standard to evaluate the accuracy of the analytic measures of our simplified panel for all 37 specimens.

The multiplex PCR assay was set up for NR-21, BAT-26, BAT-25, NR-24, MONO-27, Penta C, and Penta D markers, according to the manufacturer-provided protocol. Subsequently, PCR products were analyzed using an ABI PRISM 3500 Genetic Analyzer (Applied Biosystems), as recommended by Promega. The peaks were assessed using GeneMarker software, version HID V3.00 (SoftGenetics). The size shift of electropherograms in DNA tumor specimens, compared with

TABLE 1. The Promega Panel Mononucleotide Markers, Compared with the Single Marker BAT34c4

Marker	Gene	Location	Major Repeat Sequence	Size Range (bp)	Primer Dye
BAT25	c-Kit	Intron 16	$(A)_{25}$	114–124	JOE
NR21	*SLC7A8*	5′UTR	$(A)_{21}$	94–101	JOE
NR24	*ZNF2*	3′UTR	$(A)_{24}$	130–133	TMR
MONO27	*MAP4K3*	5′UTR	$(A)_{27}$	142–154	JOE
BAT26	*MSH2*	Intron 5	$(A)_{26}$	103–111	FAM
BAT34c4	*TP53*	3′UTR	(T)3C(T)6C(T)17C(T)5C(T)3	130–133	HEX
BAT26	*MSH2*	Intron 5	$(A)_{26}$	124–130	HEX

bp, base pair.

their adjacent normal DNA tissues, was measured for classification of specimens as MSI-H or MSS. Based on the pentamarker panel results, MSI-H is defined as being when at least 2 of 5 markers in tumor cells show size variation, compared with the normal cells. If only one marker alteration in the tumor cells is observed, it would be classified as MSI-low (MSI-L). The absence of microsatellite alteration is also considered to indicate MSS status.

The Novel Mononucleotide-Markers Assay

The sequences BAT34c4 $(T)_3C(T)_6C(T)_{17}C(T)_5C(T)_3$ and BAT26 $(A)_{26}$ were taken from the NCBI Genome Browser and UCSC Genome Browse. We used the Primer3 Plus online software tool to design primers for these 2 loci (**TABLE 2**), along with an indirect labeling strategy. Nineteen nucleotides (CACGACGTTGTAAAACGAC) of the M13 phage (N19M13) with no homology to the human genome were added to the 5′ end of each forward primers. The third primer, universal M13 primer, was the same N19M13 sequence with HEX fluorescent dye-label at the 5′ end. The third primer was the solitary source of fluorescent labeling. This primer can be used with any M13-forward primer to make a labeled PCR product that can be analyzed on any DNA analyzer.

The amplification of 2 mononucleotide markers was carried out in a total volume of 10 μL containing 50 ng extracted DNA of tumor material or normal tissue, 5 μL of 2X PCR master mix, including dNTP, MgCl2, Taq DNA polymerase, and enzyme buffer, 0.2 μL of each reverse and forward primers, 0.3 μL of M13 labeled primer, and 3.3 μL dH2O.

Then, touchdown PCR was performed in a thermal cycler device (Eppendorf AG 22331, BIO-RAD T100) as follows: initial denaturation at 94°C for 5 minutes, followed by 40 cycles at 94°C for 30 seconds; annealing started at 64°C and decreased 1°C per cycle until 57°C. The rest cycles were performed at an annealing temperature of 57°C for 30 seconds, followed by an extension at 72°C for 30 seconds and 1 final extension at 72°C for 5 minutes. Then, PCR products were analyzed via an ABI PRISM 3500 Genetic Analyzer (Applied Biosystems) using the GeneScan 500 LIZ size standard (Thermo Fisher Scientific). We read the peaks using GeneMarker software, version HID V3.00 (SoftGenetics). The 2-marker panel classified tumors as MSI-H if instability is present in 2 markers. Tumors were reclassified as MSS or MSI-L, in the cases of no instability or single-marker instability, respectively.

Results

Statistical Analysis and Epidemiological Findings

We analyzed the sensitivity, specificity and positive predictive values of clinical and molecular parameters with SPSS software, version 25 (IBM). Among 685 registered patients who had CRC between the years 2011 and 2018, a total of 210 patients (30.7%) had a positive family history of cancer, and 63 cases (9.2%) fulfilled Amsterdam II criteria. Finally, 37 patients (5.4%) were included in the study; they were representative of 37 affected families. The following cancers were frequently detected in MSI-H family members: 13 colorectal (35.1%), 4 gastric (10.8%), and 4 prostate (10.8%) cancer.

In the family members of patients with MSS, however, 4 cases of gastric cancer (12.1%), 3 of lung cancer (9.0%), and 7 of breast cancer (21.2%) were detected as the most frequent cancer types. The average age at diagnosis was 39.6 years (range, 29.0-52.0 years) for patients with MSI-H, and 46.6 years (range, 31.0-61.0) for patients with MSS. Moreover, mucinous adenocarcinoma has been reported as the most common histopathologic feature in MSI-H tumors (20.0%); the most frequent features among patients with MSS was well-differentiated adenocarcinoma (40.7%).

MSI Testing

Altogether, according to the Promega Kit results, 10 specimens (27.0%) showed instability in more than 2 microsatellite markers defined as MSI-H (**FIGURE 1**), and 27 specimens (72.9%) showed MSS (**FIGURE 2**). The female-to-male proportion in MSI-H cases was 4/6 (0.7) and in MSS was 15/12 (1.2). All 5 quasimononucleotide markers, as tested by the Promega kit, showed instability in all 10 specimens (**FIGURES 1** and **2**).

In contrast, 10 specimens were detected as MSI-H using BAT34c4 as a stand-alone marker, and the same specimens presented the MSI-H phenotype with BAT26 used as a stand-alone marker (**FIGURES 3** and **4**). These 10 specimens were the same that had been previously detected as being MSI-H via the Promega kit.

Sensitivity and Specificity of BAT34c4 and BAT26 Markers

BAT34c4 and BAT26 were unstable in all 10 patients with MSI-H and showed stability in all 27 patients with MSS CRC. All MSI-H tumors were correctly identified as MSI-H by BAT34c4 and BAT26 markers. Therefore, the sensitivity of these 2 markers was 100%, compared with the Promega results. Also, the specificity of these quasimonomorphic markers was 100%. No MSS tumors were incorrectly identified as MSI-H by the BAT34c4 and BAT26, compared with the Promega system. Positive predictive values (PPVs) for BAT34c4 and BAT26 markers were 100%.

Discussion

MSI is an important prognostic and predictive marker for screening LS and sporadic CRC.[29] National Comprehensive Cancer Network guidelines suggest that MSI should be evaluated across all solid tumors.[30]

Dinucleotide repeats showed lower sensitivity, compared with mononucleotide ones. Further, they showed polymorphism among individuals and were required to be matched with normal tissue, which could be laborious and costly.[31] The results of some studies[32,33] suggest panels with small number of highly sensitive mononucleotide markers with monomorphism features at the population level, to remove the need for normal tissue. This method could provide cost-effective, rapid, and easy performance with simplified interpretation.[19,26,29] BAT26 was suggested to be used by itself, without the need to match for normal tissue for MSI testing.[34,35] In our set of MSI-H tumors, all cases were detected by using BAT26 and BAT34c4 as a single diagnostic MSI

TABLE 2. Sequences of Forward and Reverse Primers Used for MSI Testing in the Novel Testing Kit

Primer Name	Sequence	Length
BAT34c4 F	CACGACGTTGTAAAACGACTGATGATCTGGATCCACCAAG	40
BAT34c4 R	CAACAAAGCGAGACCCAGTC	20
BAT26 F	CACGACGTTGTAAAACGACGCAGTCAGAGCCCTTAACC	38
BAT26 R	CTTCTTCAGTATATGTCAATGAAAACAT	28
M13 Labelled F	CACGACGTTGTAAAACGAC	19

marker and as a dual panel. Moreover, the Bethesda revised guideline (CNI/ICG) offered a 5-marker panel with high sensitivity and specificity.[36] Important criteria for the ideal marker for MSI analysis are 100% mutation frequency in MSI-H tumors, no mutation in MSS tumors, and a quasimonomorphic allele in the total population.[24] Our data demonstrate that BAT26 and BAT34c4 fulfill all of these criteria.

Within the *p53* gene, the expression of which has been associated with tumor suppression and apoptosis, a mononucleotide repeat was detected in 3′-UTR that displays a monomorphic pattern in CRC specimens.[37] We decided to investigate the MSI profile of this marker in a series of patients in an Iranian population who have CRC and whose cases fulfilled the Amsterdam II criteria. The marker was tested by itself and in a dual panel with BAT26.

In comparison with Promega markers, such as BAT25, BAT26, NR21, MONO27, and NR24,[33] in our series, BAT34c4 and BAT26 in a dual panel and each marker by itself seem to possess high sensitivity for detecting the MSI phenotype, with great similarity to the sensitivity previously found for CAT25[22] and MybT22.[38] We did not observe MSI in MSS cases for BAT34c4 and BAT26, so these markers revealed absolute specificity. No MSI-L tumors were found among the patients via the Promega kit, and therefore, we could not evaluate the ability of the in-house-developed dual panel to detect this type of tumor. From a genetic standpoint, BAT34c4 and BAT26 were found to be monoallelic for all cases. To evaluate MSI in cases without normal DNA specimens, this feature would be helpful.

MSI status could be also observed in 15%–20% of sporadic CRC due to *MLH1* gene promoter hypermethylation. According to the findings of 1 study,[6] there is an association between a somatic hot-spot mutation on the *BRAF* proto-oncogene and the sporadic MSI-H CRC phenotype. So, if the V600E *BRAF* variant on the tumor DNA of a patient with MSI-H CRC is found, the disease would be considered the sporadic type. MSI occurs in approximately 15%–20% of sporadic colorectal tumors. Hence, to capture more MSI events in the pilot phase of the study, patients were merely involved based on Amsterdam criteria, as in primary studies. Further investigations using a set of sporadic CRCs will need to introduce this panel for the clinical setting.

Although findings in this study show 100% sensitivity and specificity of BAT34c4 and BAT26 markers, the narrow sample size would affect the results. This is one of the current study limitations. This study is a pilot investigation to evaluate a simplified panel for MSI testing.

According to the findings of various studies,[39] a total of 70%–90% of patients with LS show instability in the microsatellite sequence repeats due to the germline mutations of 1 or more MMR genes. In the current study, only 27% of LS cases, determined according to Amsterdam II criteria, showed MSI-H in molecular investigation, which is much lower than is typical. One important reason for this difference is familial colorectal cancer type X (FCCTX) syndrome. FCCTX is defined as cases that fulfill Amsterdam criteria but show MMR-stable tumors.[40] The results of a previous study[2] demonstrate that the incidence of FCCTX is high in Iran.

Given the cost of fluorescent-labeled primers, M13 tailed primer was used, to economize by reducing the number of fluorescent labels. The use of 3 primers in a PCR run could lead to greater convenience and reduce the costs of genotyping output.[41]

Considering the standard testing procedure recommended by the NCI/ICG-HNPCC, and the fact that data were obtained by our novel panel containing 2 absolutely sensitive and specific mononucleotide BAT34c4 and BAT26 markers, we propose the wider use of this simple method, which has a short turnaround time and limited cost, for detection of MSI. The use of this panel is easy, and simultaneous data analysis allows for a significant reduction in the complexity and costs of MSI testing.

Conclusion

Because the status of MSI as a well-established predictive and prognostic marker is growing worldwide, it seems necessary to develop

FIGURE 1. DNA electropherograms from the Promega MSI Analysis System (GeneMapper software, v.3.7 [SoftGenetics]), indicating the unstable state of tumor tissue DNA (A) compared with normal paired tissue DNA (B).

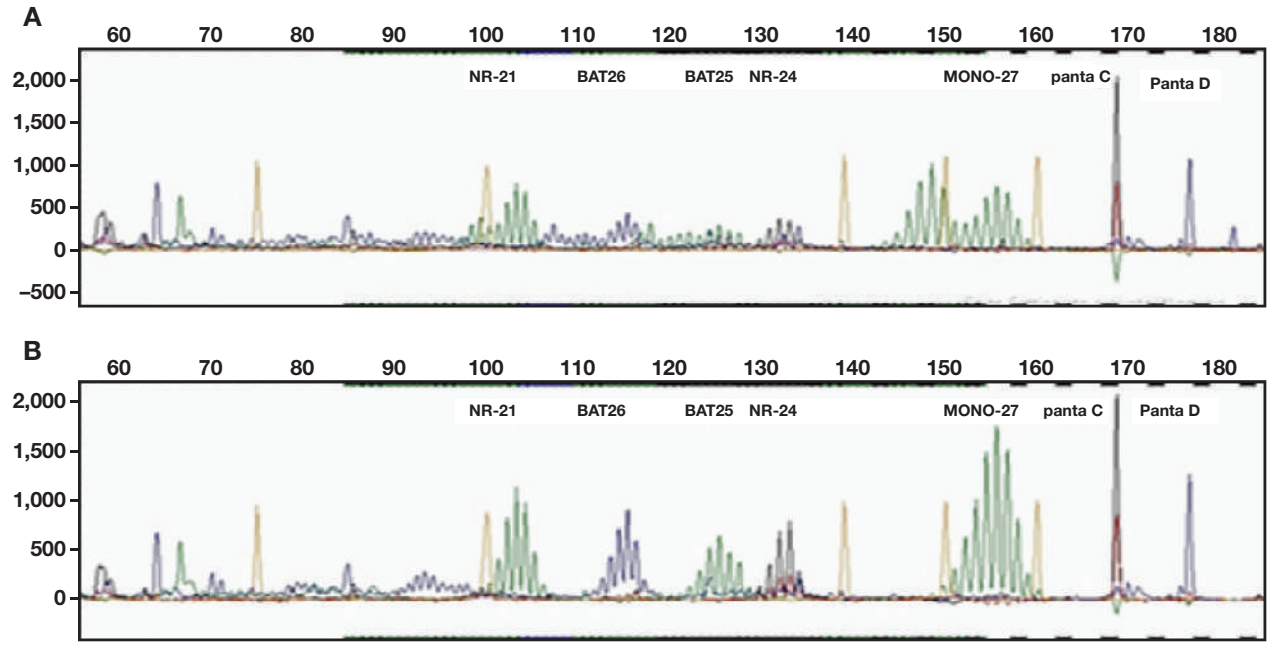

FIGURE 2. DNA electropherograms from the Promega MSI Analysis System (GeneMarker HIDSoftware, v.3.00 [SoftGenetics]), indicating stable status of tumor DNA tissue (A) and normal DNA (B).

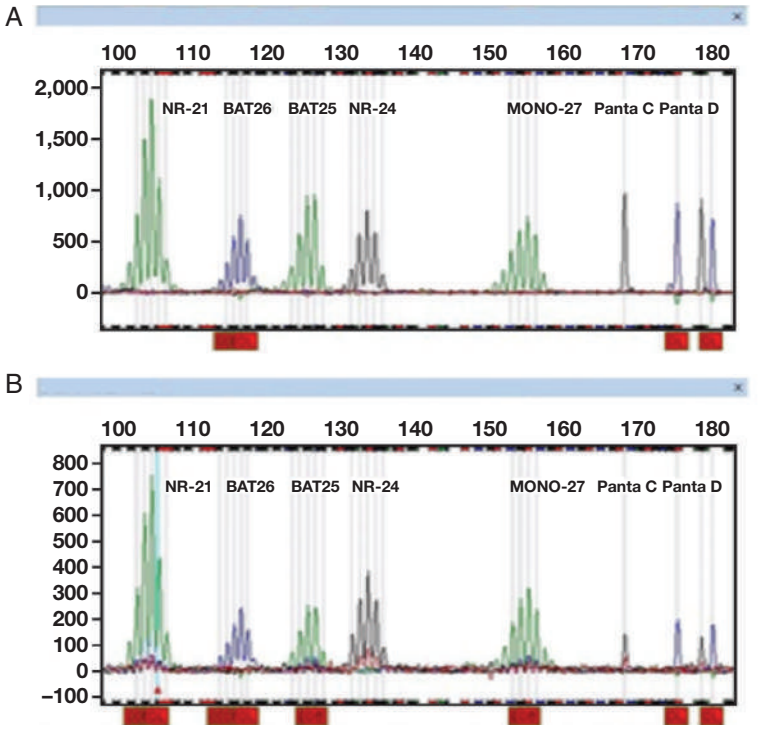

FIGURE 3. DNA electropherograms from the BAT34c4 MSI Analysis System (GeneMapper software, v.3.7 [Thermo Fisher Scientific]), indicating the unstable state of tumor tissue DNA (A), compared with normal paired-tissue DNA (B).

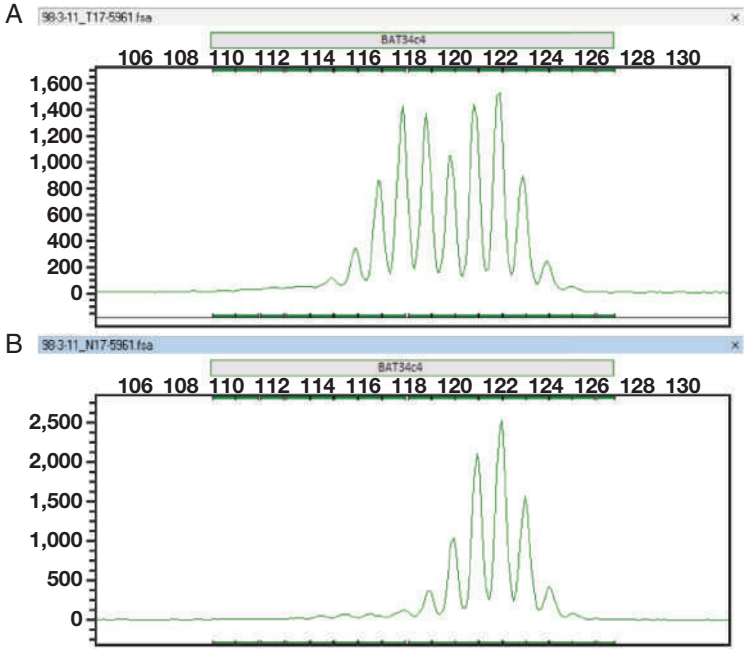

less-expensive, customized kits for MSI testing, while maintaining the diagnostic accuracy of such kits among different populations. This study was an attempt to customize a simplified diagnostic kit for MSI testing of colorectal tumors among Iranian patients. We declare that this novel 2-marker kit could present lower costs due to fewer markers and the use of M13 phage sequencing for labeling the PCR product. Meanwhile, further evaluations using larger sample sizes are suggested to confirm the current results.

FIGURE 4. **DNA electropherograms from thef BAT26 MSI Analysis System (GeneMapper software, v.3.7 [Thermo Fisher Scientific), indicating the unstable state of tumor tissue DNA (A), compared with normal paired-tissue DNA (B).**

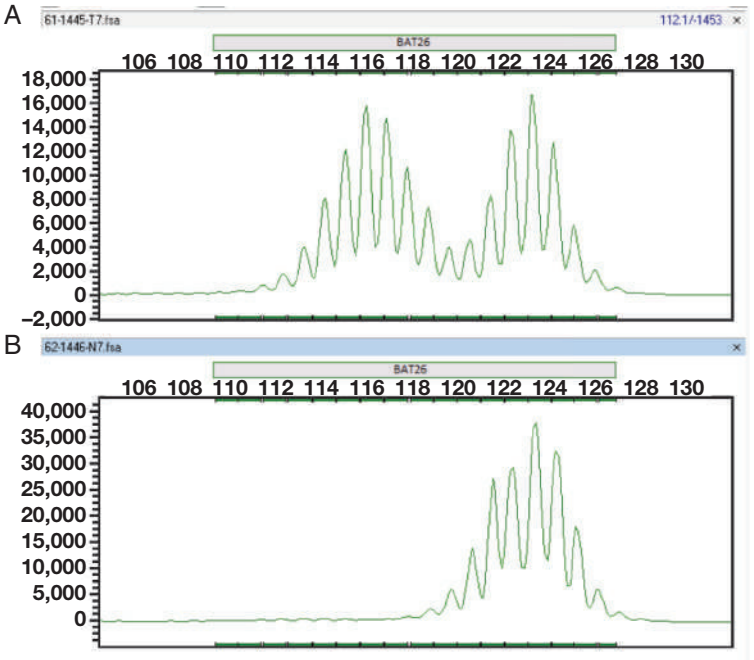

Personal and Professional Conflicts of Interest

None declared.

Acknowledgment

We thank the patients and their families for their valuable contributions. We also thank the healthcare workers of the Ala Cancer Prevention and Control Center (MACSA), Isfahan, Iran. This study was supported by an MSc grant from Isfahan University of Medical Sciences, Iran (grant no. 396958).

REFERENCES

1. Siegel RL, Miller KD, Jemal A. Cancer statistics, 2016. *CA Cancer J Clin.* 2016;66(1):7–30.
2. Zeinalian M, Hashemzadeh-Chaleshtori M, Akbarpour MJ, Emami MH. Epidemioclinical feature of early-onset colorectal cancer at-risk for Lynch syndrome in central Iran. *Asian Pac J Cancer Prev.* 2015;16(11):4647–4652.
3. Giardiello FM, Allen JI, Axilbund JE, et al. Guidelines on genetic evaluation and management of Lynch syndrome: a consensus statement by the US Multi-Society Task Force on Colorectal Cancer. *Am J Gastroenterol.* 2014;109(8):1159–1179.
4. Goodenberger M, Lindor NM. Lynch syndrome and MYH-associated polyposis: review and testing strategy. *J Clin Gastroenterol.* 2011;45(6):488–500.
5. Markowitz SD, Bertagnolli MM. Molecular origins of cancer: molecular basis of colorectal cancer. *N Engl J Med.* 2009;361(25):2449–2460.
6. Cox VL, Saeed Bamashmos AA, Foo WC, et al. Lynch syndrome: genomics update and imaging review. *Radiographics.* 2018;38(2):483–499.
7. Lynch HT, Snyder CL, Shaw TG, Heinen CD, Hitchins MP. Milestones of Lynch syndrome: 1895-2015. *Nat Rev Cancer.* 2015;15(3):181–194.
8. Boland CR, Goel A. Microsatellite instability in colorectal cancer. *Gastroenterology.* 2010;138(6):2073–2087.e3.
9. Pérez-Carbonell L, Ruiz-Ponte C, Guarinos C, et al. Comparison between universal molecular screening for Lynch syndrome and revised Bethesda guidelines in a large population-based cohort of patients with colorectal cancer. *Gut.* 2012;61(6):865–872.
10. Pasche B, Pennison MJ, DeYoung B. Lynch syndrome testing: a missed opportunity in the era of precision medicine. *JAMA.* 2016;316(1):38–39.
11. Desselle F, Verset G, Polus M, Louis E, Van Daele D. Lynch syndrome and microsatellite instability: a review. *Rev Med Liege.* 2012;67(12):638–643.
12. Lee KS, Kwak Y, Ahn S, et al. Prognostic implication of CD274 (PD-L1) protein expression in tumor-infiltrating immune cells for microsatellite unstable and stable colorectal cancer. *Cancer Immunol Immunother.* 2017;66(7):927–939.
13. Tikidzhieva A, Benner A, Michel S, et al. Microsatellite instability and beta2-microglobulin mutations as prognostic markers in colon cancer: results of the FOGT-4 trial. *Br J Cancer.* 2012;106(6):1239–1245.
14. Gan C, Love C, Beshay V, et al. Applicability of next generation sequencing technology in microsatellite instability testing. *Genes.* 2015;6(1):46–59.
15. Boland CR, Thibodeau SN, Hamilton SR, et al. A National Cancer Institute workshop on microsatellite instability for cancer detection and familial predisposition: development of international criteria for the determination of microsatellite instability in colorectal cancer. *Cancer Res.* 1998;58(22):5248–5257.
16. Pagin A, Zerimech F, Leclerc J, et al. Evaluation of a new panel of six mononucleotide repeat markers for the detection of DNA mismatch repair-deficient tumours. *Br J Cancer.* 2013;108(10):2079–2087.
17. Bacher JW, Flanagan LA, Smalley RL, et al. Development of a fluorescent multiplex assay for detection of MSI-high tumors. *Dis Markers.* 2004;20(4-5):237–250.
18. Farahani N, Nikpour P, Emami MH, Zeinalian M, Shariatpanahi SS. Evaluation of MT1XT20 single quasi-monomorphic mononucleotide marker for characterizing microsatellite instability in Persian lynch syndrome patients. *Asian Pac J Cancer Prev.* 2016;17(9):4259–4265.

19. Buhard O, Cattaneo F, Wong YF, et al. Multipopulation analysis of polymorphisms in five mononucleotide repeats used to determine the microsatellite instability status of human tumors. *J Clin Oncol.* 2006;24(2):241–251.
20. Deschoolmeester V, Baay M, Wuyts W, et al. Detection of microsatellite instability in colorectal cancer using an alternative multiplex assay of quasi-monomorphic mononucleotide markers. *J Mol Diagn.* 2008;10(2):154–159.
21. Xicola RM, Llor X, Pons E, et al; Gastrointestinal Oncology Group of the Spanish Gastroenterological Association. Performance of different microsatellite marker panels for detection of mismatch repair-deficient colorectal tumors. *J Natl Cancer Inst.* 2007;99(3):244–252.
22. Findeisen P, Kloor M, Merx S, et al. T_{25} repeat in the 3′ untranslated region of the *CASP2* gene: a sensitive and specific marker for microsatellite instability in colorectal cancer. *Cancer Res.* 2005;65(18):8072–8078.
23. Bianchi F, Galizia E, Catalani R, et al. CAT25 is a mononucleotide marker to identify HNPCC patients. *J Mol Diagn.* 2009;11(3):248–252.
24. Morandi L, de Biase D, Visani M, et al. T([20]) repeat in the 3′-untranslated region of the MT1X gene: a marker with high sensitivity and specificity to detect microsatellite instability in colorectal cancer. *Int J Colorectal Dis.* 2011;27(5):647–656.
25. Performance of different microsatellite marker panels for detection of mismatch repair–deficient colorectal tumors. *J Natl Cancer Inst.* 2007;99(3):244–252.
26. Esemuede I, Forslund A, Khan SA, et al. Improved testing for microsatellite instability in colorectal cancer using a simplified 3-marker assay. *Ann Surg Oncol.* 2010;17(12):3370–3378.
27. Liu Z, Wang Z, Li Y, et al. Association of genomic instability, and the methylation status of imprinted genes and mismatch-repair genes, with neural tube defects. *Eur J Hum Genet.* 2012;20(5):516–520.
28. Tabanifar B, Salehi R, Asgarani E, Faghihi M, Heidarpur M, Allame TS. An efficient method for DNA extraction from paraffin wax embedded tissues for PCR amplification of human and viral DNA. *Iran J Pathol.* 2008;3:173–178.
29. Berardinelli GN, Scapulatempo-Neto C, Durães R, Antônio de Oliveira M, Guimarães D, Reis RM. Advantage of HSP110 (T17) marker inclusion for microsatellite instability (MSI) detection in colorectal cancer patients. *Oncotarget.* 2018;9(47):28691–28701.
30. Benson AB 3rd, Venook AP, Cederquist L, et al. Colon Cancer, version 1.2017, NCCN Clinical Practice Guidelines in Oncology. *J Natl Compr Canc Netw.* 2017;15(3):370–398.
31. Goel A, Nagasaka T, Hamelin R, Boland CR. An optimized pentaplex PCR for detecting DNA mismatch repair-deficient colorectal cancers. *PLoS One.* 2010;5(2):e9393.
32. Hause RJ, Pritchard CC, Shendure J, Salipante SJ. Classification and characterization of microsatellite instability across 18 cancer types. *Nat Med.* 2016;22(11):1342–1350.
33. Murphy KM, Zhang S, Geiger T, et al. Comparison of the microsatellite instability analysis system and the Bethesda panel for the determination of microsatellite instability in colorectal cancers. *J Mol Diagn.* 2006;8(3):305–311.
34. Hoang JM, Cottu PH, Thuille B, Salmon RJ, Thomas G, Hamelin R. BAT-26, an indicator of the replication error phenotype in colorectal cancers and cell lines. *Cancer Res.* 1997;57(2):300–303.
35. Zhou X-P, Hoang J-M, Li Y-J, et al. Determination of the replication error phenotype in human tumors without the requirement for matching normal DNA by analysis of mononucleotide repeat microsatellites. *Genes Chromosomes Cancer.* 1998;21(2):101–107.
36. Umar A, Boland CR, Terdiman JP, et al. Revised Bethesda Guidelines for hereditary nonpolyposis colorectal cancer (Lynch syndrome) and microsatellite instability. *J Natl Cancer Inst.* 2004;96(4):261–268.
37. Cicek MS, Lindor NM, Gallinger S, et al. Quality assessment and correlation of microsatellite instability and immunohistochemical markers among population- and clinic-based colorectal tumors results from the Colon Cancer Family Registry. *J Mol Diagn.* 2011;13(3):271–281.
38. Mead LJ, Jenkins MA, Young J, et al. Microsatellite instability markers for identifying early-onset colorectal cancers caused by germ-line mutations in DNA mismatch repair genes. *Clin Cancer Res.* 2007;13(10):2865–2869.
39. Vatandoost N, Ghanbari J, Mojaver M, et al. Early detection of colorectal cancer: from conventional methods to novel biomarkers. *J Cancer Res Clin Oncol.* 2016;142(2):341–351.
40. Dominguez-Valentin M, Therkildsen C, Da Silva S, Nilbert M. Familial colorectal cancer type X: genetic profiles and phenotypic features. *Mod Pathol.* 2015;28(1):30–36.
41. Venkatesan M, Hauer MC, Rasgon JL. Using fluorescently-labeled M13-tailed primers to isolate 45 novel microsatellite loci from the arboviral vector *Culex tarsalis*. *Med Vet Entomol*. 2007;21(2):204–208.

Variations in Nomenclature of Clinical Variants between Annotation Tools

Kyoung-Jin Park, MD, PhD,[1*] *Jong-Ho Park, PhD*[2]

[1]Department of Laboratory Medicine & Genetics, Samsung Changwon Hospital, Sungkyunkwan University School of Medicine, Changwon, South Korea; [2]Department of Laboratory Medicine & Genetics, Samsung Medical Center, Seoul, South Korea; *To whom correspondence should be addressed: unmar21@gmail.com

Keywords: Human Gene Mutation Database (HGMD), ANNOVAR, snpEff, nomenclature, variant, annotation

Abbreviations: HGVS, Human Genome Variation Society; EQA, external quality assessment; VEP, Variant Effect Predictor; VR, Variation Reporter; HGMD, Human Gene Mutation Database; VCF, variant call format; cDNA, complementary DNA; Chr, chromosome.

Laboratory Medicine 2022;53:242–245; https://doi.org/10.1093/labmed/lmab074

ABSTRACT

Background: Accurate nomenclature of variants is an essential element for genetic diagnosis and patient care.

Objective: To investigate annotation differences of clinical variants between annotation tools.

Methods: We analyzed 218,156 clinical variants from the Human Gene Mutation Database. Multiple nomenclatures based on RefSeq transcripts were provided using ANNOVAR and snpEff.

Results: The concordance rate between ANNOVAR and snpEff was approximately 85%. Based on the Human Genome Variation Society (HGVS) nomenclature, snpEff was more accurate than ANNOVAR (coding variants, 99.3% vs 84.9%; protein variants, 94.3% vs 79.8%). When annotating each variant with ANNOVAR and snpEff, the accuracy of nomenclature was 99.5%.

Conclusions: There were substantial differences between ANNOVAR and snpEff annotations. The findings of this study suggest that simultaneous use of multiple annotation tools could decrease nomenclature errors and contribute to providing standardized clinical reporting.

Accurate nomenclature of variants is an essential element for genetic diagnosis and patient care. Incorrect nomenclature can cause pathogenic variants to be missed or benign variants to be selected, and may lead to misinterpretation. Hence, the use of standardized nomenclature is important in clinical reports and in data sharing. To address this issue, standardized nomenclature system was proposed by the Human Genome Variation Society (HGVS) in 1998 and updated in 2016.[1,2] Further, many external quality assessment (EQA) providers have promoted the use of the HGVS nomenclature and evaluated variant nomenclature errors among clinical laboratories.[3] Recently, major journals[4,5] also require the authors to verify HGVS nomenclature of variants in their manuscripts before submission.

There are many annotation tools that generate HGVS nomenclature, as commercial or open-source software: Alamut, ANNOVAR, Variant Effect Predictor (VEP), snpEff, Variation Reporter (VR), and conversion tools such as Mutalyzer and VariantValidator.[6–10] However, the accuracy of the HGVS-generation tools on variant call format (VCF) is far from complete.[11,12] Discordant variant nomenclature among annotation tools is one of the well-documented limitations. The findings of a previous study[11] demonstrate that concordance of nomenclature between ANNOVAR and VEP was 65% for loss-of-function variants. Another study report[12] states that there was significant discordance among annotation tools such as snpEff, VEP, and VR. In addition to annotation tools, concordance of nomenclature-generation tools depends on choice of transcript sets (Ensemble vs RefSeq) and variant type (SNV vs indels).[11,12]

Currently, there are no standardized transcripts for clinical reporting. Therefore, individual laboratories select the longest transcript rather than the most biologically relevant transcript, or depend on reference transcripts reported from a database such as the HGMD or from Alamut software. However, recent study findings[13–15] have demonstrated that simultaneous interrogation of several alternative transcripts could improve discovery of disease-relevant variants and alter variant reporting in a wide range of undiagnosed inherited disorders.

The reports from previous studies that compare annotation tools have selected only 1 transcript and 1 nomenclature with the most severe consequence, not considering multiple alternative transcripts for each variant. In this study, multiple annotations were performed with the multiple alternative transcripts within RefSeq.

The aim of this study was to investigate the differences in annotations of the HGMD variants between ANNOVAR and snpEff, which are the most commonly used free tools in the clinical setting.[6,7,16]

Further, the accuracy of the annotation tools was evaluated based on the standardized HGVS nomenclature.

Materials and Methods

We studied clinical variants (n = 229,161) registered in the HGMD (professional version 2019.01). The HGVS nomenclature and VCF (hgmd_pro_2019.1_hg19.vcf) were obtained from the licensed HGMD Professional download version. Among a total of 229,161 HGMD variants, no variants or incompletely annotated variants (n = 4214) were excluded. HGVS-compliant descriptions of the HGMD variants (n = 224,947) were validated using the VariantValidator (Version 0.5; June 4, 2020: http://variantvalidator.org) and Mutalyzer (version 2.0.34; June 4, 2021: https://mutalyzer.nl/batch-jobs?job_type=name-checker).[9,10] The predicted consequences described in parentheses were not assessed in this study; for example, p.(Arg727Ser) was considered to be p.Arg727Ser. Regulatory or noncoding variants (n = 6791) were also excluded. Variant types were categorized into substitution, deletion, duplication, insertion, and deletion-insertion, according to the HGVS nomenclature.

We ran ANNOVAR (version 2019 Oct 24) and snpEff (v4_3_GRCh37.p13.RefSeq) on the HGMD variants (n = 218,156) with RefSeq transcript set using the default command line. To select all exonic and intronic variants of 5 bp around each exon, the following options were used; -arg "--hgvs --exonicsplicing --splicing 5" for ANNOVAR and -spliceSiteSize 5 for snpEff. Multiple nomenclatures from several alternative transcripts for each variant were annotated. For example, HGMD CS941514 (rs1057518904) variants could be annotated as splicing variant (NM_000267.3:c.1721+3A>G) and nonsynonymous variant (NM_001128147.2: c.1724A>G [p.Tyr575Cys]), according to the choice of alternative transcripts.

If one of multiple nomenclatures for each variant would be in ANNOVAR or snpEff annotations, the variant was considered to be concordant. In this study, we did not consider the differences between 1-letter code and 3-letter code because ANNOVAR describes the 1-letter code, whereas snpEff uses the 3-letter code for all protein variants. The accuracy of the annotation tools was assessed based on the standardized HGVS nomenclature. If one nomenclature from ANNOVAR or snpEff was correct, the nomenclature derived by the combined use of the tools was considered to be correct.

Results

The concordance rates between ANNOVAR and snpEff at the level of complementary DNA (cDNA) and the protein were 85.2% and 85.6%, respectively (**TABLE 1**). Discordant coding variant nomenclature was more identified in deletion-insertion (100%), deletion (63.1%), or duplication (51.9%) than insertion (16.2%) or substitution variants (0.2%) (**FIGURE 1A**). Similarly, discordance at the protein level was also higher in deletion-insertion (58.5%), duplication (66.4%), or insertion (52.3%) variants than substitution variants (1.3%) (**FIGURE 1B**). The examples of discordant variants between ANNOVAR and snpEff according to variant type was shown in **TABLE 2**.

The discordance at the level of cDNA was attributed to the following factors: alternative expression of deletion (50.6%), difference in nucleotide numbering (25.5%), duplications described as insertion with/without nucleotide numbering (12.0%), incomplete annotation (10.5%), longer expression of deletion-insertion (1.2%), use of alternative transcripts (0.2%) (**TABLE 2**). The reasons for discordance of protein variants were the difference in amino-acid numbering (72.8%), no description of amino acids with/without different amino-acid numbering (13.4%), use of X in the translation termination codon (7.3%), wrong expression of indels (3.3%), and translation initiation codon not to be predicted (3.2%) (**TABLE 3**).

Based on the standardized HGVS nomenclature, snpEff was more accurate than ANNOVAR: 99.3% vs 84.9% at the cDNA level and 94.3% vs 79.8% at the protein level (**TABLE 1**). When annotating for each variant by the combined use of ANNOVAR and snpEff, the accuracy of the variant nomenclature was 99.5% at the cDNA level and also at the protein level) (**TABLE 1**).

Discussion

The current study showed that concordance of ANNOVAR and snpEff annotations for HGMD variants was approximately 85% (**TABLE 1**). The concordance of the annotation tools (ANNOVAR vs snpEff) was more significantly improved than previously reported, despite that comparisons with exact software tools (VEP vs ANNOVAR or VEP vs snpEff) and transcript sets (Ensembl vs RefSeq) were not performed.[11,12] This finding might be attributed to continual update of databases and software, as well as choices of multiple alternative transcripts. Similar to the findings of previous studies, discordant nomenclature was more identified in indels than substitutions in this study (**FIGURE 1**).[12] Generation of accurate nomenclature on VCF is still challenging, especially in indels, because VCF has been left-aligned, which contradicts the 3′ rule of HGVS.[1,2]

Our study findings showed that differences in nucleotide/amino-acid description and/or numbering were most common cause of discordance between the tools (**TABLE 3**). That means that the main reason

TABLE 1. Concordance between ANNOVAR and snpEff

Variable	ANNOVAR vs snpEff	ANNOVAR vs HGVS	snpEff vs HGVS	ANNOVAR and/or snpEff vs HGVS
Coding Level				
Concordance	185,940 (85.2%)	185,305 (84.9%)	216,681 (99.3%)	217,068 (99.5%)
Discordance	32,216 (14.8%)	32,851 (15.1%)	1475 (0.7%)	1088 (0.5%)
Total	218,156 (100.0%)	218,156 (100.0%)	218,156 (100.0%)	218,156 (100.0%)
Protein Level				
Concordance	168,972 (85.6%)	144,164 (79.8%)	138,351 (94.3%)	145,982 (99.5%)
Discordance	28,428 (14.4%)	36,548 (20.2%)	8411 (5.7%)	723 (0.5%)
Total[a]	197,400 (100.0%)	180,712 (100.0%)	146,762 (100.0%)	146,705 (100.0%)

Abbreviation: *HGVS, Human Genome Variation Society.*
[a]*The number of annotations for protein variant was different according to the tool used.*

FIGURE 1. Concordance between ANNOVAR and snpEff across variant types at the complementary DNA (cDNA) level (A) and at the protein level (B).

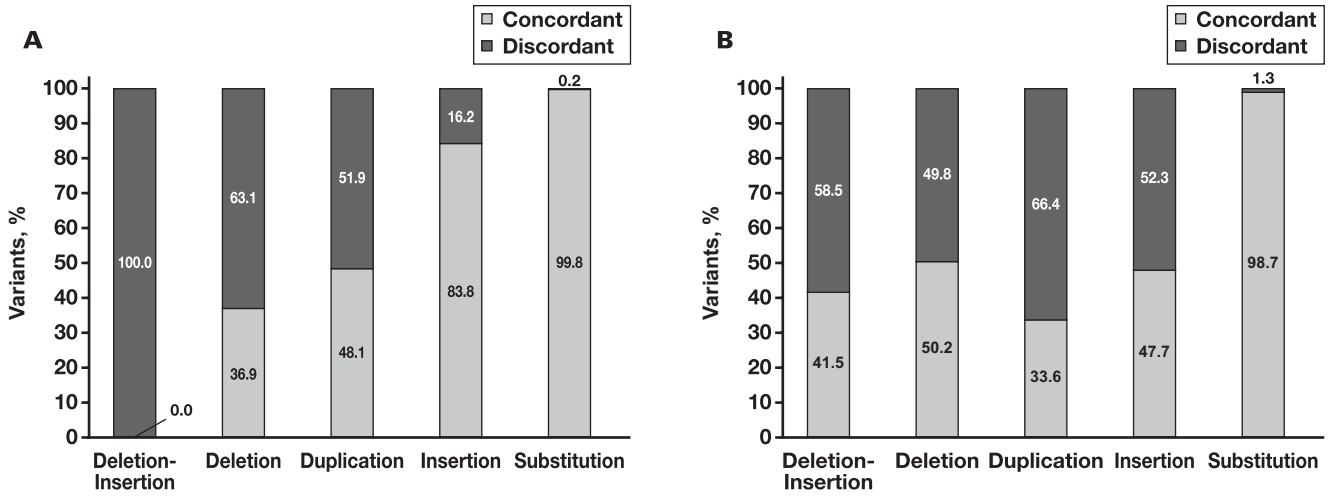

TABLE 2. Examples of Discordant Variants between ANNOVAR and snpEff According to Variant Type

Type	Chr	Start	End	Ref	Alt	HGVS Nomenclature	ANNOVAR	snpEff
Deletion-insertion	1	21894598	21894598	T	CTAA	NM_000478.5:c.650delTinsCTAA (p.Val217delinsAlaLys)	NM_000478.5:c.650delinsCTAA[a]	NM_000478.4:c.650delTinsCTAA (p.Val217delinsAlaLys)
Deletion	1	1168240	1168240	G	…	NM_080605.3:c.588delG (p.Arg197Alafs81)	NM_080605.3:c.582delG (p.P194fs)	NM_080605.3:c.588delG (p.Arg197fs)
Duplication	1	12030831	12030831	…	GC	NM_000302.3:c.1863_1864dupGC (p.Pro622Argfs3)	NM_000302.3:c.1860_1861insGC (p.I620fs)	NM_000302.3:c.1863_1864dupGC (p.Pro622fs)
Insertion	1	12294395	12294395	…	CG	NM_015378.3:c.73_74insGC (p.Gln25Argfs14)	NM_015378.3:c.72_73insCG (p.D24fs)	NM_015378.2:c.73_74insGC (p.Gln25fs)
Substitution	1	17720537	17720537	C	T	NM_207421.4:c.1141C>T (p.Gln381)	NM_207421.4:c.1141C>T (p.Q381X)	NM_207421.3:c.1142C>T (p.Ser381Leu)

Abbreviations: *Chr, chromosome; HGVS, Human Genome Variation Society; … , nonapplicable.*
[a]*A corresponding protein variant was not produced from ANNOVAR.*

TABLE 3. Causes and Examples of Discordant Variants between ANNOVAR and snpEff[a]

Variable	Cause	No. (%)	Transcript	ANNOVAR	snpEff
Coding level	Alternative expression of deletion (no description of nucleotide)	16,292/32,216 (50.6%)	NM_198317.2	**c.1375_1376del**	**c.1375_1376delCT**
	Difference in nucleotide numbering	8227/32,216 (25.5%)	NM_005101.3	c.337dupG	**c.339dupG**
	Duplications described as insertion with/without nucleotide numbering	3871/32,216 (12.0%)	NM_000527.4	c.313_314insG	**c.313+1dupG**
	Incomplete annotation	3388/32,216 (10.5%)	NM_000302.3	c.975+1->TT	**c.975+2_975+3insTT**
	Longer expression of deletion-insertion	382/32,216 (1.2%)	NM_015102.4	**c.1839delinsGA**	c.1839delTinsGA
	Use of alternative transcripts	57/32,216 (0.2%)	NM_194456.1, NM_001350671.1	**NM_001350671.1:c.15+3C>G**	**NM_194456.1:c.601C>G**
Protein level	Difference in amino acid numbering	20,699/28,428 (72.8%)	NP_940978.2	p.L786fs	**p.Ala787fs**
	No description of amino acid with/without different amino acid numbering	3818/28,428 (13.4%)	NP_542172.2	p.136_139del	**p.Met139_Ala141del**
	Use of X in the translation termination codon	2065/28,428 (7.3%)	NP_001121897.1	p.E480X	**p.Glu480***
	Wrong expression of indels	927/28,428 (3.3%)	NP_000365.3	p.E315fs	**p.Glu316del**
	Translation initiation codon not to be predicted	919/28,428 (3.2%)	NP_542172.2	p.Met1Val	**p.Met1?**

[a]*Bolding indicates accurate description.*

of discordance between tools was incorrect nomenclature. Considering that variant nomenclature could influence downstream interpretation, genetic diagnosis, treatment decisions, and genetic counselling, accurate annotation is important in clinical genetics. Therefore, variant annotations should be verified using another software tool before clinical reporting. Recognition of discordant variants between annotation tools could be a red flag warning that arises from investigating incorrect nomenclature. In this study, the accuracy of coding variants and protein variants was 99.5%, with simultaneous use of 2 annotation tools (**TABLE 1**). Combined use of multiple annotation tools could decrease nomenclature errors of clinical variants.

The current HGVS guideline recommends the use of "Ter" or "*" instead of "X" at the translation termination codon.[2] Also, HGVS recommends the use of duplication rather than insertion when a variant could, technically, be described as a duplication or an insertion.[2] The current study findings showed that duplication described as insertion was identified in 12.0% of discordance of coding variants, and use of an "X" in the translation termination codons made up 7.3% of discordance of protein variants (**TABLE 3**). Generally, the snpEff was more accurate than ANNOVAR. However, in case of deletion-insertion, ANNOVAR was more accurate than snpEff. For example, NM_015102.4:c.1839delinsGA from ANNOVAR and NM_015102.4:c.1839delTinsGA from snpEff are technically the same (**TABLE 3**). However, the HGVS recommends the former delins format rather than the latter because the description of deleted nucleotides increases the chance of error.

This study revealed that the discordance between the tools due to the use of alternative transcripts was 0.2%. The use of alternative transcripts is recently receiving increased attention.[13–15] In previous studies, only 1 transcript was selected, although there are several alternative transcripts for each variant.[11] Single annotation with canonical transcript may lead to discordance of annotations between tools. More importantly, the possibility of missed causative variants and misdiagnosis may be elevated with no consideration of multiple alternative transcripts. In the current study, because we did not investigate the confidence interval of annotation using relevant alternative transcripts, we could not demonstrate biological impacts of multiple annotation using alternative transcripts.

The data regarding the variant nomenclature from this study are the key element for accurate variant interpretation. We recommend further studies to determine whether multiple class variants from alternative transcripts can be associated with interpretations of HGMD variants.

Conclusions

This study demonstrated that there were substantial differences between ANNOVAR and snpEff. The accuracy of the annotation tools was more significantly improved than previously reported. The findings of this study suggest that simultaneous use of multiple annotation tools could decrease nomenclature errors of clinical variants and contribute to providing of standardized clinical reporting.

Personal and Professional Conflicts of Interest

None disclosed.

REFERENCES

1. Antonarakis SE. Recommendations for a nomenclature system for human gene mutations. Nomenclature Working Group. *Hum Mutat.* 1998;11(1):1–3.
2. den Dunnen JT, Dalgleish R, Maglott DR, et al. HGVS recommendations for the description of sequence variants: 2016 update. *Hum Mutat.* 2016;37(6):564–569.
3. Tack V, Deans ZC, Wolstenholme N, Patton S, Dequeker EM. What's in a name? A coordinated approach toward the correct use of a uniform nomenclature to improve patient reports and databases. *Hum Mutat.* 2016;37(6):570–575.
4. Higgins J, Dalgleish R, den Dunnen JT, et al. Verifying nomenclature of DNA variants in submitted manuscripts: guidance for journals. *Hum Mutat.* 2021;42(1):3–7.
5. Vasiliou V, Veselkov K, Bruford E, Reichardt JKV. Standardized nomenclature and open science in human genomics. *Hum Genomics.* 2021;15(1):13.
6. Wang K, Li M, Hakonarson H. ANNOVAR: functional annotation of genetic variants from high-throughput sequencing data. *Nucleic Acids Res.* 2010;38(16):e164.
7. Cingolani P, Platts A, Wang LL, et al. A program for annotating and predicting the effects of single nucleotide polymorphisms, SnpEff: SNPs in the genome of *Drosophila melanogaster* strain w^{1118}; iso-2; iso-3. *Fly (Austin).* 2012;6(2):80–92.
8. McLaren W, Gil L, Hunt SE, et al. The ensembl variant effect predictor. *Genome Biol.* 2016;17(1):122.
9. Freeman PJ, Hart RK, Gretton LJ, Brookes AJ, Dalgleish R. VariantValidator: accurate validation, mapping, and formatting of sequence variation descriptions. *Hum Mutat.* 2018;39(1):61–68.
10. den Dunnen JT. Sequence variant descriptions: HGVS nomenclature and mutalyzer. *Curr Protoc Hum Genet.* 2016;90:7.13.1–7.13.19.
11. McCarthy DJ, Humburg P, Kanapin A, et al. Choice of transcripts and software has a large effect on variant annotation. *Genome Med.* 2014;6(3):26.
12. Yen JL, Garcia S, Montana A, et al. A variant by any name: quantifying annotation discordance across tools and clinical databases. *Genome Med.* 2017;9(1):7.
13. DiStefano MT, Hemphill SE, Cushman BJ, et al. Curating clinically relevant transcripts for the interpretation of sequence variants. *J Mol Diagn.* 2018;20(6):789–801.
14. Bodian DL, Kothiyal P, Hauser NS. Pitfalls of clinical exome and gene panel testing: alternative transcripts. *Genet Med.* 2019;21(5):1240–1245.
15. Schoch K, Tan QK-G, Stong N, et al; Undiagnosed Diseases Network. Alternative transcripts in variant interpretation: the potential for missed diagnoses and misdiagnoses. *Genet Med.* 2020;22(7):1269–1275.
16. Choi KT. Current status of bioinformatics pipeline [article in Korean]. *Korean Soc Genet Diagn.* Accessed September 14, 2021. https://ksgd.org/index.php?hCode=REF_VIEW&cl_Type=W&cl_Idx=35

A UFLC-MS/MS Method for the Simultaneous Analysis of Urinary Podocin and Podocalyxin in Patients with Nephrotic Syndrome

Bilge Karatoy Erdem, PhD,[1] Mualla Özcan, PhD,[2] Vural Taner Yılmaz, MD,[3] Bahar Akkaya, MD,[2] Ramazan Çetinkaya, MD,[3] Fevzi Ersoy, MD,[3] Gültekin Süleymanlar, MD,[3] Halide Akbas, MD[1,]*

[1]Akdeniz University Faculty of Medicine Department of Clinical Biochemistry, Antalya, Turkey; [2]Akdeniz University Faculty of Medicine Department of Pathology, Antalya, Turkey; [3]Akdeniz University Faculty of Medicine Department of Nephrology, Antalya, Turkey; *To whom correspondence should be addressed. halideakbas@akdeniz.edu.tr

Keywords: nephrotic syndrome, podocyte damage, podocin, podocalyxin, UFLC-MS/MS, tryptic peptide analysis

Abbreviations: NS, nephrotic syndrome; LC-MS/MS, liquid chromatography with tandem mass spectrometry; UFLC-MS/MS, ultrafast liquid chromatography with tandem mass spectrometry; MRM, multiple reaction monitoring; ELISA, enzyme-linked immunosorbent assay; CRP, C-reactive protein; PBS, phosphate-buffered saline; DAPI, 4-6-diamidino-2-phenylindole; SEM, standard error of the mean; LOD, limit of detection; LOQ, limit of quantitation; CV, coefficient of variation.

Laboratory Medicine 2022;53:246–254; https://doi.org/10.1093/labmed/lmab089

ABSTRACT

Objective: To create an efficient and robust mass spectrometric method for the simultaneous quantitation of podocin and podocalyxin in urine samples and to evaluate urinary podocin and podocalyxin levels in patients with nephrotic syndrome (NS).

Methods: A mass spectrometric method was generated for the measurement of tryptic peptides in urine sediment. Separation of peptides was achieved via liquid chromatography, and mass spectrometric analyses were conducted by electrospray ionization triple-quadrupole mass spectrometry in the multiple reaction monitoring mode.

Results: Intra- and interassay precision values were below 12% and accuracies ranged from 87% to 111% for both of peptides. The validated method was successfully applied to detect these peptides in patients with NS. Urine podocin and podocalyxin levels were significantly higher in patients with NS compared to healthy controls.

Conclusions: This proposed mass spectrometric method provides technological evidence that will benefit the clinical field in the early diagnosis and follow-up of NS.

Nephrotic syndrome (NS) is a syndrome characterized by diffuse edema, proteinuria, hypoalbuminemia, and hyperlipidemia.[1] Diagnostic criteria for NS are (1) proteinuria >3 to 3.5 g/24 hours or a spot urine protein/creatinine ratio >300 to 350 mg/mmol, (2) serum albumin <25 g/L, (3) clinical evidence of peripheral edema, or (4) severe hyperlipidemia.[2] In addition, NS, which may occur at any age, can be classified as primary or secondary.

Despite positive improvements in nephrology, many of the proteinuric kidney diseases result in end-stage renal failure. Structures constituting the glomerular filtration barrier have important contributions in proteinuria resulting from systemic and renal diseases.[3] Glomerular endothelial cells, the glomerular basement membrane, podocytes, and the slit diaphragm between podocytes are in the glomerular filtration barrier.[4] In diseases such as NS, in which glomerular barrier functions are impaired, significant macromolecules pass through the urine.[5] In NS, there is also disruption of endothelial cell integrity, loss of fenestrations, diffuse or focal thickening of the glomerular basement membrane, and deletion and shrinkage of the podocyte foot process. Podocytes are cells that cover the outer surface of the glomerular capillaries and exhibit a highly specialized appearance with the foot process. In most glomerulopathy, the lesion is in glomerular epithelial cells, ie, podocytes.[6,7]

Renal biopsy is important in the diagnosis and classification of glomerular diseases, but it has limitations such as the difficulty in sampling and the need for re-biopsy for the evaluation of treatment efficacy.[8] Performing proteomic measurements showing podocyte damage in noninvasive urine specimens may provide an early diagnosis of glomerular disease by implementing information on the type or activity of the disease. Total proteinuria and albuminuria are widely used in the diagnosis and monitoring of glomerular diseases. However, they are not very specific for glomerular damage. Because the main lesion is in podocytes in many glomerulopathies, the development of measurements related to podocyturia is important in the diagnosis and follow-up. Drugs used in the treatment of NS have limited effect on general podocyte injury and

the repair of glomerular damage. For this reason, it is very important to expand the large-scale research on podocytes and to develop direct treatments specific to podocyte components in light of these studies in the future.[9-11]

Liquid chromatography and tandem mass spectrometry (LC-MS/MS) technology is a highly advantageous method offering good sensitivity and high specificity for analysis with a lower specimen volume. It is suitable for protein/peptide analysis and protein quantification simultaneously. The MS method is based on the analysis of ions obtained from the fragmentation products of targeted proteins. In the preliminary stage of protein analysis, peptide bonds are usually hydrolyzed using trypsin.[12]

The main goal of this study was to create an efficient and robust ultrafast LC-MS/MS (UFLC-MS/MS) method for the simultaneous quantitation of podocalyxin and podocin in urine specimens and to evaluate urine podocin and podocalyxin levels in patients with NS. In accordance with this purpose, podocyte damage was revealed using a noninvasive method, the proteomic analysis of urine specimens in patients with NS. First, the presence of podocytic protein podocin was confirmed in the specimens using immunofluorescence microscopy. Next, to reveal podocyte damage and podocyturia, simultaneous analysis of specific tryptic peptides of podocin and podocalyxin was performed using UFLC-MS/MS with the multiple reaction monitoring (MRM) method. In addition, the cross-validation of podocin and podocalyxin quantitation using MS was performed using enzyme-linked immunosorbent assay (ELISA).

Overall, this proposed MS methodology showing the simultaneous quantitation of podocin and podocalyxin in urine provides technological evidence that will benefit the clinical field in the early diagnosis and follow-up of NS.

Materials and Methods

Study Design and Individuals

This research was approved by the Ethics Committee of Akdeniz University Faculty of Medicine (decision number: 237) and conducted in accordance with the Declaration of Helsinki principles and related ethical guidelines.

We included 81 individuals who were approved by the local ethics committee in this study. Forty-five participants were patients diagnosed with NS with proteinuria, hypoalbuminemia, and hyperlipidemia who were followed up in the Akdeniz University Hospital Nephrology Outpatient Clinic. Thirty-six participants were healthy volunteers without proteinuria, hypoalbuminemia, hyperlipidemia, or history of kidney disease and who had no first-degree relatives with diabetes or renal failure.

Blood specimens required for the study were taken after 8 to 12 hours of fasting. Serum specimens obtained from blood specimens were stored at –80°C before analysis. Spot and sterile urine specimens (50 mL) were taken at the same time interval as blood specimens. Urine specimens were stored at –80°C for analyses (except immunofluorescent analysis).

Biochemical Measurements

Serum total protein and albumin levels were measured using the colorimetric method, and serum C-reactive protein (CRP), urinary protein, and albumin levels were measured using turbidimetric method with commercial kits in the COBAS 8000 autoanalyzer (Roche Diagnostics, Mannheim, Germany).

Immunofluorescent Analysis

First, 15 mL of a fresh urine specimen was centrifuged at 2000 rpm for 5 minutes. After the supernatant was discarded, 3 mL of phosphate buffered saline (PBS) solution was added onto the remaining pellet. The pellet was disseminated to the microscope slides in the cytocentrifuge using Shandon Papspin. The prepared slides were fixed in pure methanol for 10 minutes at room temperature. Then the slides were washed with PBS for 5 minutes and treated with 0.3% Triton X-100 (Sigma-Aldrich, St Louis, MO) for 10 minutes to increase the permeability of the material. The slides were washed once again in PBS solution for 5 minutes and then incubated with a blocking buffer solution at room temperature for 1 hour. After further washing with PBS, slides with 1/1000 dilution were incubated with a rabbit anti-podocin antibody (Abcam; # ab50339) at 4°C for 16 hours. After washing, the slides were incubated with fluorescent-labeled goat anti-rabbit IgG (FITC, Abcam; # ab6717) with 1/1000 of secondary antibodies for 45 minutes at room temperature. We used 4-6-diamidino-2-phenylindole (DAPI) dye to mark the nucleic acid. Slides were photographed at 400× magnification using the Olympus BX61 fluorescence microscope, and podocin-stained podocytes in the designated area were counted. The podocyte count was divided into urine creatinine and expressed podocyturia.

ELISA

Podocin and podocalyxin were measured in urine specimens using immunoassay kits (catalog numbers MBS763522 and MBS765311; MyBiosource, San Diego, CA). With this method, specimens added to antibody-coated wells or molecules in standards were linked together by incubation. With the washing steps, unbound parts were removed. The second antibody labeled with Biotin was then added to the medium and bound to the analyte previously bound with the first antibody in the wells. In the next step, streptavidin-horseradish peroxidase (HRP) was added to the medium. Then, by adding the substrate reacting with HRP to the wells, colored product was formed in direct proportion to the amount of protein in the specimen. The reaction was stopped by adding acid to the medium, and the absorbance of the resulting colored product was read at 450 nm. Podocin and podocalyxin concentrations were calculated according to the calibration curves obtained from the standards.

UFLC-MS/MS Analyses

After various extractions in urine sediment, tryptic peptides of podocin and podocalyxin were quantified using MS. These analyses were performed using the LCMS-8040 (Shimadzu Corporation, Japan) combined with electrospray ionization welded UFLC (LC-20 AD UFLC XR, Shimadzu Corporation, Japan). In the electrospray ionization (ESI) positive (+) mode, an optimized MRM method was used.

Reagents and Chemicals

The RapiGest SF Surfactant, which helps solubilize proteins, making them more susceptible to enzymatic cleavage without inhibiting enzyme activity, was purchased from Waters (Milford, MA). Acetonitrile, formic acid, methanol, and water (gradient grade for LC) were obtained from Merck (Darmstadt, Germany). Dithiothreitol, iodoacetamide, ammonium bicarbonate, and trypsin (from porcine pancreas, proteomics grade) were purchased from Sigma-Aldrich (St Quentin-Fallavier, France). Podocin APAATVVDVDEVR (purity >98%), podocalyxin ATFNPAQDK (purity >98%), tryptic peptides with isotope-labeled podocin APAAT (VAL [13C5,15N]) VDVDEVR (purity >98%), and

podocalyxin ATFNP (Ala [13C3,15N]) QDK (purity >98%) peptides were synthesized by Matreya (State College, PA).

Preparation of Specimens

We added 20 µL of RapiGest to 1 mL of the urine specimens and vortexed it, then added 100 µL of 1,4-dithiothreitol solution (150 mM). It was kept in the incubator at 60ºC for 40 minutes. Next, 250 µL of the iodoacetamide solution (150 mM) was added to the cooled specimens. It was stored in a dark place at room temperature for 40 minutes. After 40 µL of trypsin was added, it was kept in the incubator at 37ºC for approximately 18 hours. The reaction was stopped by the addition of a 0.5% formic acid/methanol/water solution to each specimen. Then, a 200 µL specimen was added to the insert vials. An MS analysis was performed by adding both 1 µL labeled podocin (10 ng/mL) and 1 µL labeled podocalyxin (10 ng/mL) peptides as internal standards to each specimen. The concentrations of the tryptic peptides of podocin and podocalyxin were determined using the calibration curve.

Preparation of Mobile Phases

Mobile phase A was prepared using distilled water containing 0.1% (v/v) formic acid, and mobile phase B was prepared using acetonitrile containing 0.1% (v/v) formic acid.

Optimization and Calibration Studies

The tryptic peptide of podocin (APAATVVDVDEVR), the tryptic peptide of podocalyxin (ATFNPAQDK), labeled podocin (APAAT [VAL (13C5,15N)] VDVDEVR), and labeled podocalyxin (ATFNP [Ala (13C3,15N)] QDK) peptides were dissolved in methanol, and stock standards at a concentration of 1 mg/mL were prepared.[10,11] Working standards were prepared by making advanced dilutions with water/methanol (90/10, v/v) containing 0.5% formic acid from labeled stocks of 1 mg/mL. Calibrators were prepared in 7 different ng/mL concentrations (0, 1.562, 3.125, 6.25, 12.5, 25, and 50 ng/mL). Next, 200 µL of each calibrator was taken into the insert vials. Then 1 µL of 10 ng/mL of the labeled podocin internal standard and 1 µL of 10 ng/mL of the labeled podocalyxin internal standard were added to the vials. In the positive electrospray ionization mode, a 5500 V ion spray was used. The UFLC-MS/MS conditions and the *m/z* values of selected ions for the tryptic peptides are shown in **TABLE 1**.

Chromatographic separations were carried out on an HPLC Column (Raptor C18, 100 × 2.1 mm, 1.8 µm; Restek, UK). The flow rates for mobile phase A and mobile phase B were determined to be 300 µL/minutes. The gradient program was mobile phase B, 10% (0–3 minutes), 20% (3.1–13 minutes), 100% (13.1–17 minutes), and 10% (17.1–25 minutes). The injection volume was 20 µL. At approximately 5.97 minutes into the analysis, peaks belonging to podocalyxin were observed, and at 11.45 minutes into the analysis, peaks belonging to podocin were observed. The chromatograms of the podocin and podocalyxin tryptic peptides are shown in **FIGURE 1** and the mass spectra are shown in **FIGURE 2**. The total analysis time for column cleaning and reconditioning was determined as 25 minutes. Three repeated linear calibration curves were drawn on different days with the prepared calibrators.

Statistical Analyses

Statistical analysis was performed using the SPSS software for Windows 20.0. Results are expressed as mean ± standard error of the mean (SEM). The data were checked using the Kolmogorov-Smirnov test for normal distribution, the Student's *t*-test was used for normal distribution, and the Mann-Whitney *U* test was used for nonnormal distribution. The values obtained were considered as statistically significant if $P < .05$. Correlation analyses were performed using Pearson correlation analysis for parametric data and Spearman correlation analysis for nonparametric data.

Results

Forty-five adult patients with primary idiopathic NS (31 men, 14 women) and 36 healthy control participants (12 men, 24 women) were included for this study. The mean age of the patients was 43.09 ± 2.81 years (mean ± SEM) and that of the control participants was 32.36 ± 1.96 years (mean ± SEM).

Biochemical Measurements

Creatinine, CRP, total protein, and albumin levels were measured in serum obtained from blood specimens, and a significant difference was observed in serum creatinine and albumin levels of the patients with NS compared to the control group. There were significant differences in urine protein, urine albumin, and urine protein/creatinine ratios, but no significant difference in urine creatinine was observed between the patient and control groups. All differences in groups are listed in **TABLE 2**.

Immunofluorescence Imaging

In sterile and fresh urine specimens, immunofluorescence staining was performed using a fluorescence microscope. Under the immuno-

TABLE 1. ESI-Positive Welded UFLC-MS/MS Conditions and *m/z* Values of Selected Precursor and Product Ions in UFLC-MS/MS

UFLC/MS-MS Conditions			
Ion spray	5500 V	DL temperature	250ºC
Evaporator gas flow	1.5 L/min	Heating block	400ºC
Desiccant gas flow	0.1 L/min	Decomposition potential	120 V
CID gas flow	230 kPa	Collision energy	32 V
***m/z* Values of Selected Ions**			
	Precursor Ion (*m/z*)	**Product Ion (*m/z*)**	
Podocin tryptic peptide	671.5	274.2	
Isotope-labeled podocin tryptic peptide	674.5	240.2	
Podocalyxin tryptic peptide	496.4	558.4	
Isotope-labeled podocalyxin tryptic peptide	498.4	562.1	

CID, collision-induced dissociation; ESI, electrospray ionization; UFLC-MS/MS, ultrafast liquid chromatography with tandem mass spectrometry.

FIGURE 1. A, The chromatogram of tryptic peptide APAATVVDVDEVR from podocin in urine. B, The chromatogram of tryptic peptide ATFNPAQDK from podocalyxin in urine.

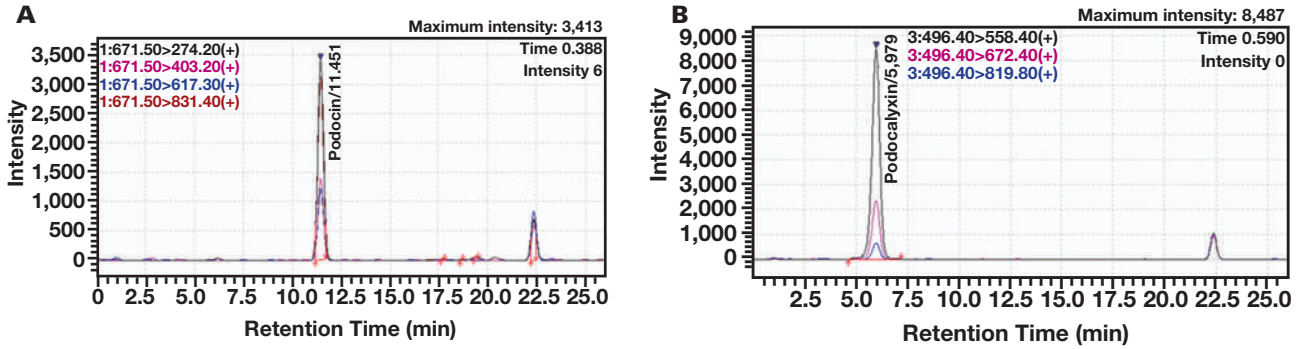

FIGURE 2. The MS/MS spectra of podocin (A) and podocalyxin (B) tryptic peptides.

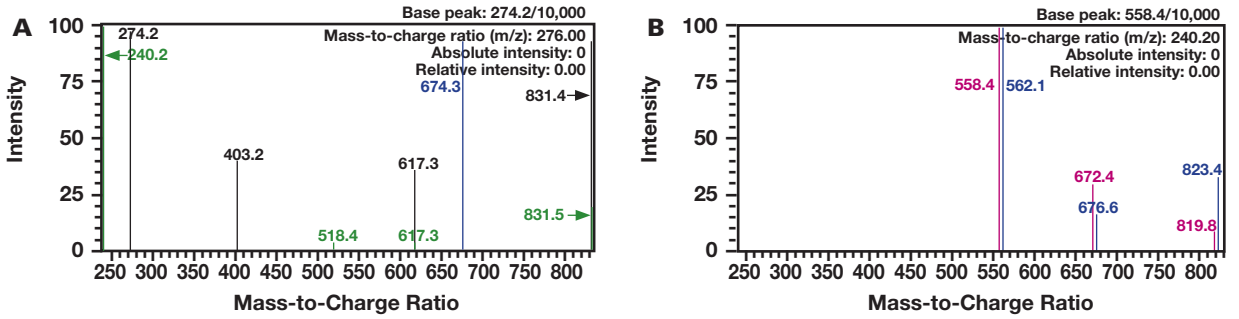

TABLE 2. NS and Control Group Mean Values of Analyzed Serum and Urine Parameters and Differences Between Groups

	NS Group, Mean ± SEM (n = 45)	Control Group, Mean ± SEM (n = 36)	*P* Value[a]
Serum creatinine (mg/dL)	1.65 ± 0.20	0.57 ± 0.03	**<.0001**
Serum albumin (g/dL)	2.98 ± 0.13	3.84 ± 0.06	**.001**
CRP (mg/dL)	0.85 ± 0.17	0.67 ± 0.24	.340
Total protein (g/dL)	5.69 ± 0.18	7.07 ± 0.11	.067
Urine albumin (mg/L)	1808.62 ± 312.64	8.60 ± 3.85	**<.0001**
Urine creatinine (mg/dL)	93.26 ± 8.34	112.78 ± 17.66	.164
Urine albumin:creatinine ratio (mg/g)	2855.32 ± 1043.04	4.95 ± 0.66	**.006**
Urine protein:creatinine ratio	5.89 ± 0.69	0.06 ± 0.007	**<.0001**
IF podocyte count	205.89 ± 49.78	ND	**.0006**
IF podocyturia (podocyte count/mg creatinine)	4.11 ± 1.08	ND	**.001**
ELISA podocin (ng/mL)	89.86 ± 33.17	0.47 ± 0.32	**.017**
ELISA podocalyxin (ng/mL)	6.11 ± 0.75	0.97 ± 0.10	**<.0001**
UFLC-MS/MS podocin peptide (ng/mL)	25.98 ± 7.72	ND	**.0007**
UFLC-MS/MS podocalyxin peptide (ng/mL)	1.92 ± 0.76	ND	**.008**
Podocin (ng/mL; podocin peptide × 31.45)	817.11 ± 242.84	ND	**.0018**
Podocalyxin (ng/mL; podocalyxin peptide × 59.2)	113.4 ± 44.82	ND	**.014**
Podocin (μg)/urine creatinine (mg)	1.47 ± 0.64	ND	**.014**
Podocalyxin (μg)/urine creatinine (mg)	0.11 ± 0.04	ND	**.008**

CRP, C-reactive protein; ELISA, enzyme-linked immunosorbent assay; IF, immunofluorescence; ND, not detected; NS, nephrotic syndrome; SEM, standard error of the mean.

[a] *P <.05 was significant, indicated by boldface P values. Nondetectable values were accepted as zero. Differences between groups were calculated using the Student's t-test for normally distributed groups and the Mann-Whitney U test for nonnormally distributed groups.*

fluorescence microscope, round or oval-looking cells were identified as podocytes; the membranes had a green fluorescence and the nuclei were stained blue with DAPI. The ratio of podocytes to urine creatinine was calculated, and podocyturia was defined as a podocin positive cell count per mg urine creatinine ≥0.85 (**FIGURE 3**). In the urine of patients with NS, podocyturia was found to be 4.11 ± 1.08 podocyte count/mg creatinine, but it was not detected in the healthy control participants.

Comparison of ELISA and UFLC-MS/MS Results

Urine podocin and podocalyxin levels measured by ELISA are shown in **TABLE 2**. Podocin and podocalyxin levels measured in patients with NS were significantly higher than those measured in the control group (P = .017 and P <.0001, respectively).

Urine podocin and podocalyxin protein levels measured by ELISA and urine podocin and podocalyxin tryptic peptide levels measured by UFLC-MS/MS were compared. Moderate correlations were found according to Spearman correlation analysis (r = .646, P <.0001 for podocin and r = .705, P <.0001 for podocalyxin).

UFLC-MS/MS Measurements

Method Validation

The standards containing tryptic peptides, prepared at different concentrations (0, 1.562, 3.125, 6.25, 12.5, 25, and 50 ng/mL), were measured by injection 3 times using UFLC-MS/MS. The calibration curve was drawn with the mean values of the intensity and field/concentration data that were obtained. The correlation coefficients of these curves were calculated, and the r^2 value for each calibration curve obtained was found to be >.99 (.998 for podocin and .996 for podocalyxin).

The limit of detection (LOD) and the limit of quantitation (LOQ) were calculated for the peptides of both podocin (LOD = 0.93, LOQ = 2.79) and podocalyxin (LOD = 0.62, LOQ = 1.86). The detection limits of the method were calculated according to the formula "$x_{LOD} = x_{Blank} + 3 * SD$," where SD was the standard deviation. The LOQ was then calculated according to the formula "$x_{LOQ} = 3 * x_{LOD}$."

For reproducibility, the intra-assay and interassay accuracies at 4 different concentrations (3.125, 12.5, 25, and 50 ng/mL) of peptides ranged from 87% to 105% and 89% to 104% for podocin, 89% to 111% and 90% to 109% for podocalyxin, and the intra-assay and interassay precisions (coefficient of variation [CV]) were 0.25% to 11.83% and 1.07% to 10.24% for podocin and 0.23% to 9.4% and 2.27% to 9.85% for podocalyxin, respectively. The CV values were calculated with the following formula: CV% = (standard deviation of the measurement/mean of the measurement) × 100.

FIGURE 3. Image of cells with podocin expression, which was marked by immunofluorescence method (100x). Hoechst nuclear stain (blue); podocin antibody followed with a secondary fluorescein isothiocyanate-labeled antibody (green).

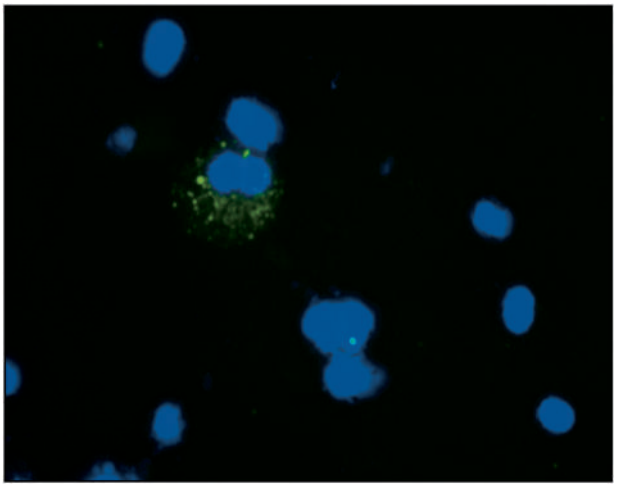

Standards of 25 ng/mL were prepared by spiking podocin and podocalyxin to human urine. As a result of the 6 repetitive measurements obtained, recovery percentages were calculated according to the following formula: percent recovery = measured concentration/reference concentration × 100. Recovery percentages were 101.36% and 92.02% for podocin and podocalyxin, respectively.

The carryover was evaluated by injecting a blank specimen after the upper LOQ specimens of the calibration standard. Carryover in the blank specimens after the upper LOQ specimens was not greater than 20% of the lower LOQ of both the podocin and the podocalyxin peptides.

To observe the matrix effect, we monitored the ion suppression on the targeted peptides during MS/MS quantification with 3 different urine specimen matrices with protein/creatinine ratios of 3.78, 10.70, and 361.73 mg/mmol. In the 2 urine matrices without proteinuria, ion suppression was <20%. However, the effect of ion suppression in urine with proteinuria was <30% for the podocin peptide and <20% for the podocalyxin peptide.

For dilution integrity, specimens were prepared at a 150 ng/mL concentration equivalent to 3 times the upper LOQ, followed by dilutions of 1/6 and 1/12. The diluted specimens were processed and analyzed according to the specimen preparation procedure. The precision and accuracy of the dilution integrity of the podocin and podocalyxin peptides were below 15%. Nominal concentrations were found to be 103.99% (1/6 dilution) to 95.87% (1/12 dilution) and 90.15% (1/6 dilution) to 105.36% (1/12 dilution) for the podocin and podocalyxin peptides, respectively.

The stability of the peptides in the calibrators and in human urine was evaluated under different temperature and timing conditions. All stability studies were performed at 2 concentration levels (3.125 ng/mL and 25 ng/mL as low and high values) with 3 determinations for each. The stability of the specimens kept in the autosampler for 18 hours was evaluated. The results showed that the podocin and podocalyxin peptides in the calibrators and the urine specimens could remain in the autosampler for at least 18 hours without a significant loss in quantitative values. Calibrators at the 2 concentration levels were tested over 3 freeze-and-thaw cycles. The podocin and podocalyxin peptides in the calibrators were found to be stable for 3 freeze-and-thaw cycles within 4 weeks when they were stored at below –20°C.

Levels of Podocin and Podocalyxin in Patients with NS

Because the podocin/APAATVVDVDEVR molecular weight ratio was 31.45 and the podocalyxin/ATFNPAQDK molecular weight ratio was 59.2, the concentrations of the peptides measured in urine were multiplied by these factors to determine the levels of podocin and podocalyxin. **TABLE 2** shows the results (mean ± SEM) of both peptides and the factor-multiplied podocin (817.11 ± 242.84 ng/mL) and podocalyxin (113.4 ± 44.82 ng/mL). Also, urinary podocin and podocalyxin levels were divided into urine creatinine levels for standardization. In the healthy control group, no evidence of podocin and podocalyxin was observed in the urine.

Furthermore, the NS group was divided into 2 groups (micro and macro) according to urine protein and albumin/creatinine levels. Then, podocin and podocalyxin peptide levels in micro and macro groups were compared with the control group. Although the podocin peptide levels were significantly different from each other in the micro and macro groups, the podocalyxin peptide levels did not differ between the groups. The mean podocin peptide levels of the groups and the P coefficients of the differences between the groups are shown in **TABLE 3**.

Relationship Between Proteinuria, Albuminuria, and Podocyturia

There were significant positive correlations between urinary podocin levels with urinary albumin and protein levels, but urinary podocalyxin levels did not show a correlation with these parameters. All significant correlations are shown in **TABLE 4** with coefficients. When the urinary protein and podocin peptide levels in patients with NS were compared using Spearman correlation analysis, a moderate correlation was found between them (r = .568, P <.0001). In addition, a strong positive correlation (r = .783, P = .004) was observed between urine protein and podocin peptide levels in the microproteinuria (30–300 mg/mmol urine protein/creatinine) group when the groups formed according to proteinuria levels were examined.

The sensitivity and specificity of this method, in which we determined urine podocin and podocalyxin peptide levels using UFLC-MS/MS, were calculated by receiver operating characteristic analysis. The area under the curve values were calculated as 0.898 (P <.0001) for the podocin peptide and 0.852 (P <.0001) for the podocalyxin peptide. The urine protein/creatinine ratio, which is one of the diagnostic criteria of NS, was evaluated in our study group by accepting the cutoff value of 300 mg/mmol. The sensitivity and specificity values for the peptides and the protein/creatinine ratio are shown in **TABLE 5** with 95% confidence intervals.

Discussion

Peripheral edema, heavy proteinuria, and hypoalbuminemia are often observed in patients with NS. Patients typically present to the clinic with edema and fatigue. The diagnosis of NS is based on typical clinical features with confirmation of severe proteinuria and hypoalbuminemia. Renal biopsy is often recommended, but the role of kidney biopsy in patients with NS is controversial and there are no evidence-based guidelines on biopsy indications. Biopsy may be more useful for treatment and prognosis in patients with idiopathic NS with an unknown histologic disease type or in patients with suspected other kidney disorders.[13]

Heavy proteinuria is mentioned when a protein:creatinine ratio of >3 to 3.5 mg protein/mg creatinine (300–350 mg/mmol) is observed in spot urine or a protein:creatinine ratio of >3 to 3.5 g protein is observed in 24-hour urine collection. Confirmation of proteinuria by 24-hour urine collection is cumbersome for patients, and the specimen may be collected incorrectly. The protein:creatinine ratio from a single urine specimen is commonly used to diagnose proteinuria in the nephrotic range. Although the accuracy of this spot test is limited in patients who exercise heavily, have altered muscle mass, or have similar factors, it is generally sufficient for the diagnosis of heavy proteinuria.[14]

TABLE 3. Comparison of Urine Podocin and Podocalyxin Peptide Levels in Proteinuria Groups[a]

	Proteinuria Group			*P* Value		
	Control (G1) (0–30 mg/mmol) Mean ± SEM	Microproteinuria (G2) (30–300 mg/mmol) Mean ± SEM	Macroproteinuria (G3) (>300 mg/mmol) Mean ± SEM	G1–G2	G1–G3	G2–G3
Podocin peptide (ng/mL)	ND	4.50 ± 1.52	44.08 ± 13.02	**.001**	**<.0001**	.313
Podocin/urine creatinine (ng/mg)	ND	432.42 ± 225.62	2454.43 ± 1129. 60	**.003**	**<.0001**	.86
Podocalyxin peptide (ng/mL)	ND	1.54 ± 1.10	2.90 ± 1.23	**.034**	**<.0001**	**.006**
Podocalyxin/urine creatinine (ng/mg)	ND	154.01 ± 91.80	101.85 ± 55.87	**.030**	**<.0001**	**.013**

ND, not detected; SEM, standard error of the mean.
[a]Nondetectable values were accepted as zero. Differences between the groups were calculated using the Kruskal-Wallis H test. P <.05 was significant, indicated by boldface values.

TABLE 4. Significant Correlations Between Podocin and Podocalyxin Peptides with Proteinuria and Albuminuria

Correlation Coefficient (*r*)	Podocalyxin Peptide	Urinary Albumin	Urinary Albumin/Creatinine	Urinary Protein	Urinary Protein/Creatinine
Podocin peptide	.411[a]	.720[a]	.820[a]	.568[a]	.530[b]
Urinary albumin/creatinine	.470[b]	…	…	…	…
Urinary podocin/creatinine	…	…	…	…	.618[b]

[a]P <.0001,
[b]P <.05.

TABLE 5. Sensitivity and Specificity of Podocin, Podocalyxin, and Protein:Creatinine Ratio[a]

	Sensitivity	95% CI	Specificity	95% CI
Podocin	79.55	64.7–90.2	100	82.2–100
Podocalyxin	70.45	54.8–83.2	100	85.2–100
Protein:creatinine	70.45	54.8–83.2	100	90.3–100

CI, confidence interval; ROC, receiver operating characteristic.
[a]Nondetectable results were considered zero when performing the ROC analysis. The cutoff value was >0 ng/mL for podocin and podocalyxin and >300 mg/mmol for the protein:creatinine ratio.

Several studies have shown that the evaluation of podocyturia may be an effective biochemical indicator of kidney damage.[7,10,11] Podocytes damaged for various reasons can be excreted in the urine. The detachment of podocytes caused by membrane damage may lead to effacement of the foot process, proteinuria, and progressive kidney failure.[15] Performing proteomic measurements showing podocyte damage in noninvasive urine specimens is important because it may facilitate an early diagnosis of glomerular disease by providing information on the type or activity of the disease.

In the scope of this study, podocyte injury and podocyturia were investigated using MS, immunofluorescence analysis, and ELISA in urine specimens of patients with NS. We have shown the association of 2 podocytic proteins with glomerular proteinuria in NS, the efficacy of the analytical methods used, and the utilization of the data to determine the degree of glomerular damage.

In this study, podocytes in urine were identified by UFLC-MS/MS technology using tryptic peptides. The presence of tryptic peptides (APAATVVDVDEVR for podocin and ATFNPAQDK for podocalyxin) in urine indicated the release of podocytes to the urine.[10,11,15] In 1996, Barr et al[16] were able to determine the level of a protein using tryptic peptide. The concentration of the protein can be calculated by comparing the ratio of the peak area of the tryptic product in the patient specimen to the internal standard area. This approach has been used successfully in measuring many proteins. For example, in 1 study, a very sensitive measurement was made using an LC-MS/MS technique for urine albumin measurement, and urinary albumin levels were determined correctly in patients with a normal albumin level.[17] This and similar studies reveal the role of LC-MS/MS in the identification of urinary markers, especially in renal diseases.

In the literature, some studies investigating podocyturia using LC-MS/MS were conducted in patients with preeclampsia, suggesting that podocyturia is present only in active glomerular diseases.[9] In some glomerular diseases such as diabetic nephropathy, lupus nephritis, and focal segmental glomerulosclerosis, the excretion of live podocytes has been reported in urine sediments.[18-20] In this study, it was possible to determine the excretion of podocytes in fresh urine specimens using immunofluorescence, but this method cannot be applied for specimens that cannot be analyzed immediately. Studies on the detection of podocyturia in the literature have suggested that urine sediment should be kept overnight in cell culture conditions and then stained with podocyte-specific proteins.[21] However, in this study we did not obtain reproducible results when we tried podocyte cell culture. Therefore, we performed immunofluorescence imaging using a specific antibody. However, the procedures for imaging when compared to quantitative measurement using LC-MS/MS were not practical because fresh specimens require 3 hours to process. Current methodologies for the evaluation of podocyturia are challenging.

Garovic et al[9] developed a method for the detection of podocyturia using MS in patients with preeclampsia. In their study, podocin tryptic peptide analysis was performed using a 50 mL urine specimen using LC-MS/MS with a 15-minute gradient. Szczepankiewicz et al[22] performed tryptic podocin peptide analysis in dogs with kidney and cardiac disorders using LC-MS/MS. Their study, published in 2019, described a method using 0.7 mL of urine sediment and involving a 30-minute gradient.[22] Simon et al[10] quantified podocin, a potential glomerular injury marker, using LC-MS/MS. In their study, a 30-minute analysis method was created using 1 mL of a human urine specimen. Analyses were performed on urine specimens from healthy volunteers. In 2015, Biarc et al[11] presented a 17.5-minute LC-MS/MS method for the quantification of the podocalyxin tryptic peptide using 1 mL of a human urine specimen from healthy volunteers, similar to the Simon et al study. In Martineau et al,[15] published in 2019, the quantification of the tryptic peptides of podocin and podocalyxin simultaneously using LC-MS/MS was performed, similar to the current study. Martineau et al used 1 mL of a human urine specimen in the 25-minute analysis performed in patients with preeclampsia and patients with Fabry disease.

There are similarities between the methods of Simon et al,[10] Biarc et al,[11] and Martineau et al[15] and the current method. The same tryptic peptide sequences and an equal specimen volume were used in these studies. However, in the current study, unlike the other 3 studies, solid-phase extraction was not performed during specimen preparation. This is the second study to present simultaneous LC-MS/MS analysis of podocin and podocalyxin tryptic peptides and the first to present peptide levels in patients with NS. This method is promising for the future screening, staging, and evaluation of the treatment efficacy of all proteinuric kidney diseases.

The MS measurement of urine podocin and podocalyxin tryptic peptides was performed in the study conducted by Martineau et al,[15] who examined patients with preeclampsia and with Fabry disease. Detection and quantitation limits obtained in their study were 19 pmol/L and 63.3 pmol/L for podocin and 17.1 pmol/L and 56.9 pmol/L for podocalyxin, respectively. The LOD and LOQ values calculated in our study were 22.14 pmol/L and 66.42 pmol/L for podocin and 11.27 pmol/L and 33.81 pmol/L for podocalyxin, respectively. When comparing both studies, note that the Martineau et al study had lower detection and quantitation limits for podocin measurement, whereas our study had lower limits for podocalyxin. Martineau et al[15] evaluated the matrix effect and showed that ion suppression was higher in proteinuric specimens, especially for the podocin peptide, similar to our results. They stated that the increased ion suppression in proteinuric specimens resulted from the association of some tryptic peptides of albumin.[15]

Four studies with the same tryptic peptides are compared in **TABLE 6**, which shows the limits of quantitation and analysis times of the studies.

Proteomic studies on podocyte injury in NS have not been widely performed in the medical world because of the need for high-level infrastructure. It is possible to perform simultaneous measurements for multiple analytes in a single analysis, after tryptic digestion in small amounts using LC-MS/MS technology. In this study, we simultaneously measured podocin and podocalyxin tryptic peptides in a single 1 mL specimen. It is considered an advantage that analysis can be performed with noninvasive urine specimens using LC-MS/MS with a volume as low as 1 mL.

Research has shown that LC-MS/MS methodologies have advantages such as good sensitivity, high specificity, lower specimen volume, and the possibility of simultaneous protein/peptide analysis. However, studies on podocyturia in the literature have usually included staining and immunofluorescence imaging with podocin-specific antibodies. There are very few studies in the literature about the measurement of podocytic proteins using LC-MS/MS.[9–11,15,22] Presenting and publishing the results of this study in

TABLE 6. Detection and Quantitation Limits, Analysis Times, and Sample Groups of Similar Studies in the Literature

Methods[a]	Podocin		Podocalyxin		Analysis Time (min)	Sample Group
	LOD	LOQ	LOD	LOQ		
1	…	0.39 ng/mL	…	…	30	Healthy volunteers
2	…	…	…	0.78 ng/mL	17.5	Healthy volunteers
3	19 pmol/L	63.3 pmol/L	17.1 pmol/L	56.3 pmol/L	10	Healthy volunteers, patients with preeclampsia, patients with Fabry disease
4	0.93 ng/mL (22.14 pmol/L)	2.79 ng/mL (66.42 pmol/L)	0.62 ng/mL (11.27 pmol/L)	1.86 ng/mL (33.82 pmol/L)	25	Healthy volunteers, patients with NS

LOD, limit of detection; LOQ, limit of quantitation; NS, nephrotic syndrome.
[a]See the following references for methods: 1,[10] 2,[11] 3.[15] This study is referred to as method number 4.

scientific environments will make a great contribution to the literature. The use of reliable and highly efficient proteomics technologies in this and similar studies will accelerate scientific research in renal diseases on national and international platforms.

The detection of podocyturia may become a more sensitive marker of glomerular disease activity and damage than proteinuria.[23] This study also supports this information. Results of the receiver operating characteristic analysis showed that urine podocin levels may be a more sensitive and specific marker than proteinuria for the diagnosis of NS. Similarly, Yu et al[24] showed that podocyturia is a more specific marker of glomerular damage than proteinuria. Furthermore, there are many research studies showing that in human glomerular disease, urinary podocytes can become a marker of disease activity.[18,19,25]

In this study, podocin results using MS and showing significant and strong correlations with proteinuria and albuminuria suggest that this analysis can be used to evaluate the efficacy of various treatments in glomerular diseases in the future. However, levels of podocytic protein in urine did not show significant correlations with serum creatinine. This finding may be related to patients with NS who have not yet developed chronic kidney disease.

Because the primary lesion is in podocytes in many glomerulopathies, the development of measurements related to podocyturia is important in diagnosis and follow-up. Studies have shown that urinary podocyte biomarkers can be used in glomerular diseases. Our findings show that urinary podocin and podocalyxin levels were significantly higher in patients with NS compared to control group. In addition, only urinary podocin levels and podocalyxin levels differed significantly in the control and microproteinuria groups. Finally, urine podocin concentrations showed a significant correlation with urine proteinuria levels, whereas urine podocalyxin concentrations did not show a significant correlation.

Conclusion

These findings suggest that urinary podocin levels may be a potential marker for the early diagnosis and monitoring of NS. The major limitation of our study is the small sample size; a larger sample set of patients with NS is needed to establish a normal range for podocin and podocalyxin tryptic peptides in urine in the future. This article presents a reliable and reproducible measurement method for determining urinary podocin and podocalyxin levels simultaneously. Podocytic proteins other than podocin and podocalyxin can also be analyzed in light of the information obtained here.

Acknowledgments

This study is supported by Akdeniz University Scientific Research Projects (grant number 2014.01.0103.007).

Conflict of Interest

None.

REFERENCES

1. Kelepouris E, Rovin BH. Overview of heavy proteinuria and the nephrotic syndrome. https://www.uptodate.com/contents/overview-of-heavy-proteinuria-and-the-nephrotic-syndrome. Accessed September 9, 2021.
2. Hull RP, Goldsmith DJ. Nephrotic syndrome in adults. *BMJ.* 2008;336(7654):1185–1189.
3. Kawachi H, Fukusumi Y. New insight into podocyte slit diaphragm, a therapeutic target of proteinuria. *Clin Exp Nephrol.* 2020;24(3):193–204.
4. Kerjaschki D. Caught flat-footed: podocyte damage and the molecular bases of focal glomerulosclerosis. *J Clin Invest.* 2001;108(11):1583–1587.
5. Tryggvason K, Patrakka J, Wartiovaara J. Hereditary proteinuria syndromes and mechanisms of proteinuria. *N Engl J Med.* 2006;354(13):1387–1401.
6. Wang P, Li M, Liu Q, Chen B, Ji Z. Detection of urinary podocytes and nephrin as markers for children with glomerular diseases. *Exp Biol Med.* 2015;240(2):169–174.
7. Sun D, Zhao X, Meng L. Relationship between urinary podocytes and kidney diseases. *Ren Fail.* 2012;34(3):403–407.
8. Imaizumi T, Nakatochi M, Akiyama S, et al. Urinary podocalyxin as a biomarker to diagnose membranous nephropathy. *PLoS One.* 2016;11(9):e0163507.
9. Garovic VD, Craici IM, Wagner SJ, et al. Mass spectrometry as a novel method for detection of podocyturia in pre-eclampsia. *Nephrol Dial Transplant.* 2013;28(6):1555–1561.
10. Simon R, Lemoine J, Fonbonne C, et al. Absolute quantification of podocin, a potential biomarker of glomerular injury in human urine, by liquid chromatography-multiple reaction monitoring cubed mass spectrometry. *J Pharm Biomed Anal.* 2014;94:84–91.
11. Biarc J, Simon R, Fonbonne C, et al. Absolute quantification of podocalyxin, a potential biomarker of glomerular injury in human urine, by liquid chromatography-mass spectrometry. *J Chromatogr A.* 2015;1397:81–85.
12. Ozcan F, Akbas H, Kırac E, Suleymanlar G, Aslan M, Yucel G. Mass spectrometric quantification of urinary human liver fatty acid binding protein in renal transplant recipients. *Rapid Commun Mass Spectrom.* 2016;30(5):603–610.

13. Kodner C. Diagnosis and management of nephrotic syndrome in adults. *Am Fam Physician.* 2016;93(6):479–485.
14. Hull RP, Goldsmith DJ. Nephrotic syndrome in adults. *BMJ.* 2008;336(7654):1185–1189.
15. Martineau T, Boutin M, Côté AM, Maranda B, Bichet DG, Auray-Blais C. Tandem mass spectrometry analysis of urinary podocalyxin and podocin in the investigation of podocyturia in women with preeclampsia and Fabry disease patients. *Clin Chim Acta.* 2019;495:67–75.
16. Barr JR, Maggio VL, Patterson DG Jr, et al. Isotope dilution–mass spectrometric quantification of specific proteins: model application with apolipoprotein A-I. *Clin Chem.* 1996;42(10):1676–1682.
17. Seegmiller JC, Barnidge DR, Burns BE, Larson TS, Lieske JC, Kumar R. Quantification of urinary albumin by using protein cleavage and LC-MS/MS. *Clin Chem.* 2009;55(6):1100–1107.
18. Nakamura T, Ushiyama C, Suzuki S, et al. Urinary excretion of podocyte in patients with diabetic nephropathy. *Nephrol Dial Transpl* 2000;25(9):1379–83.
19. Nakamura T, Ushiyama C, Suzuki S, et al. Urinary podocytes for the assessment of disease activity in lupus nephritis. *Am J Med Sci.* 2000;320(2):112–116.
20. ElShaarawy A, Behairy MA, Bawady A, Abdelsattar HA, Shadad E. Urinary podocin level as a predictor of diabetic kidney disease. *J Nephropathol*. 2019;8(3):e26.
21. Garovic VD, Wagner SJ, Turner ST, et al. Urinary podocyte excretion as a marker for preeclampsia. *Am J Obstet Gynecol.* 2007;196(4):320.e1–320.e7.
22. Szczepankiewicz B, Bąchor R, Pasławski R, et al. Evaluation of tryptic podocin peptide in urine sediment using LC-MS-MRM method as a potential biomarker of glomerular injury in dogs with clinical signs of renal and cardiac disorders. *Molecules*. 2019;24(17):3088.
23. Camici M. Urinary detection of podocyte injury. *Biomed Pharmacother.* 2007;61(5):245–249.
24. Yu D, Petermann A, Kunter U, Rong S, Shankland SJ, Floege J. Urinary podocyte loss is a more specific marker of ongoing glomerular damage than proteinuria. *J Am Soc Nephrol.* 2005;16(6):1733–1741.
25. Vogelmann SU, Nelson WJ, Myers BD, Lemley KV. Urinary excretion of viable podocytes in health and renal disease. *Am J Physiol Renal Physiol.* 2003;285(1):F40–F48.

AQ22
AQ24
AQ8
AQ10
AQ18
AQ20

Novel Methods for Detecting Human Cholesterol Crystals from Sampled Blood

Nobuzo Iwa, PhD,[1] Chikao Yutani, MD, PhD,[1] Sei Komatsu, MD, PhD,[2,] Satoru Takahashi, MD,[2] Mitsuhiko Takewa, MD, PhD,[2] Tomoki Ohara, MD,[2] Kazuhisa Kodama, MD, PhD[2]*

[1]Division of Pathology, Cardiovascular Center, Osaka Gyoumeikan Hospital, Osaka, Japan, [2]Department of Cardiology, Cardiovascular Center, Osaka Gyoumeikan Hospital, Osaka, Japan; *To whom correspondence should be addressed. plaquemap@yahoo.co.jp

Keywords: spontaneous ruptured aortic plaques, debris, human cholesterol crystals, nonobstructive general angiography, filter paper, atherosclerosis

Abbreviations: NOGA, nonobstructive general angiography; SRAPs, spontaneous ruptured aortic plaques; CCs, cholesterol crystals; H&E, hematoxylin and eosin.

Laboratory Medicine 2022;53:255–261; https://doi.org/10.1093/labmed/lmab078

ABSTRACT

Objective: Nonobstructive general angiography (NOGA) is a novel modality to detect and sample spontaneous ruptured aortic plaques (SRAPs). We aimed to establish novel methods to detect cholesterol crystals (CCs) in sampled SRAPs.

Methods: Blood specimens containing SRAPs were obtained from patients using NOGA. Blood was instantly frozen on a glass slide and subsequently thawed for quantitative analysis and spread onto a filter paper that was rinsed using distilled water. Qualitative analysis was performed for the rinsed water using polarized light microscopy, and the filter paper was embedded in paraffin for histologic analysis.

Results: The CCs were clearly observed after hemolysis using the instant freeze-thaw method. The filter paper rinse method indicated free CCs of varying shapes under polarized light microscopy without erythrocytes. On the filter paper, sampled SRAPs showed Lamé-like small particles. Histopathology revealed various atheromatous components.

Conclusion: A set of novel methods for detecting CCs from sampled blood was established.

During the last 50 years, filter papers have been used as substrates for specimens and diagnostic tools for infectious agents such as bacteria, viruses, and parasites, in addition to their use in genetic and serological analysis. Usually, a filter paper is used to identify infectious specimens in whole blood, dried blood spots, dried plasma spots, and dried buffy coat spots because it requires simple, economical, and minimal technical application.[1,2] Many harvesting methods are available for specimens with a low cell count, including centrifugation, aspiration, cell block preparation,[3] and membrane filtration.[4] However, it is difficult to collect aspirated plaques in sufficiently high numbers because specimen transfer causes their distortion and loss during whole blood specimen processing. Furthermore, these methods are inadequate for processing large amounts of blood specimens. During radiological diagnostic imaging, it is difficult to observe atheromatous materials or directly detect cholesterol crystals (CCs) from plaques as real images. Recently, Komatsu et al[5] and Komatsu et al[6] introduced the novel nonobstructive general angiography (NOGA) technique to enable the visualization, characterization, and identification of the inner surface of the aortic lumen and revealed that spontaneous ruptured aortic plaques (SRAPs) occur in up to 80.9% of evaluated patients. In addition, they reported that this modality can be used to successfully obtain specimens from puff-chandelier and puff ruptures in the aorta.[7,8] In this study, we aimed to evaluate the usefulness of a filter paper technique for detecting plaque components, including human CCs or foamy macrophages, and assessing atheromatous materials from SRAPs.

Methods

We established a set of novel methods for quantitative and qualitative analyses of CCs and histologic analysis of direct paraffin-embedded filter papers. The preparation procedures for the new filter paper technique are summarized in **FIGURE 1**.

Statement of Ethics

This study was approved by the local ethics committee of the Osaka Gyoumeikan Hospital (Osaka, Japan), and all patients provided written informed consent (#20–0033).

Sampling SRAPs

Blood specimens were obtained from patients with confirmed or suspected coronary artery disease who had undergone emergency or

FIGURE 1. A set of novel methods for detecting cholesterol crystals (CCs) sampled from spontaneous ruptured aortic plaques using nonobstructive general angiography.

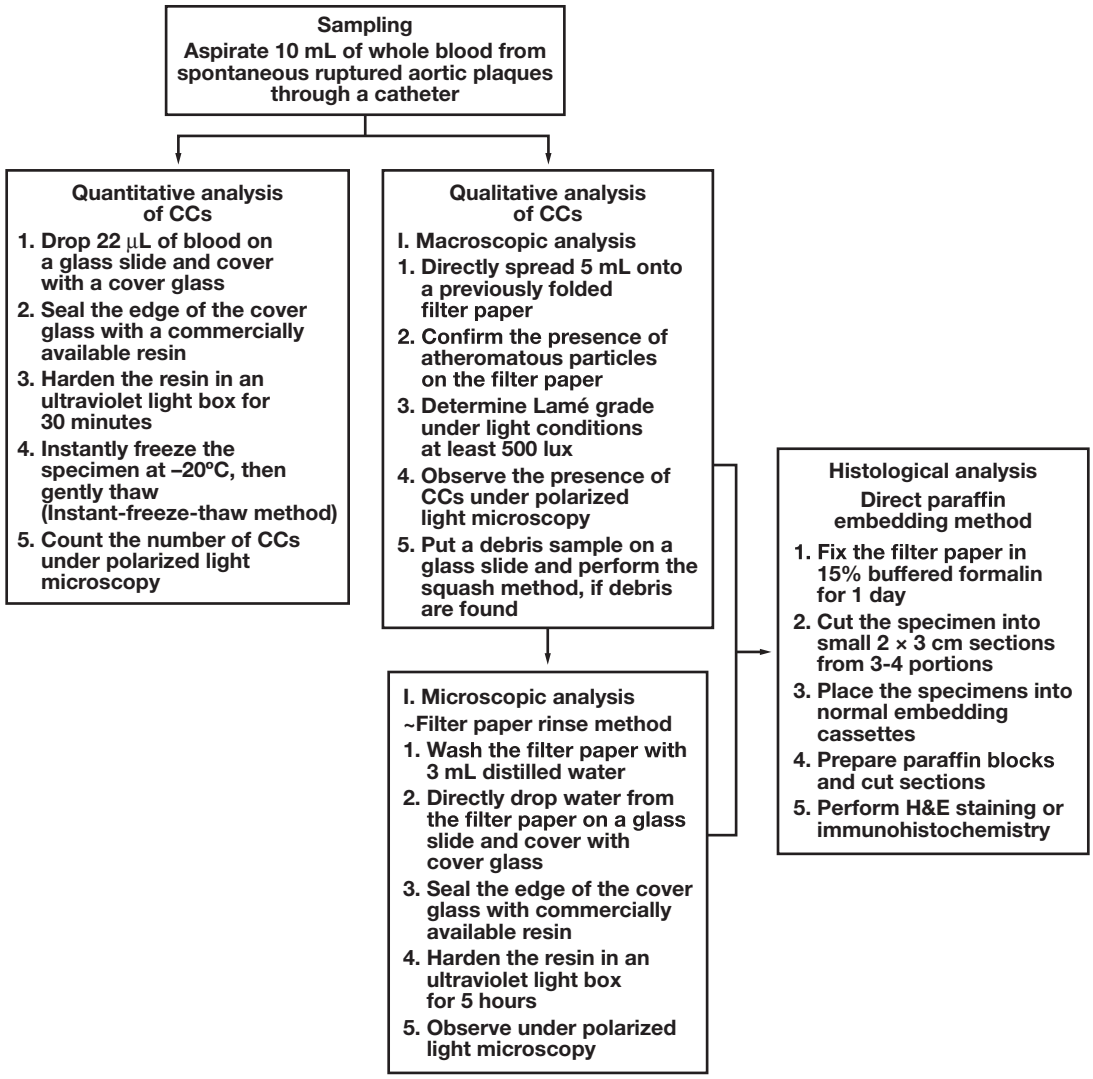

elective cardiac catheterization for identifying SRAPs via NOGA to evaluate aortic atherosclerosis. The sampling of aortic plaques was performed as reported in previous studies.[5-8] The NOGA system allows the clear visualization and identification of aortic lesions, including plaque ruptures, fissures, bleeding, ulcers, and erosion using an infusion of low-molecular dextran. The catheter system was previously described in detail.[7] In this method, ruptured plaques from puff or puff-chandelier rupture of plaques (white or white-yellow puff-like materials easily and spontaneously released from advanced aortic lesions) were naturally collected into a catheter and used as the specimen.

Quantitative Analysis of CCs

A total of 22 μL blood was sampled, placed on a glass slide, and covered with a cover slip. The edges of the cover slip were sealed with resin that was allowed to harden for approximately 30 minutes in an ultraviolet light–irradiated box. The specimens were instantly frozen at –20°C using a freezing solvent and then gently thawed to 25°C to destroy erythrocytes. The numbers of single layers or multilayers of CCs were counted under a polarized light microscope.

Qualitative Analysis of CCs

Spreading Blood onto a Filter Paper

Whole blood (10 mL) was sampled through a catheter, aspirated into a disposable syringe, and transferred into a heparinized test tube. The specimen was slightly stirred and directly spread onto a previously folded qualitative fine-pore cellulose filter paper (pore size 7 μm, diameter 15 cm, spherical type No. 5A, Advantech, Tokyo, Japan) with a single piece of tissue paper to absorb excess blood plasma. The filter paper was half-dried at 25°C for approximate 30 minutes. During this time, the specimen blood seeped into the filter paper, and plaque components were caught within the fine-pore cellulose. The SRAPs were easily visualized under normal light conditions.

Macroscopic analysis of filter papers. Under light conditions of at least 500 lux, the gross appearance of plaques on filter paper post drying is of a smooth to rough surface or chandelier-like particles, glistening granules, and gray atheromatous particles.[6,8] We classified the glittering level into several grades. If debris was found, then

we put a debris specimen on a glass slide and performed the squash method.

Microscopic analysis of a filter paper. The filter paper containing the blood components was rinsed with approximately 3 mL of distilled water. The filter paper was gently swung around, and a few drops of the distilled water from the filter paper were directly dropped onto the glass slide and covered with a cover slip. Thereafter, the edges of the cover slip were sealed with commercially available resin to prevent air infiltration. The resin was hardened for approximately 30 minutes in an ultraviolet light box to prevent drying. Evaluation of CCs was performed using polarized light microscopy,[8] and photographic images of the same were taken.

Histologic Analysis

The filter paper with SRAPs was directly fixed in 15% formalin for 1 day using a round-shaped fixative plastic bowl 15.5 × 59.5 cm in size. After fixation, the filter paper was cut into 3 × 2 cm pieces from 4 different portions containing SRAPs, and even portions where no visible components were found. Subsequently, the specimens were placed into normal embedding cassettes. These specimens were dehydrated in a graded series of ethanol and xylene and prepared as good-quality paraffin blocks. Histopathologic sections of 3 to 4 μm thickness were easily cut with a sliding-type microtome. Hematoxylin and eosin (H&E) staining was performed to confirm the presence of atheromatous components. This paraffin preparation was performed in a manner similar to conventional methods.

Results

Quantitative Analysis of CCs

Representative images are shown in **IMAGE 1**. The level of hemolysis using the freeze-thaw method could be controlled as **IMAGE 1A** and **IMAGE 1B**. The level of hemolysis, as seen in **IMAGE 1A**, was more than that, as seen in **IMAGE 1B**. The shape and borders of the CCs in **IMAGE 1A** are relatively clearer than those in **IMAGE 1B**. These images provide information regarding the quantitative analysis of CCs in 22 μL of blood.

Qualitative Analysis of CCs

Expression of the Gross Appearance of Filter Paper: Lamé Grade

Under light conditions of at least 500 lux, the gross appearance of the filter paper surface was as follows: rough-surface or chandelier-like particles, glistening granules, and gray atheromatous particles (including CCs, fibrin, macrophages, and calcification). Thus, the filter paper–based gross appearances were important for the confirmation of SRAPs.

The number of CCs in plaques on the filter paper was classified using the following 4 grades:

Grade 0, zero particles (**IMAGE 2A**);
Grade 1, <5 glistening particles (arrows, **IMAGE 2B**);
Grade 2, >5 glistening particles (arrows, **IMAGE 2C** and **Supplemental Video 1**); and
Grade 3, mixture of many glistening particles and gray atheromatous particles of various shapes and sizes (arrows, **IMAGE 2D**).

The glittering grade was named after lamé, the French word for glittering.[6,8] The filter paper surface was carefully observed to detect CCs as chandelier-like particles, glistening particles, or gray particles. Light conditions of <500 lux could have resulted in an underestimation of the grade.

Because debris coated by a fibrous cap was difficult to examine for CCs using polarized light microscopy, the squash method was performed for the evaluation of atheromatous materials, revealing a cluster of CCs as calcified particles stained with hematoxylin (**IMAGE 2E**). Furthermore, many CCs were released from the edge of the cluster with blue or orange refraction under polarized light microscopy (**IMAGE 2F**).

Filter Paper Rinse Method

In the rinse method, only free CCs and those released from SRAPs could be detected as either a single layer with orange refraction (**IMAGE 3A**) or multiple layers of various shapes and sizes with blue

IMAGE 1. Polarized light microscopic images of cholesterol crystals. Cholesterol crystals demonstrated with instant freeze-thaw method from spontaneous ruptured aortic plaques. A, High level of hemolysis caused by the strong freeze. B, Low level of hemolysis caused by the weak freeze. (×200)

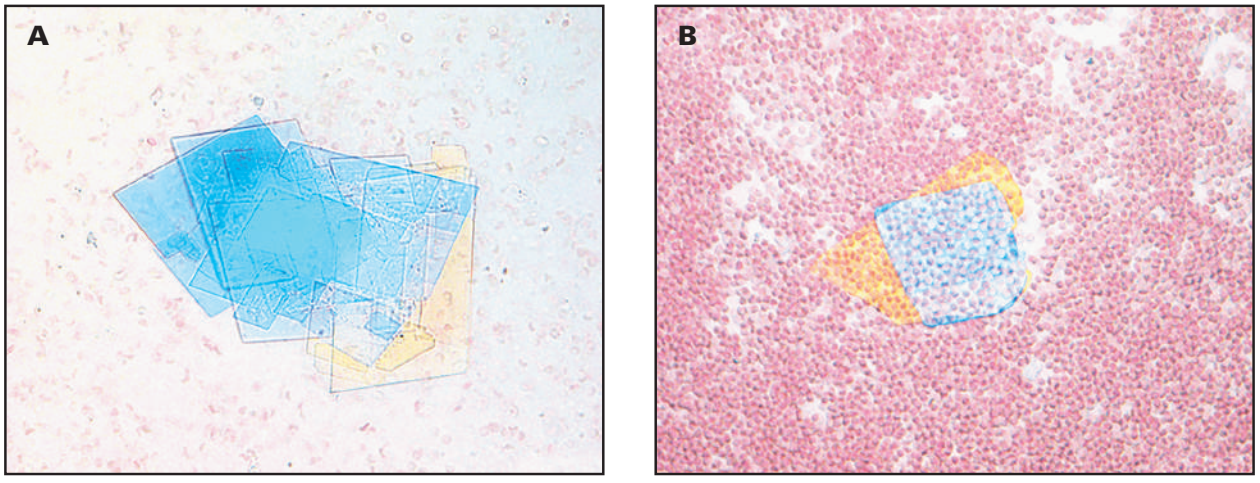

IMAGE 2. Lamé grade based on gross appearance. A, No crystal is seen, Lamé grade 0. B, Less than 5 glistening particles (arrow) seen, Lamé grade 1. C, More than 5 glistening particles (arrows) seen, Lamé grade 2. D, Mixtures of glistening particles and gray particles with irregular sizes and shapes (arrows) seen around the portions of the filter paper surface, Lamé grade 3. E, Polarized light microscopic images of the debris. Cholesterol crystals (CCs) and calcification with rock-like rough surfaces (smash method) (×12.5). F, Various-shaped CCs released from the edge of the cluster (squash method) (×100).

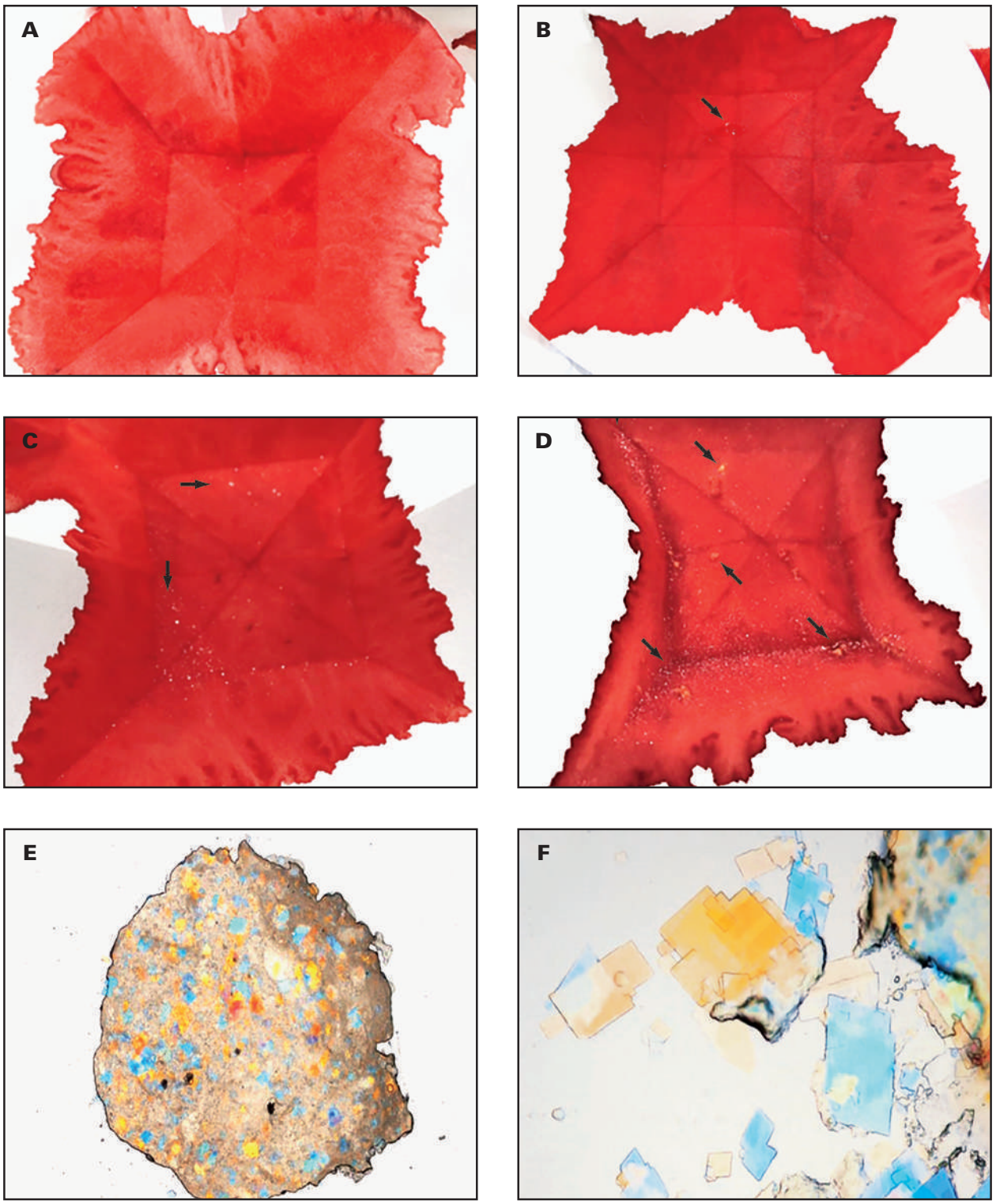

or orange refraction against a clean background without erythrocytes (**IMAGE 3B**). Research has shown that CCs are a hallmark of atherosclerosis,[9] and CCs within the plaque play a key role in splitting the plaque and also inducing inflammation.[10] This method provides qualitative information, indicating whether the atherosclerotic plaque includes CCs or not.

Histologic Analysis

In general, filter devices are used to isolate debris from blood.[11] The yield rate is quite low because the size of a single mesh is 100 to 150 μm, which is larger than the size of the debris. We hypothesized that the direct-paraffin embedding method could be performed to isolate Lamé grade 2 or 3 particles, wherein a filter paper with debris directly embedded into paraffin might increase the yield rate. Direct paraffin embedding followed by H&E staining showed various atheromatous components with good-quality staining and different features. Spindle-shaped ghost images of CCs were observed in the amorphous cellulose fiber substrate (**IMAGE 4A**). Furthermore, many lipid vacuoles or granules, foamy macrophages with enlarged cytoplasm, and calcifications with hematoxylin stain were also visible (**IMAGE 4B**). In addition, many macrophage-rich clusters were prominent, showing eccentric nuclei with foamy cytoplasm–containing calcifications with amorphous eosinophilic substances (**IMAGE 4C**). Finally, eosinophilic fibrin fragments in the cellulose filter substrates were observed with inflammatory cells against a red blood cell background (**IMAGE 4D**). This technique proved to be a useful method for the evaluation of various atheromatous components in SRAPs.

Discussion

A set of novel methods for sampling SRAPs using NOGA and detecting CCs may clarify the mechanism of symptomatic or asymptomatic systemic embolism.[6,8] It is well known that the presence of CCs may lead to the development of stroke,[12,13] heart disease,[14] renal disease,[15] and CC embolization.[16,17] The incidence of embolic disease was not always thought to be common; however, 1 study using NOGA detected SRAPs in 80.9% of patients with confirmed or suspected coronary artery disease.[8] In our study, SRAPs were found to be unlike those observed earlier via static images such as computed tomographic images or autopsy images.[6,8] Thus, the incidence of systemic embolism resulting from SRAPs was expected to be higher than that presumed before.[6,8]

Several studies have suggested an important role of the nucleotide-binding domain, leucine-rich repeat-containing family, pyrin domain–containing 3 inflammasome induced by the formation of CCs in the progression of local atherosclerosis and plaque rupture.[18] Experimental human CCs were found to be unlike the commercially available CCs (**IMAGE 5**) in diversity.[8] Quantitative and qualitative analysis of CCs in SRAPs may have great significance for evaluating the inflammatory level of each SRAP.

Distal protection devices have been used in clinical intervention for collecting plaques from live patients through the coronary arteries[9] and carotid arteries.[19] However, there is no device to detect and sample aortic atherosclerosis except for the trap of distal protection device. The size of plaques varies from millimeters to below micrometers.[8] In general, the mesh size of the filters is 150 μm. The yield rate of sampling plaques is low in conventional methods because the mesh size of the filters used is bigger than the plaques.

In our study, CCs were observed as needle-shaped ghost images because the CCs may have dissolved in the solvents (ethanol and xylene) used during paraffin block preparations.[6] Cytological specimens containing low cell numbers are routinely prepared using cell block,[20] fine-needle aspiration and brushing,[21] and Millipore filtration.[22] In 1999, Baloch et al[4] used the cell block method to reprocess their Papanicolaou-stained membrane filter paper with a limited specimen portion. Although we agree with the usefulness of this method, it is less suited for the evaluation of atheromatous materials because the sampling portion of materials is smaller than that used in our filter paper technique. In addition, CCs were only expressed as real images using electron microscopy,[23] which is relatively very costly. Our set of methods may help illustrate CCs at a low cost and provide information for the quantitative and qualitative analysis of CCs.

There are 2 prerequisites for the quantitative and qualitative analysis of CCs in sampled blood. The first is that mechanical or chemical shock should be minimized for quantitative analysis. Mechanical or chemical shock may destroy the CCs, thereby affecting their quantitative analysis. The second prerequisite is the necessity of hemolysis because multilayers of erythrocytes may hinder the detection of CCs in blood when viewed via polarized light microscopy. However, dilution by agents is not desirable for quantitative analysis. Instant freeze-thaw effectively removed erythrocytes and dispersed multilayer CCs into countable crystals. In

IMAGE 3. A, A single cholesterol crystal (CC) showing orange refraction (filter-paper rinse method, polarized light microscopy). B, Multilayer formation of CCs with blue or orange refraction (filter-paper rinse method, polarized light microscopy). (×400)

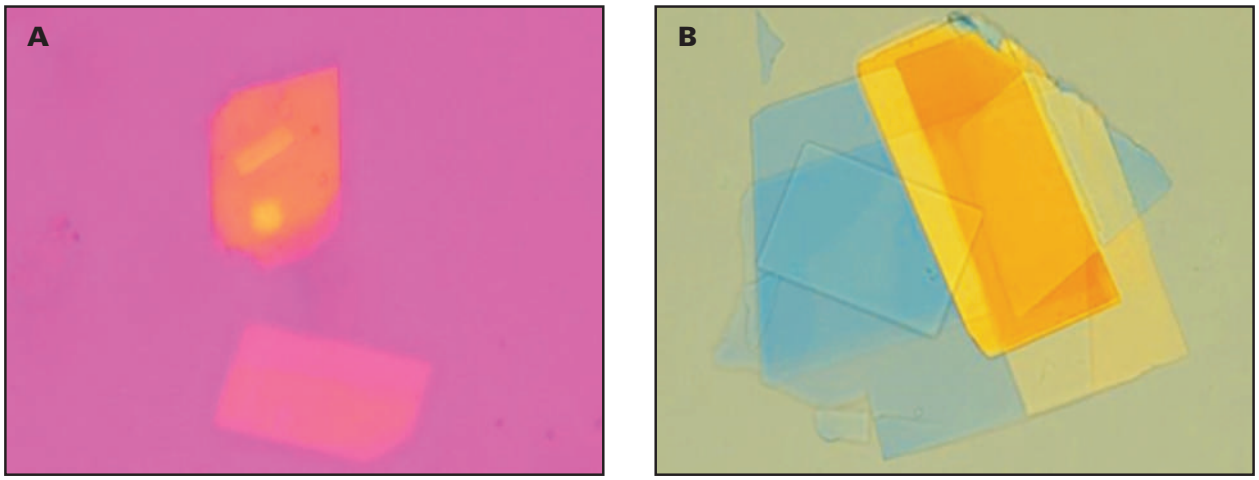

IMAGE 4. **Direct paraffin-embedding method for atheromatous particles. Hematoxylin and eosin stain of atheroma. A, Spindle-shaped ghost images of cholesterol crystals (CCs) with homogeneous eosinophilic substances (×40). B, Spindle-shaped ghost images of CCs and foamy macrophages (×200). C, Rich foamy macrophages and scant CCs as atheromatous materials (×40). D, Fibrin fragments with amorphous substances (×40).**

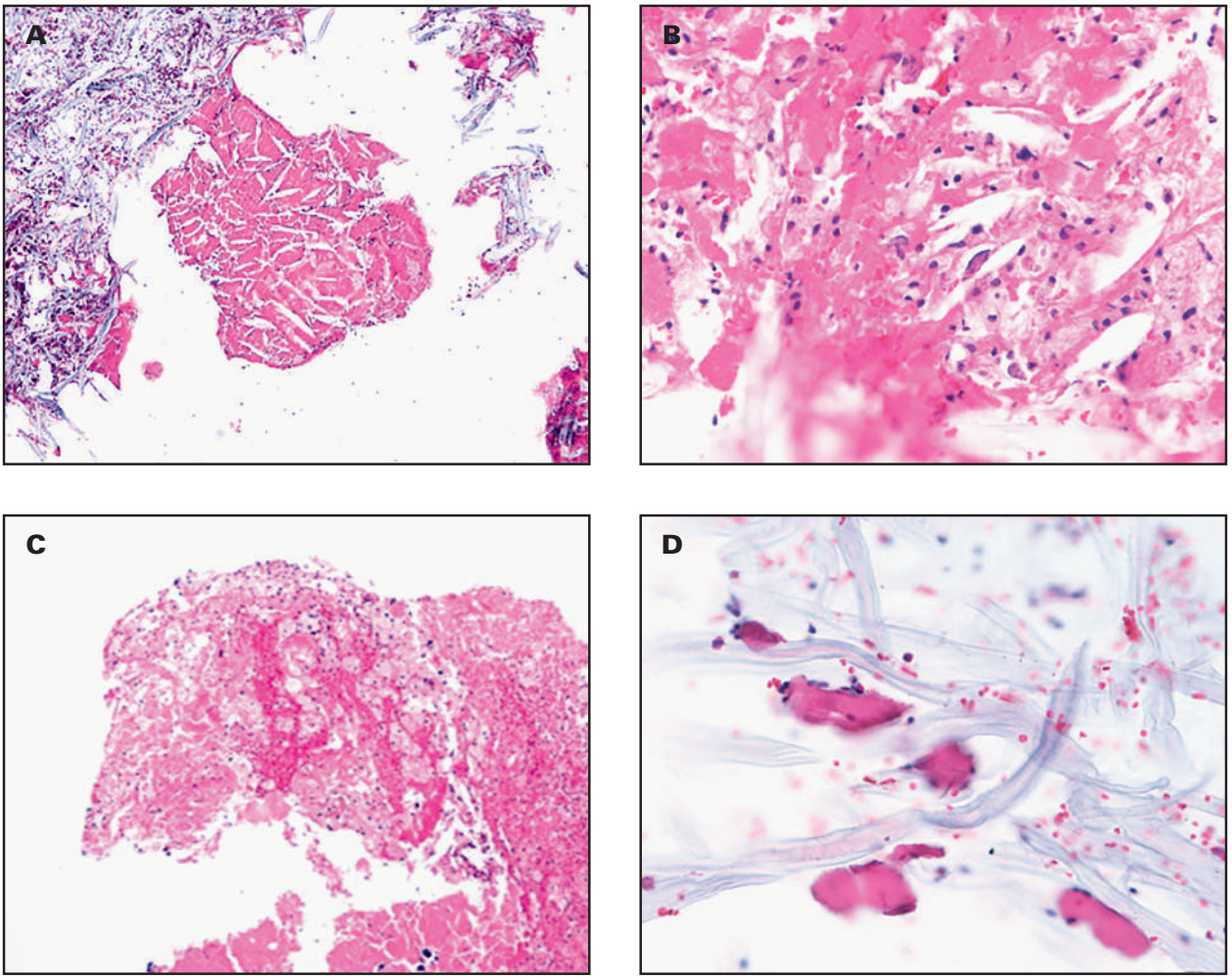

IMAGE 5. **Representative image of the commercially available cholesterol crystals (CCs) (Sigma C8667) made from sheep wool (×200). The shape is different from human CCs shown in Image 1.**

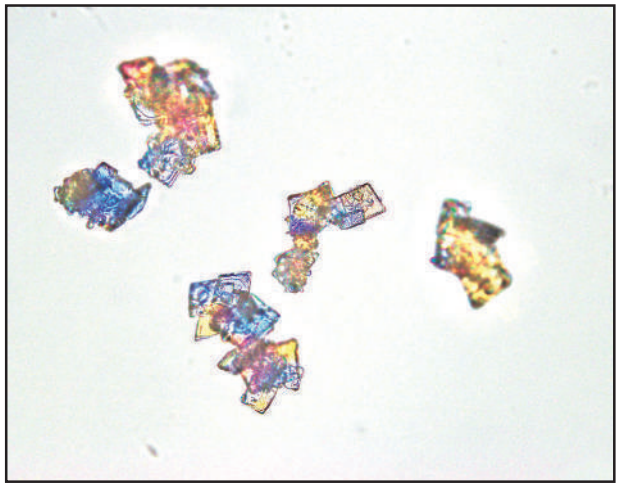

addition, blood on a glass slide can be frozen more easily than can blood in a test tube.

The selection of filter paper is based on the diameter of erythrocytes. If the pore size of a filter paper is smaller than the diameter of erythrocytes, then it may be difficult to distinguish plaque components and erythrocytes. If the pore size of a filter paper is too large as compared to the diameter of erythrocytes, then plaque components may pass through unfiltered. In considering the diameter of erythrocytes, we selected a filter paper with a pore size of 7 μm. The glittering shown by the crystals may obey the all-or-none law. A small amount of glittering may be different kinds of crystals such as uric acid if CCs were not detected from a filter paper. We were unable to visually detect a single CC with a diameter of 40 × 30 μm.[8] Lamé grade 0 may mean that there are few or no CCs. Lamé grade 1 may mean that there are CCs or other kinds of crystals. The filter-paper rinse method involves transferring CCs from a filter paper to a glass slide with minimized force. If a filter paper is rinsed with distilled water, then hemolysis may occur while transferring the CCs. The direct paraffin-embedding method was therefore applied for both H&E staining and immunohistochemistry.

2022;53;255–261 | https://doi.org/10.1093/labmed/lmab078

Using this set of methods, CCs may be detected in the aorta or any of the arteries, such as the coronary arteries[24] and peripheral arteries.[25] Free multilayer CCs were observed in blood obtained from the femoral artery using polarized light microscopy in a patient with cholesterol embolization syndrome.[25]

Conclusion

A set of novel methods for isolating and detecting CCs from sampled blood was established.

Supplementary Data

Supplemental video can be found in the online version of this article at www.labmedicine.com

Acknowledgments

The authors thank Daisuke Tamamoto, Koichi Matsumoto, Kaoru Irita, Sayaka Yamamoto, and Yuka Maekawa for technical assistance.

Conflict of Interest Statement

Kazuhisa Kodama is the president of Inter-tec Medicals. Sei Komatsu is a technical consultant for NemotoKyorin-do. The other authors have no conflicts of interest to declare.

REFERENCES

1. Mei JV, Alexander JR, Adam BW, Hannon WH. Use of filter paper for the collection and analysis of human whole blood specimens. *J Nutr.* 2001;131(5):1631S–1636S.
2. Pieter WS, Smit PW, Ivo E, et al. An overview of the clinical use of filter paper in the diagnosis of tropical diseases. *Am J Trop Med Hyg*. 2014;90(2):195–210.
3. Irmeen Q, Suhailur R, Ghazala M, et al. Utility of cytospin and cell block technology in evaluation of body fluids and urine samples: a comparative study. *J Cytol*. 2018;35(2):79–82.
4. Baloch ZW, Lee A, Cobbs C, et al. Millipore filter cell block preparation: an alternative to cell block in nongynecologic specimens of limited cellurarity. *DiganCytopathol*. 1999;20(6):389–392.
5. Komatsu S, Ohara K, Takahashi S, et al. Early detection of vulnerable atherosclerotic plaque for risk reduction of aortic rupture and thromboemboli and atheroemboli using non-obstructive angioscopy. *Cir J*. 2015;79(4):742–750.
6. Komatsu S, Takahashi S, Yutani C, et al. Spontaneous ruptured aortic plaque and injuries: insights for aging and acute aortic syndrome from non-obstructive general angioscopy. *J Cardiol.* 2020;75(4):344–351.
7. Komatsu S, Ohara T, Takahashi S, Takewa M, Yutani C, Kodama K. Improving the visual field in coronary artery by with non-obstructive angioscopy: dual infusion method. *Int J Cardiovasc Imaging.* 2017;33(6):789–796.
8. Komatsu S, Yutani C, Ohara T, et al. Angioscopic evaluation of spontaneously ruptured aortic plaques. *J Am Coll Cardiol.* 2018;71(25):2893–2902.
9. Nymo S, Niyonzima N, Espevik T, Mollnes TE. Cholesterol crystal-induced endothelial cell activation is complement-dependent and mediated by TNF. *Immunobiology.* 2014;219(10):786–792.
10. Janoudi A, Shamoun FE, Kalavakunta JK, Abela GS. Cholesterol crystal induced arterial inflammation and destabilization of atherosclerotic plaque. *Eur Heart J.* 2016;37(25):1959–1967.
11. Angelini A, Rubartelli P, Mistrorigo F, et al. Distal protection with a filter device during coronary stenting in patients with stable and unstable angina. *Circulation.* 2004;110(5):515–521.
12. Ezzeddine MA, Primavera JM, Rosand J, Hedley-Whyte ET, Rordorf G. Clinical characteristics of pathologically proved cholesterol emboli to the brain. *Neurology.* 2000;54(8):1681–1683.
13. Brown WP, Thore CR. Review: cerebral microvascular pathology in aging and neurodegeneration. *Neuropathol Appl Neurobiol*. 2011;37(1):56–74.
14. Yutani C, Nagano T, Komatsu S, Kodama K. Visible-free cholesterol crystal emboli adjunct to microinfarcts in myocardial capillaries and arterioles on H&E-stained frozen sections of an autopsied patient. *BMJ Case Rep*. 2018;2018:bcr2018225558. doi: 10.1136/bcr-2018-225558.
15. Scolari F, Ravani P. Atheroembolic renal disease. *Lancet.* 2010;375(9726):1650–1660.
16. Yutani C, Imakita M, Ishibashi-Ueda H, et al. Cerebro-spinal infarction caused by atheromatous emboli. *Acta Pathol Jpn.* 1985;35(4):789–801.
17. Masuda J, Yutani C, Ogata J, Kuriyama Y, Yamaguchi T. Atheromatous embolism in the brain: a clinicopathologic analysis of 15 autopsy cases. *Neurology.* 1994;44(7):1231–1237.
18. Duewell P, Kono H, Rayner KJ, et al. NLRP3 inflammasomes are required for atherogenesis and activated by cholesterol crystals. *Nature.* 2010;464(7293):1357–1361.
19. Goto S, Ohshima T, Kato K, Izumi T, Wakabayashi T. Efficacy of carotid artery stenting by the universal protection method. *J Stroke Cerebrovasc Dis.* 2018;27(8):2187–2191.
20. Nathan NA, Narayan E, Smith MM, et al. Cell block cytology. Improved preparation and its efficacy in diagnosis cytology. *Am J Clin Pathol*. 2000;114(4):559–606.
21. Krogerus LA, Andersson LC. A simple method for the preparation of paraffin-embedded cell blocks from fine needle aspirates, effusions and brushings. *Acta Cytol.* 1988;32(4):585–587.
22. Nassan A, Chohen C, Siddiqui MT. Utility of millipore filter and cell block in thyroid needle aspirations: which method is superior? *Diagn Cytopathol*. 2007;35(1):34–38.
23. Abela GS. Cholesterol crystals piercing the arterial plaque and intima trigger local and systemic inflammation. *J Clin Lipidol.* 2010;4(3):156–164.
24. Komatsu S, Yutani C, Takahashi S, Kodama K. Acute myocardial infarction caused by distal embolization from a proximal ruptured plaque. *JACC Case Rep*. 2020;2(1):33–34.
25. Komatsu S, Yutani C, Takewa M, Takahashi S, Kodama K. Detecting free cholesterol crystals in a patient with spontaneous cholesterol embolization syndrome. *JACC Case Rep.* 2020;2(4):615–618.

Efficacy of POC Antibody Assays after COVID-19 Infection and Potential Utility for "Immunity Passports"

Akram Shalaby, MD,[1,] Hansini Laharwani, MD,[1] John T. Bates, PhD,[1] Patrick B. Kyle, PhD[1]*

[1]University of Mississippi Medical Center, Jackson, Mississippi, US; *To whom correspondence should be addressed. akramshalaby91@gmail.com

Keywords: COVID-19, SARS-CoV-2, antibody tests, ELISA, lateral flow assays

Abbreviations: ELISA, enzyme-linked immunosorbent assay; RT-PCR, real-time polymerase chain reaction; UMMC, University of Mississippi Medical Center; RBD, receptor binding domain; PBS, phosphate-buffered saline.

Laboratory Medicine 2022;53:262–265; https://doi.org/10.1093/labmed/lmab093

ABSTRACT

Objective: Numerous manufacturers market lateral flow assays for the detection of SARS-CoV-2 antibodies, but there are many questions about the reliability and efficacy of these tests.

Materials and Methods: Serum specimens from 60 individuals were analyzed using 2 lateral flow antibody assays, an in-house enzyme-linked immunosorbent assay (ELISA), and the Abbott SARS-CoV-2 IgG chemiluminescent immunoassay.

Results: The BioMedomics and Premier Biotech lateral flow assays were positive for IgM in 73.3% and 70% and for IgG in 80% and 73.3% of specimens, respectively. The ELISA assay was positive for IgM and IgG in 73.3% and 86.7% of specimens from infected individuals, whereas the Abbott assay was positive in 80%. The specificities of the 4 assays ranged from 96.7% to 100% for IgM and from 93.3% to 100% for IgG.

Conclusion: Results of the 2 lateral flow assays were comparable to those of the ELISA and Abbott assays. Assay efficacy depended on length of time after SARS-CoV-2 infection.

COVID-19, caused by the SARS-CoV-2 virus, rapidly spread globally and was declared a worldwide pandemic in March 2020. The gold standard test methodology for the diagnosis of SARS-CoV-2 infection involves real-time polymerase chain reaction (RT-PCR) of viral RNA collected via a nasopharyngeal swab.[1] The detection of antibodies formed in response to SARS-CoV-2 could be a useful methodology to safely return adults to the workplace and children to school. Given estimates of asymptomatic COVID-19 infections ranging from 16% to 30%,[2] antibody tests may help us understand how the epidemic has progressed and provide crucial information about the true mortality of the disease. Early data suggested that convalescent plasma infusion and antibody tests were used to identify potential plasma donors as a treatment option for patients with COVID-19.[3-5]

Some reservations exist regarding the accuracy of available antibody tests, which became evident when the United Kingdom determined that 1 million test kits purchased from China lacked sufficient accuracy and could not be used for testing.[6] In addition, not all point-of-care tests have been properly vetted, and the results of these assays may vary.[7] A study comparing the performance of 7 lateral-flow IgM/IgG assays found sensitivities ranging from 50% to 97.4% in specimens collected 14 to 25 days after symptom onset.[8] In the current study, we sought to evaluate 2 point-of-care assays manufactured for the detection of human antibodies to the SARS-CoV-2 virus by comparing them to an in-house enzyme-linked immunosorbent assay (ELISA) and a commercially available assay.

Materials and Methods

Sixty previously tested patient specimens designated for disposal were obtained from the University of Mississippi Medical Center (UMMC) laboratory for this evaluation. Each specimen was collected from patients who presented to UMMC with symptoms suspicious for COVID-19 from late March to mid-April 2020. Of the 60 specimens, 30 originated from individuals positive for SARS-CoV-2 and 30 from negative individuals as determined by RT-PCR using the Abbott RealTime SARS-CoV-2 on an Abbott M2000 analyzer. The serum specimens were collected at a mean of 13.4 days after symptom onset (range, 7–30 days; lower quartile, 9.75; upper quartile, 15.5). The mean age of all patients included in the study was 54 years (range, 5–95 years). Thirty-one of the patients in the study were males and 29 were females. See **TABLE 1** and **TABLE 2** for patient demographics.

BioMedomics and Premier Biotech Rapid IgG-IgM Antibody Assays

Two commercially available point-of-care lateral flow assays manufactured in China and distributed in the United States by BioMedomics (Morrisville, NC) and Premier Biotech (Minneapolis, MN) were evaluated. Each of the assays are qualitative in nature and are designed to detect IgG and IgM antibodies specific to SARS-CoV-2 in serum, plasma, or whole blood. Package inserts do not state the antigen(s) used in either test or the expression systems used to generate the antigens. Each test cassette was received

sealed in a foil pouch with a desiccant and buffer. An alcohol pad and lancet were also provided with each Premier Biotech test cassette. Each test cassette has 3 regions that contain reaction antigen for IgG antibodies, IgM antibodies, and a positive control. The presence of antibodies is indicated by the appearance of a purple line in the IgM or IgG regions, which indicates a functioning test. Testing was performed as per each manufacturer's instructions. We added 10 μL of serum to the sample well in the respective device, followed by 2 drops of buffer solution in the buffer well. Results were determined visually after 15 minutes had elapsed.

IgM and IgG ELISA Assays

Per Stadlbauer et al,[9] ELISAs were developed for the measurement of human IgM and IgG antibodies specific for the receptor-binding domain (RBD) of the SARS-CoV-2 spike protein. We coated 384-well MaxiSorp plates (Thermo Fisher Scientific) with purified recombinant RBD at a concentration of 3 μg/mL in phosphate-buffered saline (PBS). Recombinant RBD that was produced in Sf9 insect cells was purchased from Genescript. The coating volume and reaction volumes were 25 μL per well. Plates were incubated overnight at 4°C, washed 3 times with PBS containing 0.1% Tween20, and blocked with PBS containing 3% dry milk for 1 hour at room temperature. The blocking buffer was removed, and specimens (1-log dilutions in blocking buffer, 5×10^1-5×10^4) were added to the wells. Plates were incubated for 2 hours at room temperature before washing 3 times. Horseradish peroxidase conjugated to anti-human IgG FC (Southern Biotech) or anti-human IgM (Southern Biotech) was diluted 1:3000 in PBS containing 1% dry milk, added to the wells, and incubated at room temperature for 1 hour. The plates were washed 5 times and developed with tetramethyl-benzidine (Southern Biotech). After 30 minutes, development was stopped by adding 25 μL of 2N H_2SO_4 to each well. Absorbance was measured at 450 nm. The endpoint dilution titer was set to the serum dilution that resulted in an absorbance of 0.2 absorbance units over background. A specimen was counted as having a positive result if the reciprocal of the endpoint dilution was >5000 absorbance units.

Abbott SARS-CoV-2 IgG Assay

The SARS-CoV-2 IgG assay (Abbott Diagnostics, Abbott Park, IL) is a chemiluminescent microparticle immunoassay designed for the detection of IgG antibodies to the nucleocapsid protein of SARS-CoV-2. For this assay, 150 μL of serum or plasma is mixed with SARS-CoV-2 antigen-coated microparticles and allowed to react. After a wash step, anti-human IgG acridinium-labeled conjugate is added, is allowed to incubate, and is washed. Chemiluminescence is measured as relative light units. The presence of antibodies is associated with increasing luminescence. A cutoff of 1.4 S/C was used for positivity as per the manufacturer. All analyses were performed on an Architect i2000SR (Abbott Diagnostics) after proper calibration as recommended by the assay manufacturer.

TABLE 1. Demographics of Patients Who Tested Positive by RT-PCR (n = 30)

Feature	n (%)
Sex	
Male	14 (47)
Female	16 (53)
Age at time of presentation (y)	
Range	5–95
Mean	57
Race/ethnicity	
Black	23 (77)
White	5 (17)
Hispanic	1 (3)
Asian	0 (0)
Unknown	1 (3)

RT-PCR, real-time polymerase chain reaction.

TABLE 2. Demographics of Patients Who Tested Negative by RT-PCR (n = 30)

Feature	n (%)
Sex	
Male	17 (57)
Female	16 (43)
Age at time of presentation (y)	
Range	18–91
Mean	51
Race/ethnicity	
Black	18 (60)
White	10 (33)
Hispanic	1 (3)
Asian	1 (3)
Unknown	0 (0)

RT-PCR, real-time polymerase chain reaction.

Results

Of the 30 specimens from infected patients, the in-house ELISA assay was positive for IgM and IgG in 22 (73.3%) and 26 (86.7%) patients, respectively. The BioMedomics antibody assay found 73.3% and 80% positivity for IgM and IgG, respectively, whereas the Premier Biotech assay found 70% and 73.3% positivity for IgM and IgG, respectively. The Abbott chemiluminescence microparticle assay was positive in 24 patients who were RT-PCR–positive and negative in all patients who were RT-PCR–negative. The 4 serological assays showed a specificity ranging from 96.7% to 100% for IgM and from 93.3% to 100% for IgG. The control line formed in each of the BioMedomics and Premier Biotech tests, indicating that the assays were properly functioning (**FIGURE 1**). See **TABLE 3** for the sensitivity and specificity of all antibody assays included in our study.

Our results also showed an increased sensitivity and specificity of the BioMedomics and Premier Biotech assays over time. The sensitivity and specificity of both assays for IgM and/or IgG in specimens collected >14 days after RT-PCR testing was 100%. See **TABLE 4** for the sensitivity and specificity of the BioMedomics and Premier Biotech assays for IgM and/or IgG in specimens collected at different time intervals from the RT-PCR testing date.

Discussion

Point-of-care antibody tests for SARS-CoV-2 have several advantages: They are inexpensive, easy to perform, and offer rapid results. Antibody tests for SARS-CoV-2 antibodies may provide an insight into the prevalence of COVID-19 in specific geographic locations. This concept was shown in a pilot study in Chelsea, MA, involving 200 apparently healthy individuals, of whom 64 (approximately 30%) were positive for antibodies to SARS-CoV-2. These findings provided a valuable snapshot in a community known

to have a high prevalence of disease at the time.[10] The Florida Department of Health reported that 4.4% of 123,552 healthcare workers, firefighters, police officers, and first responders were positive for antibodies.[11,12]

In this study, 2 of the immunoassays, ELISA and BioMedomics, exhibited false-positive results that reduced their specificities to 93.3% and 96.7%, respectively. Assays with very high specificities are required for population screening because when prevalence is low, even a few false-positive results cause a significant overestimation of disease.[13] For example, if the prevalence of the disease in the population is 5%, the positive predictive value of a test that exhibits 95% sensitivity and 95% specificity will be 50.0%, essentially a coin toss. Meanwhile, tests that exhibit 95% sensitivity but 99% and 99.5% specificity would exhibit positive predictive values of 83.3% and 90.8%, respectively. Therefore, positive results from assays that exhibit low specificity should be followed with another test whenever the prevalence of disease is low.[14] Although these antibody tests correlated well with RT-PCR results, they did not meet the 99% specificity recommended for population surveillance. In this dataset, a follow-up test would have eliminated all false-positive results.

Interestingly, 3 patients with COVID-19 who tested positive by RT-PCR were negative on all 4 serological assays. This outcome could have resulted from antibody concentrations below the detection limit, which could occur with a weak immune response to the virus or during the early stages of disease before sufficient antibody concentrations have formed. A study of sailors infected during the USS Theodore Roosevelt outbreak found that only 90% of infected individuals who reported a positive RT-PCR test before the study made detectable levels of SARS-CoV-2 spike-specific antibody after infection,[15] which generally agrees with the 87% seroconversion we observed. Reasons for the low seroconversion rate among RT-PCR–confirmed infections remain unknown but are likely related to the length of time after infection.

Our results showed sensitivities of 50% and 100% for both the BioMedomics and Premier Biotech assays in specimens collected <7 days and >14 days after the RT-PCR testing, respectively. Others have attributed negative SARS-CoV-2 antibody results after confirmed infection to delayed specific antibody responses in patients with severe illness.[16,17] The 3 specimens that were negative by both lateral flow assays, ELISA, and the Abbott ARCHITECT but collected from patients who were RT-PCR–confirmed positive were collected at 7, 9, and 10 days after the onset of symptoms. These specimens would have been expected to contain sufficient concentrations of IgM, if not IgG.[18] Given the reported variability of the antibody response to SARS-CoV-2 infection, the agreement between these assays raises the possibility that these specimens represent true biological negatives rather than false negatives.

Antibodies are likely to offer protection against reinfection with SARS-CoV-2; therefore, antibody assays may have a role in identifying immune individuals. One study involving 3.2 million people who had undergone SARS-CoV-2 antibody testing concluded that seropositive individuals have a significantly decreased risk for future SARS-CoV-2 infection.[19] Animal studies investigating immune response in rhesus macaque monkeys[20,21] also showed humoral and cellular immune response to SARS-CoV-2, suggesting that some level of protective immunity may occur. The transfer of sera from immunized primates to hACE2 transgenic mice in another study protected against a challenge with SARS-CoV-2.[22] Antibodies are the correlate of protection for the great majority of viral infections and seem to correlate with protection against SARS CoV-2 infection.[23]

There is an ongoing debate about the use of "immunity passports" and their role in travel restrictions.[24] Several European countries began issuing certificates of travel to verify vaccination against SARS-CoV-2, receipt of a negative test result, or recovery from the virus.[25] Italy, Iceland, Spain, Greece, and other countries were opening their borders to travelers who have been vaccinated or recently tested negative for COVID-19.[26] Note that at this time, the U.S. Food & Drug Administration does not recommend antibody tests to assess immunity or protection from vaccination.[27] Because

TABLE 3. Results of Serologic Antibody Assays

	BioMedomics	Premier Biotech	ELISA	Abbott
Sensitivity				
IgM	73.3%	70%	73.3%	N/A
IgG	80%	73.3%	86.7%	80%
Specificity				
IgM	96.7%	100%	100%	N/A
IgG	96.7%	100%	93.3%	100%

ELISA, enzyme-linked immunosorbent assay.

TABLE 4. Sensitivity and Specificity of BioMedomics and Premier Biotech Assays for SARS-CoV-2 IgG and/or IgM Antibodies at Different Time Intervals From RT-PCR Testing Date

	BioMedomics	Premier Biotech
Sensitivity		
<7 days	50%	50%
7–14 days	93%	93%
>14 days	100%	100%
Specificity		
<7 days	86%	86%
7–14 days	100%	100%
>14 days	100%	100%

RT-PCR, polymerase chain reaction.

FIGURE 1. Premier Diagnostics (top row) and BioMedomics (bottom row) lateral flow assays. Cartridges 13–15 illustrate positive results for both IgG and IgM, whereas cartridge 16 illustrates negative results for both IgG and IgM.

the presence of antibodies to COVID-19 likely indicates immunity,[19] antibody tests could play a role as one modality to prove immunity in previously infected individuals. This testing could benefit travelers from underserved countries with limited vaccination rates or limited COVID-19 testing. Given the results observed in this study, antibody tests may provide variable results within the first 10 days after the development of symptoms of SARS-CoV-2 infection. Point-of-care tests are inexpensive, easy to perform, offer rapid results, and may have a utility in screening for immunity and resuming international travel even at the point of travel. A limitation of antibody tests could involve the potential misinterpretation of results in that (1) days or weeks are required for seroconversion after infection and (2) assay sensitivities and specificities may vary considerably.

Conclusion

One limitation of our study is the small sample size, in that we only examined 30 specimens from patients who were RT-PCR–positive and 30 specimens from patients who were negative. In addition, all our specimens were collected within 21 days of the RT-PCR testing. Larger studies evaluating specimens collected at longer time intervals are needed to assess the utility of serological assays in confirming past SARS-CoV-2 infection and immunity.

Conflict of Interest Statement

The authors certify that they have no affiliations with or involvement in any organization or entity with any financial interest in the subject matter or materials discussed in this article.

REFERENCES

1. Corman V, Landt O, Kaiser M, et al. Detection of 2019 novel coronavirus (2019-nCoV) by real-time RT-PCR. *Euro Surveill*. 2020;25(3):2000045.
2. Byambasuren O, Cardona M, Bell K, et al. Estimating the extent of asymptomatic COVID-19 and its potential for community transmission: systematic review and meta-analysis. Preprint. Posted online September 13, 2020. *medRxiv*. doi: 10.1101/2020.05.10.20097543.
3. Duan K, Liu B, Li C, et al. Effectiveness of convalescent plasma therapy in severe COVID-19 patients. *Proc Natl Acad Sci U S A.* 2020;117(17):9490–9496.
4. Shen C, Wang Z, Zhao F, et al. Treatment of 5 critically ill patients with COVID-19 with convalescent plasma. *JAMA.* 2020;323(16):1582–1589.
5. Bloch EM, Shoham S, Casadevall A, et al. Deployment of convalescent plasma for the prevention and treatment of COVID-19. *J Clin Invest.* 2020;130(6):2757–2765.
6. Kirkpatrick DD, Bradley J. UK paid $20 million for new coronavirus tests. They didn't work. https://www.nytimes.com/2020/04/16/world/europe/coronavirus-antibody-test-uk.html. Updated December 17, 2020. Accessed September 29, 2021.
7. Li Z, Yi Y, Luo X, et al. Development and clinical application of a rapid IgM-IgG combined antibody test for SARS-CoV-2 infection diagnosis. *J Med Virol.* 2020;92(9):1518–1524.
8. Van Elslande J, Houben E, Depypere M, et al. Diagnostic performance of seven rapid IgG/IgM antibody tests and the Euroimmun IgA/IgG ELISA in COVID-19 patients. *Clin Microbiol Infect.* 2020;26(8):1082–1087.
9. Stadlbauer D, Amanat F, Chromikova V, et al. SARS-CoV-2 seroconversion in humans: a detailed protocol for a serological assay, antigen production, and test setup. *Curr Protoc Microbiol.* 2020;57(1):e100.
10. Saltzman J. Nearly a third of 200 blood samples taken in Chelsea show exposure to coronavirus. https://www.bostonglobe.com/2020/04/17/business/nearly-third-200-blood-samples-taken-chelsea-show-exposure-coronavirus/. Updated April 17, 2020. Accessed September 29, 2021.
11. Florida Department of Health now reporting antibody test results. https://www.capecoralbreeze.com/news/local-news/2020/05/29/florida-department-of-health-now-reporting-antibody-test-results/. Updated May 29, 2020. Accessed September 29, 2021.
12. Chang D. After weeks of antibody testing, Florida to report results for the first time Friday. https://www.miamiherald.com/news/health-care/article243028726.html. Updated May 28, 2020. Accessed September 29, 2021.
13. Horvath K, Semlitsch T, Jeitler K, Krause R, Siebenhofer A. Antibody tests for COVID-19: what the results tell us [in German]. *Z Evid Fortbild Qual Gesundhwes.* 2020;153:54–59.
14. Centers for Disease Control and Prevention. Interim guidelines for COVID-19 antibody testing. https://www.cdc.gov/coronavirus/2019-ncov/lab/resources/antibody-tests-guidelines.html. Updated September 21, 2021. Accessed September 29, 2021.
15. Payne DC, Smith-Jeffcoat SE, Nowak G, et al; CDC COVID-19 Surge Laboratory Group. SARS-CoV-2 infections and serologic responses from a sample of U.S. Navy service members—USS Theodore Roosevelt, April 2020. *MMWR Morb Mortal Wkly Rep.* 2020;69(23):714–721.
16. Xie J, Ding C, Li J, et al. Characteristics of patients with coronavirus disease (COVID-19) confirmed using an IgM-IgG antibody test. *J Med Virol.* 2020;92(10):2004–2010.
17. Shen L, Wang C, Zhao J, et al. Delayed specific IgM antibody responses observed among COVID-19 patients with severe progression. *Emerg Microbes Infect.* 2020;9(1):1096–1101.
18. Padoan A, Cosma C, Sciacovelli L, Faggian D, Plebani M. Analytical performances of a chemiluminescence immunoassay for SARS-CoV-2 IgM/IgG and antibody kinetics. *Clin Chem Lab Med.* 2020;58(7):1081–1088.
19. Harvey RA, Rassen JA, Kabelac CA, et al. Association of SARS-CoV-2 seropositive antibody test with risk of future infection. *JAMA Intern Med.* 2021;181(5):672–679.
20. Chandrashekar A, Liu J, Martinot AJ, et al. SARS-CoV-2 infection protects against rechallenge in rhesus macaques. *Science.* 2020;369(6505):812–817.
21. Bongiovanni M, Basile F. Re-infection by COVID-19: a real threat for the future management of pandemia? *Infect Dis (Lond).* 2020;52(8):581–582.
22. Yang J, Wang W, Chen Z, et al. A vaccine targeting the RBD of the S protein of SARS-CoV-2 induces protective immunity. *Nature.* 2020;586(7830):572–577.
23. Plotkin SA. Correlates of protection induced by vaccination. *Clin Vaccine Immunol.* 2010;17(7):1055–1065.
24. Brown RCH, Kelly D, Wilkinson D, Savulescu J. The scientific and ethical feasibility of immunity passports. *Lancet Infect Dis.* 2021;21(3):e58–e63.
25. Zakrzewski C. The Technology 202: European countries are starting to issue vaccine passports. The system is very different than the U.S. approach. https://www.washingtonpost.com/politics/2021/06/02/technology-202-european-countries-are-starting-issue-vaccine-passports-system-is-very-different-than-us-approach/. Updated June 2, 2021. Accessed September 29, 2021.
26. Josephs L. Covid vaccine passports: everything we know so far. https://www.cnbc.com/2021/05/22/covid-vaccine-passports-everything-we-know-so-far.html. Updated May 22, 2021. Accessed September 29, 2021.
27. U.S. Food & Drug Administration. FDA in brief: FDA advises against use of SARS-CoV-2 antibody test results to evaluate immunity or protection from COVID-19, including after vaccination. https://www.fda.gov/news-events/press-announcements/fda-brief-fda-advises-against-use-sars-cov-2-antibody-test-results-evaluate-immunity-or-protection. Updated May 19, 2021. Accessed September 29, 2021.

Is Cryoprecipitate-Reduced Plasma an Efficacious Replacement Fluid for Therapeutic Plasma Exchange for Patients with Thrombotic Microangiopathy? A Single-Center Retrospective Experience

Han Joo Kim, MD, MSc,[1] John Jeongseok Yang, MD, MSc,[1] Hyungsuk Kim, MD, MSc,[2] Sang-Hyun Hwang, MD, PhD,[1] Heung-Bum Oh, MD, PhD,[1] Yousun Chung, MD, MSc,[3] Dae-Hyun Ko, MD, PhD[1,]*

[1]Department of Laboratory Medicine, Asan Medical Center, University of Ulsan College of Medicine, Seoul, Republic of Korea, [2]Department of Laboratory Medicine, Seoul National University Hospital, Seoul, Republic of Korea, [3]Department of Laboratory Medicine, Kangdong Sacred Heart Hospital, Seoul, Republic of Korea; *To whom correspondence should be addressed. daehyuni1118@amc.seoul.kr

Keywords: therapeutic plasma exchange, cryoprecipitate-reduced plasma, fresh frozen plasma, thrombotic microangiopathy, thrombotic thrombocytopenic purpura, microangiopathic hemolytic anemia

Abbreviations: CRP, cryoprecipitate-reduced plasma; FFP, fresh froen plasma; TMA, thrombotic microangiopathy; TPE, therapeutic plasma exchange; LD, lactate dehydrogenase; TTP, thrombotic thrombocytopenic purpura; TA-TMA, transplantation-associated thrombotic microangiopathy; Hb, hemoglobin; fRBC, fragmented red blood cell; vWF, von Willebrand factor.

Laboratory Medicine 2022;53:266–272; https://doi.org/10.1093/labmed/lmab092

ABSTRACT

Objective: We designed a study to compare the efficacy of cryoprecipitate-reduced plasma (CRP) and fresh frozen plasma (FFP), at the level of individual sessions, for treating refractory thrombotic microangiopathy (TMA) with therapeutic plasma exchange (TPE).

Materials and Methods: Platelet counts (× $10^3/\mu L$) and lactate dehydrogenase (LD; IU/L) levels were measured before and after each session. We compared the mean-percentage and absolute changes in platelet count and LD after each TPE session.

Results: The data from 33 patients treated for TMA between 2009 and 2018 were collected for this study. Both absolute and percentage increases in the platelet count were statistically significant (P = .003 and P = .011, respectively) when CRP was used. However, when patients were divided into subgroups according to specific diagnosis, no significant differences were found among the groups, except in terms of the absolute platelet count increase in the thrombotic thrombocytopenic purpura group (P <.001).

Conclusion: The platelet count increase was higher when patients received CRP than when they received FFP. We found that CRP may be a rescue option for patients with refractory TMA.

Thrombotic microangiopathy (TMA) is a pathologic and clinical term that refers to various disorders. The pathologic features of TMA are vascular occlusion with intraluminal thrombi and endotheliosis, along with luminal and vessel-wall fibrin deposition, typically observed in kidney biopsy findings. The clinical characteristics of TMA include microangiopathic hemolytic anemia with thrombocytopenia, often accompanied by organ injury.[1] Primary TMAs are classified into different diseases according to pathophysiology, which also include thrombotic thrombocytopenic purpura (TTP), Shiga toxin–mediated hemolytic-uremic syndrome, drug-induced TMA, complement-mediated TMA, and cobalamin-deficiency TMA. For these primary TMAs, urgent treatment targeting the pathophysiology of each entity is essential to optimize patient outcomes. In the case of TTP, immediate initiation of therapeutic plasma exchange (TPE) is the most important first-line intervention.[2,3]

In general, fresh frozen plasma (FFP) is the recommended replacement fluid for plasma exchange for patients with TTP or TMA. According to guidelines disseminated by the American Society for Apheresis, replacement by plasma exchange for TTP and other TMAs should be performed with FFP or FFP used together with albumin.[3,4] The British Society for Haematology recommends solvent/detergent-treated FFP as the sole replacement fluid.[4] However, few studies have investigated the efficacy of cryoprecipitate-reduced plasma (CRP) as a replacement fluid for patients with TTP. A study investigating the influence of replacement fluid on survival found no significant difference between CRP and FFP for patients with refractory TTP even with repeated TPE.[5,6] This finding indicates that CRP is an acceptable replacement fluid. In contrast, a study evaluating the efficacy of CRP as a replacement fluid concluded that CRP should not be used as a first-line alternative fluid for patients with newly diagnosed TTP.[7] A few

more studies have compared the prognosis associated with CRP and FFP for plasma exchange in the context of TTP or TMA. In this study, we compared the responses in each plasma exchange session when using CRP and FFP as replacement fluids for patients diagnosed with TMA, including TTP.

Materials and Methods

This study was approved by the institutional review board of the Asan Medical Center (2019-0588).

Study Sample

The data from 33 nonselected patients with TMA treated with TPE using CRP as a replacement fluid were retrospectively collected from December 2009 through December 2018. Only 2 patients had TTP confirmed by ADAMTS-13 activity levels. Patients whose ADAMTS-13 activity test results were less than 10% were classified as having TTP. Patients with TMA features, having previously undergone hematopoietic stem cell or solid organ transplantation, were classified as having transplantation-associated TMA (TA-TMA). Patients who did not fall into either category were classified as having "TMA, others."

Patients for whom laboratory results such as platelet count and lactate dehydrogenase (LD) levels did not improve despite plasmapheresis with FFP were defined as refractory. Therefore, patients with refractory TTP were those for whom there was no choice but to devise a treatment method other than TPE using FFP.

Study data were obtained from electronic medical records at the Asan Medical Center (Seoul, Republic of Korea). Analyzed patient-level variables included age, sex, diagnosis, underlying disease, transplantation history, number of TPEs, platelet count, serum LD level, hemoglobin (Hb) concentration, fragmented red blood cell (fRBC) count, ADAMTS-13 activity, serum haptoglobin level, and last follow-up date.

TPE

Plasma exchange was performed using the COBE Spectra (Terumo BCT, Lakewood, CO), Amicus Separator (Fresenius-Kabi, Bad Homburg, Germany), or Spectra Optia (Terumo BCT, Lakewood, CO) devices. We used FFP or CRP as replacement fluids. The latter was used for patients with refractory TMA despite several sessions of TPE using FFP. All patients underwent 1.0 plasma volume exchange regardless of the replacement fluids, instruments, or diagnosis.

Efficacy Variables

The changes in fRBC count, plasma Hb, and haptoglobin could not be analyzed because there were too many missing data points. The effectiveness of the replacement fluids was estimated by comparing the absolute and percentage changes in platelet counts and LD levels, which are the most important variables for monitoring TMA. The Hb levels were also compared with the platelet counts and LD levels. These observations were documented and compared before and after each TPE session. An increase in platelet counts or Hb or a decrease in LD after each TPE session was considered as evidence of effective treatment.

Statistical Analysis

Continuous variables are summarized as mean ± standard deviation and were compared using the Mann-Whitney *U* test. Categorical data are presented as numbers and proportions. All statistical analyses were conducted using PASW Statistics for Windows (version 18.0; IBM, Chicago, IL). Statistical significance was set at $P \leq .05$.

Results

Patient Demographic and Clinical Characteristics

The patients' demographic and clinical characteristics are summarized in **TABLE 1**. A total of 33 patients were enrolled, with an age range of 1 to 91 years (median age, 50 years). Two patients were diagnosed with TTP, for whom the ADAMTS-13 activity results were <5% and 0%, respectively. Eleven patients had previously undergone transplantation, 7 of whom had undergone hematopoietic stem cell transplantation. Twenty other patients without ADAMTS-13 deficiency or transplantation history were classified as TMA, others.

Comparison of Changes in Each Variable

The mean (standard deviation) changes in platelet count, LD levels, and Hb levels before and after TPE were calculated (**TABLE 2**). The mean

TABLE 1. Patient Demographics and Clinical Characteristics[a]

Characteristic	Observation (n = 33)
Age (y)[b]	50 (1–91)
Sex	
Male	13 (39.4%)
Female	20 (60.6%)
Diagnosis	
TTP	2 (6.1%)
TA-TMA	11 (33.3%)
TMA, others	20 (60.6%)
Underlying disease	
None	8 (24.2%)
Rheumatic disease	5 (15.2%)
Solid tumor	6 (18.2%)
Hematopoietic malignancy	6 (18.2%)
Others	8 (24.2%)
Transplantation history	
Liver	2 (6.1%)
Kidney	2 (6.1%)
Hematopoietic stem cell	7 (21.2%)
Total	11 (33.3%)
Total plasma volume exchanged each TPE session (L)[c]	3.37 (3.38)
Number of TPEs per patient[b]	
Replaced by FFP or 5% albumin	7 (2–25)
Replaced by CRP	4 (1–21)
Total	12 (3–38)
Initial platelet count (/μL)[d]	53,000 (49,000)
Initial lactate dehydrogenase (IU/L)[d]	2060 (3674)
Initial Hb (g/dL)[d]	8.4 (1.6)

CRP, cryoprecipitate-reduced plasma; FFP, fresh frozen plasma; Hb, hemoglobin; TA-TMA, transplantation-associated thrombotic microangiopathy; TMA, thrombotic microangiopathy; TMA, others, patients who did not fall into TPE or TA-TMA categories; TPE, therapeutic plasma exchange; TTP, thrombotic thrombocytopenic purpura.
[a]Data are presented as number (%), unless otherwise specified.
[b]Ages and number of TPEs are presented as median (range).
[c]Total plasma volume exchanged per each TPE session is presented as mean (median).
[d]Initial laboratory results are presented as mean (standard deviation).

absolute and percentage changes according to the type of replacement fluid were compared. There were 459 TPE sessions, of which 183 used CRP. Overall, when TPE involved CRP replacement, both the mean absolute and percentage changes in platelet count increased significantly (**FIGURE 1**; $P = .003$, $P = .011$).

Although the mean Hb concentrations did not increase significantly, there was a nonsignificant improvement, particularly in association with TPEs using CRP (**FIGURE 1E** and **1F**). However, when the study sample was divided into groups according to diagnosis (TTP; TA-TMA; and TMA, others), no statistically significant differences were found except for the mean absolute increase in platelet count among patients with TTP (**FIGURE 2**; $P < .001$).

Discussion

Research has suggested that TPE is an effective treatment for TMA, because the replaced fluid can replenish the missing enzymes and eliminate factors such as autoantibodies, complement, and ultralarge von Willebrand factor (vWF), known to be responsible for TMA pathophysiology. Although TPE is known to be the most important component of TMA management (including TTP), not all patients respond to TPE, and the reasons for refractoriness to plasmapheresis are not clearly understood. Previous studies have investigated replacement fluids other than FFP, such as CRP, solvent-/detergent-treated plasma, psoralen-treated plasma, or methylene blue–treated FFP. In particular, CRP has ADAMTS-13 activity equivalent to that of other plasma products and lower levels of high-molecular vWF than regular FFP, and several studies have been conducted to evaluate its efficacy as a substitute for patients with TTP.

In 1985, there was also an attempt to utilize CRP even before TPE was established as a standard treatment for TMA.[8] The authors compared the effects of FFP and CRP infusions. They observed 3 patients with chronic relapsing TTP and concluded that the infusion of the cryosupernatant fraction was as effective as FFP in the treatment or prevention of chronic relapsing TTP.

TABLE 2. Mean and Standard Deviation of Absolute and Percentage Changes in Platelet Count, LD Level, and Hb Concentration[a]

Parameters		Replacement Fluid		*P* Value[b]
		FFP	CRP	
Total (n = 33)				
Platelet count (× 10^3/μL)	% change	20.24 ± 119.7	24.69 ± 90.6	**.011**
	Absolute change	−1.0 ± 54.7	7.0 ± 20.9	**.003**
LD (IU/L)	% change	−10.1 ± 37.3	−8.2 ± 19.9	.590
	Absolute change	−125.6 ± 438.0	−80.0 ± 297.9	.313
Hb (g/dL)	% change	0.2 ± 15.2	0.1 ± 14.0	.721
	Absolute change	0.0 ± 1.4	0.1 ± 2.3	.766
TTP (n = 2)				
Platelet count (× 10^3/μL)	% change	13.3 ± 62.9	32.3 ± 36.1	.061
	Absolute change	1.8 ± 12.6	20.7 ± 20.4	**<.001**
LD (IU/L)	% change	−10.7 ± 17.4	−6.9 ± 15.0	.614
	Absolute change	−171.4 ± 353.2	−27.4 ± 60.8	.080
Hb (g/dL)	% change	1.3 ± 18.5	1.1 ± 12.2	.489
	Absolute change	0.0 ± 1.5	0.8 ± 4.4	.363
TA-TMA (n = 11)				
Platelet count (× 10^3/μL)	% change	16.9 ± 130.3	6.4 ± 76.8	.777
	Absolute change	−11.3 ± 83.0	−1.7 ± 11.6	.509
LD (IU/L)	% change	−8.8 ± 18.5	−7.3 ± 22.1	.916
	Absolute change	−64.4 ± 153.0	−116.1 ± 475.0	.807
Hb (g/dL)	% change	0.6 ± 12.4	0.3 ± 15.5	.725
	Absolute change	0.1 ± 1.4	0.0 ± 1.3	.697
TMA, others (n = 20)				
Platelet count (× 10^3/μL)	% change	23.2 ± 118.7	31.0 ± 109.4	.277
	Absolute change	5.2 ± 27.0	6.2 ± 22.2	.338
LD (IU/L)	% change	−10.9 ± 47.1	−9.2 ± 20.7	.660
	Absolute change	−159.4 ± 555.6	−82.5 ± 229.2	.610
Hb (g/dL)	% change	−0.1 ± 16.5	−0.5 ± 14.0	.599
	Absolute change	−0.1 ± 1.5	−0.1 ± 1.0	.523

CRP, cryoprecipitate-reduced plasma; FFP, fresh frozen plasma; LD, lactate dehydrogenase; TA-TMA, transplantation-associated thrombotic microangiopathy; TMA, thrombotic microangiopathy; TMA, others, patients who did not fall into TPE or TA-TMA categories; TPE, therapeutic plasma exchange; TTP, thrombotic thrombocytopenic purpura.

[a]*All data are presented as mean ± standard deviation.*

[b]*Bold values indicate significance (P < .05).*

FIGURE 1. **Mean absolute and percentage changes in platelet counts, lactate dehydrogenase (LD) levels, and hemoglobin (Hb) concentrations in association with individual sessions of therapeutic plasma exchange with fresh frozen plasma (FFP) and cryoprecipitate-reduced plasma (CRP) (n = 33).**

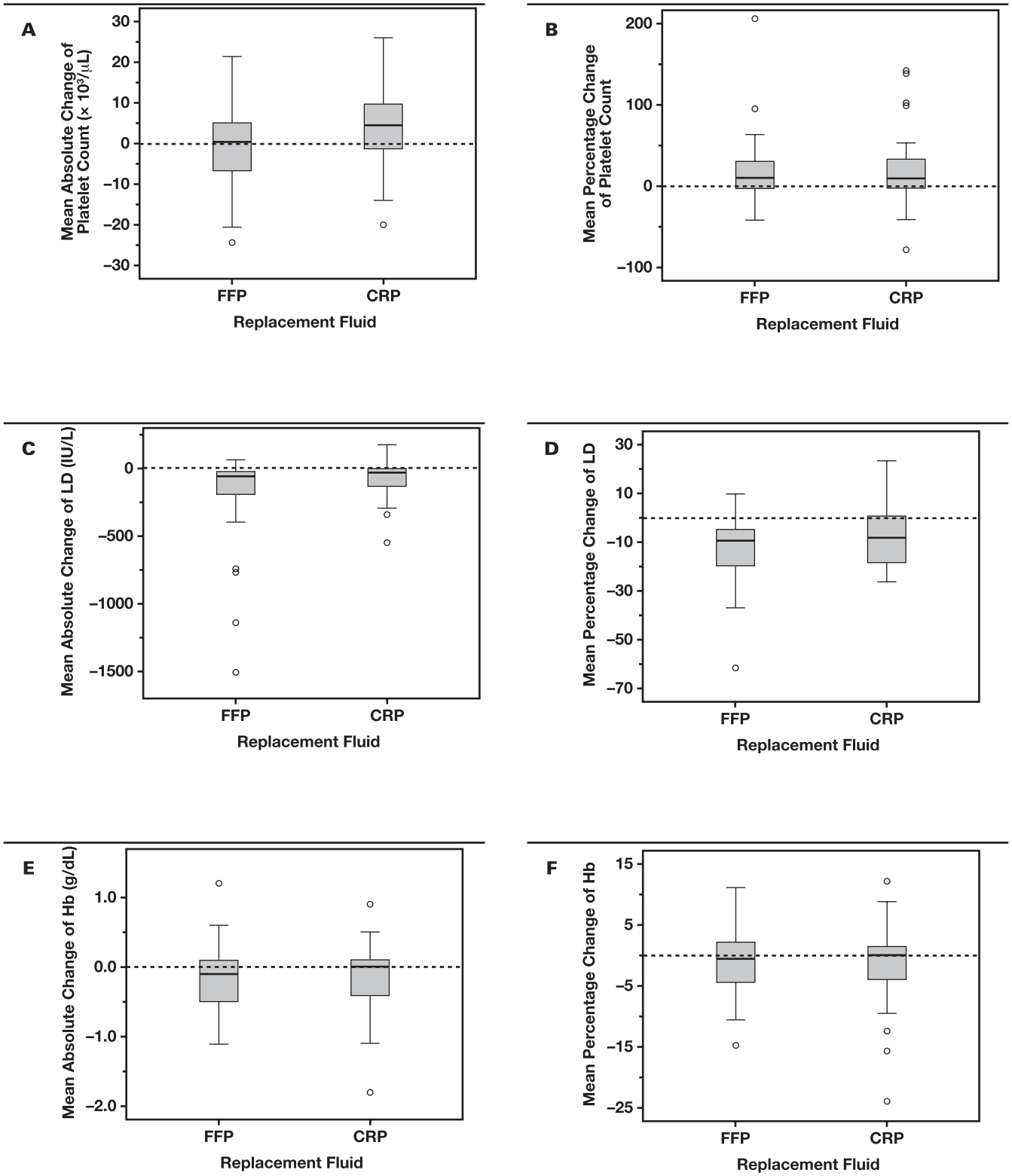

After an early study, various studies using CRP as a replacement fluid for TPE were conducted by several researchers. In a 1990 study,[9] CRP was used for 7 patients with TTP with poor responses to TPE using FFP. All 7 patients showed clinical improvements, and it was concluded that CRP could be considered as an alternative to FFP for patients with refractory TTP. In subsequent studies, it has been reported that CRP is

FIGURE 2. Mean absolute and percentage changes in platelet count, lactate dehydrogenase (LD) levels, and hemoglobin (Hb) in association with the therapeutic plasma exchange sessions of two patients (solid line and dashed line, respectively) who were diagnosed with thrombotic thrombocytopenic purpura, confirmed by ADAMTS-13 positivity, using fresh frozen plasma (FFP) and cryoprecipitate-reduced plasma (CRP).

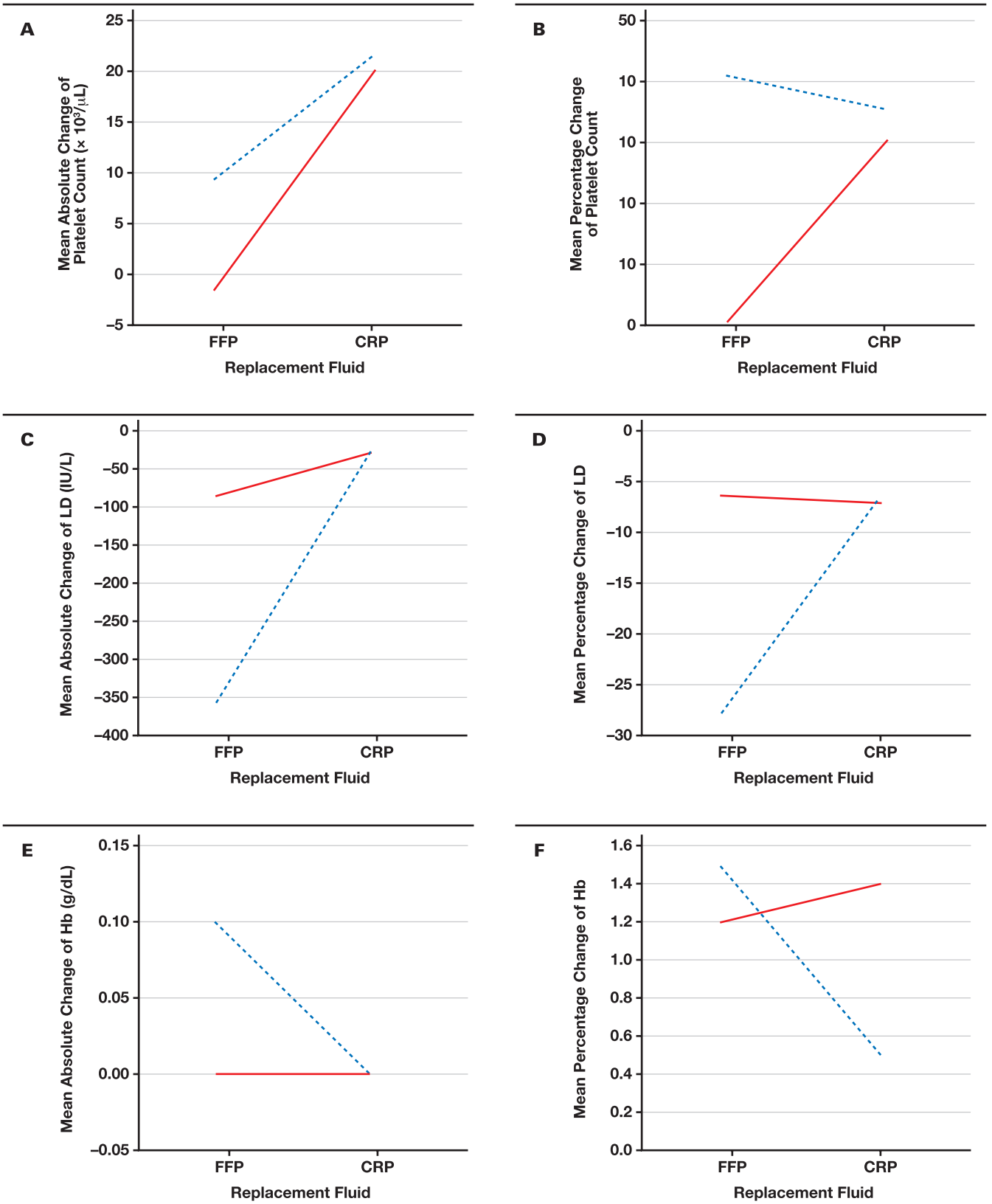

associated with a better prognosis as a replacement fluid than FFP for patients with TTP.[6,10,11] And in other studies, it has been shown that CRP as a replacement fluid is as acceptable as FFP, although the data have not shown an apparent advantage of the use of CRP in patients with TTP.[12-14]

Contrary to these previous studies, a retrospective study of newly diagnosed patients with TTP comparing the effects of FFP and CRP as replacement fluids suggested some negative effects of CRP. The CRP group underwent more TPE and was therefore exposed to larger volumes. However, this difference was not statistically significant. Notably, acute exacerbations of TTP were significantly more frequent in the CRP group. The study concluded that CRP should not be used as a first-line replacement fluid for patients with newly diagnosed TTP.[7]

The previous studies described above compared the outcomes of 2 groups of patients using either CRP or FFP as an alternative fluid. There is only 1 study that was carried out in which the combination of FFP and CRP was applied for TPE in patients with TTP, and outcomes were compared between groups depending on which replacement solution predominated.[15] The study concluded that CRP-dominant TPE was more effective than FFP-dominant TPE in early responses. However, the overall survival did not vary significantly.

Our study had a few limitations. This study was small, and there may not have been enough patients to elicit statistically significant findings. In addition, this was a retrospective study. Considering that TMA (including TTP) is rare and has a variety of clinical features, large-scale randomized controlled trials are difficult to develop. Therefore, it is meaningful to build evidence through observational studies and small clinical trials. Evidence-based apheresis guidelines do not recommend TPE as a first-line treatment for most types of TMA other than TTP.[3] However, the patients included in this study underwent multiple TPEs because the disease course worsened even with other treatments. Because there are differences in TPE conditions and complementary treatments other than TPE, our results should be interpreted with caution. Another limitation of this study was the absence of a definitive indication for the use of CRP. Because there are no guidelines for using CRP instead of FFP, dose effects and improvements over time could not be evaluated in our study.

The patients included in our study were not newly diagnosed with TTP or TMA when they were treated with TPE. Some patients relapsed and some were not fully responsive to the previous plasmapheresis using regular FFP.

In summary, although the changes in platelet count, LD levels, and Hb levels of each session using CRP as a replacement fluid did not differ significantly from those observed with FFP across the entire study sample, mean absolute platelet counts tended to increase in association with CRP-mediated TPE. The LD levels decreased more in sessions with FFP than in sessions with CRP, although this finding was not statistically significant. We considered this decrease to be the result of the initial effect for sessions with FFP. In most patients, FFP was used in the early days of the disease course when LD levels were very high. Most important, for the 2 patients with TTP with decreased ADAMTS-13 activity, the platelet counts improved in TPE sessions using CRP rather than FFP with statistical significance.

Ours is the first study to compare the laboratory findings of each TPE session using CRP or FFP for individual patients. The study was unique in that each patient was the control group for himself or herself. In this respect, the effects of CRP-mediated TPE may be reflected better than in previous studies comparing 2 completely different patient groups.

Conclusion

With this single-center experience, we have shown the possibility of using CRP as an alternative replacement fluid for refractory or relapsing TMA. We determined that CRP as a replacement product is not inferior to FFP in terms of platelet, LD, and Hb changes. Further randomized controlled studies with larger sample sizes would further elucidate the efficacy of CRP relative to that of FFP.

Acknowledgments

This research did not receive any specific grant from funding agencies in the public, commercial, or not-for-profit sectors. The overall research was conceived and led by D.H. Ko and Y. Chung. H.J. Kim wrote the manuscript and performed statistical analysis. J.J. Yang, H. Kim, S.H. Hwang, and H.B. Oh directly contributed to the acquisition of clinical data, interpretation, or revision of the article.

REFERENCES

1. Moake JL. Thrombotic microangiopathies. *N Engl J Med.* 2002;347(8):589–600.
2. Rock GA, Shumak KH, Buskard NA, et al. Comparison of plasma exchange with plasma infusion in the treatment of thrombotic thrombocytopenic purpura. Canadian Apheresis Study Group. *N Engl J Med.* 1991;325(6):393–397.
3. Padmanabhan A, Connelly-Smith L, Aqui N, et al. Guidelines on the use of therapeutic apheresis in clinical practice—evidence-based approach from the Writing Committee of the American Society for Apheresis: the Eighth Special Issue. *J Clin Apher.* 2019;34(3):171–354.
4. Howell C, Douglas K, Cho G, et al. Guideline on the clinical use of apheresis procedures for the treatment of patients and collection of cellular therapy products. British Committee for Standards in Haematology. *Transfus Med.* 2015;25(2):57–78.
5. Röthele E, Krumme B, Rump LC. Design of the prospective randomized study for the treatment of patients with thrombotic microangiopathy. *Ther Apher.* 2000;4:327–331.
6. Rock G, Shumak KH, Sutton DM, Buskard NA, Nair RC. Cryosupernatant as replacement fluid for plasma exchange in thrombotic thrombocytopenic purpura. Members of the Canadian Apheresis Group. *Br J Haematol.* 1996;94(2):383–386.
7. Stefanello B, De Paula EV, Andrade Orsi F, et al. Safety and efficacy of cryoprecipitate-poor plasma as a replacement fluid for therapeutic plasma exchange in thrombotic thrombocytopenic purpura: a single center retrospective evaluation. *J Clin Apher.* 2014;29(6):311–315.
8. Moake JL, Byrnes JJ, Troll JH, et al. Effects of fresh-frozen plasma and its cryosupernatant fraction on von Willebrand factor multimeric forms in chronic relapsing thrombotic thrombocytopenic purpura. *Blood.* 1985;65(5):1232–1236.
9. Byrnes JJ, Moake JL, Klug P, Periman P. Effectiveness of the cryosupernatant fraction of plasma in the treatment of refractory thrombotic thrombocytopenic purpura. *Am J Hematol.* 1990;34(3):169–174.
10. Obrador GT, Zeigler ZR, Shadduck RK, Rosenfeld CS, Hanrahan JB. Effectiveness of cryosupernatant therapy in refractory and chronic relapsing thrombotic thrombocytopenic purpura. *Am J Hematol.* 1993;42(2):217–220.
11. Owens MR, Sweeney JD, Tahhan RH, Fortkolt P. Influence of type of exchange fluid on survival in therapeutic apheresis for thrombotic thrombocytopenic purpura. *J Clin Apher.* 1995;10(4):178–182.

12. Zeigler ZR, Shadduck RK, Gryn JF, et al; North American TTP Group. Cryoprecipitate poor plasma does not improve early response in primary adult thrombotic thrombocytopenic purpura (TTP). *J Clin Apher.* 2001;16(1):19–22.
13. Rock G, Anderson D, Clark W, et al; Canadian Apheresis Group; Canadian Association of Apheresis Nurses. Does cryosupernatant plasma improve outcome in thrombotic thrombocytopenic purpura? No answer yet. *Br J Haematol.* 2005;129(1):79–86.
14. Altuntas F, Aydogdu I, Kabukcu S, et al. Therapeutic plasma exchange for the treatment of thrombotic thrombocytopenic purpura: a retrospective multicenter study. *Transfus Apher Sci.* 2007;36(1):57–67.
15. Lin Q, Fan L, Huang H, Zeng F, Fu D, Wei S. Combination of fresh frozen plasma and cryosupernatant plasma for therapeutic plasma exchange in thrombotic thrombocytopenic purpura: a single institution experience. *Biomed Res Int.* 2019;2019:1756109.

Relationships Between Circulating Tenascin-C Levels and Gonadal Hormones in Male Patients with Depressive Disorder: A Retrospective, Cross-Sectional Study

Rui Peng, MD,[a] Di Li, Yan Li, MD[a,]*

Department of Clinical Laboratory, Renmin Hospital of Wuhan University, Wuhan, Hubei Province, P.R. China; *To whom correspondence should be addressed. yanlitf1120@163.com; [a]Jointly supervised this work.

Keywords: tenascin-C, gonadal hormones, depression, inflammation, serum, ratio

Abbreviations: TNC, tenascin-C; T, testosterone; E2, estradiol; FT3, free tri-iodothyronine; TSH, thyroid-stimulating hormone; MDD, major depressive disorder; HPT, hypothalamic-pituitary-thyroid; SAH, subarachnoid hemorrhage; hsCRP, high-sensitivity C-reactive protein; FT4, free thyroxine; PC12, pheochromocytoma 12.

Laboratory Medicine 2022;53:273–277; https://doi.org/10.1093/labmed/lmab094

ABSTRACT

Objective: Tenascin-C (TNC) is an extracellular matrix glycoprotein closely associated with the progression of psychiatric disorders. The present study was performed to investigate the possible association between serum gonadal hormones and TNC levels in male patients with depressive disorder.

Materials and Methods: We measured serum TNC levels by enzyme-linked immunosorbent assay. In addition, we investigated the influence of testosterone (T) and estradiol (E_2) on TNC levels in primary neuronal cultures.

Results: Patients with depression had lower levels of T, free tri-iodothyronine (FT3), thyroid-stimulating hormone (TSH), and the T/E_2 ratio than healthy control patients. Levels of TNC and high-sensitivity C-reactive protein were significantly higher in patients than in healthy volunteers. Serum TNC concentrations were negatively associated with levels of E_2 and T and with the T/E_2 ratio. Levels of TNC, TSH, and FT3 and the T/E_2 ratio were predictors of depression. Among men with depression, TNC was negatively associated with T levels and with the T/E_2 ratio. Incubating pheochromocytoma 12 cells with the combination of T and E_2 greatly decreased TNC levels in the culture medium.

Conclusion: Increased TNC levels may predict imbalance between T and E_2 in patients with depression, and gonadal hormones may modulate TNC expression in vivo.

Major depressive disorder (MDD) is a complex psychiatric disorder with a lifetime prevalence of approximately 16%.[1] It shows a highly variable pathogenesis, clinical presentation, course, and response to treatment. Research has linked MDD to neurasthenia disorder, dysregulation of monoamine, dysfunction of the hypothalamic-pituitary-thyroid (HPT) axis, and inflammation.[2,3] The detailed pathophysiology of MDD remains poorly understood. One study found a negative correlation between serum testosterone (T) levels and the severity of depression in men, with serum T levels significantly lower in male patients with depression than in healthy control patients.[4] Indeed, partial androgen deficiency in older men has been linked to weakness, depressive mood, anxiety, and memory impairment, and T treatment shows promise as an antidepressant therapy.[5] Increasing evidence suggests that low T should be regarded as an independent risk factor for depression in men.[6,7]

Tenascin-C (TNC) is an extracellular matrix glycoprotein that many organisms express during development, and elevated TNC levels have been linked to inflammation, tissue impairment, and psychiatric disorders. Inhibition of TNC activity can ameliorate Alzheimer's disease, indicating that TNC may be a potential therapeutic target.[8] Subarachnoid hemorrhage (SAH) can lead to brain edema and disrupt the blood-brain barrier, inducing TNC expression, so targeting TNC may also be useful for counteracting SAH injury.[9] The induction of TNC occurs during angiogenesis in the central nervous system.[10]

Studies have shown that TNC may also be a biomarker for MDD and may contribute to the pathophysiology of the disorder.[11] For example, TNC may induce an inflammatory response in the brain, involving tumor necrosis factor-α and high-sensitivity C-reactive protein (hsCRP), which activate the HPT axis and may increase the risk of depression.[12] In addition, TNC may mediate molecular pathways involved in inflammation, apoptosis, and oxidative stress, which may affect the onset and progression of MDD.

Estrogen and androgens may downregulate TNC,[13,14] suggesting that these gonadal hormones may help protect against depression. The present cross-sectional study explored potential relationships between TNC levels and gonadal hormones in men with MDD. In the current study,

we analyzed the association between TNC levels and gonadal hormones with other parameters that are changed in male patients with depression.

Materials and Methods

Characteristics of Male Patients and Healthy Control Patients

A total of 127 men diagnosed with depression, ranging from ages 18 to 72 years (median, 36.48 years), and 109 healthy men, ranging from ages 21 to 76 years (median, 33.29 years), were recruited into the current study. All patients with depression and healthy volunteers underwent a structured clinical interview for the *Diagnostic and Statistical Manual of Mental Disorders,* 4th edition, in the Department of Psychiatry at Renmin Hospital of Wuhan University (Wuhan, P.R. China). Patients were excluded if they suffered from bipolar depression, reported using illegal substances within the past 2 months, or had a history of acute or chronic infection, cancer, major somatic disorder, or heart, kidney, or inflammatory disease. Control patients were excluded if they had a history of recent medication or if they had diseases that might interfere with the study, including hyperthyroidism, other mental disorders, or neurologic disease.

Sociodemographic information, cigarette consumption, alcohol use, symptom duration, and drug treatment were recorded at the beginning of hospitalization. Patients were evaluated using the Hamilton Depression Scale to assess depression severity, hopelessness, impulsivity, and suicidal ideation. None of the recruited patients had used antidepressants for at least 2 months before the study.

This research was approved by and performed in accordance with the guidelines of the Medical Ethics Review Committee of Renmin Hospital, Wuhan University. The requirement for written informed consent was waived because the patients at admission provided written consent for their anonymized medical data to be analyzed and published for research purposes.

Specimen Collection

Antecubital vein blood was drawn from patients and healthy volunteers at 8:00–9:00 AM, after participants had fasted for at least 8 hours. Blood serum was recovered, aliquoted into 1.5 mL tubes, and stored at –80°C until analysis.

Analytical Methods

Serum levels of TNC in patients and healthy volunteers were measured using a commercial enzyme-linked immunosorbent assay (CusaBio, Wuhan, China) according to the manufacturer's guidance. All serum specimens were also assayed for hsCRP using a Siemens Advia 2400 automatic biochemistry analyzer (Siemens, Erlangen, Germany). Levels of estradiol (E_2), T, free thyroxine (FT4), FT3, and TSH were measured using a Siemens Advia Centaur CP system (Siemens).

Cell Culture and Treatment

Pheochromocytoma 12 (PC12) cells were cultured in 1640 medium supplemented with penicillin (100 U/mL), streptomycin (100 U/mL), and 10% fetal bovine serum (Gibco) in a humidified atmosphere of 5% CO_2 at 37°C. Cells were divided into 5 groups, which were treated with corticosterone (200 μmol/L), T (10^{-8} mol/L), or E_2 (10^{-9} mol/L). Cells were incubated with these agents for 24 hours. The culture medium was collected and stored at –80°C until the assay of the TNC levels.

Statistical Analysis

Statistical analysis was carried out using SPSS 19.0 (IBM, Chicago, IL). Normal distribution and homogeneity of data were tested using Levene's test. Normally distributed data were reported as mean ± standard deviation. Intergroup differences in the following variables were assessed using the independent *t*-test: cigarette consumption, alcohol use, symptom duration, drug treatment, TSH, T, E_2, and T/E_2 ratio. Intergroup differences in the following variables were assessed using the Mann-Whitney *U* test: age, TNC, FT3, FT4, and hsCRP. Pearson analysis was used to identify correlations of TNC with levels of T, E_2, TSH, FT3, FT4, or hsCRP or with the T/E_2 ratio. Factors associated with depression risk were identified using uni- and multivariate logistic regression, and potential associations between such risk factors and TNC levels were explored using multiple linear regression. All variables associated with $P \leq .05$ were regarded as statistically significant.

Results

Characteristics of the Study Population

The levels of gonadal hormones and thyroid hormones in healthy volunteers and patients are summarized in **TABLE 1**. Patients had lower TSH and FT3 levels but higher hsCRP levels than control patients

TABLE 1. Characteristics of Hormone Levels Between Healthy Control Patients and Matched Patients with Depression

Characteristics	Control Patients (n = 109)	Patients (n = 127)	*P* Value[a]
Age (y)	33.29 ± 10.71	36.48 ± 15.73	.584
Cigarette consumption (%)	39 (30.7%)	44 (34.6%)	.546
Alcohol use (%)	26 (23.9%)	16 (12.6%)	.054
Symptom duration (mo)	…	36.47 ± 31.72	…
TNC (ng/mL)	6.92 ± 2.87	11.79 ± 6.06	**<.001**
T (241–376.72 ng/dL)	441.47 ± 142.96	336.28 ± 150.53	**<.001**
E_2 (19.5–144.2 pg/mL)	30.28 ± 11.51	28.80 ± 12.87	.354
T/E_2 ratio	15.74 ± 6.01	12.74 ± 5.81	**<.001**
TSH (0.55–4.78 μIU/mL)	2.26 ± 0.93	1.75 ± 1.03	**<.001**
FT3 (2.3–4.2 pg/mL)	3.50 ± 0.30	3.38 ± 0.43	**.006**
FT4 (0.89–1.80 ng/mL)	1.23 ± 0.14	1.27 ± 0.22	.310
hsCRP (0–3.0 mg/L)	0.39 ± 0.41	1.22 ± 3.14	**.008**
Treatment			
Imipramine	…	44 (34.6%)	…
Mirtazapine	…	31 (24.4%)	…
Fluoxetine	…	27 (21.3%)	…
Other antidepressants	…	25 (19.7%)	…

E_2, estradiol; FT3, free tri-iodothyronine; FT4, free thyroxine; hsCRP, high-sensitivity C-reactive protein; T, testosterone; TNC, tenascin-C; TSH, thyroid-stimulating hormone.
[a]*Bold values represent significant differences.*

(all P <.01). Patients also had significantly lower levels of serum T and the T/E_2 ratio (both P <.001). In contrast, E_2 and FT4 levels were similar between patients and healthy volunteers. The TNC levels were significantly higher in patients (P <.05).

Correlations Between TNC and Hormone Levels in Patients

Pearson partial correlation was used to explore associations of TNC levels with concentrations of thyroid and gonadal hormones. After adjustment for age, we found that serum TNC concentrations were negatively associated with levels of E_2 and T and with the T/E_2 ratio (**FIGURE 1**). Conversely, TNC concentrations positively correlated with FT4 levels. In other words, patients with lower serum TNC levels had higher serum T levels and T/E_2 ratio.

Predictors of MDD

Uni- and multivariate logistic regression was carried out to identify variables that might predict depression (**TABLE 2**). Univariate analyses indicated that T, hsCRP, the T/E_2 ratio, TNC, TSH, and FT3 correlated with the incidence of depression. Of these variables, multivariate analysis identified the last 4 as independent predictors of depression.

Association Between TNC Levels and Predictors of Depression

Relationships of TNC with the risk factors of depression were evaluated using multivariate regression. We found that TNC negatively correlated with T levels and the T/E_2 ratio in patients (**TABLE 3**).

Synergy Between T and E_2 Downregulated TNC in PC12 Cells

To further verify the effects of gonadal hormones on the TNC level, we examined how T and E_2 affected TNC expression in PC12 cells. Exposing cells to T or E_2 on their own significantly increased levels of TNC in the culture medium (both P <.05; **FIGURE 2**). These increases were smaller when the 2 hormones were coadministered (both P <.05). These results suggest that T and E_2 synergize to downregulate TNC levels relative to the level stimulated by either hormone on its own.

Discussion

Few studies have evaluated the role of TNC in the occurrence of depression, even though TNC is considered to play important roles during neural development, axonal regeneration, and synaptic plasticity. The purpose of the current research was to investigate the relationship

FIGURE 1. Scatter diagram depicting associations of tenascin-C (TNC) levels with estradiol (E_2) levels (r = 0.276; P <.001) (A), T levels (r = 0.268; P <.001) (B), T/E_2 ratio (r = 0.204; P =.002) (C), and free thyroxine (FT4) levels (r = 0.141; P =.032) (D).

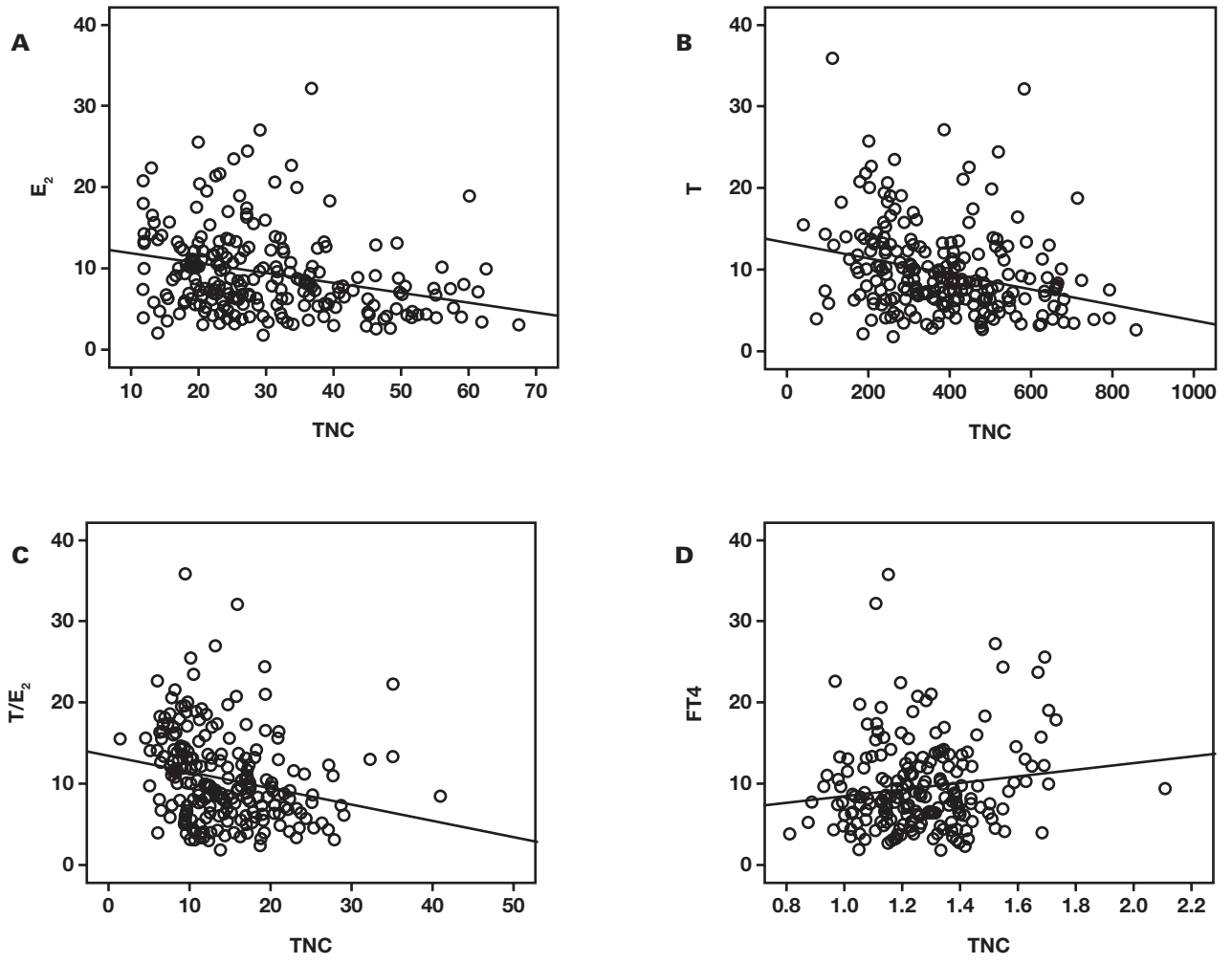

TABLE 2. Univariate and Multivariate Logistic Regression Analyses for Depression

Factor	Univariate			Multivariate		
	OR	95% CI	*P* Value[a]	OR	95% CI	*P* Value[a]
Age	1.018	0.998–1.037	.077	…	…	…
E_2	0.990	0.970–1.011	.352	…	…	…
T	0.995	0.993–0.997	**<.001**	1.002	0.999–1.005	.180
T/E_2 ratio	0.916	0.873–0.960	**<.001**	1.090	1.019–1.166	**.012**
TNC	1.312	1.204–1.429	**<.001**	0.757	0.686–0.836	**<.001**
TSH	0.578	0.433–0.772	**<.001**	1.818	1.286–2.570	**.001**
FT3	0.421	0.205–0.862	**.018**	3.332	1.232–9.017	**.018**
FT4	3.455	0.821–14.539	.091	…	…	…
hsCRP	1.542	1.095–2.171	**.013**	0.762	0.524–1.108	.154

CI, confidence interval; E_2, estradiol; FT3, free tri-iodothyronine; FT4, free thyroxine; hsCRP, high-sensitivity C-reactive protein; OR, odds ratio; T, testosterone; TNC, tenascin-C; TSH, thyroid-stimulating hormone.
[a]*Bold values represent significant differences.*

TABLE 3. Multiple Regression Analyses for Association Among TNC and Depressive Risk Factors in Male Patients with Depression

	T	T/E_2	TSH	FT3	hsCRP
β-coefficient	–0.244	–0.187	–0.075	–0.074	0.041
P value[a]	**<.001**	**.007**	.094	.512	.241

E_2, estradiol; FT3, free tri-iodothyronine; hsCRP, high-sensitivity C-reactive protein; T, testosterone; TNC, tenascin-C; TSH, thyroid-stimulating hormone.
[a]*Bold values represent significant differences.*

FIGURE 2. TNC levels in the medium of PC12 cultures after different treatments. Data shown as mean ± SD. *P <.05 vs control group; **P <.05 vs corticosterone + T/E_2 group. E_2, estradiol; PC12, pheochromocytoma 12; SD, standard deviation; T, testosterone; TNC, tenascin-C.

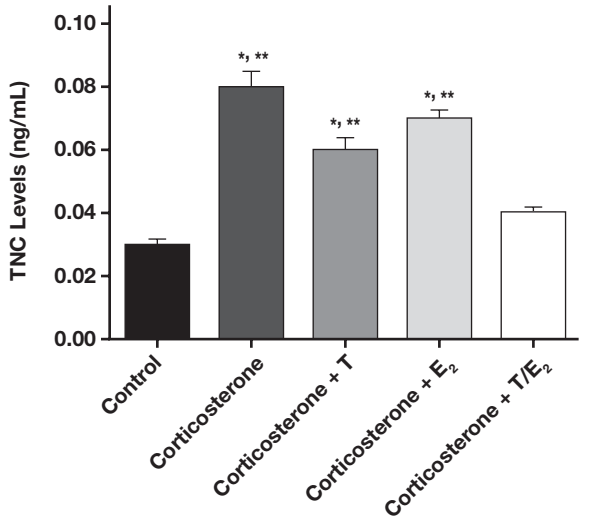

between serum gonadal hormone concentrations and TNC levels in men with depression. In our patients, serum TNC concentrations were significantly higher than in healthy volunteers (P <.001). Thus, TNC may be involved in the development of MDD, which may reflect that high TNC levels can suppress the regeneration of nervous tissue.[15–17] For example, TNC deficiency can weaken climbing-fiber paired-pulse depression and strengthen parallel-fiber paired-pulse facilitation.[16]

In addition, TNC levels in our patients positively correlated with FT4 levels, suggesting that TNC overexpression may disrupt the HPT axis. This disruption may reflect the ability of TNC to inhibit neurite outgrowth and bind with neuritogenic substrate,[8] along with promoting inflammation, neuronal apoptosis, and oxidative stress.[10] Our findings support the idea that TNC levels may be key to understanding the pathophysiology of MDD and useful for diagnosing the disorder.[11]

Serum TNC levels in our patients negatively correlated with T levels and the T/E_2 ratio such that patients showed significantly lower serum T levels and T/E_2 ratios than the healthy control patients. In fact, multiple linear regression indicated that serum TNC levels closely correlated with T levels in patients. Our patients also showed significantly lower serum levels of TSH and FT3 than the healthy volunteers, which is consistent with another study.[16]

The patients in our study showed lower alcohol consumption than the control patients, but the difference did not reach statistical significance. Nevertheless, alcohol consumption may have confounded the observed differences in TNC and hormone levels between the 2 groups, so large prospective studies are needed to verify and extend our results.

Estrogen has been shown to improve depression-like behaviors by suppressing inflammation, activating indoleamine-2,3-dioxygenase, and maintaining serotonin levels.[18] Similarly, T can exert antidepressant effects by activating extracellular signal-regulated kinase 2 signaling within the dentate gyrus of the hippocampus.[19] Therapy with T may be even more effective than antidepressants for treating MDD in men who are hypogonadal, resistant to antidepressant therapy, or infected with HIV, and in men with early-onset depression.[20] In other male populations, however, T may not be as effective against depression as antidepressants.[20,21] Ablation with T stimulates TNC expression in the rat prostate,[14] and consistent with that work, our study found significantly lower T levels and T/E_2 ratios but significantly higher TNC levels in patients than in healthy control patients. Furthermore, TNC levels in our patients negatively correlated with T levels and T/E_2 ratios. Our results imply that synergy between exogenous T and E_2 may suppress the expression of TNC via the androgen/estrogen receptor, mitigating MDD. Our experiments with PC12 cultures suggest that reduced T levels may upregulate TNC and increase the risk of depression, whereas the combination of T with E_2 can reduce TNC expression.

Our findings should be interpreted with caution given several limitations of the study. We recruited only patients who had not taken antidepressants or other medication for at least 2 months previously, so whether our results can be generalized to patients on antidepressant therapy remains to be seen. Such therapy may affect the serum levels of TNC and multiple hormones.[22] The patients and healthy volunteers in our study showed T, E_2, TSH, FT3, FT4, and hsCRP levels within the normal ranges, indicating a certain homogeneity in the study population, so future work should verify our findings in more diverse populations. Our sample lacked the statistical power to assess the impact of other depression risk factors on TNC and hormone levels. Large prospective studies are needed to assess the prognostic power of TNC serum concentrations for men with MDD and to clarify the association between TNC and T levels in such patients. The roles of TNC and T in depression remain poorly understood and need to be further analyzed in in vivo and in vitro studies, as does the question of how T and E_2 synergize to influence TNC expression. Despite these limitations, the present study is the first to report that TNC levels correlate with the T/E_2 ratio.

Conclusion

We propose that serum TNC levels are closely associated with the balance between T and E_2 in men and with the development of depression. Assaying TNC may help predict imbalance in the T/E_2 ratio in men with depression.

Acknowledgments

This study was supported by the Fundamental Research Funds for the Central Universities (number 2042020kf0064).

Conflict of Interest Statement

All authors declare that they have no conflict of interest.

REFERENCES

1. Müller S, Rohde P, Gau JM, Stice E. Moderators of the effects of indicated group and bibliotherapy cognitive behavioral depression prevention programs on adolescents' depressive symptoms and depressive disorder onset. *Behav Res Ther.* 2015;75:1–10.
2. Krishnan V, Nestler EJ. The molecular neurobiology of depression. *Nature.* 2008;455(7215):894–902.
3. Belmaker RH, Agam G. Major depressive disorder. *N Engl J Med.* 2008;358(1):55–68.
4. Hisashi M, Hitoshi M, Sayaka K, et al. Gender differences in serum testosterone and cortisol in patients with major depressive disorder compared with controls. *Int J Psychiatry Med.* 2013;46:203–221.
5. Amore M, Scarlatti F, Quarta AL, Tagariello P. Partial androgen deficiency, depression and testosterone treatment in aging men. *Aging Clin Exp Res.* 2009;21(1):1–8.
6. Kawato S. Role of androgen in the elderly. Modulation of synaptic plasticity by brain-synthesized androgens [in Japanese]. *Clin Calcium.* 2013;23(8):1141–1150.
7. Sankar JS, Hampson E. Testosterone levels and androgen receptor gene polymorphism predict specific symptoms of depression in young men. *Gend Med.* 2012;9(4):232–243.
8. Xie K, Liu Y, Hao W, et al. Tenascin-C deficiency ameliorates Alzheimer's disease-related pathology in mice. *Neurobiol Aging.* 2013;34(10):2389–2398.
9. Fujimoto M, Shiba M, Kawakita F, et al. Deficiency of tenascin-C and attenuation of blood-brain barrier disruption following experimental subarachnoid hemorrhage in mice. *J Neurosurg.* 2016;124(6):1693–1702.
10. Zagzag D, Capo V. Angiogenesis in the central nervous system: a role for vascular endothelial growth factor/vascular permeability factor and tenascin-C. Common molecular effectors in cerebral neoplastic and non-neoplastic "angiogenic diseases." *Histol Histopathol.* 2002;17(1):301–321.
11. Bot M, Chan MK, Jansen R, et al. Serum proteomic profiling of major depressive disorder. *Transl Psychiatry.* 2015;5:e599.
12. Piotr G, Monika T, George A, et al. Mechanisms underlying neurocognitive dysfunctions in recurrent major depression. *Med Sci Monit.* 2015;21:1535–1547.
13. Giinter V, Horst M, Grsten E, et al. Androgen ablation induces tenascin expression in the rat prostate. *The Prostate.* 1994;25:81–90.
14. Gottschalk MG, Cooper JD, Chan MK, Bot M, Penninx BW, Bahn S. Discovery of serum biomarkers predicting development of a subsequent depressive episode in social anxiety disorder. *Brain Behav Immun.* 2015;48:123–131.
15. Andjus PR, Bajić A, Zhu L, Schachner M, Strata P. Short-term facilitation and depression in the cerebellum: some observations on wild-type and mutant rodents deficient in the extracellular matrix molecule tenascin C. *Ann N Y Acad Sci.* 2005;1048:185–197.
16. Jia Y, Zhong S, Wang Y, Liu T, Liao X, Huang L. The correlation between biochemical abnormalities in frontal white matter, hippocampus and serum thyroid hormone levels in first-episode patients with major depressive disorder. *J Affect Disord.* 2015;180:162–169.
17. Evers MR, Salmen B, Bukalo O, et al. Impairment of L-type Ca2+ channel-dependent forms of hippocampal synaptic plasticity in mice deficient in the extracellular matrix glycoprotein tenascin-C. *J Neurosci.* 2002;22(16):7177–7194.
18. Xu Y, Sheng H, Tang Z, Lu J, Ni X. Inflammation and increased IDO in hippocampus contribute to depression-like behavior induced by estrogen deficiency. *Behav Brain Res.* 2015;288:71–78.
19. Carrier N, Kabbaj M. Extracellular signal-regulated kinase 2 signaling in the hippocampal dentate gyrus mediates the antidepressant effects of testosterone. *Biol Psychiatry.* 2012;71(7):642–651.
20. Amiaz R, Seidman SN. Testosterone and depression in men. *Curr Opin Endocrinol Diabetes Obes.* 2008;15(3):278–283.
21. Johnson JM, Nachtigall LB, Stern TA. The effect of testosterone levels on mood in men: a review. *Psychosomatics.* 2013;54(6):509–514.
22. Francesca V, Elena DB, Paola T, et al. Effect of adipose-derived mesenchymal stromal cells on tendon healing in aging and estrogen deficiency: an in vitro co-culture model. *Cytotherapy.* 2015;4:1–9.

AQ22

Validation of an In-House-Developed GC-MS Method for 5α-Cholestanol According to ISO 15189:2012 Requirements

Canan Coker, MD,[1,*] *Sezer Uysal, MD,*[1]

[1]Dokuz Eylül University Faculty of Medicine, Department of Biochemistry, Izmir, Turkey; *To whom correspondence should be addressed. sezer.uysal@deu.edu.tr

Keywords: cholestanol, GC-MS, measurement uncertainty, proficiency testing, clinical laboratory, method performance

Abbreviations: GC-MS, gas chromatography-mass spectrometry; NCS, noncholesterol sterol; CTX, cerebrotendinous xanthomatosis; LC-MS/MS, liquid chromatography-tandem mass spectrometry; BSTFA, *N,O*-bis-(trimethylsilyl) trifluoroacetamide; TMCS, trimethylchlorosilane; IS, internal standard; 7-DHC, 7-dehydrocholesterol; LOD, limit of detection; LOQ, limit of quantitation; RSD, relative standard deviation; LLLI, lower limit of linearity interval; ERNDIM, European Research Network for Evaluation and Improvement of Screening, Diagnosis and Treatment of Inherited Disorders of Metabolism; PT, proficiency testing; MU, measurement uncertainty; CV, coefficient of variation; GUM, Guide to the Expression of Uncertainty in Measurement.

Laboratory Medicine 2022;53:278–284; https://doi.org/10.1093/labmed/lmab095

ABSTRACT

Objective: The aim of this study was to validate a gas chromatography-mass spectrometry (GC-MS) method for the measurement of 5α-cholestanol in the clinical laboratory in agreement with ISO 15189:2012.

Materials and Methods: The GC-MS performance was evaluated and proficiency testing data were used to estimate the measurement uncertainty of the method considering the recommendations of international guidelines.

Results: The calibration curves were linear from 6 to 50 μmol/L, with r^2 >.99. The limit of detection and limit of quantitation were determined to be 0.36 and 2.58 μmol/L, respectively. The bias ranged from –18.9% to 15.2% for 6.5, 18.3, and 66 μmol/L. The intra- and interassay reproducibility was <20% at the various concentrations studied. The expanded uncertainty was determined to be 50.9%.

Conclusion: The GC-MS method for the measurement of 5α-cholestanol has proved to have acceptable analytical performance for use in the clinical laboratory.

5α-cholestanol, a noncholesterol sterol (NCS), is a biomarker for cerebrotendinous xanthomatosis (CTX), a rare inherited disorder of bile metabolism that occurs because of a deficiency of sterol 27-hydroxylase, which has a key role in the conversion of cholesterol into bile acids.[1] This deficiency leads to an accumulation of 5α-cholestanol and other bile acid precursors in plasma and tissues. In addition, the urinary excretion of bile alcohols increases.[2,3] To prevent neurologic disability in patients with CTX, early diagnosis and replacement therapy introduced on time are crucial.[1,4] In addition to its utility as a diagnostic marker, 5α-cholestanol is used for monitoring the therapy of patients with CTX.[4] Furthermore, 5α-cholestanol is a promising surrogate marker for cholesterol absorption, and its assessment in plasma specimens may be useful during dietary control and/or lipid-lowering lifestyle/drug therapy monitoring.[5]

Gas chromatography with flame ionization detector and gas chromatography-mass spectrometry (GC-MS) have been the most widely used methods for the measurement of plasma 5α-cholestanol in the biochemical diagnosis of CTX.[6-9] Although the capillary columns used in GC methods are suggested to provide good chromatographic separation, MS analysis is crucial to assuring correct structural identification.[5,7] More recently, liquid chromatography-tandem mass spectrometry (LC-MS/MS) methods have emerged for the analysis of NCSs including 5α-cholestanol.[9,10] Yet there is still no reference method for the isolation, identification, and quantification of NCSs in biological matrices. Moreover, the existing methods lack harmonization.[5,11]

One of the major problems with 5α-cholestanol determination is related to the fact that it has very similar properties to cholesterol, whose concentration is 300-fold higher.[5] Therefore, GC-MS has been considered as a key option for the successful separation and identification of 5α-cholestanol in plasma. This study was undertaken to establish a GC-MS method modified from previously reported methods for the routine analysis of 5α-cholestanol.[7,8] Furthermore, we aimed to achieve this in compliance with ISO 15189:2012, the standard describing requirements for quality and competence in medical laboratories.[12]

Materials and Methods

Specimen Collection

Plasma specimens were obtained from venous blood drawn into test tubes containing potassium EDTA (1.0 mg mL^{-1}; Beckton Dickinson). Donors were adult outpatients who presented to clinics other than oncology,

hematology, and endocrinology and who were referred to the central laboratory of the hospital for various blood tests. After centrifugation at 1750*g* for 10 minutes at room temperature, plasma specimens were marked "anonymous," transferred into vials, and stored at −80°C until the analyses. Plasma specimens with total cholesterol levels that were not within the reference range were not used in the experiments. Total cholesterol levels were measured by an enzymatic photometric method. After enzymatic hydrolysis and oxidation, quinoneimine, the colorimetric indicator, was generated from 4-aminoantipyrine and phenol by hydrogen peroxide under the catalytic action of peroxidase (Tinder reaction). The analysis was performed on a Beckman Coulter AU-5800 autoanalyzer using a Beckman Coulter commercial kit (catalog number OSR6516).

Reagents and Standards

All the chemicals and organic solvents used were high-performance LC grade. Hexane, ethanol, and toluene were purchased from Aldrich (Milwaukee, WI). Silylation-grade pyridine and high-purity derivatization solvents, *N*,*O*-bis-(trimethylsilyl) trifluoroacetamide (BSTFA) with 1% trimethylchlorosilane (TMCS), were obtained from Supelco (Bellefonte, PA). The standards cholest-5-en-3-ol (cholesterol), 5α-cholestan-3-ol (5α-cholestanol), and 5α-cholestane (internal standard [IS]) and KOH and butylated hydroxytoluene were purchased from Sigma Chemical (St Louis, MO).

Standard Solutions

A 5α-cholestane stock solution was prepared at 1 mg/25 mL in toluene. For the working internal standard, 5α-cholestane stock solution was diluted as (1:49) (v/v) in toluene. Cholesterol stock solution was prepared at a concentration of 39 mg/100 mL in toluene. Similarly, 5α-cholestanol stock solution was prepared at a concentration of 39 mg/100 mL in toluene. Afterward, 5 working calibration standards were freshly prepared in toluene for each analytical batch: 400, 500, 625, 750, and 833 μmol/L for cholesterol and 6, 16.7, 25, 37.5, and 50 μmol/L for 5α-cholestanol.

Specimen Preparation

Specimen preparation consisted of saponification, extraction, and derivatization. It was modified from the method previously reported by Ahmida et al.[7] Saponification was carried out by adding 1 mL of KOH/ethanol (5.6 g KOH/100 mL ethanol) to 100 μL of plasma or calibration standard in a glass tube containing 100 μL of the internal standard. Tubes were well mixed and heated at 65°C for 60 minutes in the dark. The reaction was stopped by cooling the tubes with cold water. The solution was then diluted with 1 mL of water and the lipids were extracted with 2 mL of extraction solution (hexane:ethanol; 20:1, v/v) containing 130 mg/L butylated hydroxytoluene. The specimens were vortexed and then centrifuged at 1800*g* at 20°C for 10 minutes. The organic phase was transferred to glass tubes and evaporated to dryness with nitrogen. Derivatization was achieved by adding 100 μL BSTFA with 1% TMCS and 100 μL pyridine. After incubation at 65°C for 60 minutes in the dark, the derivatized extracts were transferred to autosampler vials for GC-MS analysis.

Analytical Conditions

The GC-MS measurements were performed on a Shimadzu GC-2010 Plus Gas Chromatograph, equipped with an AOC-20i autoinjector and coupled to a Shimadzu QP 2010 SE mass spectrometer. The injection volume was 1 μL. The separation was achieved on a Restek C18 capillary column with 60 m × 0.25 mm internal diameter and 0.25 μm film thickness; helium of 99.999% purity was used as the carrier gas. The analytical conditions for GC were applied as previously described.[7] The temperatures of the injector and the ion source were held at 300°C and 206°C, respectively. Injection mode was splitless. The temperature program applied was as follows: The initial column temperature was 90°C and was held for 3 minutes, then increased to 260°C with a heating rate of 25°C/minute, held there for 28 minutes and then increased to 275°C with a rate of 1°C/minute and maintained at this temperature for another 13 minutes. The total analysis time was 50 minutes.

Mass spectra were collected in selected ion monitoring mode (with ions with *m/z* 306 and 445 monitored for 5α-cholestanol and ions with *m/z* 217 and 357 for 5α-cholestan). Cholesterol and 7-dehydrocholesterol (7-DHC) were also detected in the same run, with ions with *m/z* 458 and 329 for cholesterol and ions with *m/z* 343 and 351 for 7-DHC.

Evaluation of the Method Performance

The method described above allowed the quantitation of 5α-cholestanol, cholesterol, and 7-DHC. Method validation was performed for 5α-cholestanol. To determine the experimental design, the procedures necessary to apply for method validation, and the acceptance criteria, we used the guidelines of the Clinical and Laboratory Standards Institute,[13,14] the U.S. Food & Drug Administration,[15,16] and the directive of the European Council.[17] Peer-reviewed articles were taken into consideration as well.[18,19] The performance characteristics evaluated were as follows: measurement range, limit of detection (LOD), limit of quantitation (LOQ), trueness, imprecision, robustness, and carryover.

Calibration Curve, Linearity, LOD, and LOQ

Calibration curves for cholesterol, 5α-cholestanol, and 7-DHC were drawn by plotting the peak-area ratio between each analyte and the IS as a function of analyte concentration. A regression line was then calculated using the method of least-squares for each calibration curve. An 8-point standard curve from 3 μmol/L to 100 μmol/L was used to determine the linearity for 5α-cholestanol. Three consecutive calibration curves were drawn to evaluate the stability of the calibration curve. Relative standard deviation (RSD) (%) and mean bias (%) were determined for each calibration point.

The LOD was calculated as the concentration corresponding to 3 times the noise level of the negative standard. Toluene containing no standard was considered as the negative standard. After 10 replicates, the concentration of 5α-cholestanol corresponding to a signal-to-noise ratio of >3:1 was accepted as the LOD.[13]

As for the LOQ, which represented the lowest concentration measured with acceptable precision, we analyzed matrix-matched plasma specimens with gradually decreasing 5α-cholestanol concentrations that were less than the lower limit of linearity interval (LLLI). Intra-assay (n = 10) and interassay (n = 3) precision were calculated for each specimen.[13,16]

Measurement range and sensitivity were evaluated according to the intended use and the expected concentrations in pathologic conditions. Previously reported values for healthy volunteers and patients are summarized in **TABLE 1**.

Trueness

The indirect evaluation of trueness was carried out by determining the recovery, the efficiency of the extraction, and the integrity of the

TABLE 1. Previously Reported 5α-Cholestanol Levels in Serum/Plasma for Healthy Volunteers and Patients

Reference	5α-Cholestanol Levels in Serum/Plasma			
	Healthy Volunteers		Patients	
	μmol/L	n	μmol/L	n
Mignarri et al[1]	5.67 ± 2.06	17	74.7 ± 30.9	37
Nie at al[3]	8.50 ± 0.77	Not indicated	5- to 10-fold	Not indicated
Pilo de la Fuente et al[4]	2–12.6	Not indicated	56–238	14
Seyama et al[6]	8.60 ± 1.39	18	42.52–79.80	3
Ahmida et al[7]	4.73 ± 2.57	161	…	…
DeBarber et al[8]	2.06–4.64	20	21.65–170.10	10

serial dilution. For recovery, a plasma pool was fortified to 50 μmol/L and analyzed in duplicate. To evaluate the efficiency of the extraction, 5α-cholestanol standards at 2 different concentrations (50 μmol/L and 20 μmol/L) were added to aliquoted specimens from a common plasma pool either before or after the extraction step. Extraction efficiency was determined for each concentration by dividing the mean peak area of the 5α-cholestanol in the specimens that were spiked before extraction (n = 3) by those that were spiked after extraction (n = 3). For dilution integrity, a plasma pool was prepared, fortified to 50 μmol/L, and then diluted to 1/5 and 1/10. After GC-MS analysis, the mean peak area of 5α-cholestanol in the diluted specimens was divided by that of the undiluted plasma pool. The requirement criteria for recovery was accepted as being 80% to 110% in the concentration range of 5α-cholestanol.[16]

Bias was assessed by analyzing matrix-matched quality control specimens, ie, lyophilized spiked human specimens that were obtained from the European Research Network for Evaluation and Improvement of Screening, Diagnosis and Treatment of Inherited Disorders of Metabolism (ERNDIM) scheme, and which were proven to have *z* scores of <2. Triplicate analysis of 3 specimens at different levels—6.5 μmol/L, 18.3 μmol/L, and 66 μmol/L—was performed on separate days and with different batches. Measured values were compared with the reported consensus values. The acceptable range for trueness was considered to be –20% to +10%.[15]

Imprecision

Intra-assay reproducibility was determined using plasma pools at 3 different concentrations for 10 replicates for each assay. For interassay reproducibility, 2 replicates were analyzed for each assay on 5 different runs, each using a new calibration curve. To evaluate the reproducibility of the instrument, injection stability was determined by injecting the same specimen 10 times consecutively.[17]

Robustness

Extraction with hexane:ethanol accomplished by a single step was compared to the double-step extraction previously reported.[7] Three specimens at concentrations of 15 μmol/L, 16.7 μmol/L, and 25.6 μmol/L were extracted using both procedures in duplicate, and bias was determined.

Carryover

To evaluate the possible effects of carryover, 1 patient's specimen was analyzed in duplicate both before and after the triplicate injection of a plasma pool at 61 μmol/L, which is a high concentration of 5α-cholestanol exceeding the upper limit of linearity.

Measurement Uncertainty

Proficiency testing (PT) data were used for the estimation of measurement uncertainty (MU) in accordance with the recommendations of international guidelines, mainly applying the Nordtest approach.[20-24] The PT program that our laboratory participated in was the ERNDIM Quality Assurance in Laboratory Testing for Inborn Errors of Metabolism, and the data were obtained between April 2018 and July 2019.

The measurement of each PT specimen was performed on a different day in accordance with the timetable of the PT program, and a new calibration curve was plotted for each run. The data from 9 different specimens from the PT program at the lowest, midrange, and highest levels are presented in **TABLE 2**. These data were used to calculate the uncertainty of bias, which represented the systematic component of MU, using equations (2), (3), and (4) shown in **TABLE 3**.

The random component of MU, represented by the within-laboratory reproducibility, was calculated using the data obtained from duplicate assays of 2 different plasma pools for 5 days at mean 5α-cholestanol concentrations of 11.18 μmol/L and 17.26 μmol/L, according to equation (1) in **TABLE 3**.

The random and systematic components were combined using equation (5) in **TABLE 3** to calculate the combined standard uncertainty, which was then multiplied by the coverage factor to obtain the expanded MU with 95% confidence. The calculations for the determination of MU for 5α-cholestanol were performed using Microsoft Excel 2013.

Results

Representative total ion chromatograms for low- and high-plasma 5α-cholestanol concentrations are shown in **FIGURE 1**. A satisfactory resolution was accomplished for 5α-cholestanol from the preceding peak of cholesterol, which was remarkably high and non-Gaussian in shape. The chromatographic run was completed in 50 minutes.

Calibration Curve, Linearity, LOD, and LOQ

The calibration curve was determined to be linear from 6 to 50 μmol/L and had a correlation coefficient (r^2) ≥.99, which is the acceptable criterion for the linearity range. For all individual calibration points, the RSD of the replicates and the mean bias at each concentration were found

TABLE 2. Data of the PT Program for 5α-Cholestanol Analysis

Specimen	Result (μmol/L)	*z* Score	Bias (%)	CV (%)	n[a]
1	19.1	0.2	2.1	14.2	31
2	5.27	1	–19.3	23.8	31
3	53.6	1.8	–19.5	13.4	32
4	22.4	1.7	25.1	14.3	33
5	9.14	1.8	32.6	19	34
6	64.5	1.4	–27.12	18.9	33
7	7.85	0.2	6.5	27.8	32
8	18.9	0.2	3.28	18.4	31
9	48.9	2	–29	15.1	33

CV, coefficient of variation; GC-MS, gas chromatography-mass spectrometry; PT, proficiency testing.
[a]These numbers represent only the laboratories that used the GC-MS method.

to be acceptable as presented in **TABLE 4**. The LOD and LOQ are also presented in **TABLE 4**. The intra-assay and interassay coefficients of variation (CVs) of the LOQ were determined to be 3.1% and 19.6%, respectively.

Trueness

Results of the recovery, extraction efficiency, and dilution integrity experiments are presented in **TABLE 4**. The recovery values for the entire analytical process and the extraction step proved to be acceptable.

TABLE 3. Equations Used and Values Obtained for MU

Term	Equation			Result (%)
U(Rw)	(1)	$\sqrt{(CV_A^2 + CV_B^2)}$	$\sqrt{(8.16^2 + 10.88^2)}$	13.58
RMS_{bias}	(2)	$\sqrt{(\sum bias^2)/n}$	$\sqrt{(453)}$	21.29
U(Cref)	(3)	interlab CV /$\sqrt{n}$	18.3/$\sqrt{32.2}$	3.23
U(bias)	(4)	$\sqrt{(RMS_{bias}^2 + U(Cref)^2)}$	$\sqrt{21.29^2 + 3.23^2}$	21.5
Uc	(5)	$\sqrt{(U(Rw)^2 + U(bias)^2)}$	$\sqrt{21.5^2 + 13.59^2}$	25.45
U	(6)	k × Uc	2 × 25.45	50.91

CV, coefficient of variation; k, coverage factor (accepted as 2; the result represents the interval where the "true" value lies with 95% confidence); MU, measurement uncertainty; RMS_{bias}, root mean square of the bias values; U, expanded uncertainty; U(bias), uncertainty component for bias; Uc, combined standard uncertainty; U(Cref), uncertainty of assigned values; U(Rw), within-laboratory reproducibility standard deviation.

Bias values obtained from the repeated analyses of the external quality control specimens were considered acceptable (**TABLE 4**).

Imprecision

Intra-assay and interassay reproducibility and injection stability proved to be sufficient (**TABLE 4**).

Robustness

Bias between single and double extractions was observed to be between –8.4% and 1.88% for specimens at different concentrations between 15 and 25.6 μmol/L.

Carryover

The 5α-cholestanol level showed an increase from 8.7 μmol/L to 9.2 μmol/L (5.7%) in the patient specimen, which was analyzed both before and after a plasma pool with high 5α-cholestanol concentration. This increase was found to be acceptable, corresponding to <20% of the LOQ.[17]

Measurement Uncertainty

Results of the proficiency testing scheme, which provided the data used for the calculation of the systematic component of MU, were satisfactory considering that *z* scores were ≤2 for all of the 9 specimens (**TABLE 2**). The interlaboratory CV was reported to be 20.2% (n = 41) in the annual report of 2019. Results of the calculations for MU are presented in **TABLE 3**.

FIGURE 1. Selected ion monitoring chromatograms of patients with low and high concentrations of cholestanol. A, Internal standard. B, Cholesterol: 2743 μmol/L; cholestanol: 2.7 μmol/L. C, Cholesterol: 5161 μmol/L; cholestanol: 25.19 μmol/L. The black lines indicate the ions with m/z of 217 (A) and 445 (B and C); the magenta lines indicate the ions with m/z of 357 (A) and 306 (B and C). The red arrows indicate the start and/or the end of the peaks.

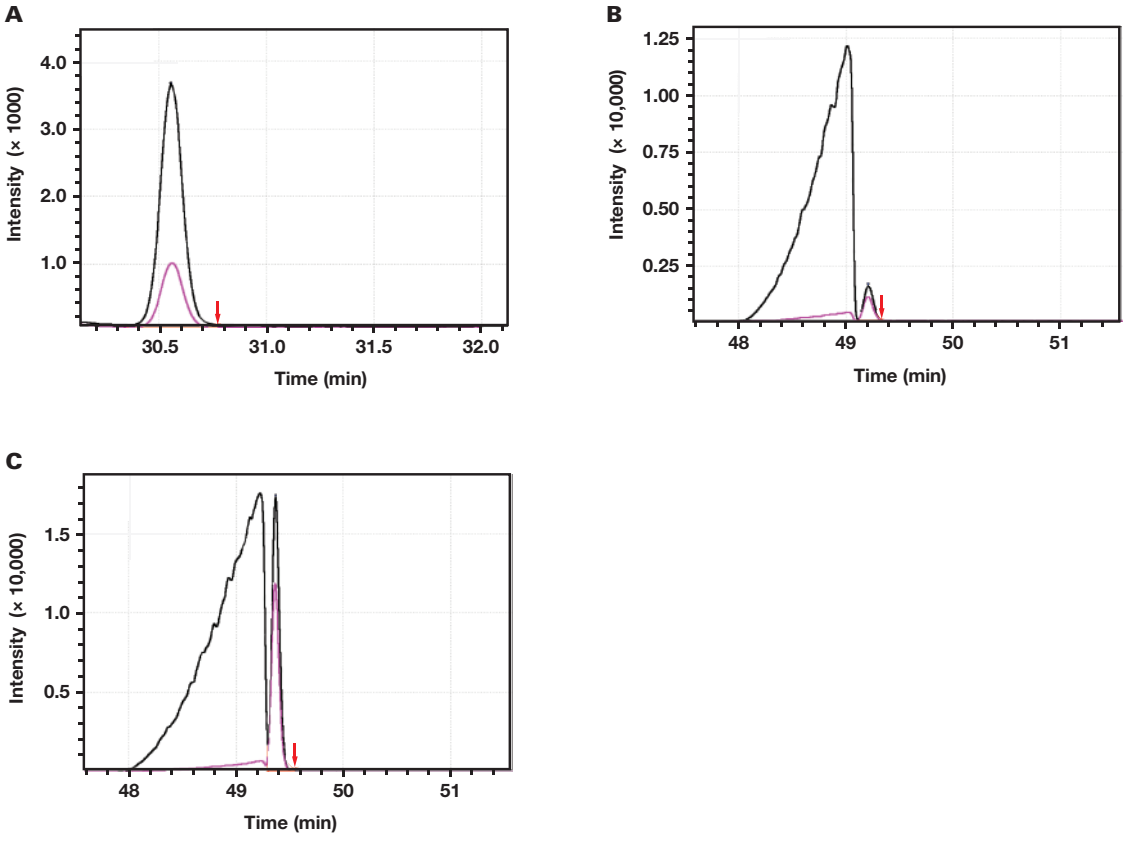

AQ17

TABLE 4. Results of Method Validation Experiments and Acceptability Criteria

Performance Characteristics	Results	Acceptability Criteria
Linearity	$r^2 \geq 0.99$ (6–50 μmol/L)	$r^2 \geq 0.99$
	For all individual calibration points (n = 3): RSD <20%	For all individual calibration points: RSD <20%
	Bias:	Bias: ±20%[14,15]
	19.5% for 6 μmol/L	
	3.0% for 16.67 μmol/L	
	8.5% for 25 μmol/L	
	1.8% for 37.5 μmol/L	
	5.0% for 50 μmol/L	
LOD	0.36 μmol/L	S/N >3[13]
LOQ	2.58 μmol/L	RSD <20%[16]
Trueness		
Recovery		80%–110%
Whole procedure	86.9% for 50 μmol/L (n = 2)	80%–110%[16]
Extraction efficiency	92.5% for 50 μmol/L (n = 3)	
	88.7% for 20 μmol/L (n = 3)	
Dilution integrity	r^2 = 0.83 (3-point calibration)	± 15% of nominal concentrations[17]
	(5.42, 10.84, 54.20 μmol/L)	
	1/10 dilution: 111.6%	
	1/5 dilution: 85%	
Bias	(n = 3) for each concentration	Bias: ± 20%[17]
	−18.3% to + 9.9% for 6.5 μmol/L	
	+4.3% to +15.2% for 18.3 μmol/L	
	−18.9% to + 4.2% for 66 μmol/L	
Imprecision		
Intra-assay	(n = 10) for each concentration	<8% (obtained from Horwitz equation)[15,16]
	3.8% for 5.9 μmol/L	
	6.6% for 9.4 μmol/L	
	1.5% for 13.1 μmol/L	
Interassay	(n = 5 × 2) for each concentration	<16% (obtained from Horwitz equation)[15,16]
	8.2% for 11.1 μmol/L	
	13.3% for 11.4 μmol/L	
	10.9% for 17.3 μmol/L	
Injection stability	6.73% for 5.8 μmol/L	

LOD, limit of detection; LOQ, limit of quantitation; RSD, relative standard deviation; S/N, signal-to-noise ratio.

Discussion

We found the GC-MS method established in our laboratory for the measurement of 5α-cholestanol to have an acceptable analytical performance. The method was modified from the previously reported method[7] at 2 steps: specimen preparation and chromatographic separation. To make specimen preparation faster and simpler, the extraction process was performed as a single step rather than as double steps. The single-step extraction proved to be efficient considering the results of the extraction efficiency and robustness experiments. The main modification regarding the chromatographic separation was using the splitless injection mode because we focused on 5α-cholestanol and tried to increase the sensitivity and achieve good resolution for this molecule. As observed in **FIGURE 1**, our optimized method yielded highly resolved peaks at both low and high concentrations of 5α-cholestanol. A drawback of the method was the relatively long chromatographic run time. The run time was similar to that of the previously reported GC-MS method.[7] Shorter run times have been reported for LC-MS/MS methods that analyze other bile acids along with 5α-cholestanol.[8-11] However, the GC-MS method was more convenient for routine measurement of 5α-cholestanol in our laboratory considering that the instrument is less expensive, the method is easier to apply, and it is currently in widespread use in clinical laboratories.[5,11]

Previously reported 5α-cholestanol levels in healthy volunteers and in patients were taken into consideration while choosing the standard concentrations for the calibration curve (**TABLE 1**). Linear calibration curves showed correlation coefficients equal to or higher than 0.99 up to 50 μmol/L at all batches. The linearity range of the calibration curve obtained in this study encompasses the values of the healthy volunteers and extends to the diagnostic values as well.

The LOD value of this modified method is very close to that reported by Ahmida et al (0.36 μmol/L and 0.40 μmol/L, respectively).[7] The relatively high difference between LOD and LOQ probably resulted from the use of plasma specimens with low 5α-cholestanol concentrations instead of blank specimens for the determination of LOQ. According to our findings, it seems to be a better laboratory practice not to report a definite numerical value for levels lower than 2.6 μmol/L, a value nearly half of the LLLI.

To evaluate the trueness of the method, both recovery and bias were evaluated as indirect and direct parameters, respectively. The recovery for the entire analytical procedure was evaluated by either specimen spiking or dilution. The recovery assessed by dilution is also closely related to the concept of dilution integrity, which encompasses the linear relationship between diluted specimens. Recovery values were found to be acceptable. The recovery for extraction, also called the extraction efficiency, was determined to be very satisfactory, indicating minimum matrix effects.[18] The extraction efficiency also indicated that it was appropriate to apply the extraction as a single step. The method also proved to be robust considering the relatively low values of bias. Several guidelines have indicated that the required bias should be between −20% and 10%, but there are also reports considering ±20% as an acceptable bias.[15,16,18]

Assessment of bias was performed using specimens with concentrations covering the previously reported reference ranges.[1,3,4,6-8] Furthermore, the concentration of the third specimen used was close to the concentrations reported for patients and just above the upper linearity limit of our method.

The trueness and reproducibility of the method also proved to be within the acceptable limits. All these validation experiments showed that our method meets the performance criteria for routine measurement in clinical laboratories and that further evaluation regarding MU is applicable.

In recent years, the adoption of ISO 15189:2012 for the accreditation of clinical laboratories has made the estimation of MU, in addition to method validation, a required activity.[12] It may be challenging for clinical laboratories to predict MU, especially for tests that are required for the diagnosis of rare diseases and are usually performed by in-house developed methods. While calculating MU for in-house developed methods, a bottom-up approach can be adopted in accordance with the Guide to the Expression of Uncertainty in Measurement (GUM) principles.[25] On the other hand, it has been stated that the practical application of the GUM model is not possible in routine laboratory work considering the large number of preanalytical, analytical, and postanalytical factors that

influence MU in routine laboratory diagnostics.[26] Proficiency testing is considered an alternative tool in evaluating the performance of a diagnostic test for a rare disease. The Nordic countries technical report, Nordtest TR 537, provides the clearest explanation of the top-down model in MU assessment based on proficiency testing data.[20]

The data obtained from participation in a PT can be a good basis for uncertainty estimates if the type of material and range of values of the measurand are appropriate, the number of PT rounds is sufficient (minimum 6 trials), and the number of laboratories participating is sufficient for a reliable estimation of the consensus values.[27] The PT data used for the estimation of uncertainty of bias for 5α-cholestanol in this study were obtained over a period of 18 months and included 9 different specimens with a relatively large span of concentrations. The number of participating laboratories (n = 31–34, as presented in **TABLE 2**) was sufficient from a statistical point of view. As reported by Belli et al,[28] consensus mean values and observed standard deviations of measurement/analytical results of laboratories participating in a PT with a limited number of participants (<20–30) are not reliable for the assessment of a laboratory's performance. As for the between-laboratory standard deviations, their contribution to the uncertainty of bias was relatively small as noted in **TABLE 4**.

In the estimation of measurement uncertainty for 5α-cholestanol in our study, the method bias appeared to be the main determinant. As observed in **TABLE 2**, our bias values changed in a relatively large spectrum. Similarly, the results of the survey for chromatographic analysis of 5α-cholestanol reported by Lütjohann et al[5] indicated that in an interlaboratory comparison study, none of the 10 participating laboratories determined 5α-cholestanol concentrations within ±15% range of the mean value. It is well known that the bias may vary over time, over concentration range, and because of matrix variations in patient specimens. It has been noted that using PT data instead of a reference material may lead to the overestimation of measurement uncertainty, especially if the estimated bias component is the dominant component.[27] The reason is that when a reference material is used, the bias is the mean value obtained over a long period of time. On the other hand, when only 1 measurement on a certain day is performed for each external quality control material, the bias contains both a systematic and a random component. Thus, by using the existing quality control data, the highest possible method bias and consequently the highest possible uncertainty were calculated for our method of measurement of 5α-cholestanol in plasma.

One of the limitations of this study is that it does not include reference values obtained from healthy volunteers. The main reason is the difficulty in finding a sufficient number of healthy children. Thus, in the course of the adaptation of the method before beginning the routine measurement of 5α-cholestanol, previous reports about the levels of this diagnostic parameter in healthy volunteers and patients were taken into consideration and method validation was carried out accordingly.

This study also does not include values obtained from patients with CTX. Because CTX is a rare disease and the number of patients receiving a definitive diagnosis of CTX is small, monitoring of the laboratory results is required over a long period of time. Therefore, it is hard to show the clinical effectiveness of the test before its routine use in the laboratory, which is true for all the biochemical markers for rare diseases.

Conclusion

According to the performance evaluation that was carried out using the existing guidelines and tools, this GC-MS method has proven to be suitable and applicable for the determination of 5α-cholestanol in medical laboratories in compliance with ISO 15189:2012.

Acknowledgments

We thank Sevinc Gezginciler and Elcin Berker for their technical assistance. We acknowledge the use of data derived from ERNDIM EQA materials in this manuscript. The use of ERNDIM EQA materials does not imply that ERNDIM endorses the methods used or the scientific validity of the findings in this manuscript. ERNDIM (www.erndim.org) is an independent, not for profit foundation that provides EQA schemes in the field of inborn errors of metabolism with the aim of improving diagnosis, treatment, and monitoring of inherited metabolic diseases.

REFERENCES

1. Mignarri A, Gallus GN, Dotti MT, Federico A. A suspicion index for early diagnosis and treatment of cerebrotendinous xanthomatosis. *J Inherit Metab Dis.* 2014;37(3):421–429.
2. Björkhem I, Hansson M. Cerebrotendinous xanthomatosis: an inborn error in bile acid synthesis with defined mutations but still a challenge. *Biochem Biophys Res Commun.* 2010;396(1):46–49.
3. Nie S, Chen G, Cao X, Zhang Y. Cerebrotendinous xanthomatosis: a comprehensive review of pathogenesis, clinical manifestations, diagnosis, and management. *Orphanet J Rare Dis.* 2014;9:179.
4. Pilo de la Fuente B, Sobrido MJ, Girós M, et al. Usefulness of cholestanol levels in the diagnosis and follow-up of patients with cerebrotendinous xanthomatosis. *Neurología*. 2011;26:397–404.
5. Lütjohann D, Björkhem I, Friedrichs S, et al. First international descriptive and interventional survey for cholesterol and non-cholesterol sterol determination by gas- and liquid-chromatography—urgent need for harmonisation of analytical methods. *J Steroid Biochem Mol Biol.* 2019;190:115–125.
6. Seyama Y, Ichikawa K, Yamakawa T. Quantitative determination of cholestanol in plasma with mass fragmentography. Biochemical diagnosis of cerebrotendinous xanthomatosis. *J Biochem.* 1976;80(2):223–228.
7. Ahmida HSM, Bertucci P, Franzo L, et al. Simultaneous determination of plasmatic phytosterols and cholesterol precursors using gas chromatography-mass spectrometry (GC-MS) with selective ion monitoring (SIM). *J Chromatogr B*. 2006;842:43–47.
8. DeBarber AE, Connor WE, Pappu AS, Merkens LS, Steiner RD. ESI-MS/MS quantification of 7alpha-hydroxy-4-cholesten-3—one facilitates rapid, convenient diagnostic testing for cerebrotendinous xanthomatosis. *Clin Chim Acta.* 2010;411(1–2):43–48.
9. DeBarber AE, Luo J, Star-Weinstock M, et al. A blood test for cerebrotendinous xanthomatosis with potential for disease detection in newborns. *J Lipid Res.* 2014;55(1):146–154.
10. Vaz FM, Ferdinandusse S. Bile acid analysis in human disorders of bile acid biosynthesis. *Mol Aspects Med.* 2017;56:10–24.
11. Andrade I, Santos L, Ramos F. Advances in analytical methods to study cholesterol metabolism: the determination of serum noncholesterol sterols. *Biomed Chromatogr.* 2013;27(10):1234–1242.
12. ISO 15189:2012. Medical laboratories—requirements for quality and competence. https://www.iso.org/standard/56115.html. Updated November 2012. Accessed September 30, 2021.
13. Clinical and Laboratory Standards Institute. C43-A2. Gas chromatography/mass spectrometry confirmation of drugs; approved guideline—second edition; 2010. https://webstore.ansi.org/preview-pages/CLSI/preview_C43-A2+Vol.+30+No.+6.pdf. Updated March 2010. Accessed September 30, 2021.
14. Clinical and Laboratory Standards Institute. C50-A. Mass spectrometry in the clinical laboratory: general principles and guidance;

approved guideline. https://clsi.org/standards/products/clinical-chemistry-and-toxicology/documents/c50/. Updated October 29, 2007. Accessed September 30, 2021.

15. European Commission. 2002/657/EC: Commission decision of 12 August 2002 implementing Council Directive 96/23/EC concerning the performance of analytical methods and the interpretation of results. https://op.europa.eu/en/publication-detail/-/publication/ed928116-a955-4a84-b10a-cf7a82bad858/language-en. Updated August 12, 2002. Accessed September 30, 2021.
16. U.S. Food & Drug Administration. Memorandum: guidelines for the validation of chemical methods for the FDA Foods Program, 3rd edition. https://www.fda.gov/media/81810/download. Updated October 17, 2019. Accessed September 30, 2021.
17. U.S. Food & Drug Administration. Guidance document: bioanalytical method validation guidance for industry. https://www.fda.gov/regulatory-information/search-fda-guidance-documents/bioanalytical-method-validation-guidance-industry. Updated May 2018. Accessed September 30, 2021.
18. Smith CR, Truver MT, Swortwood MJ. Quantification of U-47700 and its metabolites in plasma by LC-MS/MS. *J Chromatogr B Analyt Technol Biomed Life Sci.* 2019;1112:41–47.
19. Padoan A, Antonelli G, Aita A, Sciacovelli L, Plebani M. An approach for estimating measurement uncertainty in medical laboratories using data from long-term quality control and external quality assessment schemes. *Clin Chem Lab Med.* 2017;55(11):1696–1701.
20. Magnusson B, Näykki T, Hovind H, Krysell M, Sahlin E. Handbook for calculation of measurement uncertainty in environmental laboratories. NT TR 537-Edition 4. http://nordtest.info/images/documents/nt-technical-reports/NT_TR_537_edition4_English_Handbook_for_calculation_of_measurement_uncertainty_in_environmental_laboratories.pdf. Updated November 2017. Accessed September 30, 2021.
21. Guidelines on measurement uncertainty: CAC/GL 54-2004. http://www.fao.org/input/download/standards/10129/CXG_054e.pdf. Updated 2004, 2011. Accessed September 30, 2021.
22. Quantifying uncertainty in analytical measurement. Eurachem/CITAC Guide CG 4, 3rd ed. https://eurachem.org/images/stories/Guides/pdf/QUAM2012_P1.pdf. Accessed September 30, 2021.
23. Eurolab. Measurement uncertainty revisited: alternative approaches to uncertainty evaluation. Technical report No.1/2007. https://eurolab-d.de/files/measurement_uncertainty_revisited_-_alternative_approaches_to_uncertainty_evaluation.pdf. Updated March 2007. Accessed September 30, 2021.
24. ISO/TS 20914:2019. Medical laboratories—practical guidance for the estimation of measurement uncertainty. https://www.iso.org/standard/69445.html. Updated July 2019. Accessed September 30, 2021.
25. Joint Committee for Guides in Metrology. International vocabulary of metrology—basic and general concepts and associated terms (VIM), 3rd edition. https://www.bipm.org/documents/20126/2071204/JCGM_200_2012.pdf/f0e1ad45-d337-bbeb-53a6-15fe649d0ff1. Updated 2012. Accessed September 30, 2021.
26. Milinković N, Ignjatović S, Šumarac Z, Majkić-Singh N. Uncertainty of measurement in laboratory medicine. *J Med Biochem.* 2018;37(3):279–288.
27. Magnusson B, Ossowicki H, Rienitz O, Theodorsson E. Routine internal- and external-quality control data in clinical laboratories for estimating measurement and diagnostic uncertainty using GUM principles. *Scand J Clin Lab Invest.* 2012;72(3):212–220.
28. Belli M, Ellison SLR, Faljgelj A, et al. Implementation of proficiency testing schemes for a limited number of participants. *Accred Qual Assur.* 2007;12:391–398.

Semaphorin 3A Levels in Lupus with and without Secondary Antiphospholipid Antibody Syndrome and Renal Involvement

Gözde Sevgi Kart Bayram, MD,[1,] Abdulsamet Erden, MD,[2] Doğan Bayram, MD,[1] Bahar Özdemir, MD,[2] Özlem Karakaş, MD,[2] Hakan Apaydın, MD,[2] Ortaç Ateş, MD,[3] Serdar Can Güven, MD,[2] Berkan Armağan, MD,[2] Kevser Gök, MD,[2] Yüksel Maraş, MD,[2] Ahmet Omma, MD,[4] Orhan Küçükşahin, MD,[5] Canan Topçuoğlu, MD,[6] Şükran Erten, MD[5]*

[1]Ankara City Hospital, Internal Medicine, Üniversiteler Mahallesi, Ankara, Turkey, [2]Ankara City Hospital, Rheumatology, Ankara, Turkey, [3]Ankara City Hospital, Biochemistry, Ankara, Turkey, [4]TC Saglik Bakanligi Ankara Numune Egitim ve Arastirma Hastanesi, Ankara, Turkey, [5]Ankara Yildirim Beyazit University, Rheumatology, Ankara, Turkey, [6]Ankara Numune Education and Research Hospital, Biochemistry Department, Ankara, Turkey, *To whom correspondence should be addressed. gzdsvg@gmail.com

AQ5

Keywords: semaphorin 3A, antiphospholipid antibody syndrome, systemic lupus erythematosus, lupus nephritis, vasculopathy, thromboembolism

Abbreviations: SLE, systemic lupus erythematosus; APS, antiphospholipid antibody syndrome; VEGF, vascular endothelial growth factor; SLICC, Systemic Lupus International Collaborating Clinics; ANA, antinuclear antibodies; anti-dsDNA, anti-double-strand DNA antibodies; ESR, erythrocyte sedimentation rate; CRP, C-reactive protein; SLEDAI, Systemic Lupus Erythematosus Disease Activity Index; ELISA, enzyme-linked immunosorbent assay.

Laboratory Medicine 2022;53:285–289; https://doi.org/10.1093/labmed/lmab096

ABSTRACT

Objective: The aim of this study is to evaluate semaphorin 3A levels in patients with systemic lupus erythematosus (SLE) with and without renal involvement and secondary antiphospholipid antibody syndrome (APS).

Methods: Patients with SLE were grouped according to the presence of secondary APS or renal involvement. The control group consisted of age-matched, nonsmoking, healthy volunteers. Semaphorin 3A levels were compared among groups. All patients with SLE were regrouped according to the presence of thrombotic events, miscarriages, and proteinuria, and semaphorin 3A levels were investigated. Finally, semaphorin 3A levels of all patients with SLE as a single group were compared to those of the control patients.

Results: The mean semaphorin 3A values were 16.16 ± 2.84 ng/mL in the control group, 9.05 ± 5.65 ng/mL in patients with SLE without nephritis and APS, 11.28 ± 5.23 ng/mL in the SLE with APS group, and 8.53 ± 5.11 ng/mL in the lupus nephritis group. When all 3 patient groups were examined as a single group, the mean semaphorin 3A value was significantly lower than that of the control group. Semaphorin 3A was reduced in patients with SLE with thromboembolism and/or history of miscarriage.

Conclusion: Semaphorin 3A levels were lower in all patient groups compared to the control group. Moreover, the reduced semaphorin 3A levels in patients with a history of thromboembolism and/or miscarriage suggest that semaphorin 3A may play an important role in the pathogenesis of vasculopathy.

Systemic lupus erythematosus (SLE) is a chronic, systemic, autoimmune, inflammatory connective tissue disease. Although multiple genetic, hormonal, and environmental factors have been associated with disease development, its etiopathogenesis is yet to be fully clarified.[1]

Research has shown that SLE may result in a wide range of clinical presentations, and renal involvement (lupus nephritis) is one of the major predictors of mortality and morbidity. The clinical presentation of lupus nephritis is highly variable, ranging from subclinical involvement to end-stage renal disease. Renal involvement is a classic immune complex–mediated glomerulonephritis in most patients, caused by the binding of circulating immune complexes or autoantibodies to glomerular antigens. Vascular lesions in SLE are commonly referred as lupus vasculopathy, in which endothelial cell activation, vascular wall necrosis, inflammation, and thrombosis play a major role.[2] Antiphospholipid antibody syndrome (APS) is an autoimmune condition often associated with thrombotic events, microangiopathy, and/or pregnancy morbidities, which can frequently present in patients with SLE as a part of the clinical scenario, further contributing to the vascular complications. It is characterized by the presence of lupus anticoagulant, anti-cardiolipin, and anti-β2 glycoprotein I antibodies, collectively known as anti-phospholipid antibodies.[3]

Semaphorins were initially described as neural guidance cues that guide axons to their targets. Subsequent studies have shown that semaphorins are membrane-associated proteins that are involved in numerous physiological processes, including vascular growth, regulation of the tumor microenvironment, bone homeostasis, retinal homeostasis, and regulation of immune response.[4] Semaphorins are divided into 8 subclasses according to their C terminal structures. Classes 1 and 2 are found in invertebrates, classes 3 through 7 are found in vertebrates, and class 8 semaphorins are specific to viruses. Class 3 semaphorins are secreted proteins, and class 4 to 6 semaphorins are membrane-bound. Plexins and neurophilins have been identified as the primary semaphorin receptors.[5] Although most membrane-bound semaphorins bind plexins directly, class 3 semaphorins need neurophilins as a coreceptor to bind to plexins.[6] Neurophilin-1, identified as the receptor of semaphorin 3A, also acts as a receptor for vascular endothelial growth factor (VEGF) in both endothelial and tumor cells. Consequently, semaphorin 3A acts as an antiangiogenic because of the competitive inhibition of VEGF.[7]

Both secreted and membrane-bound semaphorins have various roles in immune response and contribute to the pathogenesis of autoimmune diseases. Studies from the last decade have examined the relationship of semaphorins with rheumatoid arthritis, SLE, systemic sclerosis, and antineutrophil cytoplasmic antibody–associated vasculitis and have shown their potential as targets in the diagnosis and treatment of these rheumatic diseases.[8]

In this study, we aimed to evaluate semaphorin 3A levels in patients with SLE with and without renal involvement or secondary antiphospholipid antibody syndrome (APS) to further elucidate the contribution of semaphorin 3A to the etiopathogenesis of these conditions.

Methods

All procedures in this cross-sectional study were approved by the institutional ethics committee and were therefore performed in accordance with the ethical standards laid down in the 1964 Declaration of Helsinki and its later amendments.

Patients aged 18 to 70 years who presented to the rheumatology outpatient clinic at Ankara Yıldırım Beyazıt University Medical School, Ankara City Hospital (Ankara, Turkey) between October 2019 and March 2020 with a diagnosis of SLE meeting the 2012 Systemic Lupus International Collaborating Clinics (SLICC) classification criteria were enrolled consecutively upon acceptance.[9]

Patient demographics, smoking status, years of diagnosis, comorbidities, history of thrombotic events, thrombus location, history of miscarriage, involved organ systems according to SLICC 2012 definitions, and medications were recorded.[9] The presence of positive antinuclear antibodies (ANA), anti-double-strand DNA antibodies (anti-dsDNA), anticardiolipin and anti-β2 glycoprotein IgG and M antibodies, and lupus anticoagulant positivity were investigated from the hospital database. Levels of serum complement 3 and 4, erythrocyte sedimentation rate (ESR), C-reactive protein (CRP), creatinine, spot urine protein excretion, and whole blood count numbers from the last visit were also recorded. Disease activity of the patients was calculated with respect to the Systemic Lupus Erythematosus Disease Activity Index (SLEDAI) and categorized as no activity (0), mild activity (1–5), moderate activity (6–10), high activity (11–19), and very high activity (≥20).

Venous blood specimens from all participants were collected into serum separator tubes and centrifuged at 4°C at 1000*g* for 10 minutes to separate the serum. Serum specimens were kept at –80°C until analysis. Before the analysis, serum specimens were thawed at room temperature and homogenized by vortexing. Serum semaphorin 3A levels were determined quantitatively using an enzyme-linked immunosorbent assay (ELISA) with the Cusabio commercial kit (CSB-E15913h; Cusabio Technology LLC, Wuhan Hi-Tech Medical Devices Park, Wuhan, China) and an ELISA microplate reader (Thermo Scientific Varioskan Flash, Finland). The detection range of the assay was 0.156 to 10 ng/mL with a sensitivity of 0.039 ng/mL. Intra-assay and interassay coefficient of variation percentage values were <8% and <10%, respectively. Specimens were diluted 1/4 before analysis in accordance with the manufacturer's recommendations. The serum semaphorin 3A concentration was calculated by multiplying the results obtained after the analysis by 4.

Patients were thereafter grouped as (1) patients without secondary APS or renal involvement (group A), (2) patients with secondary APS (meeting the revised Sapporo classification criteria[10] [group B]), and (3) patients with biopsy-proven lupus nephritis (group C). Patients with both secondary APS and lupus nephritis were enrolled in group B. A control group of 19 healthy volunteers was formed afterward from individuals aged 18 to 70 years without a history of any systemic, autoimmune, or thromboembolic disease, smoking, or malignancy and who were not receiving any medication. Semaphorin 3A levels were compared across groups. Thereafter, patients were regrouped with respect to the presence of thrombotic events, miscarriages, and proteinuria, regardless of meeting APS classification criteria or biopsy-proven lupus nephritis. In our study, a spot urine protein/creatinine ratio >150 mg/g was taken as a proteinuria criterion.[11] Differences in semaphorin 3A levels were further investigated accordingly.

Data were analyzed using SPSS 24.0 software. The groups were compared using the *t*-test, and quantitative variables were expressed using descriptive statistics (means and standard deviations). Nominal variables were presented using percentages, and *P* values ≤.05 were considered statistically significant.

Results

A total of 78 participants (59 patients with SLE, 19 healthy control patients) were enrolled in the study. Demographics, clinical features, and the distribution of participants across groups are noted in **TABLE 1**.

In terms of SLEDAI scores, the majority of patients in all 3 groups had mild activity. Hydroxychloroquine and corticosteroids were the most commonly used medications in patients without APS (groups A and C), whereas hydroxychloroquine and acetylsalicylic acid were the most common in patients with secondary APS (group B). According to the SLICC classification system definitions, the most common clinical findings related to lupus were acute cutaneous lupus in groups A and B and synovitis (after renal involvement) in group C.

The mean semaphorin 3A level was 9.05 ± 5.65 ng/mL in group A, 11.28 ± 5.23 ng/mL in group B, 8.53 ± 5.11 ng/mL in group C, and 16.16 ± 2.84 ng/mL in the control group. In pairwise comparisons, all patient groups had significantly reduced semaphorin 3A levels when compared to those of the control group. No statistically significant differences were observed in pairwise comparisons between patient groups (**TABLE 2**, **FIGURE 1**).When the patient groups were examined as a single group, their mean semaphorin 3A value was again

TABLE 1. Demographics and Clinical Features of Patients with SLE and Control Patients[a]

	Group A (n = 20)	Group B (n = 20)	Group C (n = 19)	Control Patients (n = 19)
Age, mean ± SD (y)	41.55 ± 12.92	40.7 ± 12.08	33.89 ± 8.68	40.74 ± 8.54
Sex, female, n (%)	20 (100)	16 (80)	17 (89.5)	17 (89.50)
Active smokers, n (%)	5 (25)	4 (20)	5 (26.3)	0 (0.00)
Clinical features, n (%)				…
ACL	11 (55.0)	11 (55.0)	7 (36.8)	…
CCL	4 (20.0)	5 (25.0)	2 (10.5)	…
Alopecia	11 (55.0)	9 (45.0)	5 (26.3)	…
Oral/nasal ulcers	8 (40.0)	3 (15.0)	7 (36.8)	…
Serositis	0 (0.0)	0 (0.0)	3 (15.8)	…
Synovitis	10 (50.0)	10 (50.0)	9 (47.4)	…
Renal involvement	0 (0.0)	4 (20.0)	18 (100)	…
Neurologic involvement	0 (0.0)	0 (0.0)	1 (5.3)	…
Hematologic involvement	1 (5.0)	1 (5.0)	0 (0.0)	…
Thrombotic event	1 (5.0)	13 (65)	2 (10.5)	…
DVT	1	8	1	…
PTE	0	2	0	…
CVE	0	6	1	…
Mesenteric ischemia	0	0	0	…
MI	0	0	0	…
Retinal thrombosis	0	1	0	…
Miscarriage	17 (85.0)	6 (30.0)	11 (64.71)	
SLEDAI score, n (%)				…
Remission	0 (0.0)	1 (5.0)	1 (5.3)	…
Mild activity	11 (55.0)	14 (70.0)	11 (57.9)	…
Moderate activity	8 (40.0)	5 (25.0)	6 (31.6)	…
High activity	1 (5.0)	0 (0.0)	1 (5.3)	…
Very high activity	0 (0.0)	0 (0.0)	0 (0.0)	
Current medications, n (%)				…
Hydroxychloroquine	18 (90.0)	17 (85.0)	14 (73.7)	…
Corticosteroid	11 (55.0)	8 (40.0)	14 (73.7)	…
Azathioprine	3 (15.0)	4 (20.0)	1 (5.3)	…
Mycophenolate mofetil	0 (0.0)	4 (20.0)	11 (57.9)	…
Acetylsalicylic acid	2 (10.0)	9 (45.0)	8 (42.1)	…
Warfarin	1 (5.0)	7 (35.0)	0 (0.0)	

ACL, acute cutaneous lupus; CCL, chronic cutaneous lupus; CVE, cerebrovascular event; DVT, deep vein thrombosis; MI, myocardial infarction; PTE, pulmonary thromboembolism; SD, standard deviation; SLE, systemic lupus erythematosus; SLEDAI: Systemic Lupus Erythematosus Disease Activity Index.
[a]Groups: (A) Patients with SLE without secondary antiphospholipid syndrome or renal involvement, (B) patients with secondary antiphospholipid syndrome, and (C) patients with biopsy-proven lupus nephritis.

TABLE 2. Pairwise Comparisons of Semaphorin 3A Levels Between Patient Groups and Control Patients[a]

	Patient Group				*P* Value
	Group A (n = 20)	Group B (n = 20)	Group C (n = 19)	Control (n = 19)	
Semaphorin 3A, ng/mL, mean ± SD	9.05 ± 5.65	11.28 ± 5.23	8.53 ± 5.11	16.16 ± 2.84	Group A vs control <.001
					Group B vs control <.001
					Group C vs control <.001
					Group A vs B = .203
					Group A vs C = .766
					Group B vs C = .106
	All Patients (n = 59)		Control (n = 19)		<.001
	9.64 ± 5.38		16.16 ± 2.84		

SD, standard deviation; SLE, systemic lupus erythematosus.
[a]Groups: (A) Patients with SLE without secondary antiphospholipid syndrome or renal involvement, (B) patients with secondary antiphospholipid syndrome, and (C) patients with biopsy-proven lupus nephritis.

FIGURE 1. Semaphorin 3A levels in patient groups. APS, antiphospholipid antibody syndrome; SLE, systemic lupus erythematosus.

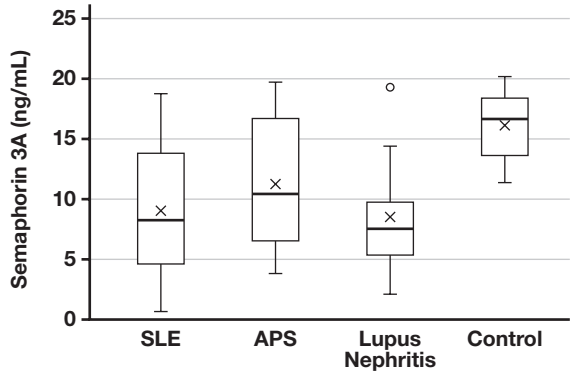

TABLE 3. Comparison of Semaphorin 3A Levels with History of Thrombus, Miscarriage, and Proteinuria

	Semaphorin 3A, ng/mL, mean ± SD	*P* Value
Patients with thrombotic events and/or miscarriages (n = 31)	9.96 ± 5.11	.032
Patients without thrombotic events and/or miscarriages (n = 47)	12.33 ± 5.84	
Patients with proteinuria and/or thrombotic events and/or miscarriages (n = 44)	9.05 ± 5.09	<.001
Patients without proteinuria and/or thrombotic events and/or miscarriages (n = 34)	14.91± 4.50	

significantly lower than that of the control group (9.64 ± 5.38 ng/mL vs 16.16 ± 2.84 ng/mL; P <.001).

In our study, no significant correlations were observed between semaphorin 3A levels and age, ANA positivity, anti-dsDNA, antiphospholipid antibody complement levels, hemoglobin, leukocyte count, international normalized ratio, ESR, CRP, and creatinine values. Likewise, no statistically significant correlation was found between the SLEDAI scores and semaphorin 3A values.

When patient groups were reorganized according to the presence of proteinuria and/or thrombotic events and/or miscarriages, the mean semaphorin 3A levels were significantly lower in patients with a history of thrombotic event and/or miscarriage when compared to patients without this history (9.96 ± 5.11 ng/mL vs 12.33 ± 5.84 ng/mL; P = .032). When proteinuria was added as a factor to thrombosis and miscarriages, a more significant reduction was observed in semaphorin 3A levels (**TABLE 3**).

Discussion

Our results showed that semaphorin 3A levels were significantly lower in patients with SLE with or without secondary APS and lupus nephritis without significant differences between patient subgroups. Furthermore, the mean semaphorin 3A levels were significantly reduced in patients with a history of thrombosis and/or a history of miscarriage when compared to patients without this history, and adding the presence of proteinuria as a factor for vascular events resulted in further lowered semaphorin 3A levels.

Semaphorin signaling plays a role in cardiovascular and lymphatic development. In addition, it is also involved in the maintenance of hemostasis and vascular permeability by providing communication between platelets in cases such as vascular injury. In the immune system, semaphorin is involved in tasks such as the regulation of immune cell migration, thymocyte differentiation, and cytokine production in cases of infection. In animal studies, it has been observed that the administration of exogenous semaphorin 3A activates innate immune cells and increases cytokine production in response to bacterial sepsis. It has also been shown that semaphorin 3A regulates dendritic cell migration between lymphatics and has positive effects on the innate immune response.[12]

Semaphorin 3A is well known as a powerful immune regulator and participates in all stages of inflammatory processes. Semaphorin 3A can suppress T- and B-cell proliferation and reduce the production of proinflammatory cytokines by T cells.[13] The literature indicates that the reduced expression of semaphorin 3A plays a role in the exacerbation of many autoimmune diseases. There are multiple studies comparing semaphorin 3A levels in control patients to those in patients with autoimmune conditions, including SLE, rheumatoid arthritis, and systemic sclerosis. However, there are no other studies investigating semaphorin 3A levels in APS.

Wang et al[14] evaluated semaphorin 3A levels in 80 patients with SLE and 80 control patients; similar to our results, they found that semaphorin 3A levels were significantly lower in patients with SLE. Vadasz et al[15] investigated the relationship between semaphorin 3A levels and renal involvement among patients with SLE. They reported renal involvement in 73% of patients with semaphorin 3A levels <50 ng/mL and in only 5% of patients with semaphorin 3A levels >50 ng/mL and an inverse correlation between semaphorin 3A levels and disease activity. Contrary to their results, we did not find a statistically significant difference in semaphorin 3A levels in patients with SLE with and without renal involvement. Gao et al[16] similarly found a negative correlation between disease activity and semaphorin 3A levels whereas Wang et al[14] did not report a significant correlation between disease activity and semaphorin 3A levels.

Our study further indicated that the mean semaphorin 3A level was significantly reduced in patients with a history of thrombosis and/or a history of miscarriage when compared to patients without this history. Neurophilin-1, a semaphorin 3A receptor, also acts as a receptor for VEGF, a factor involved in angiogenesis, which allows semaphorin 3A to act as an antiangiogenic because of the competitive inhibition of VEGF. An imbalance between semaphorin 3A and VEGF can result in structural and functional vascular abnormalities.[17] Maione et al[18] also showed that semaphorin 3A is an endogenous antiangiogenic that reduces the growth and abnormal vascularization of tumoral tissues, particularly without causing persistent hypoxia and disrupting vascularity in normal vessels. Therefore, semaphorin 3A may be potentially involved in thromboembolism in pathological conditions such as autoimmune diseases. Decreased semaphorin 3A levels in patients with a history of thromboembolism and/or miscarriage may be ascribed to its increased consumption in the case of vascular involvement.

Increased urine semaphorin 3A excretion has previously been reported to correlate with kidney damage and proteinuria in patients with diabetes and hypertension, suggesting a relation between chronic kidney disease and semaphorin 3A malfunction.[19,20]

Although semaphorin 3A levels were not significantly different between patients with or without nephritis in our study, adding the presence of proteinuria as a factor to vascular events resulted in further lowered semaphorin 3A levels. However, this finding should be interpreted with caution because proteinuria was not evaluated as a single variable in our study.

Our study had some limitations. First, the study was conducted in a single center and was cross-sectional. In addition, the patient number could be considered low and because most of the patients were under effective treatment, most of them had only mild disease activity.

Conclusion

Semaphorins play an important role in the pathogenesis and prognosis of autoimmune diseases. They are potentially valuable tools for the diagnosis and follow-up of autoimmune diseases and can serve as a potential target for treatment in the near future. In our study, semaphorin 3A levels were reduced in all patients with SLE regardless of secondary APS and renal involvement. However, semaphorin 3A levels were found to be lower in patients with thrombotic events and/or miscarriage, suggesting that low semaphorin 3A levels may be a predictor of vasculopathic events in the context of SLE. The evaluation of semaphorin 3A levels in larger groups with more treatment-naïve patients may further indicate the effect of semaphorin 3A on vascular involvement.

Acknowledgments

The study protocol was approved by the institutional committee on Human Research Ethics. The datasets used in this study are available from the corresponding author upon valid request. All authors substantially contributed to study design and acquisition, analysis, and interpretation of the data. All authors revised the final version of the work and approved for publication in agreement on all aspects of the study. There is no editing support to acknowledge.

REFERENCES

1. Gualtierotti R, Biggioggero M, Penatti AE, Meroni PL. Updating on the pathogenesis of systemic lupus erythematosus. *Autoimmun Rev.* 2010;10(1):3–7.
2. Cieślik P, Hrycek A, Kłuciński P. Vasculopathy and vasculitis in systemic lupus erythematosus. *Pol Arch Med Wewn.* 2008;118(1–2):57–63.
3. Chaturvedi S, Brodsky RA, McCrae KR. Complement in the pathophysiology of the antiphospholipid syndrome. *Front Immunol.* 2019;10:449.
4. Gu C, Yoshida Y, Livet J, et al. Semaphorin 3E and plexin-D1 control vascular pattern independently of neurophilins. *Science.* 2005;307(5707):265–268.
5. Pasterkamp RJ. Getting neural circuits into shape with semaphorins. *Nat Rev Neurosci.* 2012;13(9):605–618.
6. Takamatsu H, Okuno T, Kumanogoh A. Regulation of immune cell responses by semaphorins and their receptors. *Cell Mol Immunol.* 2010;7(2):83–88.
7. Guttmann-Raviv N, Shraga-Heled N, Varshavsky A, Guimaraes-Sternberg C, Kessler O, Neufeld G. Semaphorin-3A and semaphorin-3F work together to repel endothelial cells and to inhibit their survival by induction of apoptosis. *J Biol Chem.* 2007;282(36):26294–26305.
8. Nishide M, Kumanogoh A. The role of semaphorins in immune responses and autoimmune rheumatic diseases. *Nat Rev Rheumatol.* 2018;14(1):19–31.
9. Petri M, Orbai AM, Alarcón GS, et al. Derivation and validation of the Systemic Lupus International Collaborating Clinics classification criteria for systemic lupus erythematosus. *Arthritis Rheum.* 2012;64(8):2677–2686.
10. Gerosa M, Meroni PL, Erkan D. Recognition and management of antiphospholipid syndrome. *Curr Opin Rheumatol.* 2016;28(1):51–59.
11. Yasar E, Ozger HS, Yeter HH, et al. Could urinary kidney injury molecule-1 be a good marker in subclinical acute kidney injury in mild to moderate COVID-19 infection? *Int Urol Nephrol.* Published online ahead of print July 2, 2021. doi: 10.1007/s11255-021-02937-0.
12. Takamatsu H, Takegahara N, Nakagawa Y, et al. Semaphorins guide the entry of dendritic cells into the lymphatics by activating myosin II. *Nat Immunol.* 2010;11(7):594–600.
13. Yamamoto M, Suzuki K, Okuno T, et al. Plexin-A4 negatively regulates T lymphocyte responses. *Int Immunol.* 2008;20(3):413–420.
14. Wang P, Mao YM, Liu LN, Zhao CN, Li XM, Pan HF. Decreased expression of semaphorin 3A and semaphorin 7A levels and its association with systemic lupus erythematosus. *Immunol Invest.* 2020;49(1≠2):69–80.
15. Vadasz Z, Haj T, Halasz K, et al. Semaphorin 3A is a marker for disease activity and a potential immunoregulator in systemic lupus erythematosus. *Arthritis Res Ther.* 2012;14(3):R146.
16. Gao H, Ma XX, Guo Q, et al. Expression and clinical significance of semaphorin 3A in serum and mononuclear cells in patients with systemic lupus erythematosus. *Zhonghua Yi Xue Za Zhi.* 2017;97(5):370–374.
17. Serini G, Valdembri D, Zanivan S, et al. Class 3 semaphorins control vascular morphogenesis by inhibiting integrin function. *Nature.* 2003;424(6947):391–397.
18. Maione F, Molla F, Meda C, et al. Semaphorin 3A is an endogenous angiogenesis inhibitor that blocks tumor growth and normalizes tumor vasculature in transgenic mouse models. *J Clin Invest.* 2009;119(11):3356–3372.
19. Mohamed R, Ranganathan P, Jayakumar C, et al. Urinary semaphorin 3A correlates with diabetic proteinuria and mediates diabetic nephropathy and associated inflammation in mice. *J Mol Med (Berl).* 2014;92(12):1245–1256.
20. Viazzi F, Ramesh G, Jayakumar C, Leoncini G, Garneri D, Pontremoli R. Increased urine semaphorin-3A is associated with renal damage in hypertensive patients with chronic kidney disease: a nested case-control study. *J Nephrol.* 2015;28(3):315–320.

The Relationship of Thyroid Functions with ADMA, IMA, and Metabolic Laboratory Parameters in Euthyroid Adults with and without Autoimmune Thyroiditis

Zeynep Cetin,[1,] Arzu Kosem,[2] Merve Catak,[3] Bulent Can,[4] Ozden Baser,[5] Serdar Guler[6]*

[1]Division of Endocrinology and Metabolism, Department of Internal Medicine, Amasya University Medicine Faculty, Amasya, Turkey, [2]Department of Clinical Biochemistry, University of Health Sciences, Ankara City Hospital, Ankara, Turkey current affiliation: University of Health Sciences, Diskapi Education and Research Hospital, Ankara, Turkey, [3]Division of Endocrinology and Metabolism, Department of Internal Medicine, Gaziosmanpaşa University Medicine Faculty, Tokat, Turkey, [4]Division of Endocrinology and Metabolism, Department of Internal Medicine, Medeniyet University Medicine Faculty, Istanbul, Turkey, [5]Department of Endocrinology and Metabolism, Yozgat City Hospital, Yozgat, Turkey, [6]Department of Endocrinology and Metabolism, Liv Hospital, Ankara, Turkey; *To whom correspondence should be addressed. drzeynepcetin@gmail.com

Keywords: euthyroid, autoimmune thyroiditis, asymmetric dimethylarginine, ischemia-modified albumin, metabolic, risk

Abbreviations: ADMA, asymmetric dimethylarginine; IMA, ischemia-modified albumin; AIT, autoimmune thyroiditis; fT4, free thyroxine; fT3, free tri-iodothyronine; DM, diabetes mellitus; IMA-alb, IMA corrected to albumin; anti-TPO, anti-thyroid peroxidase antibody; anti-TG, anti-thyroglobulin antibody; FPG, fasting plasma glucose; CRP, C-reactive protein; ABSU, absorbance unit; SD, standard deviation; HDL, high-density lipoprotein; LDL, low-density lipoprotein; ROS, free-oxygen radical.

Laboratory Medicine 2022;53:290–295; https://doi.org/10.1093/labmed/lmab098

ABSTRACT

Objective: To investigate the relationship between thyroid functions and asymmetric dimethylarginine (ADMA), ischemia-modified albumin (IMA), and other metabolic laboratory markers in euthyroid adults and whether narrower thyroidal targets are required for lower metabolic risk.

Materials and Methods: Thyroid functions, antithyroid autoantibodies, and metabolic parameters were measured for 115 patients. Forty-seven had autoimmune thyroiditis (AIT). Analyses were performed according to cutoff values of 1, 2, 2.5, and 3 mIU/L for thyrotropin, 0.84 ng/dL for free thyroxine (fT_4), and 3.59 ng/dL for free tri-iodothyronine (fT_3).

Results: There was no relationship between thyrotropin and fT_3 cutoff values and metabolic parameters. Only C-reactive protein was lower in the group with thyrotropin ≤2.5 μIU/L. A weak positive correlation was found between fT_4 with IMA and IMA corrected for albumin ($r = 0.187$, $P = .05$; $r = 0.204$, $P = .034$, respectively). There was no difference between AIT and the metabolic laboratory parameters examined in the study.

Conclusion: This study is the first to evaluate ADMA in AIT. Narrower thyroid function targets are not required for better metabolic control in euthyroid adults.

Thyroid hormones have an essential role in conducting normal metabolic activities. They regulate metabolism and provide energy and weight balance by acting mainly on the brain, adipose tissue, skeletal muscle, liver, and pancreas. Problems in thyroid function lead to disruption in metabolic activities and increased oxidative stress, leading to cardiovascular and metabolic diseases.[1]

Asymmetric dimethylarginine (ADMA) is a protein that inhibits nitric oxide synthase.[2] Nitric oxide is one of the major vasodilators and platelet aggregation inhibitors and is effective in cardiovascular protection of the organism; ADMA causes a decrease in nitric oxide levels. It has been shown in many studies that ADMA increases in cardiovascular and renal diseases and in diabetes mellitus (DM).[3] Similarly, ADMA levels are high in hyperthyroidism and metabolic syndrome.[2,4]

Ischemia-modified albumin (IMA) is an ischemia marker that was first found to be high in patients with acute myocardial ischemia.[5] During ischemia, the binding of albumin to exogenous cobalt decreases, and the degree of ischemia is determined by detecting an increase in IMA levels. The IMA index corrected for albumin (IMA-alb) is used because it is affected by changes in albumin levels. In addition, IMA elevation, which is found in many cardiovascular diseases, has been shown in patients with hyperthyroidism.[6]

In this study, the relationship between thyroid hormone levels and ADMA, IMA, and other metabolic laboratory markers in euthyroid adults with/without autoimmune thyroiditis (AIT) and the necessity of a narrower thyroid function range for normal metabolism were investigated.

Materials and Methods

Ethical Approval

The local ethics committee approved the study (number 1044/2016). All procedures were in accordance with the ethical standards of the

institutional research committee and with the 1964 Helsinki Declaration and its later amendments or comparable ethical standards. Informed consent was obtained from the participants.

Patient Selection

This is a cross-sectional study. It was conducted on 144 euthyroid individuals between October 1, 2016, and January 1, 2017. Pregnant women, applicants aged <18 years, and those with chronic diseases were excluded. Patients using any drugs effective on metabolism were also excluded. One hundred fifteen patients met the inclusion criteria (**FIGURE 1**). Eventually, 115 individuals were recruited.

Laboratory

Thyrotropin, free thyroxine (fT_4), free tri-iodothyronine (fT_3), anti-thyroid peroxidase antibody (anti-TPO), anti-thyroglobulin antibody (anti-TG), fasting plasma glucose (FPG), fasting insulin, lipids, C-reactive protein (CRP), ADMA, and IMA levels were measured.

The thyrotropin, fT_4, fT_3, anti-TPO, anti-TG, and fasting insulin levels were measured (sandwich immunoassay) on a Roche cobas E601 Analyzer; FPG, lipids, and CRP levels were measured (spectrophotometric methods) on a Roche cobas C501 Analyzer (Roche Diagnostics). The ADMA levels were studied using a Beckman-Coulter DXI-800 immunoassay device with an enzyme-linked immunosorbent assay. The normal value range is 117.6 to 573.7 ng/mL.

The IMA was measured colorimetrically using a Spekol brand spectrometer; results are given according to absorbance unit (ABSU). Values >0.400 ABSU indicate the presence of ischemia. The IMA-alb index was calculated using the formula = serum albumin concentration (g/dL) × 23 + IMA (U/mL) – 100.

Ultrasonographic evaluation of the thyroid glands of all volunteers was performed using a Hitachi EUB-7000 HV device by the same endocrinologist. Thyroid echogenicity was compared with the surrounding tissue and classified from homogeneous to advanced heterogeneous. We detected AIT in 48 participants by using autoantibody levels and sonographic characteristics. Thyroid gland volumes were calculated according to the formula of anterior-posterior diameter × transverse diameter × longitudinal diameter × 0.52.[7]

Data Analysis

Statistical analyses were performed using the IBM SPSS for Windows Version 24.0 software. Numerical variables are summarized as mean ± standard deviation (SD) and median (minimum-maximum). Categorical variables are represented as numbers and percentages. The differences between the groups in terms of categorical variables were investigated using the χ^2 test or Fisher's exact test. The Kolmogorov-Smirnov test, histograms, ratios of SD/mean, skewness, and kurtosis were used to determine whether the numerical variables showed normal distribution. Homogeneity of variance was examined using the Levene test. The *t*-test was used for normally distributed parameters, and the Mann-Whitney *U* test was used for nonnormally distributed parameters. Pearson's correlation analysis was used to determine relationships between parameters. The significance level was accepted as $P < .05$.

AQ11

Results

TABLE 1 shows the basic demographic, laboratory, and sonographic data of the participants. Those that conformed to normal distribution are shown as mean ± standard deviation, and those that did not are shown as median (minimum-maximum).

In **TABLE 2**, a comparison is made by grouping the participants according to a thyrotropin cutoff of 1, 2, 2.5, and 3 μIU/L. The CRP level was found to be lower in the group with thyrotropin ≤2.5 μIU/L than in the group with thyrotropin >2.5 μIU/L. No significant results were obtained in the correlation analysis between thyrotropin and metabolic parameters (**TABLE 3**).

Ninety-nine (86%) of the participants had fT_3; the median fT_3 was 3.59 ng/dL. One hundred eleven (96.5%) of the participants had fT_4; the median fT_4 was 0.84 ng/dL. A comparison was made according to these values; no significant difference was observed (**TABLE 4**). In the correlation analysis between fT_3, fT_4, and the same parameters, a weak positive correlation was found between fT_4 and IMA and IMA-alb (**TABLE 5**).

Forty-seven participants with AIT and 68 participants without AIT were compared for metabolic parameters and no significant differences

FIGURE 1. Patient flow diagram.

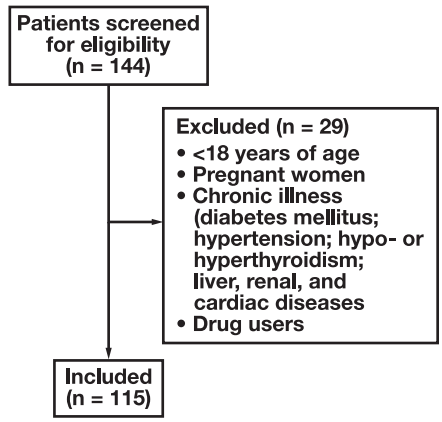

TABLE 1. Baseline Characteristics of All Participants

Parameter	All Participants (n = 115)	Parameter	All Participants (n = 115)
Age (y)	40.57 ± 11.55	ADMA (ng/mL)	213.49 (15.9–1040.46)
Sex, n (%) (female/male)	101 (87.8)/14 (12.2)	IMA (ABSU)	0.436 (0.003–0.937)
Thyrotropin (μIU/L)	2 (0.51–4)	IMA-alb (ABSU)	0.444 (0.003–1.071)
fT_4 (ng/dL)	0.84 (0.64–1.18)	Total cholesterol (mg/dL)	200.06 ± 46.18
fT_3 (ng/dL)	3.59 (0.71–4.49)	Triglyceride (mg/dL)	101 (32–447)
Anti-TPO (IU/mL)	1.45 (0.1–3460)	LDL-C (mg/dL)	121 (38–282)
Anti-TG (IU/mL)	0.9 (0.1–1049)	HDL-C (mg/dL)	51 (33–93)
FPG (mg/dL)	92.37 ± 8.29	Non-HDL-C (mg/dL)	147.66 ± 44.74
Insulin (μIU/mL)	7.62 (1.87–31.97)	CRP (mg/L)	2 (0.2–18)
HOMA-IR	1.67 (0.40–7.66)	AIT, n (%)	47 (40.8)

ADMA, asymmetric dimethylarginine; AIT, autoimmune thyroiditis; anti-TG, anti-thyroglobulin; anti-TPO, antithyroid peroxidase; CRP, C-reactive protein; FPG, fasting plasma glucose; fT_3, free tri-iodothyroinine; fT_4, free thyroxine; HDL-C, high-density lipoprotein cholesterol; HOMA-IR, homeostatic model values for insulin resistance; IMA, ischemia modified albumin; IMA-alb, IMA-corrected to albumin; LDL-C, low-density lipoprotein cholesterol; non-HDL-C, lipoproteins other than HDL.

TABLE 2. Comparison of Groups According to Thyrotropin Cutoffs

Parameter	Thyrotropin < 1 (n = 21)	Thyrotropin > 1 (n = 94)	*P* Value	Thyrotropin < 2 (n = 58)	Thyrotropin > 2 (n = 57)	*P* Value	Thyrotropin < 2.5 (n = 78)	Thyrotropin > 2.5 (n = 37)	*P* Value	Thyrotropin < 3 (n = 93)	Thyrotropin > 3 (n = 22)	*P* Value
Age (y)	41.95	40.26	.545	40.55	40.58	.990	41.17	39.3	.420	40.99	38.77	.421
Sex, n (female/male)	18/3	83/11	.743	48/10	53/4	.094	67/11	34/3	.358	79/14	22/0	.052
Thyrotropin (μIU/L)	0.82	2.38	**.000**	1.3	2.9	**.000**	1.56	3.22	**.000**	1.75	3.54	**.000**
FPG (mg/dL)	92.95	92.24	.725	93.31	91.42	.223	92.48	92.13	.833	92.29	92.72	.825
Insulin (μIU/mL)	10.30	8.77	.148	9.5	8.6	.289	9.10	8.94	.719	9.19	8.46	.717
HOMA-IR	2.42	2.04	.180	2.2	1.97	.229	2.12	2.08	.662	2.14	1.97	.760
ADMA (ng/mL)	292.56	286.11	.764	322.26	251.70	.075	311.62	235.99	.109	299.96	233.71	.160
IMA (ABSU)	0.478	0.441	.494	0.461	0.434	.506	0.450	0.442	.634	0.54	0.419	.138
IMA-alb (ABSU)	0.479	0.445	.612	0.464	0.438	.436	0.453	0.447	.575	0.460	0.417	.144
Total cholesterol (mg/dL)	194.85	201.23	.570	195.58	204.63	.296	197.80	204.83	.448	198.26	207.68	.392
Triglycerides (mg/dL)	119.76	121.93	.587	116.46	126.70	.408	120.29	124.16	.565	122.18	118.81	.834
LDL-C (mg/dL)	118.76	125.03	.471	119.81	128.03	.313	121.84	128.18	.715	122.11	131.36	.683
HDL-C (mg/dL)	52.14	52.46	.519	52.48	52.33	.529	52.65	51.89	.981	52.35	52.63	.662
Non-HDL-C (mg/dL)	142.71	148.76	.578	143.10	152.29	.272	145.15	152.94	.425	145.91	155.04	.392
CRP (mg/L)	3.66	3.93	.763	3.21	4.57	.147	3.43	4.85	**.032**	3.69	4.70	.239

ABSU, absorbance unit; ADMA, asymmetric dimethylarginine; CRP, C-reactive protein; FPG, fasting plasma glucose; HDL-C, high-density lipoprotein cholesterol; HOMA-IR, homeostatic model values for insulin resistance; IMA, ischemia modified albumin; IMA-alb, IMA-corrected to albumin; LDL-C, low-density lipoprotein cholesterol; non-HDL-C, lipoproteins other than HDL.

TABLE 3. Correlations Between Thyrotropin and Metabolic Parameters

Parameter	*r*	*P* Value
FPG (mg/dL)	–0.059	.528
Insulin (μIU/mL)	–0.146	.120
HOMA-IR	–0.149	.112
ADMA (ng/mL)	–0.164	.079
IMA (ABSU)	–0.100	.288
IMA-alb (ABSU)	–0.097	.308
Total cholesterol (mg/dL)	0.068	.472
Triglycerides (mg/dL)	–0.016	.865
LDL-C (mg/dL)	0.072	.443
HDL-C (mg/dL)	0.080	.393
Non-HDL-C (mg/dL)	0.064	.495
CRP (mg/L)	0.099	.292

ABSU, absorbance unit; ADMA, asymmetric dimethylarginine; CRP, C-reactive protein; FPG, fasting plasma glucose; HDL-C, high-density lipoprotein cholesterol; HOMA-IR, homeostatic model values for insulin resistance; IMA, ischemia modified albumin; IMA-alb, IMA-corrected to albumin; LDL-C, low-density lipoprotein cholesterol; non-HDL-C, lipoproteins other than HDL.

were found. However, a significant difference was determined in terms of sex in the subgroup analysis (**TABLE 6**). No correlation was found between antithyroid antibodies and ADMA, IMA, and IMA-alb, which were examined specifically for the study (**TABLE 7**).

The correlation between thyroid volume and thyrotropin, ADMA, IMA, and alb-IMA was investigated. A significant negative correlation was found only between thyrotropin and the right-left lobe volumes ($r = -0.385$, $P \leq .001$; $r = -0.515$, $P \leq .001$, respectively). When the same analyses were repeated for patients with Hashimoto thyroiditis, a significant negative correlation was found only between right thyroid volume and thyrotropin ($r = -0.383$, $P = .011$). No correlation was observed between other parameters and thyroid volumes (**TABLE 8**).

Discussion

Significant results obtained in this study: CRP was lower in patients with thyrotropin ≤2.5 μIU/L, and there was a weak positive correlation between fT_4 and IMA and IMA-alb. Research has shown that CRP is not a specific metabolic marker; it can be affected in many ways, so one can conclude that there is no need to control thyrotropin, fT_4, and fT_3 at a narrower level for better metabolic protection in euthyroid individuals and that the presence of AIT does not increase the metabolic risk.

In our study, in addition to the standard laboratory tests (FPG, fasting plasma insulin, lipid parameters, and CRP), ADMA, IMA, and IMA-alb were examined. Studies have shown that ADMA is an inhibitor of nitric oxide synthase. Nitric oxide is an important vasodilator and platelet aggregation inhibitor for the organism. Defects in nitric oxide metabolism play an important role in the pathophysiology of endothelial diseases, with cardiovascular diseases the leader among them.[3] In addition, nitric oxide decreases in metabolic diseases such as type 2 DM and inflammatory disorders—that is, ADMA levels increase. Therefore,

TABLE 4. Comparison of Groups According to Median fT_3 and fT_4

Parameter	fT_3			fT_4		
	≤3.59 (n = 50)	>3.59 (n = 49)	*P* Value	≤0.84 (n = 58)	>0.84 (n = 53)	*P* Value
Age (y)	42.02	39.10	.204	41.64	38.89	.214
Sex, n (female/male)	46/4	39/10	.076	53/5	45/8	.289
FPG (mg/dL)	91.72	93.83	.213	93.08	91.56	.342
Insulin (μIU/mL)	9.10	9.84	.911	9.59	8.57	.392
HOMA-IR	2.08	2.35	.748	2.26	1.97	.399
ADMA (ng/mL)	288.21	271.58	.886	288.56	279.24	.843
IMA (ABSU)	0.469	0.437	.292	0.427	0.457	.219
IMA-alb (ABSU)	0.478	0.437	.283	0.429	0.460	.161
Total cholesterol (mg/dL)	201.70	201.26	.962	200	195.39	.592
Triglycerides (mg/dL)	116.46	125.32	.718	111.27	125.50	.300
LDL-C (mg/dL)	124.66	125.18	.897	124.68	119.98	.643
HDL-C (mg/dL)	53.66	51.10	.109	53.08	51.45	.247
Non-HDL-C (mg/dL)	148.04	150.16	.813	146.91	143.94	.722
CRP (mg/L)	3.65	4.25	.227	3.88	3.70	.394

ABSU, absorbance unit; ADMA, asymmetric dimethylarginine; CRP, C-reactive protein; FPG, fasting plasma glucose; fT_3, free tri-iodothyroinine; fT_4, free thyroxine; HDL-C, high-density lipoprotein cholesterol; HOMA-IR, homeostatic model values for insulin resistance; IMA, ischemia modified albumin; IMA-alb, IMA-corrected to albumin; LDL-C, low-density lipoprotein cholesterol; non-HDL-C, lipoproteins other than HDL.

TABLE 5. Correlation Analyses of Free-Thyroid Hormones and Metabolic Parameters

Parameter	fT_3		fT_4	
	r	*P* Value	*r*	*P* Value
FPG (mg/dL)	0.059	.564	–0.022	.821
Insulin (μIU/mL)	0.124	.222	–0.023	.807
HOMA-IR	0.139	.169	–0.019	.847
ADMA (ng/mL)	–0.009	.933	–0.001	.989
IMA (ABSU)	–0.190	.060	0.187	.050
IMA-alb (ABSU)	–0.176	.082	0.204	.034
Total cholesterol (mg/dL)	–0.129	.202	–0.003	.978
Triglycerides (mg/dL)	0.067	.508	0.055	.568
LDL-C (mg/dL)	–0.050	.623	–0.012	.903
HDL-C (mg/dL)	–0.118	.244	–0.091	.343
Non-HDL-C (mg/dL)	–0.127	.209	–0.006	.947
CRP (mg/L)	0.038	.711	–0.110	.251

ABSU, absorbance unit; ADMA, asymmetric dimethylarginine; CRP, C-reactive protein; FPG, fasting plasma glucose; fT_3, free tri-iodothyroinine; fT_4, free thyroxine; HDL-C, high-density lipoprotein cholesterol; HOMA-IR, homeostatic model values for insulin resistance; IMA, ischemia modified albumin; IMA-alb, IMA-corrected to albumin; LDL-C, low-density lipoprotein cholesterol; non-HDL-C, lipoproteins other than HDL.

ADMA (and its derivatives) has been extensively studied in understanding the pathophysiology of these diseases and improving treatment.[2] The other molecule associated with oxidative stress, IMA, is higher in individuals with hyperthyroidism and hypothyroidism than in euthyroid patients.[8] Our study examined the possible relationship between different thyrotropin and free hormone levels and ADMA and IMA in euthyroid individuals.

Thyroid dysfunction has a prevalence of approximately 6.6% in adults in developed countries; it increases with age, and it is more common in women.[9] Cardiovascular diseases, on the other hand, are the most common cause of death and are constantly increasing in both developed and developing countries. Glucose intolerance, lipid diseases, obesity, hypertension, and male sex, which can be signals of metabolic syndrome, are also cardiac risk factors.[10] Thyroid hormones are closely related to both metabolic syndrome and cardiovascular diseases, with their effects on lipid metabolism, energy consumption, insulin secretion, glucose metabolism, and blood pressure.[11] Many studies have shown that overt and subclinical thyroid diseases lead to worse cardiovascular outcomes.[12-14] Based on these studies, curiosity has arisen as to whether euthyroid status also carries similar risks. In the meta-analysis conducted by Lee et al,[15] the authors accepted the range of 0.5 to 5 μIU/L as a normal thyrotropin level, and the participants with higher thyrotropin and lower fT_4 had a higher cardiometabolic risk. We did not examine fT_3 in this study. Another study[16] was performed on 180 euthyroid patients with cardiomyopathy. The patients were followed up with a thyrotropin range of 0.55 to 4.78 μIU/L. It was found that as thyrotropin increased, the risk of ventricular arrhythmia increased, and if thyrotropin was >2.67 μIU/L, then more ventricular arrhythmia was observed.

The thyrotropin range is different between laboratories—the upper limit can go up to 5.5 μIU/L. However, there are publications in the literature indicating that thyrotropin <2.5 μIU/L is associated with lower risk.[17,18] Souza et al[19] conducted a study with overweight and obese adolescents and supported this value as a cutoff because lower homeostatic model values for insulin resistance and waist-to-hip ratios and higher high-density lipoprotein (HDL) cholesterol levels were found with thyrotropin <2.5 μIU/L. However, the upper limit for thyrotropin was set at 5 μIU/L. The American Thyroid Association guideline recommends 0.4 to 4 μIU/L as the normal range in the treatment of hypothyroidism.[20] Based on this recommendation, euthyroid individuals with thyrotropin levels between 0.4 and 4 μIU/L and who did not receive levothyroxine replacement were included in the present study. When the participants with a thyrotropin level of 1, 2, 2.5 (based on the above studies), and 3 μIU/L were compared, only those with thyrotropin ≤2.5 μIU/L had a lower CRP than those with thyrotropin

TABLE 6. Comparison of Participants by Presence of AIT

Parameter	AIT (n = 47)	Non-AIT (n = 68)	*P* Value
Age (y)	39.94 ± 11.314	41 ± 11.777	.629
Sex, n (female/male)	46/1	55/13	**.007**
Thyrotropin (μIU/L)	2.46 (0.79–4)	1.65 (0.51–3.64)	**.000**
Anti-TPO	122.40 (0.3–3460)	0.7 (0.10–92.8)	**.000**
Anti-TG	4.8 (0.1–1049)	0.9 (0.1–8.8)	**.000**
FPG (mg/dL)	92.70 ± 8.03	62.14 ± 8.51	.726
Insulin (μIU/mL)	7 (1.87–31.97)	8 (1.97–24.66)	.132
HOMA-IR	1.51 (0.42–7.66)	1.75 (0.40–6.09)	.174
ADMA (ng/mL)	213.49 (15.9–1040.46)	211.56 (17.19–962.43)	.352
IMA (ABSU)	0.429 (0.233–0.937)	0.441 (0.003–0.847)	.466
IMA-alb (ABSU)	0.413 (0.264–1.071)	0.449 (0.003–0.873)	.218
Total cholesterol (mg/dL)	204 ± 44.750	197.35 ± 47.283	.450
Triglycerides (mg/dL)	95 (40–447)	108.5 (32–368)	.898
LDL-C (mg/dL)	126 (60–282)	119 (38–208)	.395
HDL-C (mg/dL)	52 (39–79)	51 (33–93)	.511
Non-HDL-C (mg/dL)	151.36 ± 44.319	145.10 ± 45.185	.463
CRP (mg/L)	3 (0.2–16)	2 (0.2–18)	.585

ABSU, absorbance unit; ADMA, asymmetric dimethylarginine; AIT, autoimmune thyroiditis; CRP, C-reactive protein; FPG, fasting plasma glucose; HDL-C, high-density lipoprotein cholesterol; HOMA-IR, homeostatic model values for insulin resistance; IMA, ischemia modified albumin; IMA-alb, IMA-corrected to albumin; LDL-C, low-density lipoprotein cholesterol; non-HDL-C, lipoproteins other than HDL.

TABLE 7. Correlation Between Antithyroid Antibodies and ADMA, IMA, and IMA-alb

Parameter	Anti-TPO		Anti-TG	
	r	*P*	*r*	*P*
ADMA (ng/mL)	–0.070	.462	–0.046	.637
IMA (ABSU)	–0.140	.137	–0.086	.376
IMA-alb (ABSU)	–0.145	.128	–0.075	.443

ABSU, absorbance unit; ADMA, asymmetric dimethylarginine; anti-TG, anti-thyroglobulin; anti-TPO, anti-thyroid peroxidase; IMA, ischemia-modified albumin; IMA-alb, IMA-corrected to albumin.

>2.5 μIU/L (**TABLE 2**). However, there was no significant correlation between thyrotropin and CRP (**TABLE 3**).

According to the meta-analysis of Baumgartner et al,[13] individuals with higher fT_4, despite being euthyroid, were found to have a higher risk of atrial fibrillation. In the study of Mehran et al,[21] fT_4 was found to be positively correlated with HDL cholesterol, low-density lipoprotein (LDL) cholesterol, and triglycerides and inversely correlated with insulin resistance. Another study conducted with 120 euthyroid women who were postmenopausal reached no significant result with thyrotropin and fT_4 but found that fT_3 was positively correlated with insulin and negatively correlated with HDL cholesterol and glucose.[22] In these studies, no cutoffs were given for free hormones. In our study, the analyses were repeated by taking the median values of fT_4 hormones as the cutoff (because normal distribution was not observed). The median fT_3 was 3.59 ng/dL and the median fT_4 was 0.84 ng/dL, and no significant results were found in the analyses performed according to these cutoffs (**TABLE 4**). Only a weak positive correlation was found between fT_4 and IMA and IMA-alb (**TABLE 5**).

Free-oxygen radicals (ROSs) play a fundamental role in tissue damage. Normal thyroid function is required for ROS metabolism. In hypo- and hyperthyroidism, ROSs are increased and thus tissue damage occurs. Furthermore, ROSs are also the basis of autoimmune diseases.[23] In a study with 35 patients with AIT and 35 healthy control patients,[24] all participants were euthyroid, and serum oxidant status, antioxidant status, IMA, and oxidized LDL levels were examined. The antioxidant level was lower in the AIT group and the IMA level was higher, and there was no correlation between IMA and anti-TPO and anti-TG (ADMA was not examined in the study). Based on these results, it was concluded that oxidative stress was involved in the pathogenesis of AIT. Accordingly, the AIT status of the participants was determined, and 47 of them had AIT.[24] Those results were contrary to those in our study, wherein no significant difference was observed between the groups in terms of metabolic parameters (**TABLE 6**). There was no correlation between autoantibodies and ADMA, IMA, and IMA-alb (**TABLE 7**). We did not find any significant correlation between thyroid volume and ADMA, IMA, and alb-IMA (**TABLE 8**). However, in the subgroup analysis, it was observed that there was a difference between the groups in terms of sex distribution; there were more women in the AIT group. This demographic factor may have contributed to the fact that no significant difference was found in our analysis. Linear regression analysis could not be performed because the data did not show a normal distribution, and logistic regression analysis could not be performed because the metabolic parameters were not categorical. Therefore, no further analysis could be made for the confounding effect of sex.

There are also limitations in our study. Although this study was related to metabolism, we could not analyze body mass index because few participants had this data. Like ADMA, tumor necrosis factor-α and interleukin-6 are also useful markers in studies investigating endothelial dysfunction. Studies on autoimmune thyroid disease are also available in this context. However, we could not include these parameters in our research because of cost reasons. The analysis of these items would affect the results of the study.

Conclusion

Based on the findings in our study, we concluded that narrower thyrotropin, fT_4, and fT_3 targets are not required for lower metabolic risk, and metabolic risk does not increase in the presence of AIT. This study is the first to evaluate ADMA levels in AIT.

TABLE 8. Correlation Between Thyroid Volumes and Thyrotropin, ADMA, IMA, and IMA-alb

Parameter	All Participants				Hashimoto's Group			
	Right Lobe Volume		Left Lobe Volume		Right Lobe Volume		Left Lobe Volume	
	r	*P* Value	*r*	*P* Value	*r*	*P* Value	*r*	*P* Value
Thyrotropin	−0.385	**<.001**	−0.515	**<.001**	−0.383	**.011**	−0.245	.111
ADMA	0.030	.764	−0.044	.665	−0.026	.868	−0.141	.369
IMA	−0.050	.617	−0.009	.928	0.017	.914	0.079	.614
IMA-Alb	−0.014	.889	0.006	.950	0.041	.798	0.106	.502

ADMA, asymmetric dimethylarginine; IMA, ischemia-modified albumin; IMA-alb, IMA-corrected to albumin.

Conflict of Interest Statement

All authors declare that they do not have any conflict of interest related to this study.

Acknowledgments

This work was supported by the Ankara Numune Education and Research Hospital Scientific Research Evaluation Commission, grant number 1182/2016.

REFERENCES

1. Mullur R, Liu YY, Brent GA. Thyroid hormone regulation of metabolism. *Physyil Rev*. 2014;94(2):355–382.
2. Tain YL, Hsu CN. Toxic dimethylarginines: asymmetric dimethylarginine (ADMA) and symmetric dimethylarginine (SDMA). *Toxins*. 2017;9:92.
3. Tsikas D, Bollenbach A, Hanff E, Kayacelebi AA. Asymmetric dimethylarginine (ADMA), symmetric dimethylarginine (SDMA) and homoarginine (hArg): the ADMA, SDMA and hArg paradoxes. *Cardiovasc Diabetol.* 2018;17(1):1.
4. Singh VP, Aggarwal R, Singh S, et al. Metabolic syndrome is associated with increased oxo-nitrative stress and asthma-like changes in lungs. *PLoS One.* 2015;10(6):e0129850.
5. Bar-Or D, Lau E, Rao N, et al. Reduction in the cobalt binding capacity of human albumin with myocardial ischaemia. *Ann Emer Med*. 1999;34(4):1–5.
6. Oncel M, Kıyıcı A, Onen S. Evaluation of the relationship between ischemia-modified albumin levels and thyroid hormone levels. *J Clin Lab Anal.* 2015;29(6):427–431.
7. Shabana W, Peeters E, Verbeek P, Osteaux MM. Reducing interobserver variation in thyroid volume calculation using a new formula and technique. *Eur J Ultrasound.* 2003;16(3):207–210.
8. Reddy VS, Bukke S, Mahato K, et al. A meta-analysis of the association of serum ischaemia-modified albumin levels with human hypothyroidism and hyperthyroidism. *Biosci Rep*. 2017;37(1):BSR20160268.
9. Canaris GJ, Manowitz NR, Mayor G, Ridgway EC. The Colorado thyroid disease prevalence study. *Arch Intern Med.* 2000;160(4):526–534.
10. Jokinen E. Obesity and cardiovascular disease. *Minerva Pediatr.* 2015;67(1):25–32.
11. van Tienhoven-Wind LJN, Dullaart RBF. Low-normal thyroid function and the pathogenesis of common cardio-metabolic disorders. *Eur J Clin Invest.* 2015;45(5):494–503.
12. Rodondi N, den Elzen WP, Bauer DC, et al; Thyroid Studies Collaboration. Subclinical hypothyroidism and the risk of coronary heart disease and mortality. *JAMA.* 2010;304(12):1365–1374.
13. Baumgartner C, da Costa BR, Collet TH, et al; Thyroid Studies Collaboration. Thyroid function within the normal range, subclinical hypothyroidism, and the risk of atrial fibrillation. *Circulation.* 2017;136(22):2100–2116.
14. Collet TH, Gussekloo J, Bauer DC, et al; Thyroid Studies Collaboration. Subclinical hyperthyroidism and the risk of coronary heart disease and mortality. *Arch Intern Med.* 2012;172(10):799–809.
15. Lee JJ, Pedley A, Marqusee E, et al. Thyroid function and cardiovascular disease risk factors in euthyroid adults: a cross-sectional and longitudinal study. *Clin Endocrinol (Oxf).* 2016;85(6):932–941.
16. Li X, Yao Y, Chen Z, et al. Thyroid-stimulating hormone within the normal range and risk of major adverse cardiovascular events in nonischemic dilated cardiomyopathy patients with severe left ventricular dysfunction. *Clin Cardiol.* 2019;42(1):120–128.
17. Wartofsky L, Dickey RA. The evidence for a narrower thyrotropin reference range is compelling. *J Clin Endocrinol Metab.* 2005;90(9):5483–5488.
18. Laurberg P, Andersen S, Carlé A, Karmisholt J, Knudsen N, Pedersen IB. The TSH upper reference limit: where are we at? *Nat Rev Endocrinol.* 2011;7(4):232–239.
19. Souza LL, Guedes EP, Teixeira PF, Moreira RO, Godoy-Matos AF, Vaisman M. Serum TSH levels are associated with cardiovascular risk factors in overweight and obese adolescents. *J Pediatr (Rio J).* 2016;92(5):532–538.
20. Jonklaas J, Bianco AC, Bauer AJ, et al. Guidelines for the treatment of hypothyroidism: prepared by the American Thyroid Association task force on thyroid hormone replacement. *Thyroid.* 2014;24(12):1670–1751.
21. Mehran L, Amouzegar A, Tohidi M, Moayedi M, Azizi F. Serum free thyroxine concentration is associated with metabolic syndrome in euthyroid subjects. *Thyroid.* 2014;24(11):1566–1574.
22. Luna-Vazquez F, Cruz-Lumbreras R, Rodríguez-Castelán J, et al. Association between the serum concentration of triiodothyronine with components of metabolic syndrome, cardiovascular risk, and diet in euthyroid post-menopausal women without and with metabolic syndrome. *Springerplus.* 2014;3:266.
23. Laddha NC, Dwivedi M, Mansuri MS, et al. Vitiligo: interplay between oxidative stress and immune system. *Exp Dermatol.* 2013;22(4):245–250.
24. Baser H, Can U, Baser S, Yerlikaya FH, Aslan U, Hidayetoglu BT. Assessment of oxidative status and its association with thyroid autoantibodies in patients with euthyroid autoimmune thyroiditis. *Endocrine.* 2015;48(3):916–923.

Influence of Tacrolimus on Serum Vitamin A Levels in Patients after Renal Transplantation

Shulin Yang, MMed,[1] Juan Le, MMed,[1] Rui Peng, MD,[1] Shaoting Wang, PhD,[1,a,] Yan Li, MD[1,a]*

[1]Department of Clinical Laboratory, Renmin Hospital of Wuhan University, Wuhan, China; *To whom correspondence should be addressed. shaotingw@whu.edu.cn; [a]The authors jointly supervised this work.

Keywords: renal transplantation, vitamin A, tacrolimus, calcineurin inhibitor, retinol, therapeutic drug monitoring

Abbreviations: CNI, calcineurin inhibitor; AST, aspartate aminotransferase; ALT, alanine aminotransferase; eGFR, estimate glomerular filtration rate; LC-MS/MS, liquid chromatography-tandem mass spectrometry; IS, internal standard; MMF, mycophenolate mofetil.

Laboratory Medicine 2022;53:296–301; https://doi.org/10.1093/labmed/lmab102

ABSTRACT

Objective: Patients after renal transplantation exhibit high levels of vitamin A, which has been previously suspected to be related with immunosuppressive medication. However, this possibility has not yet been systematically studied.

Materials and Methods: Altogether, 116 patients were included and divided into 2 groups based on serum creatinine levels. The mean values of vitamin A levels between the 2 groups were compared using the Student's *t*-test. The Pearson's correlation coefficient was calculated to assess the association between vitamin A and tacrolimus.

Results: Elevated vitamin A levels were found in both groups, and patients with kidney dysfunction after transplantation showed higher levels of vitamin A than patients with recovered kidney function. Most important, we could not identify any significant correlations between vitamin A level and tacrolimus for both groups. After long-term and short-term monitoring for different patients, obvious individual differences emerged. Such results generally ruled out previous suspicions regarding causality between immunosuppressive medication (tacrolimus) and vitamin A elevation after renal transplantation.

Conclusion: Patients after renal transplantation showed higher serum vitamin A levels than people with a normal medical exam, even if their graft function was restored. The cause of this abnormality did not seem to be related with tacrolimus.

The number of renal transplants has been increasing rapidly in recent years.[1,2] After transplantation, the immune system of patients will be significantly disrupted. For better prognosis, special attention should be paid to their nutritional status. As a typical fat-soluble vitamin, vitamin A has long been considered an important part to maintain immune activity in vivo.[3,4] However, vitamin A supplementation after renal transplantation is controversial because vitamin A concentrations in serum seem to be higher than the upper limit of suggested reference intervals (1–3 μmol/L) and hypervitaminosis A has been proven to cause serious consequences such as headache, dizziness, osteoporosis, and increased intracranial pressure.[5-8]

Such a phenomenon was first reported by Yatzidis et al in the 1970s.[9] They found that even with normal graft function the serum retinol of some patients posttransplantation could remain in the normal range for at least 2 years. Since then, a number of related studies have been carried out. For example, Kelleher et al[10] found that along with serum retinol, retinol-binding protein would also elevate in these patients. And Connolly et al[11] speculated that the high retinol concentration might be derived from anti-inflammatory or anti-infective reaction in vivo. Notably, a high level of serum vitamin A was further confirmed not only for renal transplantation but also for lung transplantation for patients with cystic fibrosis in 2005 by Stephenson et al.[12] And 6 years later, the same group expanded these findings to all patients who had lung transplantation.[8] However, despite all of these impressive contributions, the molecular mechanism behind this phenomenon is still undisclosed.

As for another fat-soluble vitamin, vitamin D, it has been confirmed that high levels of tacrolimus can inhibit the activity of the CYP3A4 enzyme such that the metabolism of $1,25(OH)_2D_3$ will be suppressed, leading to an increase in $1,25(OH)_2D_3$ reservation.[13,14] Considering that the metabolism of vitamin A is also related to the cytochrome P450 system, it is reasonable to speculate that tacrolimus could be a potential factor to impact vitamin A concentration as well.[15,16] In previous investigations, some researchers have already put forward similar conjectures that immunosuppressants, especially calcineurin inhibitors (CNIs), could possibly cause high levels of vitamin A.[8,12] Nevertheless, there is still a lack of systematic studies to clarify this issue.

Herein, we conducted the first research to investigate whether increased serum vitamin A levels in renal transplant recipients were derived from a dosage of tacrolimus. First, serum retinol was detected in the patients after renal transplantation who were divided into 2 groups based on their renal function. Second, the general relationship between vitamin A levels and tacrolimus concentrations was analyzed for both

groups. Last, the long-term and short-term correlations of vitamin A toward tacrolimus concentrations were monitored for random individuals.

Materials and Methods

Patients

Altogether, 116 patients who had undergone renal transplantation at the Renmin Hospital of Wuhan University (Wuhan, China) for chronic renal failure were included in the study (demographics are shown in **TABLE 1**). All patients were regularly monitored for liver, kidney function, and drug concentrations after transplantation. The patients were retrospectively divided into 2 groups based on the reference intervals of creatinine according to the National Health Commission of the People's Republic of China (No. WS/T404.5-2015, male aged <60 years: 57~97 μmol/L; male aged >60 years: 57~111 μmol/L; female aged <60 years: 41~73 μmol/L; female aged >60 years: 41~81 μmol/L).[17] Group 1 comprised 54 patients with normal renal function whose creatinine levels were within the reference intervals, and group 2 comprised 62 patients with abnormal renal function whose creatinine levels were above the upper limit of normal. There were no statistical significances in age and sex between the 2 groups. None of the patients received specialized vitamin A supplementation or adjustment. Immunosuppressive medications were given shortly after surgery for long-term antirejection therapy. The levels of serum vitamin A of the patients were obtained retrospectively.

Methods

Serum creatinine, aspartate aminotransferase (AST), and alanine aminotransferase (ALT) from fasting blood specimens were assayed using the Siemens Advia 2400 biochemical analyzer with matching reagents in routine clinical laboratory. The estimated glomerular filtration rate (eGFR) was calculated using the chronic kidney disease epidemiology collaboration formula. Retinol in serum was measured using liquid chromatography-tandem mass spectrometry (LC-MS/MS) per an earlier study, except that plasma was substituted with serum.[18] Tacrolimus in whole blood was also analyzed using LC-MS/MS per a previous study with some modifications.[19]

Briefly, a whole blood specimen (40 μL), $ZnSO_4$ solution (200 μL), and internal standard (IS) solution (400 μL) were mixed together. Then, the mixture was centrifuged (10,000 rcf, 5 minutes) at 4°C after supersonic disruption (30 seconds) and vortexing (4 minutes). For solid-phase extraction purification, water (400 μL) was added into the supernatant (400 μL), and the entire solution was transferred into an Oasis PRiME HLB 96-well Plate (Waters-186008054). After rinsing with a methanol-water solution (1 mL, 2/8, v/v), the plate was desorbed using a methanol-acetonitrile solution (200 μL, 1/1, v/v). Finally, the eluent (100 μL) was mixed with water (100 μL) and injected for LC-MS/MS analysis. We purchased 6PLUS1 Multilevel Whole Blood Calibrator Set Immunosuppressants (Chromsystems-28039/XL) for the calibration specimens. The blank calibrator was used as a blank matrix. Quality control specimens were obtained using MassCheck Immunosuppressants Whole Blood Controls (Chromsystems-0081). A $ZnSO_4$ solution was prepared in water (0.1 mol/L). The concentration of the stable isotopic IS solution was 0.5 ng/mL for tacrolimus-13C,d2 prepared in acetonitrile.

The basic information for all patients was obtained through the hospital information system, and all the test data were obtained with the written informed consent of the patients. The study was also supervised by the Ethics Committee of Renmin Hospital of Wuhan University.

Statistics

Statistical analyses were performed using the statistical software IBM SPSS Statistics, version 26. The Student's *t*-test was used to compare mean values between the 2 groups, and the Pearson correlation coefficient was calculated to assess the associations between vitamin A and other parameters.

Results

Demographic Analysis of Groups

After grouping, the data from group 2 (**TABLE 1**) showed that the increased mean serum creatinine and decreased eGFR were significant compared with data from group 1 (P <.0001). These results were consistent with what we predicted. In terms of liver function, AST and ALT were within the reference interval for both groups. And no significant differences were seen between the 2 groups. Thus, the metabolism and storage of vitamin A in liver between the 2 groups would not cause a significant effect upon subsequent analysis. In addition, consistent with previous reports, serum vitamin A levels in both groups (group 1: 2.5 ± 0.9 μmol/L, group 2: 3.0 ± 0.9 μmol/L) were significantly higher than the levels in those undergoing usual medical examination in our laboratory (1.5 ± 0.4 μmol/L; P <.0001). Posttransplant, all patients were treated using multiple immunosuppressive medications. There were no differences in immunosuppressive medication exposure between group 1 and group 2.

Correlation Between Vitamin A and Creatinine, eGFR, or Tacrolimus

The correlations between vitamin A and serum creatinine or eGFR in the 2 groups are shown in **TABLE 2**. For group 1, the level of vitamin A was positively correlated with serum creatinine, and the corre-

TABLE 1. Demographics of Different Groups

	Renal Transplantation (n = 116)		*P* Value
	Group 1 (n = 54)	Group 2 (n = 62)	
Age[a] (y)	44.5 ± 10.6	41.8 ± 10.3	NS
Male (%)	54	56	NS
Creatinine (μmol/L)	73.0 ± 15.7	115.8 ± 22.0	<.0001
eGFR	98.5 ± 9.9	61.4 ± 11.8	<.0001
AST (U/L)	21.8 ± 7.1	20.2 ± 6.3	NS
ALT (U/L)	22.1 ± 11.4	20.8 ± 8.1	NS
Vitamin A (μmol/L)	2.5 ± 0.9	3.0 ± 0.9	.004
Tacrolimus (ng/mL)	7.2 ± 1.6	7.4 ± 2.0	NS
Immunosuppressive medications (%)	Tacrolimus (100)	Tacrolimus (100)	
	Cyclosporine A (0)	Cyclosporine A (0)	
	Sirolimus (1.9)	Sirolimus (3.2)	
	MMF (100)	MMF (100)	
	Azathioprine (0)	Azathioprine (0)	
	Prednisone (100)	Prednisone (100)	

ALT, alanine aminotransferase; AST, aspartate aminotransferase; MMF, mycophenolate mofetil; NS, not significant.
[a]*Values are mean ± standard deviation unless otherwise stated.*

lation was significant (r = 0.44; P <.001). However, there was no such correlation in group 2. Similarly, the level of vitamin A was negatively correlated with eGFR in group 1 and the correlation was significant (r = –0.34, P = .01), whereas for group 2 no correlation was observed. Research has suggested that higher serum levels of vitamin A are associated with higher levels of creatinine and lower levels of eGFR when creatinine is within the reference range. In contrast, there was no significant correlation between vitamin A level and the predose concentration of tacrolimus in both groups (as shown in **FIGURE 1**). From this preliminary result, the immunosuppressant function of tacrolimus may not impact levels of vitamin A.

Long-Term Monitoring of Serum Vitamin A and Tacrolimus

To further investigate the relationship between tacrolimus and vitamin A level, some patients were enrolled randomly for long-term analysis. The results from 4 representative patients are shown in **FIGURE 2**. Among them, patients 1 and 2 were from group 1 and patients 3 and 4 were from group 2. In general, there was no consistent trend between vitamin A and the predose concentration of tacrolimus across different individuals. Moreover, the relative deviations of tacrolimus and vitamin A from every 2 time points were calculated, and the relationships between their relative deviations are shown in the insets (**FIGURE 2**). The fluctuations in tacrolimus levels in patients 1 and 3 were not correlated with the fluctuations of vitamin A (patient 1: r = –0.24, P = .5; patient 3: r = –0.17, P = .61), whereas patients 2 and 4 had a significant positive correlation (patient 2: r = 0.87, P = .01; patient 4: r = 0.67, P = .03).

TABLE 2. Correlation Between Vitamin A and Other Parameters in Group 1 and Group 2

	Group 1		Group 2	
	r[a]	*P* Value[b]	*r*[a]	*P* Value[b]
Creatinine (μmol/L)	0.44	<.001	0.03	NS
eGFR	–0.34	.01	0.12	NS
Tacrolimus (ng/mL)	–0.07	NS	0.04	NS

eGFR, estimated glomerular filtration rate; NS, not significant.
[a]r = *Spearman's ordinal correlation coefficient.*
[b]P = *Correlation coefficient's significance.*

Short-Term Monitoring of Serum Vitamin A and Tacrolimus

To investigate whether acute changes in tacrolimus concentration would cause vitamin A fluctuation, short-term monitoring for patients after drug administration (between 0 and 6 hours) was also conducted (n = 10). All of these patients exhibited similar results, so we only chose 2 (patient 1 from group 1 and patient 2 from group 2) for specific description. As shown in **FIGURE 3**, for both patients, the peak concentrations of tacrolimus (approximately 30 ng/mL) occurred 1 hour after taking the drug and then gradually dropped to preadministration levels (<9 ng/mL) at 6 hours. During this period of time, the vitamin A levels did not change notably (less than 15% of steady level).

Discussion

Elevated Vitamin A and Renal Function

Results from the present study confirmed that after renal transplantation, serum vitamin A levels in some patients with renal transplantation remained elevated despite a well-functioning graft. But when our analysis used 3 μmol/L as the upper threshold,[20] a much higher risk of hypervitaminosis A was shown for group 2 (51.6%, 32/62) than for group 1 (22.2%, 13/54). Given the fact that the excretion of vitamin A mainly occurs in the kidneys, such a distinction could be ascribed to the differing renal function between these 2 groups.[7] In practice, tacrolimus may cause kidney poisoning. To exclude such an effect on vitamin A metabolism, we analyzed the correlation between the predose concentration of tacrolimus and the serum creatinine level for both groups. No significant correlations could be found (as shown in **FIGURE 4**). Such results indicated that according to study, tacrolimus would not impact vitamin A concentration by suppressing renal function.

Elevated Vitamin A and Tacrolimus Medication

As shown in **FIGURE 1**, we could hardly observe any correlations between serum vitamin A and tacrolimus in both groups. These results generally ruled out previous conjectures about the potential relationship between CNIs (tacrolimus) and vitamin A fluctuation after renal transplantation.[8] Furthermore, all patients received mycophenolate mofetil (MMF) and prednisone during the immunosuppressive therapy.

FIGURE 1. Relationship between serum vitamin A and tacrolimus values in group 1 (A) and group 2 (B) after renal transplants. (group 1: r = –0.07, P = .63; group 2: r = 0.04, P = .76, not significant). The red line is the fitting line for correlation analysis.

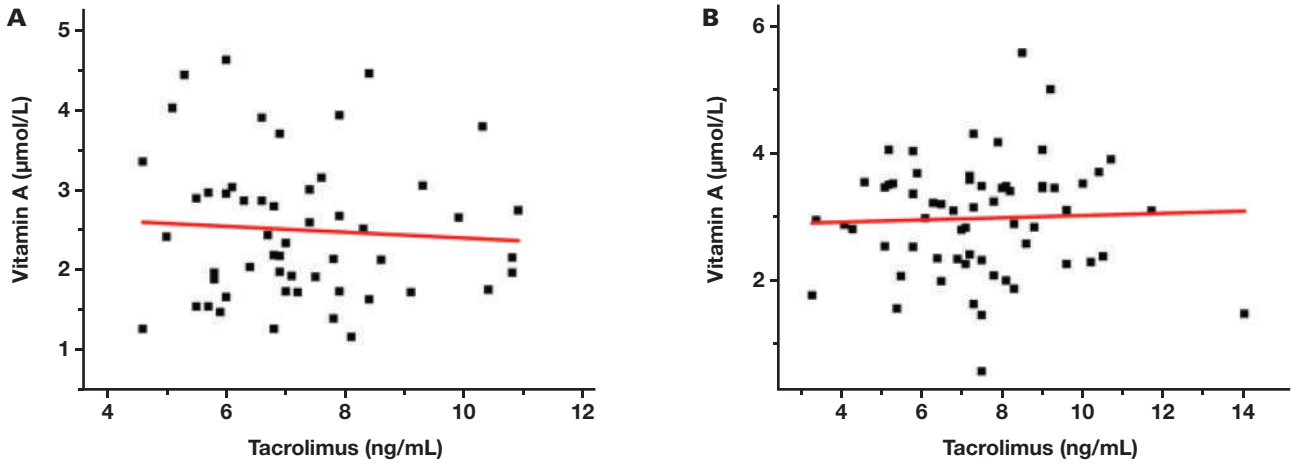

2022;53;296–301 | https://doi.org/10.1093/labmed/lmab102

FIGURE 2. Long-term changes in serum vitamin A and tacrolimus values in 4 patients from different groups. The black line represents the trend of tacrolimus concentration, and the red line represents the trend of vitamin A concentration. The relationship between the relative deviation of vitamin A and the relative deviation of tacrolimus is shown in the inset. The red line is the fitting line for correlation analysis. A, Two patients from group 1 with normal renal function: $r = -0.24$, $P = .5$; $r = 0.86$, $P = .01$, respectively. B, Two patients from group 2 with abnormal renal function: $r = -0.17$, $P = .61$; $r = 0.67$, $P = .03$, respectively.

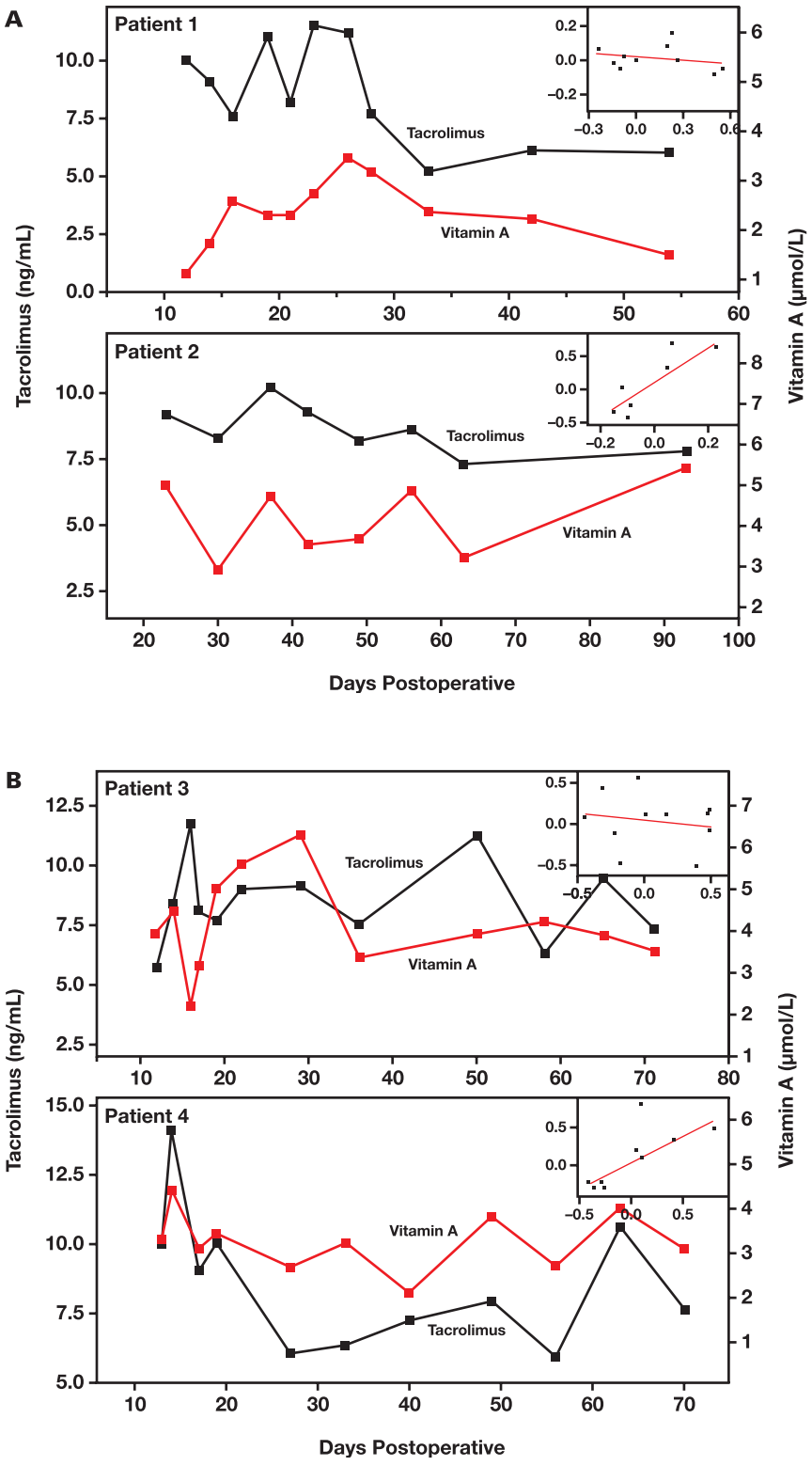

FIGURE 3. Short-term changes in serum vitamin A and tacrolimus values in 2 patients from different groups after taking the medication. A, Patient 1 from group 1 with normal renal function. B, Patient 2 from group 2 with abnormal renal function.

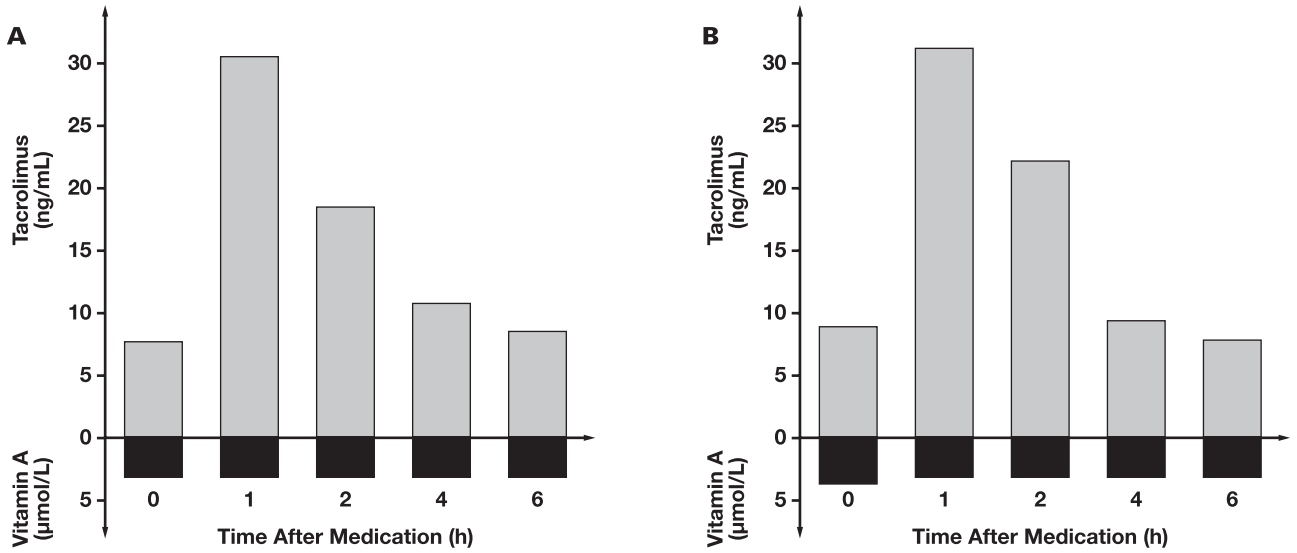

FIGURE 4. Relationship between serum creatinine and tacrolimus values in group 1 and group 2 after renal transplantation (group 1: $r = 0.15$, $P = .29$; group 2: $r = 0.20$, $P = .11$, not significant). The red line is the fitting line for correlation analysis.

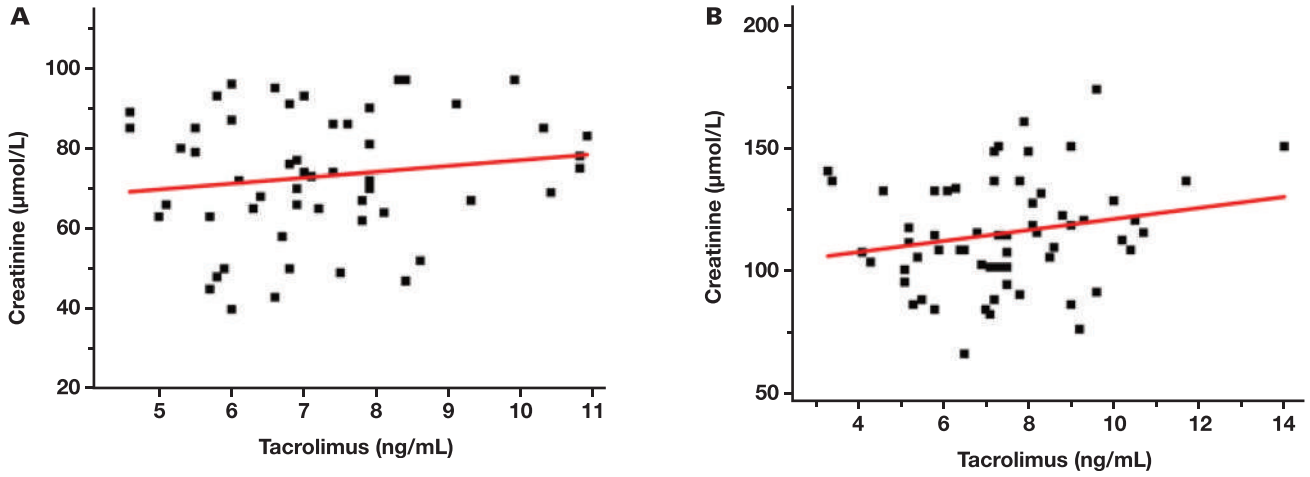

Therefore, we collected the predose concentrations of mycophenolic acid in the 2 groups of patients and analyzed the correlations between MMF and vitamin A. From the available data (group 1: n = 23; group 2: n = 29), we found that there were no significant relationships between MMF and vitamin A in either group ($r = 0.20$, $P = 0.39$ vs $r = 0.18$, $P = 0.34$). Therefore, MMF was less likely to be a potential factor affecting vitamin A levels. Furthermore, because therapeutic drug monitoring was not routinely performed for prednisone, it was not easy to analyze the correlation between prednisone concentration and vitamin A. And although the main adverse reactions of prednisone are hyperglycemia and hyperlipidemia, the potential for hypervitaminosis A posed by prednisone in this population requires further study for us.[21] Follow-up research is already scheduled in our center.

To further improve the quality of such a conclusion, data from long-term and short-term monitoring were examined for different individuals. In the case of long-term monitoring, obvious individual heterogeneity was present in both groups of patients. As shown in **FIGURE 2**, the trends in vitamin A levels for some patients (patients 2 and 4) seemed consistent with the trends in tacrolimus levels, whereas for other patients (patient 1s and 3), no similar correlation could be observed. In short-term tests (as shown in **FIGURE 3**), although the tacrolimus concentrations revealed a sharp surge within 6 hours after drug administration, the serum vitamin A levels changed just less than 15%. Such slight fluctuations were more likely from detecting deviation rather than a drug-induced physiological reaction. Taking all these phenomena together, tacrolimus medication was unlikely the reason for the abnormal vitamin A metabolism in patients with renal transplantation.

Prospects and Expansion

On the basis of this study, patients without transplant taking tacrolimus can also be included for the quantitative determination of vitamin A. If serum vitamin A in these patients did not increase significantly, it would be further proven that the elevated vitamin A in the transplant popula-

tion is not caused by pharmacological factors. Moreover, in addition to patients with kidney or lung transplantation, it is still unknown whether patients with other solid organ transplantation also present elevated serum vitamin A. If it was a universal phenomenon, then the molecular mechanism would be more likely derived from the transplantation process itself. Follow-up research is already underway in our center.

Conclusion

Patients after renal transplantation showed higher serum vitamin A levels than people with a healthy exam, even in the presence of a very well-functioning transplant. When taking 3 μmol/L as the cutoff value, we found that the risk of hypervitaminosis A could be higher than 20% for these patients. Most important, the present study provides the first evidence that excludes the long-suspected correlation between increased vitamin A and tacrolimus medication. More studies are needed to address the mechanisms of vitamin A metabolism after renal transplantation so that optimal clinical guidance for vitamin A adjustment can be given.

Acknowledgments

This work was supported by the National Natural Science Foundation of China grants 21705121 and 81772265. All authors were involved in aspects of the study design. Shulin Yang participated in performance of the research and the writing of the paper. Shulin Yang and Shaoting Wang participated in data analysis. Yan Li contributed reagents and analytic tools. All authors were involved in data review and interpretation, manuscript review and editing, and approval of the final manuscript. The basic information on all patients was obtained through the hospital information system, and all the test data were obtained with written informed consent of the patients. The study was also supervised by the Ethics Committee of Renmin Hospital of Wuhan University. There is no supplementary material for this paper, and the analysis data uploaded before are only for reviewers' use.

REFERENCES

1. Shahbazi F, Ranjbaran M, Karami-Far S, Soori H, Manesh HJ. Graft survival rate of renal transplantation during a period of 10 years in Iran. *J Res Med Sci.* 2015;20(11):1046–1052.
2. Courtney AE, McNamee PT, Maxwell AP. The evolution of renal transplantation in clinical practice: for better, for worse? *QJM.* 2008;101(12):967–978.
3. Maggini S, Pierre A, Calder PC. Immune function and micronutrient requirements change over the life course. *Nutrients.* 2018;10:1531.
4. Jomphe V, Lands LC, Mailhot G. Nutritional requirements of lung transplant recipients: challenges and considerations. *Nutrients.* 2018;10:790.
5. Penniston KL, Tanumihardjo SA. The acute and chronic toxic effects of vitamin A. *Am J Clin Nutr.* 2006;83(2):191–201.
6. Michaëlsson K, Lithell H, Vessby B, Melhus H. Serum retinol levels and the risk of fracture. *N Engl J Med.* 2003;348(4):287–294.
7. Albahrani AA, Greaves RF. Fat-soluble vitamins: clinical indications and current challenges for chromatographic measurement. *Clin Biochem Rev.* 2016;37(1):27–47.
8. Ho T, Gupta S, Brotherwood M, et al. Increased serum vitamin A and E levels after lung transplantation. *Transplantation.* 2011;92(5):601–606.
9. Yatzidis H, Digenis P, Koutsicos D. Hypervitaminosis A in chronic renal failure after transplantation. *Br Med J.* 1976;2(6043):1075.
10. Kelleher J, Humphrey CS, Homer D, Davison AM, Giles GR, Losowsky MS. Vitamin A and its transport proteins in patients with chronic renal failure receiving maintenance haemodialysis and after renal transplantation. *Clin Sci.* 1983;65(6):619–626.
11. Connolly GM, Cunningham R, Maxwell AP, Young IS. Decreased serum retinol is associated with increased mortality in renal transplant recipients. *Clin Chem.* 2007;53(10):1841–1846.
12. Stephenson A, Brotherwood M, Robert R, et al. Increased vitamin A and E levels in adult cystic fibrosis patients after lung transplantation. *Transplantation.* 2005;79(5):613–615.
13. Prytuła A, Cransberg K, Raes A. Drug-metabolizing enzymes CYP3A as a link between tacrolimus and vitamin D in renal transplant recipients: is it relevant in clinical practice? *Pediatr Nephrol.* 2019;34(7):1201–1210.
14. Christians U, Jacobsen W, Benet LZ, Lampen A. Mechanisms of clinically relevant drug interactions associated with tacrolimus. *Clin Pharmacokinet.* 2002;41(11):813–851.
15. McSorley LC, Daly AK. Identification of human cytochrome P450 isoforms that contribute to all-trans-retinoic acid 4-hydroxylation. *Biochem Pharmacol.* 2000;60(4):517–526.
16. Saadeddin A, Torres-Molina F, Cárcel-Trullols J, Araico A, Peris JE. Effect of cytochrome P450 inhibitors (diethyl dithiocarbamate, ketoconazole and grapefruit juice) on the pharmacokinetics of all-trans-retinoic acid. *Farmaco.* 2004;59(9):697–702.
17. National Health Commission of the People's Republic of China. Reference intervals for common clinical biochemistry tests—part 5: serum urea and creatinine (WS/T404.5-2015) [in Chinese]. http://www.nhc.gov.cn/wjw/s9492/201504/b396412bcbd84e1ea2b7f9e0e131ae80.shtml. Accessed October 1, 2015.
18. Le J, Yuan TF, Zhang Y, et al. New LC-MS/MS method with single-step pretreatment analyzes fat-soluble vitamins in plasma and amniotic fluid. *J Lipid Res.* 2018;59:1783–1790.
19. Seger C, Tentschert K, Stöggl W, Griesmacher A, Ramsay SL. A rapid HPLC-MS/MS method for the simultaneous quantification of cyclosporine A, tacrolimus, sirolimus and everolimus in human blood samples. *Nat Protoc.* 2009;4(4):526–534.
20. Greaves RF, Woollard GA, Hoad KE, et al. Laboratory medicine best practice guideline: vitamins A, E and the carotenoids in blood. *Clin Biochem Rev.* 2014;35(2):81–113.
21. Üsküdar Cansu D, Bodakçi E, Korkmaz C. Dose-dependent bradycardia as a rare side effect of corticosteroids: a case report and review of the literature. *Rheumatol Int.* 2018;38(12):2337–2343.

Storage Duration and Red Blood Cell–Derived Microparticles in Packed Red Blood Cells Obtained from Donors with Thalassemia

Egarit Noulsri, PhD,[1,] Surada Lerdwana, BSc,[2] Duangdao Palasuwan, PhD,[3] Attakorn Palasuwan, PhD[3]*

[1]Research Division, Faculty of Medicine Siriraj Hospital, Mahidol University, Bangkok, Thailand, [2]Department of Research and Development, Faculty of Medicine Siriraj Hospital, Mahidol University, Bangkok, Thailand, [3]Oxidation in Red Cell Disorders and Health Task Force, Department of Clinical Microscopy, Faculty of Allied Health Sciences, Chulalongkorn University, Bangkok, Thailand; *To whom correspondence should be addressed. egarit.nou@mahidol.ac.th

Keywords: transfusion, thalassemia, packed RBCs, storage, cell-derived microparticle, flow cytometry

Abbreviations: RBC, red blood cell; RMP, red blood cell–derived microparticle; PLT, platelet; MP, microparticle; ATP, adenosine triphosphate; CD235a-PE, anti-CD235a-antibody conjugated with phycoerythrin; FITC, fluorescein isothiocyanate; CBC, complete blood count; Hb, hemoglobin; HPLC, high-performance liquid chromatography; SAGM, saline-adenine-glucose-mannitol; PBS, phosphate-buffered saline; FSC, forward scatter; SSC, side scatter.

Laboratory Medicine 2022;53:302–306; https://doi.org/10.1093/labmed/lmab106

ABSTRACT

Objective: To address the effects of storage duration on red blood cell (RBC)–derived microparticles (RMPs) in packed RBCs from donors who have thalassemia.

Materials and Methods: Packed RBCs were prepared according to laboratory routine. The quantity of RMPs was determined using FACSCalibur and counting beads.

Results: Across durations of storage, the packed RBCs from donors with thalassemia (n = 28) and healthy volunteers (n = 104) showed average RMPs to be 47,426 (10,139–127,785) particles/μL vs 49,021 (13,033–126,749) particles/μL, respectively (P = .63). The peak RMP levels in donors with thalassemia and healthy volunteers, respectively, were shown in products from storage days 34 and 38. Both groups showed a trend toward a positive association between RMP concentration and the duration of storage in packed RBC bags stored under blood bank conditions.

Conclusion: Our results suggest that storage-induced RMP release has similar effects in stored packed RBCs obtained from both donors with thalassemia and healthy volunteers.

Thalassemia is a hematologic disorder common in several countries.[1,2] The disease is characterized by decreased or absent hemoglobin production in the red blood cells (RBCs), which results in anemia to varying degrees, from asymptomatic to lethal.[3,4] According to international guidelines, individuals who have thalassemia are eligible to donate blood if their hemoglobin levels are within normal ranges.[5] A recent study in India showed that the prevalence of donors with thalassemia there was 3.7%.[6] A study in Thailand reported an overall frequency of 12.9% in donors who had hemoglobinopathies.[7] Therefore, assessing the changes that occur during the processing and storage of blood products prepared from these donors is necessary for optimal therapeutic efficacy when blood products are transfused into recipients.

Cell-derived microparticles (MPs) are heterogeneous vesicles that are released from cells upon activation or when the cells are undergoing apoptosis.[8] These MPs can be obtained from RBCs (RBC-derived microparticles [RMPs]), platelets (PLTs), leukocytes, and endothelial cells. In transfusion medicine, increased levels of RMPs have been found in various blood components, including packed RBCs.[9-12] Recent proteomic analysis of stored RBC products obtained from donors with heterozygous β-thalassemia showed unique membrane proteomes of RBCs and RMPs released during storage.[13] Hashemi Tayer and colleagues[14] determined the RMP levels in 20 packed RBC bags during storage and reported increased RMP concentrations after 6 weeks of storage. This in vitro study also revealed a positive correlation between the levels of MPs and their procoagulant activities that was associated with the expression of phosphatidylserine on their surface membranes, suggesting an effect of storage on MP release. Increased MP levels during storage have been attributed to decreased adenosine triphosphate (ATP), lower pH, and increased oxidative stress.[15-17] These biochemical changes disrupt and degrade the interaction of cytoskeleton molecules, leading to MP formation and shedding. An in vivo study showed that mice injected with RMPs from stored blood products had accelerated clotting times and lower serum fibrinogen levels, suggesting that the transfusion of stored packed RBCs containing high MP levels may contribute to

thrombosis complications through the activation of thrombin.[18] However, that investigation focused on the packed RBCs obtained from healthy volunteers. Furthermore, little is known regarding the effects of storage duration on changes in MP levels in eligible donors with thalassemia.

In the present study, we quantitated the RMP levels in stored packed RBCs from donors with thalassemia and compared the results with those from healthy volunteers. Knowing this information may help optimize the quality of blood products and minimize adverse transfusion reactions in recipients.

Materials and Methods

Materials

Anti-CD235a-antibody conjugated with phycoerythrin (CD235a-PE), annexin V antibody conjugated with fluorescein isothiocyanate (FITC), and 10 × annexin V binding buffer were obtained from Becton Dickinson (San Jose, CA). CountBright absolute counting beads were obtained from Molecular Probes (Eugene, OR).

Ethics Statement

The experimental protocol was approved by the Ethics Committee of the Faculty of Medicine, Siriraj Hospital (COA number 359/2016). The study was conducted following the recommendations of the Declaration of Helsinki, and all individuals gave informed consent before undergoing blood collection.

Hematologic Analysis

To analyze complete blood counts (CBCs), whole blood specimens were collected in tubes containing tripotassium EDTA and then analyzed using the Coulter AcT 5-part differential hematology analyzer (Beckman Coulter, Fullerton, CA).

Hemoglobin Typing

Hemoglobin (Hb) typing was performed using the automated high-performance liquid chromatography (HPLC) β-Thalassemia Short Program (Variant Hemoglobin Testing System, Bio-Rad Laboratories, Hercules, CA). Next, 5 µL whole blood was dissolved in 1 mL hemolysis buffer and applied to the automated HPLC. The percentages of HbF, HbA, and HbA_2 were automatically calculated. Multiplex gap–polymerase chain reaction was used to detect α-globin gene variants.

Preparation of Packed RBCs and Sampling

Units of whole blood were collected into triple blood collecting systems (JMS Triple Blood Bag, CPD-SAGM Solution, JMS Singapore, Singapore). Each system included a 450 mL collection bag containing 63 mL citrate-phosphate-dextrose, a 400 mL bag containing 100 mL saline-adenine-glucose-mannitol (SAGM) red cell preservative solution, and a 400 mL bag for 5-day PLT storage. All units of whole blood were stored at room temperature (22 ± 2°C) for up to 8 hours before the blood components were prepared. The units of whole blood were centrifuged at 3100*g* for 5 minutes at 22 ± 2°C in a Heraeus Cryofuge 6000i centrifuge (Thermo Electron LED, Langenselbold, Germany) and separated into packed RBCs and PLT-rich plasma using a manual extractor. After 100 mL SAGM was added, the units of packed RBCs were stored at 4 ± 2°C.

After the bag was thoroughly mixed, specimens were taken from heat-sealed segments, and then the sampling pipe was stripped. The contents of each segment were transferred into a 0.5 mL microcentrifuge tube and analyzed using flow cytometry.

Flow Cytometry Analysis of RMPs

Specimens from packed RBCs were diluted 1:100 with phosphate-buffered saline (PBS). Then, 10 µL diluted specimen was incubated with 2 µL annexin V-FITC, 2 µL CD235a-PE, and 20 µL 1 × annexin V buffer at room temperature. After 15 minutes, 350 µL 1 × annexin V buffer and 10 µL counting beads were added to the tube. The specimens were analyzed using FACSCalibur (Becton Dickinson, San Jose, CA).

Forward scatter (FSC), side scatter (SSC), and fluorescent parameters were set as logarithmic scales. The threshold was set on the FSC to exclude noise signals and debris. First, the MP gate (R-1) was drawn on the FSC-vs-SSC dot plot using 1.09 µm standard microbeads. The gated MPs were analyzed on a dot plot of annexin V-FITC vs CD235a to determine the events of RMPs in the upper-right quadrant (**FIGURE 1**). Next, the recorded events of RMPs were used to calculate the concentration per mL, as previously described.[19] In brief, 50 µL counting microbeads with a known concentration were mixed gently with 300 µL PBS and then run at the beginning and end of each batch of specimens, with the average of the 2 acquired counting bead events being calculated. The volume acquired in 120 seconds was obtained by dividing the bead events counted in 120 seconds by the concentration of the counting beads. Given that the flow rate was constant throughout the analysis period, the same specimen volume would be acquired. The MP concentrations were then calculated by dividing the events of the MPs counted in 120 seconds by the previously calculated volume and multiplying the results by the dilution factor.

Statistical Analysis

Statistical analysis was conducted using GraphPad Prism Software version 5.0 for Windows (GraphPad, San Diego, CA). All data are reported as mean, standard deviation, and ranges. An unpaired *t*-test was used

FIGURE 1. Flow cytometry gating strategy of red blood cell–derived microparticles (RMPs). A, The forward scatter (FSC)-vs-side scatter (SSC) dot plot shows the microparticle gate (R-1), which is established using 1.09 µm standard microbeads. B, An annexin V-vs-CD235a dot-plot depicts the RMPs in the upper right quadrant from the previous gated population. FITC, fluorescein isothiocyanate.

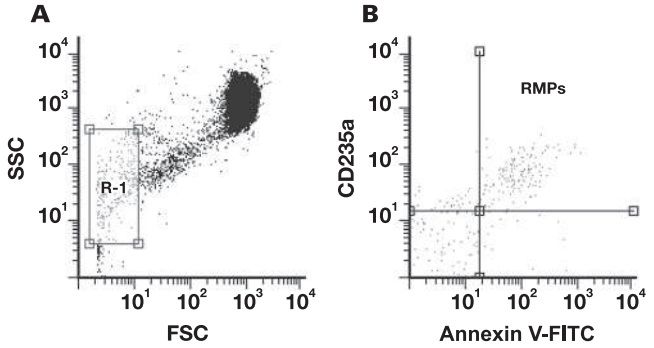

to compare the differences between the 2 groups. Those P values <.05 were considered statistically significant. A linear regression was used to assess the relationship between the duration of storage and RMP concentration.

Results

Genotype of Donors with Thalassemia

The most frequent types of donors with thalassemia were those with the α-thalassemia trait (12/28), which included 3.7 and 4.2 kb-deletion and the HbE trait (11/28). The remaining donors hadthe β-thalassemia trait, which included homozygous HbE and HbCS. The donors were informed if their hemoglobin was <10 g/dL or if other parameters indicating anemia were found.

Demographic and CBC Analysis

TABLE 1 summarizes the donors' demographic and hematologic parameters. Our data showed that the levels of mean corpuscular volume and mean corpuscular hemoglobin in donors with thalassemia were significantly lower than in healthy volunteers. However, the red cell distribution width, mean PLT volume, and RBC counts were significantly higher in donors with thalassemia than in healthy volunteers. There were no significant differences between the 2 groups in age, Hb, hematocrit, mean corpuscular hemoglobin concentration, white blood cells, or PLTs.

RMP Concentrations in Stored Packed RBCs

The duration of storage for packed RBCs obtained from donors with thalassemia ranged from 2 to 42 days, and for those from healthy volunteers it ranged from 4 to 44 days. Regression analysis showed a positive association in both groups between the RMP concentration and the duration of storage (**FIGURE 2**). The results also showed an r^2 of 0.35 (P = .0006) in donors with thalassemia and 0.41 (P <.0001) in healthy volunteers. Over the duration of storage, the packed RBCs from donors with thalassemia and healthy volunteers showed average RMPs to be 47,426 (10,139–127,785) particles/μL vs 49,021 (13,033–126,749) particles/μL, respectively (P = .63). The highest values in donors with thalassemia were found on day 34 and in healthy volunteers on day 38.

Discussion

The current study aimed to address the dynamic changes in RMP levels in packed RBCs obtained from donors who have thalassemia. This study is the first to report similar trends in donors with thalassemia and healthy volunteers regarding MP accumulation in RBC products stored under blood bank conditions.

The changes in MP levels in blood components during manufacturing and storage underscore the importance of analyzing MP quantities in these blood components.[20] The changes may be influenced by different donor characteristics (eg, thalassemia status). Previous work has characterized the MPs in blood products prepared from donors with thalassemia.[19] In the current study, we examined the RMPs in stored packed RBCs from eligible donors with thalassemia. Our main findings are (1) a trend toward a positive relationship between RMP concentration and duration of storage, indicating that longer duration of storage yields higher RMP values in stored packed RBCs in both donors with thalassemia and healthy volunteers; (2) almost identical slope values of the linear regressions, suggesting a rate of RMP accumulation in stored packed RBCs that is similar in both groups; (3) indistinguishable ranges of RMP concentration between the groups; and (4) maximum values of RMPs in the late days of storage in both groups. Together, these similar patterns suggest that storage-induced RMP release in donors with thalassemia is like that in healthy volunteers.

Studies have suggested changes in several biochemical parameters during the storage of blood components.[16,17] Examination of the markers associated with the antioxidant defense system (eg, superoxide dismutase, catalase, and glutathione peroxidase) in RBCs has found similar activity in those who have thalassemic traits and in control patients.[21] The unremarkable differences in the biochemical markers between the donors with thalassemia and healthy volunteers may explain the similar effects of storage on RMP release observed in the present study.

TABLE 1. Demographic and Hematologic Parameters of Donors with Thalassemia and Healthy Volunteers[a]

	Donors with Thalassemia Trait (n = 28)	Healthy Volunteers (n = 104)	*P* Value
Age (y)	34.07 ± 11.84 (19–56)	35.64 ± 12.01 (17–58)	.54
Female:male ratio	1 (9):2 (19)	1 (55):1 (49)	…
Hb (g/dL)	13.74 ± 1 (11.5–15.6)	13.86 ± 1.26 (11.3–17.1)	.64
HCT (%)	42.26 ± 2.8 (35.9–46.8)	42.2 ± 3.64 (33.7–51.2)	.93
MCV (fL)	76.28 ± 6.8 (57.2–85.6)	85.55 ± 6.42 (55.8–95.6)	<.0001[b]
MCH (pg)	24.28 ± 2.27 (19.5–27.5)	28.13 ± 2.39 (18.4–31.8)	<.0001[b]
MCHC (g/dL)	32.52 ± 0.9 (30.1–34.2)	32.84 ± 0.93 (30.2–35.3)	.11
RDW (%)	14.74 ± 1.2 (12.7–17.7)	13.8 ± 1 (11.8–17.3)	.006[b]
MPV (fL)	9.52 ± 0.91 (7.8–12.1)	8.99 ± 1 (6.9–12.2)	.02[b]
WBCs (cells/μL)	7411 ± 1776 (4370–1.1 × 10^4)	7437 ± 1503 (4740–1.1 × 10^4)	.9
RBC count (cells/μL)	5.5 × 10^6 ± 6 × 10^5 (4.3 × 10^6–7.1 × 10^6)	4.9 × 10^6 ± 5 × 10^5 (3.9 × 10^6–6.8 × 10^6)	<.0001[b]
PLTs (cells/μL)	2.4 × 10^5 ± 5 × 10^4 (1.5 × 10^4–3.6 × 10^5)	2.6 × 10^5 ± 6.9 × 10^4 (3.3 × 10^4–4.4 × 10^5)	.06

Hb, hemoglobin; HCT, hematocrit; MCH, mean corpuscular hemoglobin; MCHC, mean corpuscular hemoglobin concentration; MCV, mean corpuscular volume; MPV, mean platelet volume; PLTs, platelets; RBC, red blood cell; RDW, red cell distribution width; WBCs, white blood cells.
[a]*Results are expressed as mean ± standard deviation (minimum–maximum).*
[b]*Indicates significant difference between the groups.*

FIGURE 2. Regression analysis of red blood cell–derived microparticle (RMP) concentrations and durations of storage in the packed red blood cells obtained from donors with thalassemia (A) and healthy volunteers (B). A, r^2 = 0.35; y = 1695x + 5451; P =.0006. B, r^2 = 0.41; y = 1609x + 9581; P <.0001.

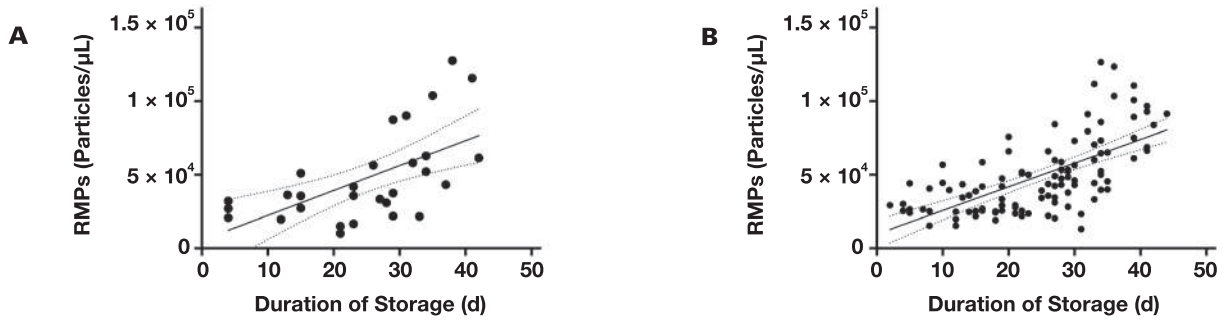

In addition to this similarity, our kinetic study makes other suggestions regarding RMPs in stored RBC products. First, it recommends that MP quantitation be performed on packed RBCs stored for more than 30 days before being sent to recipients. As **FIGURE 2** shows, some packed RBCs clearly show increased RMP levels after 30 days of storage, whereas others do not. Considering this difference, classifying packed RBCs according to RMP levels may help minimize posttransfusion complications in recipients and improve transfusion efficacy, as previously described.[22] Second, our findings assume that stored packed RBCs from donors with thalassemia and healthy volunteers are equally capable of contributing to posttransfusion complications. This assumption is supported by our finding of similarities between the groups regarding the ranges and magnitudes of RMP levels. However, further study is needed to confirm this assumption.

In the current study, our patients' demographic data included ages ranging from 17 to 60 years, and the durations of storage in both groups ranged from 4 to 44 days, indicating the broad range of information in the study. In addition, Hb typing showed that the highest frequency of the α-thalassemia trait and HbE occurred in the donor group, a result in line with those of a study that examined the prevalence of donors with thalassemia in Thailand.[7] Although the study reported the highest frequency of donors with α-thalassemia when compared to other types of thalassemia, the lower prevalence values in our study were unexpected and may be explained by the difference in study areas. Collectively, these findings suggest the validity of the sample of eligible donors with thalassemia recruited for the present study.

The study has several limitations. First, a limited number of donors with thalassemia were available for analysis. Although our results indicated a positive association between RMP levels and the duration of storage in both groups of donors, the differences between these groups in the number of packed RBCs at the longer storage durations may limit the generalizability of this research finding. Therefore, further studies that recruit more donors with thalassemia may be needed to confirm the effects of storage duration on RMP release in RBC products. Second, because our study was a cross-sectional one, we were unable to obtain data regarding either the therapeutic efficacy of packed RBC products or the adverse reactions in recipients. Finally, the present study lacked data on biochemical parameters related to cellular metabolism and RBC quality (eg, ATP, 2,3-diphosphoglycerate, and calcium and potassium content in the RBCs).[23] Addressing these parameters may help support the quality of the RBC products obtained from donors with thalassemia as compared to those from healthy volunteers.

Conclusion

In summary, our results indicate that storage-induced RMP release has similar effects in packed RBCs obtained from both donors with thalassemia and healthy volunteers.

Conflict of Interest Statement

The authors report no financial or other conflict of interest relevant to the subject of this article.

Acknowledgments

This research was funded by Chulalongkorn University (CU-GES-60-05-30-01). The authors thank the Faculty of Medicine Siriraj Hospital, Mahidol University, for supporting this research project.

REFERENCES

1. Fucharoen S, Winichagoon P. Thalassemia and abnormal hemoglobin. *Int J Hematol.* 2002;76(suppl 2):83–89.
2. Hirsch RE, Sibmooh N, Fucharoen S, Friedman JM. HbE/β-thalassemia and oxidative stress: the key to pathophysiological mechanisms and novel therapeutics. *Antioxid Redox Signal.* 2017;26(14):794–813.
3. Nienhuis AW, Nathan DG. Pathophysiology and clinical manifestations of the β-thalassemias. *Cold Spring Harb Perspect Med.* 2012;2(12):a011726.
4. Origa R. β-thalassemia. *Genet Med.* 2017;19(6):609–619.
5. World Health Organization. *Blood Donor Selection: Guidelines on Assessing Donor Suitability for Blood Donation*. Geneva, Switzerland: World Health Organization; 2012.
6. Sundh A, Kaur P, Palta A, Kaur G. Utility of screening tools to differentiate beta thalassemia trait and iron-deficiency anemia—do they serve a purpose in blood donors? *Blood Res.* 2020;55(3):169–174.
7. Nuinoon M, Kruachan K, Sengking W, Horpet D, Sungyuan U. Thalassemia and hemoglobin E in southern Thai blood donors. *Adv Hematol.* 2014;2014:932306.
8. Burnier L, Fontana P, Kwak BR, Angelillo-Scherrer A. Cell-derived microparticles in haemostasis and vascular medicine. *Thromb Haemost.* 2009;101(3):439–451.
9. Rank A, Nieuwland R, Liebhardt S, et al. Apheresis platelet concentrates contain platelet-derived and endothelial cell-derived microparticles. *Vox Sang.* 2011;100(2):179–186.

10. Kriebardis A, Antonelou M, Stamoulis K, Papassideri I. Cell-derived microparticles in stored blood products: innocent bystanders or effective mediators of post-transfusion reactions? *Blood Transfus.* 2012;10(suppl 2):s25–s38.
11. Noulsri E, Palasuwan A. Effects of donor age, donor sex, blood-component processing, and storage on cell-derived microparticle concentrations in routine blood-component preparation. *Transfus Apher Sci.* 2018;57(4):587–592.
12. Noulsri E, Udomwinijsilp P, Lerdwana S, Chongkolwatana V, Permpikul P. Differences in levels of platelet-derived microparticles in platelet components prepared using the platelet rich plasma, buffy coat, and apheresis procedures. *Transfus Apher Sci.* 2017;56(2):135–140.
13. Tzounakas VL, Anastasiadi AT, Dzieciatkowska M, et al. Proteome of stored RBC membrane and vesicles from heterozygous beta thalassemia donors. *Int J Mol Sci.* 2021;22(7):3369.
14. Hashemi Tayer A, Amirizadeh N, Ahmadinejad M, Nikougoftar M, Deyhim MR, Zolfaghari S. Procoagulant activity of red blood cell-derived microvesicles during red cell storage. *Transfus Med Hemother.* 2019;46(4):224–230.
15. Gevi F, D'Alessandro A, Rinalducci S, Zolla L. Alterations of red blood cell metabolome during cold liquid storage of erythrocyte concentrates in CPD-SAGM. *J Proteomics.* 2012;76:168–180.
16. D'Alessandro A, Gevi F, Zolla L. Red blood cell metabolism under prolonged anaerobic storage. *Mol Biosyst.* 2013;9(6):1196–1209.
17. D'Alessandro A, Kriebardis AG, Rinalducci S, et al. An update on red blood cell storage lesions, as gleaned through biochemistry and omics technologies. *Transfusion.* 2015;55(1):205–219.
18. Kim Y, Xia BT, Jung AD, et al. Microparticles from stored red blood cells promote a hypercoagulable state in a murine model of transfusion. *Surgery.* 2018;163(2):423–429.
19. Noulsri E, Lerdwana S, Palasuwan D, Palasuwan A. Cell-derived microparticles in blood products from thalassemic blood donors. *Lab Med.* 2021;52(2):150–157.
20. García-Roa M, Del Carmen Vicente-Ayuso M, Bobes AM, et al. Red blood cell storage time and transfusion: current practice, concerns and future perspectives. *Blood Transfus.* 2017;15(3):222–231.
21. Chakraborty D, Bhattacharyya M. Antioxidant defense status of red blood cells of patients with beta-thalassemia and Ebeta-thalassemia. *Clin Chim Acta.* 2001;305(1–2):123–129.
22. Noulsri E. Quantitation of cell-derived microparticles in blood products and its potential applications in transfusion laboratories. *Lab Med.* 2020;51(5):452–459.
23. Hess JR. Measures of stored red blood cell quality. *Vox Sang.* 2014;107(1):1–9.

The Impact of Sodium Dodecyl Sulfate and 2-Mercaptoethanol on Antibody and Antigen Binding

Chong Wang, BS, Hui Liu, MS, Xinyan Feng, MS*

College of Medical Laboratory, Dalian Medical University, Dalian, China; *To whom correspondence should be addressed. liuhui60@sina.com

Keywords: SDS treatment, 2-mercaptoethanol, immunodiffusion, western blot, antigenicity, methodology

Abbreviations: ENAs, extractable nuclear antigens; SDS, sodium dodecyl sulphate; PAGE, polyacrylamide gels by electrophoresis; 2-ME, 2-mercaptoethanol; HBsAg, hepatitis B surface antigen; NS, normal saline; OD, optical density; MANOVA, multivariate ANOVA

Laboratory Medicine 2022;53:307–313; https://doi.org/10.1093/labmed/lmab081

ABSTRACT

Objective: To evaluate the effect of sodium dodecyl sulfate (SDS) and 2-mercaptoethanol (2-ME) on antigen-antibody binding when incubated at 100°C, which is the pretreatment temperature required for western blots.

Methods: Serum that tested positive for hepatitis B surface antigen (HBsAg) plus loading buffer were mixed at a ratio of 4:1 and incubated in a water bath. We then detected HBsAg using double immunodiffusion and ELISA.

Results: The HBsAg titer was 1:512 in the control group when incubated at 37°C. Incubation with SDS at 100°C reduced the antigen titer to 1:32. The inhibitory effect on HBsAg titer reached 96.9% after incubation at 100°C with SDS and 2-ME.

Conclusion: We detected strong inhibition of antigens in western blots via SDS and 2-ME. It is likely that false-negative results will be obtained from western blots of antigens with weak resistance to these reagents.

Western blotting has been widely used in clinical laboratories for its unique advantages, such as identification of antibodies against HIV[1] and extractable nuclear antigens (ENAs) in autoimmune diseases.[2] Western blotting is used to identify a specific protein from complex protein matrices in biochemistry, molecular biology, and clinical-laboratory studies.[3,4] Proteins are separated by electrophoresis on a polyacrylamide slab gel and then transferred to a solid-phase carrier; next, an antibody and corresponding secondary antibody are used to detect the presence of a specific protein. Although this technology has been widely used to detect protein levels, several recent findings[5–8] suggest that western blots may not be as reliable as previously assumed. Although western blotting seems to be a straightforward and simple method for protein analysis, in practice it is an error-prone method due to its time-consuming multistep protocol.[9]

The multistep western blotting procedure mainly involves specimen preparation and separation of proteins by size on sodium dodecyl sulphate (SDS) polyacrylamide gels by electrophoresis (PAGE).[10–12] Total proteins are mixed in a buffer containing SDS and 2-mercaptoethanol (2-ME) according to a certain ratio and incubated in a water bath at 100°C for 5 minutes to denature the proteins during western blotting.[13]

SDS is an anionic surfactant that can damage the noncovalent bonds between proteins and other substances. Using a strong reducing agent such as 2-ME, disulfide bonds between the protein molecules are opened, and proteins are depolymerized into polypeptides. The polypeptides combine with SDS and include a large number of negative charges, which eliminates the difference in charge between proteins; thus, electrophoretic mobility is only related to the molecular weight of the proteins, which can then be determined.[14–17] In practical experiments, we often use 5× SDS-PAGE protein-loading buffer. Based on relevant literature, the main components of the protein-loading buffer are 1 M Tris-HCl, 10% SDS, 50% glycerol, 1% bromophenol blue, 2-ME, or other reducing agents.[18]

Because SDS treatment can change the charge of proteins and heating can destroy many conformational epitopes,[19,20] it has also been reported[21] that almost all immunochemical reactivity is destroyed at concentrations of SDS greater than 0.01%. If it actually inhibited proteins, western blotting would not have become so popular. Therefore, to assure successful detection of proteins in western blots, it is critical to check that the antibody is specific towards native and denatured protein because the denaturing treatment of protein specimens in western blotting may change the exposure and availability of the epitope, affecting antibody binding affinity.

Western blotting is the preferred method for identification of antibodies against HIV and ENAs, including RNP, Sm, SSA, SSB, Scl-70, Jo-1, and others.[1,2] However, the destruction of antigen in the process of western blotting may affect the detection of the aforementioned antibodies, which are characterized by low sensitivity and poor stability.[22]

In our experiments, we explored the damage caused to antigens during western blotting using the strongly resistant hepatitis B surface antigen (HBsAg). We detected HBsAg in western blots of HBsAg-positive serum in experimental groups treated with SDS and 2-ME, compared with a control group treated with an equal amount of normal saline (NS). Semiquantitative analyses of HBsAg using 2 immunological methods were performed to investigate the effects of SDS and 2-ME treatment on antigenicity at 2 different temperatures. ELISA was used for preliminary exploration, and double immunodiffusion tests were used for confirmation.

Materials and Methods

HBsAg-positive serum specimens provided by a randomly selected anonymous patient (6888 IU/mL) were used as test antigens in the experimental and control groups. The serum was denatured at different temperatures after adding different doses of SDS and 2-ME, and the control group was treated with an equal amount of NS. Antigens were then detected by double immunodiffusion and ELISA.

We incubated 3 different concentrations of SDS and 2-ME with the specimens at 2 different temperatures and analyzed them using multifactor analysis, with the test method designed as an orthogonal experiment. SDS, 2-ME, and temperature were set as independent variables, and optical density (OD) was measured by ELISA as the dependent variable, to investigate the effects of the 3 variables on serum antigenicity, also considering the interactions among the 3 variables. The OD values were analyzed by multivariate ANOVA (MANOVA). The double immunodiffusion test was used for the analysis and identification of antigen, antibody purity, and antigen specificity, and was also selected as a confirmatory test to verify ELISA results.

Treatment of the Experimental Specimens

Serum and loading buffer were mixed at a 4:1 ratio and incubated in a water bath. There were 2 operating temperature: 37°C for 30 minutes and at 100°C for 3 minutes. The control group was treated with an equal amount of NS. The volume of the control buffer was 100 μL, containing 20 μL of 10% SDS, 5 μL of 2-ME, and 75 μL of NS.

The concentration of SDS and 2-ME in the single-factor treatment groups were divided into 3 levels to test half and double the concentration of reagents in the control dose. The SDS doses were 10 μL, 20 μL, and 40 μL (the corresponding concentrations in the system were 0.2%, 0.4%, and 0.8%, respectively); the 2-ME doses were 2 μL, 5 μL, and 10 μL (the corresponding concentrations in the system were 0.4%, 1%, and 2%, respectively).

Orthogonal ELISA Test

The experimental method used was orthogonal experimental design, also known as orthogonal design, which is a method for scientific design of multifactor experiments. SDS, 2-ME, and temperature were the independent variables, and the OD value was the dependent variable. We carried out experiments with the multifactor treatment group in accordance with the orthogonal design table (**TABLE 1**).

Preparation of Specimens and Determining the OD Value of HBsAg

We followed the aforementioned specimen-processing procedure. A volume of 50 μL of serum from the experimental and control groups was added to wells in an ELISA plate coated with hepatitis B surface antibody.

TABLE 1. Effects of SDS, 2-ME, and Temperature on HBsAg Antigenicity[a]

Group	Concentration	OD	Temperature
Control Group	NS	1.298	
1	10 μL SDS + 2 μL 2-ME	0.870	37°C
2	10 μL SDS + 5 μL 2-ME	0.783	
3	10 μL SDS + 10 μL 2-ME	0.726	
4	20 μL SDS + 2 μL 2-ME	0.776	
5	20 μL SDS + 5 μL 2-ME	0.486	
6	20 μL SDS + 10 μL 2-ME	0.444	
7	40 μL SDS + 2 μL 2-ME	0.588	
8	40 μL SDS + 5 μL 2-ME	0.399	
9	40 μL SDS + 10 μL 2-ME	0.260	
10	10 μL SDS + 2 μL 2-ME	0.601	100°C
11	10 μL SDS + 5 μL 2-ME	0.591	
12	10 μL SDS + 10 μL 2-ME	0.364	
13	20 μL SDS + 2 μL 2-ME	0.266	
14	20 μL SDS + 5 μL 2-ME	0.246	
15	20 μL SDS + 10 μL 2-ME	0.222	
16	40 μL SDS + 2 μL 2-ME	0.184	
17	40 μL SDS + 5 μL 2-ME	0.142	
18	40 μL SDS + 10 μL 2-ME	0.108	

Abbreviations: *SDS, sodium dodecyl sulfate; 2-ME, 2-mercaptoethanol; HBsAg, hepatitis B surface antigen; OD, optical density; NS, normal saline.*
[a]The volume of the buffer was 100 μL, containing 10% SDS, 2-ME, and NS.

The plate was covered with sealing film and placed in a water bath for 60 minutes. The liquid in the wells was discarded, and the wells were washed with diluted washing liquid 5 consecutive times and then patted dried. With the exception of the blank wells, each well received 50 μL of enzyme binder, and the plate was covered with sealing film and incubated in a 37°C water bath for 30 minutes. The liquid in the wells was discarded, and the wells were washed with diluted washing liquid 5 consecutive times and then patted dried. We performed 3 parallel trials for each specimen.

Subsequently, substrate solution A (50 μL of 5% hydrogen peroxide) and 50 μL of substrate solution B (0.2 mg/mL tetramethylbenzidine) were then added to the ELISA plates and mixed thoroughly; next, the plates were incubated at 37°C in the dark to develop color for 30 minutes. Termination solution (50 μL of 2 mol/L H_2SO_4) was then added and mixed gently to terminate the reaction. An automatic microplate reader (Bio-Rad xMark; Bio-Rad Laboratories) was used to read the OD values at 450 nm.

Confirmatory Test Double Immunodiffusion

ELISA was used for preliminary exploration. Double immunodiffusion tests were used as confirmatory tests.

Preparing the Agarose Gel

We placed 10 mL of 15 g/L agar in 6-cm dishes and allowed it to solidify. Next, 3 groups of wells were created with a 4-mm punch.

Adding the Specimen

For the experimental and control specimens, 20 μL of 1:2 diluted rabbit anti–human serum antibody were added to the middle well, and 20 μL

of serum from the experimental or control groups were added to the remaining 6 wells. We performed 3 parallel experiments for each specimen.

Determining the Reaction Results

The agar plate with the added specimen was placed into a wet box, and the results were observed after 24 hours at 37°C. The precipitation line was observed, and the titer of antigen was recorded. The highest dilution with a visible precipitation line was considered to be the antigen titer.

Alternative Experiments for SDS

We chose sodium lauroyl sarcosinate (sarkosyl) as the alternative reagent for SDS. In the single-factor treatment groups, sarkosyl was added at the same concentration as SDS,[23] using the same treatment method as SDS at 37°C. The damage to protein antigenicity was observed via ELISA and double immunodiffusion tests.

Statistical Analysis

Statistical analyses were performed using SPSS software, version 17.0 (IBM Corporation). Multivariate analysis of variance was performed on the orthogonal ELISA results. The effects of the 3 factors on serum antigenicity were investigated; the interactions between SDS-temperature, SDS–2-ME, 2-ME–temperature, and the combination of these 3 factors were also examined. Data were considered to be statistically significant when the probability of type I error was .05 or less.[24] The SDS concentration corresponding to half the absorbance value of the control group was considered the half-inhibitory concentration of SDS on HBsAg (ID_{50}), which was calculated as follows. The 2 points above and below half the absorbance value of the control group were named A1 and A2, respectively, and the corresponding SDS concentrations were designated C1 and C2, respectively. The 2 points were plotted, with the concentration of SDS on the abscissa and the absorbance on the ordinate. The coordinates of these 2 points were (C1, A1) and (C2, A2). These coordinates were then substituted into the equation y = kx + b as follows: A1 = k × C1 + b and A2= k × C2 + b. Therefore, k = (A1-A2)/(C1-C2) and b = (C1 × A2-A1 × C2)/(C1-C2), and the equation was solved as

$$y = \frac{A_1 - A_2}{C_1 - C_2}x + \frac{C_1A_2 - C_2A_1}{C_1 - C_2}$$

with concentration plotted on the X-axis and absorbance on the Y-axis. We substituted half the absorbance value of the control group into the equation to obtain X, which is the ID_{50} of SDS on HBsAg.

The algorithm for inhibition of antigen titer in bidirectional immunodiffusion tests was as follows: if the serum titer of antigen is A in the control group and B in the experimental group, the inhibition rate of antigen titer is equal to

$$\left(\frac{1/A - 1/B}{1/A}\right) \times 100\%$$

Results

The changes in absorbance of HBsAg-positive serum treated with different concentrations of SDS, 2-ME, and temperature are shown in **TABLE 1**. The results showed that compared with the single-factor group, the more factors that were applied, the greater was the influence on antigenicity. The inhibitory effect was gradually enhanced with the increase in concentration. Multifactor analysis of variance was then performed for the aforementioned orthogonal experiments (**TABLE 2**).

In **TABLE 2**, we compared the F values and *P* values of SDS, 2-ME, and temperature, and the pairwise interactions between the factors, as well as the interaction among all 3 factors. The results showed that the *P* values of the 3 factors were all less than .01, indicating that the 3 factors had a significant impact on the OD values of serum antigen and were statistically significant. However, the magnitude of their influence varied greatly. According to the results of variance analysis, 2-ME had the least influence on OD values, and temperature had the greatest influence. The effect of the 3 factors on the absorbance value was in the following order: temperature > SDS > 2-ME.

In the single-factor group at 37°C, the absorbance values of the SDS group at increasing SDS concentrations were 1.159, 0.829, and 0.525; the absorbance values of the 2-ME group were 1.150, 0.802, and 0.434 (**TABLE 3**). At 100°C, the absorbance values of the SDS group were 0.662, 0.577, and 0.283. The absorbance value of the control group was 1.298 at 37°C; however, the specimen could not be solubilized without SDS at 100°C, so this detection assay was not performed. Compared with the control group, the different concentrations of SDS and 2-ME and increasing temperature had different degrees of inhibition on HBsAg. With the increase in SDS and 2-ME concentration, the absorbance values for serum antigen decreased, and the inhibitory effect became more obvious.

Because the concentration range of SDS in the control group with half of the absorbance was between 0.4% and 0.8%, when the concentration of SDS was plotted on the abscissa and the absorbance values on the ordinate, the equations using points (0.4, 0.829) and (0.8, 0.525) were calculated to obtain $y = -1.65x + 1.489$. When the absorbance was half of the control group ($y = 0.649$), $x = 0.51$ was obtained; therefore, the concentration of SDS producing half-inhibition of HBsAg was 0.51%. Similarly, the half-inhibitory concentration of 2-ME for HBsAg was 2.4%.

Double immunodiffusion is an immunoprecipitation technique. The precipitation line represents the approximate proportion of antigen and antibody when they spread from different wells of the agar gel.[25]

Rabbit anti–human serum antibody was added to the middle well in the experimental and control-group specimens. Moving from the first well, the dilution of the serum was increased in an anticlockwise manner around the middle well. The results showed that higher serum

TABLE 2. MANOVA Results from the Orthogonal Test

Source	Type III Sum of Squares	df	Mean Square	F	*P* Value
Corrected Model	3.060[a]	17	0.180	189.465	<.001
Intercept	10.776	1	10.776	11343.011	
SDS	1.419	2	0.710	746.939	
ME	0.345	2	0.173	181.612	
T	1.087	1	1.087	1144.625	
SDS * ME	0.030	4	0.008	8.002	
SDS * T	0.010	2	0.005	5.335	
ME * T	0.067	2	0.034	35.299	
SDS * ME * T	0.101	4	0.025	26.477	

Abbreviations: *MANOVA, multifactor ANOVA; SDS, sodium dodecyl sulfate; ME, mercaptoethanol.*
[a]$R^2 = 0.989$.

concentrations presented a more obvious precipitation line. The antigen titer in the control group was 1:512 at 37°C. As the concentration of SDS and 2-ME increased, the inhibitory effect of these reagents became more obvious. The antigen titers of the SDS group at 37°C for 3 parallel assays with increasing SDS concentration were 1:256, 1:256, and 1:64. The antigen titers of the 2-ME group at 37°C at 3 doses were 1:256, 1:64, and 1:64 (**FIGURE 1**).

After the boiling-water bath in the SDS group, the titer of the antigen was lower, and the antigen titers were 1:32, 1:32, and 1:1 (**FIGURE 2**), which were lower than those at 37°C. When the 3 factors were applied at the same time, the inhibition was strongest (**TABLE 4**). These results showed that the antigenicity of serum protein was significantly inhibited after exposure to SDS, 2-ME, and high temperature (**FIGURE 3**).

Alternative experiments for SDS: in the single-factor group at 37°C, the absorbance values of the SDS group at increasing SDS concentrations were 0.866, 0.333, and 0.297; the values for the sarkosyl group were 1.086, 0.474, and 0.316 (**TABLE 5**). The absorbance value of the control group was 1.650 at 37°C. At 100°C, the absorbance values of the SDS group were 0.353, 0.255, and 0.176. The antigen titers of the sarkosyl group at 37°C for the 3 assays were 1:256, 1:256, and 1:64, respectively. Comparisons of the 2 denaturing agents are shown in **TABLE 5**.

TABLE 3. Comparison of Denaturing Antigenicity between SDS and 2-ME under Different Dosage Conditions[a]

Group	ELISA (OD)		
	Low	Medium	High
SDS			
37°C	1.159	0.829	0.525
100°C	0.662	0.577	0.283
2-ME			
37°C	1.150	0.802	0.434
100°C	NA	NA	NA

Abbreviations: *SDS, sodium dodecyl sulfate; 2-ME, 2-mercaptoethanol; OD, optical density; HBsAg, hepatitis B surface antigen; NA, nonapplicable.*
[a]*The absorbance values of the control group was 1.298 at 37°C in the ELISA test. The concentration of SDS producing half-inhibition of HBsAg was 0.51%. The half-inhibitory concentration of 2-mercaptoethanol for HBsAg was 2.4%.*

Discussion

SDS and 2-ME have been used in a variety of biological experiments and have a inhibitory effect on antigen reactivity to antibody.[26] The antigen used in the present experiments was HBsAg, which can survive at 60°C for 4 hours and is tolerant to generally used concentrations of disinfectant. HBsAg resistance to heat is strong; however, heating to 60°C for 10 hours can reduce its antigenicity, and boiling at 100°C for 5 minutes can completely inactivate it. Therefore, in this experiment, HBsAg was used to observe the influence of specimen buffer reagents on antigenicity of specimens in western blots. Damage to the antigen with strong resistance implies even more damage to the antigen with weak resistance.

The experimental method used was orthogonal experimental design, also known as orthogonal design, which is a method for scientific design of multifactor experiments.[27] It uses a set of normalized orthogonal tables to arrange the experiment, and then the experimental results are statistically processed so that scientific conclusions can be drawn. It is a method designed to study multiple factors and levels, and it is convenient and rapid.

The results of orthogonal ELISA were analyzed by multivariate analysis of variance. SDS, 2-ME, and temperature were set as independent variables, and the absorbance value (OD) provided the dependent variable to investigate the effects of the 3 factors on serum antigenicity, as well as the interaction between SDS-temperature, SDS–2ME, 2-ME–temperature, and the interaction among all 3 factors.

There are various detection methods for serum HBsAg, of which the most common is ELISA. ELISA is the classic immunological experiment, combining the high efficiency and specificity of enzyme reactions with the specificity of antigen-antibody reactions, with the advantages of high sensitivity, good reproducibility, and simple operation.[28,29] Double immunodiffusion is an immunoprecipitation technique in which the precipitation lines represent the interaction between antigen and antibody as they diffuse from different wells in an agar gel. It is a test to analyze and identify antigen, antibody purity, and antigen specificity. It has strong specificity, so it can be used as confirmatory test to verify ELISA results and draw conclusions.

The results of ELISA showed that SDS and 2-ME had an inhibitory effect on HBsAg that increased with concentration. The half-inhibition of HBsAg by SDS occurred at an SDS concentration of 0.51%, and half-inhibition of HBsAg by 2-ME occurred at 2.4%, both of which values

FIGURE 1. Representative results of double immunodiffusion assays to detect the influence of 2-mercaptoethanol (2-ME) on serum antigens.

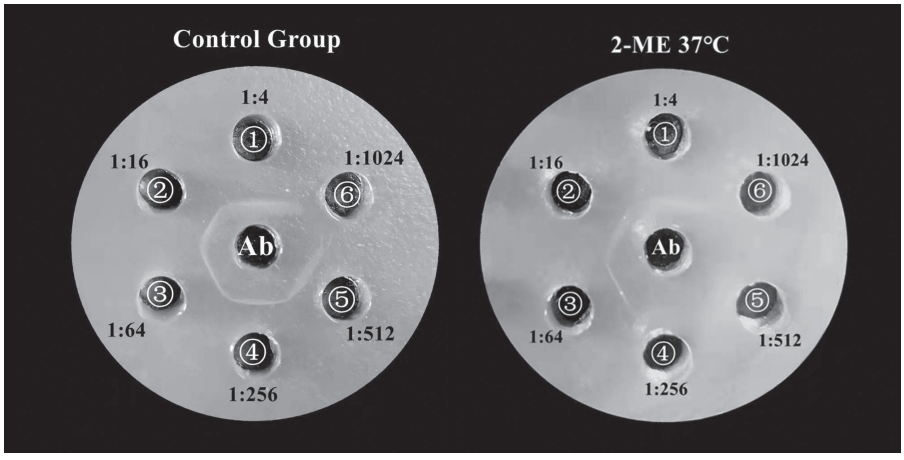

2022;53;307–313 | https://doi.org/10.1093/labmed/lmab081

FIGURE 2. Representative results from double immunodiffusion assays to detect the influence of sodium dodecyl sulfate (SDS) on serum antigens at 100°C.

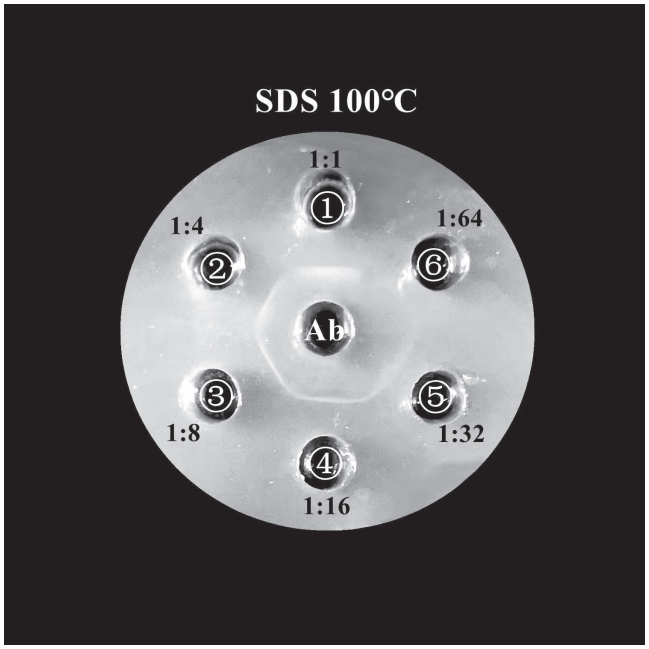

were much lower than the concentrations used in our experiment. The experimental temperature adopted was first set at 37°C, which is the normal human body temperature and the optimal temperature specified for the reagent kit.

These results indicated that inhibition of HBsAg was produced by SDS and 2-ME, which exerted a certain inhibitory effect on the antigen. Second, to explore the effect of temperature on serum antigenicity, we raised the temperature to 100°C and boiled the specimens for 3 minutes, and the results showed that antigenicity was more obviously inhibited.

A preliminary conclusion was obtained by ELISA, and a double immunodiffusion assay was used for verification. The results showed that the antigen titer in the control group was 1:512, which was 2–8 times higher than that of the single-factor group at 37°C, and was at least 16 times higher than the titer of the group at 100°C. When SDS and 2-ME were combined, the inhibition was more obvious, and the titer of antigens was significantly reduced. The titer of antigen in the 37°C group decreased to 1:64 and to 1:1 in the 100°C group when SDS and 2-ME were present. Taking the reciprocal of the antigen titer and calculating the inhibition rate showed that the inhibition rates of the SDS experimental group at 37°C were 50%, 50%, and 87.5% at 3 doses; the inhibition rates in the 2-ME experimental group were 50%, 87.5%, and 87.5%. In contrast, the inhibition rates in the SDS experimental group at 100°C at 3 doses were 93.8%, 93.8%, and 99.8%. The titer of the 2-ME group could not be detected because 2-ME coagulates at high temperatures. The results showed that SDS exerted an inhibitory effect on antigenicity at 37°C and the same effect more prominently at 100°C.

The purpose of adding some reductants and SDS to proteins in western blots is to denature proteins.[30] SDS is a protein denaturation agent that is highly effective and widely used and has been applied in many fields. In the process of protein extraction, it is used to destroy the cell membrane, so that transmembrane proteins with strong hydrophobicity are extracted into the aqueous solution, thus improving the efficiency

TABLE 4. Double Immunodiffusion Confirmation Test Results to Detect the Influence of Single Factors on Serum Antigenicity

Temperature		SDS	2-ME	SDS + 2-ME
37°C	Titer	1:256	1:64	1:128
	Inhibition rate	50%	87.5%	75%
100°C	Titer	1:32	NA	1:16
	Inhibition rate	93.8%	NA	96.9%

Abbreviations: *SDS, sodium dodecyl sulfate; 2-ME, 2-mercaptoethanol; NA, nonapplicable.*
[a]*The antigen titer in the control group was 1:512 at 37°C.*

of protein extraction.[31–33] SDS can break noncovalent bonds between proteins and other substances.[34,35]

In the presence of strong reducing agents such as 2-ME, disulfide bonds between protein molecules are opened, and proteins are depolymerized into polypeptides. The depolymerized proteins bind to SDS, forming a complex with a large amount of negative charge, which eliminates the charge difference between proteins. Therefore, electrophoretic mobility is only related to the molecular weight of proteins. According to this principle, the molecular weight of the protein is determined, but the effect of this treatment on antigenicity is ignored. Even the surface antigen of hepatitis B with strong resistance is also greatly inhibited. If the antigenicity of the protein is weak, false-negative results are likely to result from the aforementioned treatment. Therefore, it is not suitable for specimens with weak antigenicity, and alternatives should be sought for agents that demonstrate a strong inhibitory effect.

Studies have applied radioimmunoassay technology to detect and compare the effects of 3 reagents: SDS, sodium deoxycholate, and Triton X-100, on antigen-antibody reactions. The results have shown that concentrations of SDS greater than 0.01% can destroy most immune reactions, indicating that SDS has great damaging effects.[36] For mildly antigenic specimens, a milder agent is required. The search for mild detergents that can weaken and maintain enzymatic activity has been an important research subject worldwide.

There are 2 types of protein denaturants commonly used in these experiments: anionic and cationic. The anionic types include SDS and sarkosyl; the cationic types are cetylpyridine bromide and hexadecyl trimethylammonium bromide. SDS is a strong denaturing agent for proteins in gel electrophoresis. It has been shown to be an ideal detergent for the identification of high kinetic stability proteins using the PAGE method, including D2D SDS-PAGE and S-trap.[37]

Some super stable proteins, also known as kinetically stable proteins, are resistant to SDS and need to be heated to denature. The findings of a study[38] have shown that sarkosyl is a mild detergent compared with SDS, and it can identify proteins with medium-high kinetic stability. Sarkosyl is an ideal new denaturing agent that can be used to establish a set of elution methods with low toxicity, high efficiency, and no damage to the tissue structure.[38] For decades, it has been known that sarkosyl is a milder detergent than SDS, although many proteins can be denatured by sarkosyl at room temperature. Sarkosyl has been widely used to solubilize a variety of aggregation-prone proteins, including membranes, cytoskeletons, and inclusion bodies.[39–43]

Unexpectedly, we learned from the experimental results that the concentration of SDS producing half-inhibition of HBsAg was 0.22% and that the half-inhibitory concentration of sarkosyl for HBsAg was 0.29%.

FIGURE 3. Effects of sodium dodecyl sulfate (SDS), 2-mercaptoethanol (2-ME), and temperature on serum antigen titer and inhibition rate.

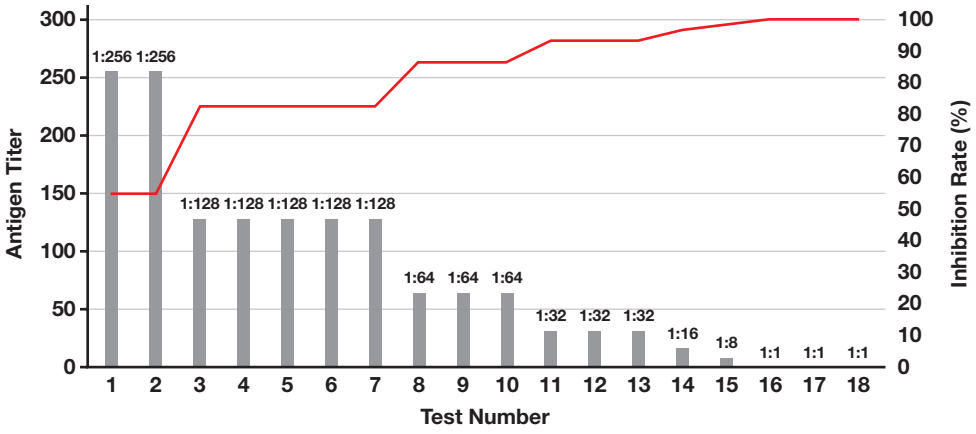

TABLE 5. Comparison of Denaturing Antigenicity between SDS and Sarkosyl under Different Dosage Conditions at 37°C[a]

Group	ELISA			Double Immunodiffusion		
	Low	Medium	High	Low	Medium	High
SDS	0.866	0.333	0.297	1:256	1:256	1:64
Inhibition rate	47.5%	79.8%	82.0%	50.0%	50.0%	87.5%
Sarkosyl	1.086	0.474	0.316	1:256	1:256	1:64
Inhibition rate	34.2%	71.3%	80.8%	50.0%	50.0%	87.5%

Abbreviation: *SDS, sodium dodecyl sulfate; HBsAg, hepatitis B surface antigen.*

[a]*The absorbance values of the control group was 1.650 in the ELISA test. The antigen titer in the control group was 1:512 in the double immunodiffusion test. The half-inhibition of HBsAg by SDS occurred at an SDS concentration of 0.22%, and half-inhibition of HBsAg by sarkosyl occurred at 0.29%.*

Similarly, the antigen titers of the sarkosyl group at 37°C at 3 doses were 1:256, 1:256, and 1:64, respectively, which show that the protein denatured by sarkosyl was similar to that denatured by SDS.

Although sarkosyl is widely considered to be milder than SDS, we have not been able to demonstrate in our experiments that its use reduces the inhibition of antigens and antibodies. As a mild anionic detergent, it is similar to SDS in size, shape, and hydrophobic tail.[23] However, it has a strong inhibitory effect on immune proteins, so it is not suitable for the replacement of denaturing agent SDS in western blots. As a denaturing agent component in the traditional western blotting method, SDS has its value and is a better choice. Western blotting is widely used in clinical practice to detect HIV antibodies and some common ENA antibodies in clinical diseases.[21] However, the damage to antigen in the western blotting process is great, and some antigens with weak expression may yield false-negative test results, which will impact the clinical results.

The limitation of this research work was that although substitute reagents were used to replace SDS, the inhibition of protein antigenicity was not greatly reduced. However, in this experiment, we did determine the main factors influencing western blots, which has laid a foundation for improving the western blotting technique. Therefore, the next step is to seek a reagent that is milder than SDS, weakens the inhibition of antigens and antibodies, and reduces the loss of experimental information caused by SDS. If such a reagent can be found, western blotting could be better applied to improve the accuracy of laboratory diagnosis and scientific research.

Acknowledgments

We thank the International Science Editing Company. Also, we thank our colleagues who have published concordance studies.

Personal and Professional Conflicts of Interest

None reported.

REFERENCES

1. Crowell TA, Ritz J, Coombs RW, et al. Novel criteria for diagnosing acute and early human immunodeficiency virus infection in a multinational study of early antiretroviral therapy initiation. *Clin Infect Dis*. 2021;73(3):e643–e651.
2. Hauke G, Lührmann R, Metz B, Peter HH. Detection of antibodies to extractable nuclear antigens with counterimmunoelectrophoresis and the Western blot technic [article in German]. *Z Rheumatol.* 1988;47(1):26–29.
3. Shapiro AL, Viñuela E, Maizel JV Jr. Molecular weight estimation of polypeptide chains by electrophoresis in SDS-polyacrylamide gels. *Biochem Biophys Res Commun.* 1967;28(5):815–820.
4. Bass JJ, Wilkinson DJ, Rankin D, et al. An overview of technical considerations for Western blotting applications to physiological research. *Scand J Med Sci Sports.* 2017;27(1):4–25.
5. Liu X, Wang Y, Yang W, Guan Z, Yu W, Liao DJ. Protein multiplicity can lead to misconduct in western blotting and misinterpretation of immunohistochemical staining results, creating much conflicting data. *Prog Histochem Cytochem.* 2016;51(3-4):51–58.
6. Gorr TA, Vogel J. Western blotting revisited: critical perusal of underappreciated technical issues. *Proteomics Clin Appl.* 2015;9(3-4):396–405.
7. Ghosh R, Gilda JE, Gomes AV. The necessity of and strategies for improving confidence in the accuracy of western blots. *Expert Rev Proteomics.* 2014;11(5):549–560.
8. Landry M, Gomes AV. Antibodies: Half of samples fail protein-blot tests. *Nature.* 2016;529(7584):25.
9. Ghosh R, Gilda JE, Gomes AV. The necessity of and strategies for improving confidence in the accuracy of western blots. *Expert Rev Proteomics.* 2014;11(5):549–560.

10. Murphy RM, Lamb GD. Important considerations for protein analyses using antibody based techniques: down-sizing Western blotting up-sizes outcomes. *J Physiol.* 2013;591(23):5823–5831.
11. Kurien BT, Scofield RH. Other notable protein blotting methods: a brief review. *Methods Mol Biol.* 2015;1312:487–503.
12. Bass JJ, Wilkinson DJ, Rankin D, et al. An overview of technical considerations for Western blotting applications to physiological research. *Scand J Med Sci Sports.* 2017;27(1):4–25.
13. Mishra M, Tiwari S, Gomes AV. Protein purification and analysis: next generation Western blotting techniques. *Expert Rev Proteomics.* 2017;14(11):1037–1053.
14. Reynolds JA, Tanford C. Binding of dodecyl sulfate to proteins at high binding ratios. Possible implications for the state of proteins in biological membranes. *Proc Natl Acad Sci U S A.* 1970;66(3):1002–1007.
15. Pederson T. Turning a PAGE: the overnight sensation of SDS-polyacrylamide gel electrophoresis. *FASEB J.* 2008;22(4):949–953.
16. Manning M, Colón W. Structural basis of protein kinetic stability: resistance to sodium dodecyl sulfate suggests a central role for rigidity and a bias toward beta-sheet structure. *Biochemistry.* 2004;43(35):11248–11254.
17. Xia K, Zhang S, Bathrick B, Liu S, Garcia Y, Colón W. Quantifying the kinetic stability of hyperstable proteins via time-dependent SDS trapping. *Biochemistry.* 2012;51(1):100–107.
18. Chen W, Bao G, Zhao L, Wang H. Analysis of circulating HMGB1 in human serum. *Methods Mol Biol.* 2020;2108:15–28.
19. Song J, Yuan Z, Tan H, Huber T, Burrage K. Predicting disulfide connectivity from protein sequence using multiple sequence feature vectors and secondary structure. *Bioinformatics.* 2007;23(23):3147–3154.
20. Kim TD, Ryu HJ, Cho HI, Yang C-H, Kim J. Thermal behavior of proteins: heat-resistant proteins and their heat-induced secondary structural changes. *Biochemistry.* 2000;39(48):14839–14846.
21. Qualtiere LF, Anderson AG, Meyers P. Effects of ionic and non-ionic detergents on antigen-antibody reactions. *J Immunol.* 1977;119(5):1645–1651.
22. Gastaldello R, Gallego S, Isa MB, et al. Immunofluorescence assay reactivity patterns of serum samples presenting indeterminate Western blot results for antibodies to HIV-1 and HTLV-I/II in Cordoba, Argentina. *Rev Inst Med Trop São Paulo*. 2001:43(5):277–282.
23. Huang L, Kou X, Zheng W, et al. 05SAR-PAGE: Separation of protein dimerization and modification using a gel with 0.05% sarkosyl. *Anal Chim Acta.* 2020;1101:193–198.
24. Yu J-W, Lim S-H, Kim B. Prefrontal functional connectivity analysis of cognitive decline for early diagnosis of mild cognitive impairment: a functional near-infrared spectroscopy study. *Biomed Opt Express*. 2020;11(4):1725–1741.
25. Mwangi JN, Ozwara HS, Motiso JM, Gicheru MM. Characterization of *Tunga penetrans* antigens in selected epidemic areas in Murang'a county in Kenya. *PLoS Negl Trop Dis.* 2015;9(3):e0003517.
26. Mishiro S, Imai M, Takahashi K, et al. A 49,000-dalton polypeptide bearing all antigenic determinants and full immunogenicity of 22-nm hepatitis B surface antigen particles. *J Immunol.* 1980;124(4):1589–1593.
27. Wang H-J, Pan M-C, Chang C-K. Optimization of ultrasonic-assisted extraction of cordycepin from Cordyceps militaris using orthogonal experimental design. *Molecules*. 2014;19(12):20808–20820.
28. Meng Y, Gao X, Chen W, et al. Methionine enkephalin (MENK) mounts antitumor effect via regulating dendritic cells (DCs). *Int Immunopharmacol.* 2017;44:61–71.
29. Mohanty S, Kamolvit W, Zambrana S, et al. Extract of *Clinopodium bolivianum* protects against *E. coli* invasion of uroepithelial cells. *J Ethnopharmacol.* 2017;198:214–220.
30. Liu ZY, Hao Q, Hou XX, et al. A study of the technique of western blot for diagnosis of lyme disease caused by *Borrelia afzelii* in China. *Biomed Environ Sci.* 2013;26(3):190–200.
31. Ning Z, Seebun D, Hawley B, Chiang CK, Figeys D. From cells to peptides: "one-stop" integrated proteomic processing using amphipols. *J Proteome Res.* 2013;12(3):1512–1519.
32. Sun L, Tao D, Han B, et al. Ionic liquid 1-butyl-3-methyl imidazolium tetrafluoroborate for shotgun membrane proteomics. *Anal Bioanal Chem.* 2011;399(10):3387–3397.
33. Chen EI, McClatchy D, Park SK, Yates JR 3rd. Comparisons of mass spectrometry compatible surfactants for global analysis of the mammalian brain proteome. *Anal Chem.* 2008;80(22):8694–8701.
34. Zhao XH, Huang CZ. Protein interaction with sodium dodecyl sulfate polarization properties of light scattering. *Chin Sci Bull*. 2006;51:2729–2732.
35. Yuan Y, Michael LM. Identification of nucleotides with identical fluorescent labels based on fluorescence polarization in surfactant solutions. *Anal Chem*. 2001;73:4508–4513.
36. Qualtiere LF, Anderson AG, Meyers P. Effects of ionic and non-ionic detergents on antigen-antibody reactions. *J Immunol*. 1977;119(5):723–730.
37. Xia K, Manning M, Hesham H, Lin Q, Bystroff C, Colón W. Identifying the subproteome of kinetically stable proteins via diagonal 2D SDS/PAGE. *Proc Natl Acad Sci U S A.* 2007;104(44):17329–17334.
38. Thibeault J, Patrick J, Martin A. Sarkosyl: A milder detergent than SDS for identifying proteins with moderately high hyperstability using gel electrophoresis. *Anal Biochem*. 2019;571:21–24.
39. Wroblewski H, Burlot R, Johansson KE. Solubilization of *Spiroplasma citri* cell membrane proteins with the anionic detergent sodium lauroyl-sarcosinate (sarkosyl). *Biochimie.* 1978;60(4):389–398.
40. Crossley R, Holberton DV. Selective extraction with sarkosyl and repolymerization in vitro of cytoskeleton proteins from *Giardia. J Cell Sci.* 1983;62:419–438.
41. Frankel S, Sohn R, Leinwand L. The use of sarkosyl in generating soluble protein after bacterial expression. *Proc Natl Acad Sci U S A.* 1991;88(4):1192–1196.
42. Burgess RR. Purification of overproduced *Escherichia coli* RNA polymerase sigma factors by solubilizing inclusion bodies and refolding from sarkosyl. *Methods Enzymol.* 1996;273:145–149.
43. Tao H, Liu W, Simmons BN, Harris HK, Cox TC, Massiah MA. Purifying natively folded proteins from inclusion bodies using sarkosyl, Triton X-100, and CHAPS. *Biotechniques.* 2010;48(1):61–64.

Adequate Antibody Response to COVID-19 Vaccine in Patients with Monoclonal Gammopathies and Light Chain Amyloidosis

Alan H.B. Wu, PhD,[1,] Chia-Ching Wang, MD,[2] Chui Mei Ong, BS,[1] Kara L. Lynch, PhD[1]*

[1]Department of Laboratory Medicine, University of California, San Francisco, California, US, [2]Department of Medicine, Division of Hematology/Oncology, University of California, San Francisco, California, US; *To whom correspondence should be addressed. alan.wu@ucsf.edu

Keywords: vaccine for SARS-CoV-2, COVID-19, multiple myeloma, immunosuppression, antibodies, monoclonal gammopathy of unknown significance

Abbreviations: MG, monoclonal gammopathy; MGUS, monoclonal gammopathy of unknown significance; MM, multiple myeloma; SMM, smoldering multiple myeloma; AL, light chain amyloidosis; HCW, healthcare workers; SPE, serum protein electrophoresis; FLC, free light chain; RFU, relative fluorescence unit; dara, daratumumab; bort, bortezomib; lena, lenalidomide; carfil, carfilzomib.

Laboratory Medicine 2022;53:314–319; https://doi.org/10.1093/labmed/lmab113

ABSTRACT

Objective: Determine the COVID-19 seroconversion rate for patients with multiple myeloma receiving a COVID-19 vaccine.

Materials and Methods: After 45 patients received their second COVID-19 vaccine dose, their serum IgG antibodies were measured: 22 with monoclonal gammopathy (MG) of unknown significance, 3 with smoldering myeloma, 2 with light chain amyloidosis, and 18 with MG (9 in remission, 6 out of remission, and 3 with free light-chain gammopathy alone). A second serum specimen was retained for 16 patients with MG. Their antibody levels were compared to those of 78 uninfected healthy vaccinated control patients.

Results: Three patients with MG had low antibody levels on blood collected 98, 100, and 113 days after the initial vaccine dose (2 with MG of unknown significance and 1 with hypogammaglobulemia). The other 40 patients with MG (seroconversion rate 93%) and both patients with amyloidosis produced antibodies. Relative to days after vaccination, patients with MG had lower antibody levels than control patients.

Conclusion: After receiving a COVID-19 vaccine, most patients with MG produce anti-SARS-CoV-2 antibodies comparable to levels in uninfected vaccinated healthy control patients.

In the past century, there have been several major pandemics caused by viral infections. The development and implementation of vaccines are among the key measures to arrest these outbreaks. Although smallpox has been eradicated and polio has largely been eliminated, influenza continues to be a major health concern, and there are no vaccines available for HIV. The release of vaccines has reduced the incidence and severity of SARS-CoV-2, the causative agent producing COVID-19. As of this report, 3 vaccines have been approved by the U.S. Food & Drug Administration under emergency use authorization. The Pfizer-BioNTech and Moderna vaccines are based on mRNA technology, and the Johnson & Johnson vaccine uses a modification of an adenovirus. Other COVID-19 vaccines are available in other parts of the world.

Multiple myeloma (MM) is a disease associated with impaired immunity, which is a manifestation of both the disease itself and the treatment given. Smoldering multiple myeloma (SMM) is a precancerous condition that is characterized by lower concentrations of myeloma proteins and the absence of symptoms. Monoclonal gammopathy of unknown significance (MGUS) is a benign condition. Both MGUS and SMM are not treated but can progress to MM over time. Amyloidosis is a disease characterized by the presence of misfolded proteins that deposit into various solid organs of the body. The most common form found in the United States is amyloid light chain (AL) amyloidosis. Many patients have excess free lambda light chains. Immunomodulatory treatment of amyloidosis[1] and medications to prevent organ transplant rejection result in immunosuppression.

The International Myeloma Working Group examined patients with myeloma who contracted COVID-19 and found significantly higher risks for death (33%) relative to individuals who had no preexisting chronic disease.[2] Therefore, vaccination against SARS-CoV-2 is recommended by many physicians.[3] There is no guarantee that a vaccination will necessarily produce adequate immune protection. In a study of a high-dose influenza vaccine, Branagan et al[4] showed that only 39% of patients with MM developed antibodies against 3 flu strains (H1N1, H3N2, and influenza B). Higher rates of antibody production were observed with administration

of a booster injection, a procedure that is not routinely performed for infection prophylaxis among healthy individuals. The vaccine used in their study was an inactivated influenza virus and different in principle from 2 mRNA vaccines released in later 2019. It is not known if the mRNA vaccines are indeed more immunogenic.

The purpose of this study was to examine COVID-19 antibody levels in patients with MM (active and in remission), SMM, MGUS, and AL after administration of a COVID-19 vaccine.

Materials and Methods

We recruited 46 patients seen at the Zuckerberg San Francisco General Hospital (ZSFG; San Francisco, CA) who exhibited a monoclonal gammopathy (MG) at one point during their medical history. Remnant serum specimens were retained from the ZSFG clinical laboratory as part of the patients' routine follow-up tests for serum protein electrophoresis (SPE) and serum free light chains (FLC). Medical records were reviewed for routine testing conducted at ZSFG for the presence of the SARS-CoV-2 virus using molecular assays in regular use at ZSFG. The manufacturer of the vaccine and the number of days from the date of the vaccine inoculations were recorded. One patient with MG tested positive for COVID-19 and was omitted from the study. Thirty-four patients tested negative for a COVID-19 infection during their hospitalization visits and had no medical history of an infection. For 16 patients with MG, a second blood specimen was retained from a follow-up visit a few weeks or months after their first specimen was retained and tested. For a control group, we recruited 78 ZSFG healthcare workers (HCW) who self-reported that they were healthy and free of a prior COVID-19 infection. Because of varying COVID-19 vaccine availability at the time, more Moderna vaccine was used for the MG group and more Pfizer-BioNTech vaccine was used for the HCW group. Protocols were reviewed and approved by the Institutional Review Board of the University of California, San Francisco with written consent from the HCW group and no consent for the MG group.

Blood from patients with MG was collected between February and July 2021. Specimens were centrifuged, and the serum was tested using SPE (Hydrasis 2 System, Sebia, Norcross, GA), total protein (Siemens Advia 1800, Tarrytown, NY) and for FLC (Diazyme, San Diego, CA). We confirmed MG using immunofixation electrophoresis (Sebia). The IgG antibodies to COVID-19 were measured with a quantitative assay using Pylon (ET Healthcare).[5] This assay produces relative fluorescence units (RFUs), which are indicative of the antibody titer, and is directed to both the nucleocapsid protein and the receptor binding domain (RBD) of the spike protein of SARS-CoV-2. As such, this assay cannot differentiate between antibodies produced as a result of a COVID-19 infection (antibodies to both proteins) and those produced by the vaccine alone (antibodies to the RBD of the spike only). A cutoff of 50 RFUs was considered as positive for this assay.

For 9 patients with MG, there were no COVID-19 molecular or antigen test results reported in the medical records. Serum from 5 of these individuals was tested for the presence of COVID-19 IgG antibodies using the Abbott Architect i2000 assay that is directed to the nucleocapsid protein. A positive result is indicative of a prior COVID-19 infection. The Student's *t*-test was used to compare the means of sex and vaccine type, and a plot of the log antibody level vs days after the first vaccine was performed for the MG and HCW groups using MedCalc version 19.6.4 (Ostend, Belgium).

Results

TABLE 1 lists the medical history of the patients with MG enrolled in the study. Overall, there were 35 men (78%; age range, 36–91 years) and 10 women (22%; age range, 49–77 years). Of the 9 patients with no record of a SARS-CoV-2 polymerase chain reaction test, 5 had negative antibodies toward the virus's nucleocapsid protein, indicating that the presence of the vaccine was responsible for the antibodies found in the sera of these individuals. There was an insufficient volume of specimen to test the remaining 4 patients. None of these patients had a medical history suggestive of a COVID-19 infection; therefore, we included them as not having been previously infected. Serum from the 1 excluded patient with MG who had a prior COVID-19 infection was positive for the presence of the nucleocapsid protein. For the purposes of this report, we presume that the other 4 nontested patients did not have a prior COVID-19 infection.

The distribution of manufacturers was as follows: 28 Moderna (62%), 16 Pfizer-BioNTech (36%), and 1 Johnson & Johnson (2%). There were 22 patients with MGUS, 3 with SMM, 18 patients with a diagnosis of MM (including 3 with FLC disease only and 6 in remission indicating hypogammaglobulinemia), and 2 with AL amyloidosis. For the latter 2 groups, patients were in various stages of medical management (the therapeutic regimens used to treat these patients are shown in **TABLE 1**). For the HCW group, there were 46 men (66%; age range, 28–75 years) and 24 women (34%; age range, 28–68 years). All of these participants were negative for the presence of antibodies directed toward the nucleocapsid protein (Abbott assay). The distribution of vaccine manufacturers was as follows: 37 Moderna (47%), 41 Pfizer-BioNTech (53%), and 0 Johnson & Johnson (0%). More patients with MG than the HCW received the Moderna vaccine ($P < .05$).

We found that 76 of 78 (99%) individuals tested had a positive IgG result within 16 days (range, 16–159 days) of their first vaccine dose (range, 199–6218 RFU). **FIGURE 1A** shows the distribution of results vs days from the first vaccination. The 1 individual who was negative (9 RFU) had blood taken at 9 days after the first vaccine. Antibody levels were generally lower per days after vaccination for the MG group vs the HCW group.

FIGURE 1B shows the SARS-CoV-2 IgG response from all patients in the MG group (including second draws). Results are plotted relative to days after the first dose of the vaccine. Similar results were obtained when plotted to days after the second dose (data not shown). Of the 45 patients with MG who received the vaccine, 42 had IgG levels above the assay's cutoff concentration. The 3 patients (numbers 41, 12, and 13 from **TABLE 1**) had a negative IgG level after blood was collected at 94, 100, and 113 days after they received the vaccine (5, 9, and 13 RFU, respectively). The first patient had MG with hypogammaglobulinemia (**FIGURE 2B**, given the Pfizer-BioNTech vaccine) and the other 2 had MGUS (**FIGURE 2C** and **2D**, given the Moderna and Pfizer-BioNTech vaccines, respectively), with 1 exhibiting immune suppression. The seroconversion rate for the MG group was 40 of 43 (93%). There was an insufficient number of patients within the MG group to determine whether IgG antibody results were different between the MGUS SMM, MG or AL groups, or the therapies used within the MG group. We were also unable to determine whether there were any differences between the types of vaccine used.

Repeat blood sampling was available for 16 patients with MG. Five of these patients initially had negative antibodies when blood was collected at 4, 16, 18, 21, and 28 days after the first dose. When these individuals

TABLE 1. Summary of Patients with MG

Patient (n)	Age (y)/ Sex	Dose Days	Vaccine Type	Free K (mg/dL)[a]	Free λ (mg/dL)	K/λ	Treatment	Myeloma Subtype	Total Protein (g/dL)[b]	Gammaglobulin (g/dL)	Prior Infection[c]
MGUS											
1	66/F	60	Moderna	2.28	1.29	1.77	None	IgG-λ	6.7	1.13	Neg
2	73/M	69	Moderna	5.12	1.93	2.65	None	IgG-K	7.2	1.11	Unknown
3	79/M	44	Moderna	6.69	4.6	1.45	None	IgG-K	6.2	0.73	Neg NP
4	60/F	71	Moderna	0.96	0.68	1.35	None	IgA-K	7.3	0.44	Neg
5	68/M	28	Moderna	0.82	0.76	1.08	None	IgM-K	7.6	0.27	Neg
6	65/M	39	Moderna	NP	NP	NP	None	IgM-K	7.2	1.11	Neg
7	66/M	70	Pfizer	4.8	1.39	3.45	None	IgG-K	8	2.2	Neg
8	69/M	27	Moderna	8.56	1.62	5.28	None	IgG-K	7.2	1.14	Neg
9	68/M	25	Moderna	NP	NP	NP	None	IgG-K	6.7	0.75	Neg
10	67/M	101	Moderna	2.43	1.08	2.25	None	IgG-K	7.1	2.5	Neg
11	69/F	96	Moderna	NP	NP	NP	None	IgG-λ	8	3.8	Neg
12	73/M	100	Moderna	6.49	2.34	2.94	None	IgG-K	8.4	2.6	Neg
13	91/M	113	Pfizer	6.66	8.33	0.8	None	IgM-K	5.9	1.4	Neg
14	54/F	64	Pfizer	9.87	2.08	4.75	None	IgG-K	8.1	2.71	Unknown
								IgM-K			
15	73/M	107	Pfizer	15.34	6.49	2.36	None	IgA-K	1.4	0.58	Neg
16	63/M	125	Moderna	NP	NP	NP	None	IgG-K	8.8	3.32	Neg
17	77/F	99	Moderna	2.6	1.75	1.49	None	IgG-λ	5.5	0.57	Unknown
18	65/M	154	Moderna	6.01	2.2	2.73	None	IgG-K	8.1	1.8	Neg
								IgM-K			
19	71/M	112	Pfizer	8.12	2.26	3.59	None	IgM-K	7.5	1.76	Neg
20	66/M	100	Moderna	4.55	3.28	1.39	None	IgG-λ	6.3	1	Neg
21	60/M	58	Pfizer	18.61	4.06	4.58	None	IgG-λ	10.4	4.79	Neg
22	70/M	154	Moderna	5.83	3.07	1.9	None	IgG-K	5.7	0.3	Neg
SMM											
23	78/M	73	Moderna	5.58	1.33	4.2	None	IgG-K	7.2	1.38	Neg
24	66/M	60	Moderna	7.23	3.83	1.89	None	IgG-K	6.4	1.38	Neg
25	82/M	84	Moderna	11.91	7.26	1.26	None	IgA-λ	6.6	2.7	Neg NP
MM											
26	76/M	47	Moderna	2.33	0.69	3.38	Dara	IgG-K	7.1	0.7	Neg NP
								Free K			
27	67/M	33	Moderna	4.08	2.37	1.72	Lena	IgA-K	6.9	0.88	Neg
								Free K			
28	59/M	18	Pfizer	0.88	8.37	0.09	Dara	IgA-λ	6.8	0.38	Neg
								IgG-λ			
29	72/M	56	Pfizer	3.06	1.51	2.03	Bort, lena	Free λ	6.8	0.46	Neg
30	68/M	21	Pfizer	57.9	2.96	19.56	Bort	IgG-K	7.6	0.27	Neg
31	55/M	28	Pfizer	2.14	0.81	2.64	Lena	IgA-K	6.6	0.4	Neg
32	52/M	70	Moderna	1.16	0.87	1.33	Bort, lena	IgG-K	7	0.5	Neg
33	62/M	40	Moderna	3.48	1.91	1.82	None	IgG-K	6.2	1.14	Neg
34	56/F	163	Moderna	53.6	0.94	57.09	Bort	IgG-K	7.6	2.31	Neg
Free light chain											
35	65/F	32	Pfizer	2.51	1.73	1.45	Lena	Free λ	6.1	0.59	Neg
36	73/F	98	Moderna	NP	NP	NP	None	Free λ	NP	NP	Neg
37	57/M	65	Pfizer	0.95	15.46	0.66	Poma, lena	Free λ	5.6	0.24	Neg
MM with hypogammaglobulinemia											
38	59/M	4	Pfizer	1.85	8.36	0.22	Bort	IgG-λ	6.4	0.33	Neg

TABLE 1. Continued

Patient (n)	Age (y)/ Sex	Dose Days	Vaccine Type	Free K (mg/dL)[a]	Free λ (mg/dL)	K/λ	Treatment	Myeloma Subtype	Total Protein (g/dL)[b]	Gammaglobulin (g/dL)	Prior Infection[c]
								Free λ			
39	36/M	14	Pfizer	0.54	8.18	0.07	Carfil	IgD-λ	6.7	4.2	Neg NP
40	49/F	66	Moderna	1.71	1.13	1.51	Lena	IgG-K	6.1	0.46	Neg
41	55/F	10	Pfizer	1.21	0.86	1.41	Dara	IgG-K	5.8	0.35	Neg
								Free K			
42	61/M	16	Moderna	0.98	0.72	1.36	Dara	IgG-K	6.3	0.32	Neg NP
43	58/M	52	Moderna	2.62	1.45	1.81	None	IgG-K	5.9	0.45	Neg
Amyloidosis											
44	59/M	2	Janssen	3.43	3.35	1.02	Dara, lena	Free λ	3.9	0.43	Unknown
45	66/M	73	Pfizer	4.05	3.68	1.1	Dara, lena	Free λ	1.1	0.56	Neg

bort, bortezomib; carfil, carfilzomib; dara, daratumumab; lena, lenalidomide; MGUS, monoclonal gammopathy of unknown significance; MM, multiple myeloma; NP, not performed; poma, pomalidomide; SMM, smoldering multiple myeloma.
[a]Reference range: free K: 0.33–1.94 mg/dL; free λ: 0.57–2.63 mg/dL; K/λ: 0.26–1.65.
[b]Reference range: total protein: 6.4–8.3 g/dL; gammaglobulin: 0.6–1.6 mg/dL.
[c]Neg NP: negative for the nucleocapsid protein (ie, no natural infection).

FIGURE 1. Log IgG antibody response vs days after the first vaccination for SARS-CoV-2. A, Healthcare workers (log[y] = –0.00225x + 3.26; r = 0.19, P = NS). B, Patients with monoclonal gammopathy (log[y) = 0.0024x + 2.40; r = 0.10; P = NS). The cutoff concentration is indicated by the dotted line. NS, not significant.

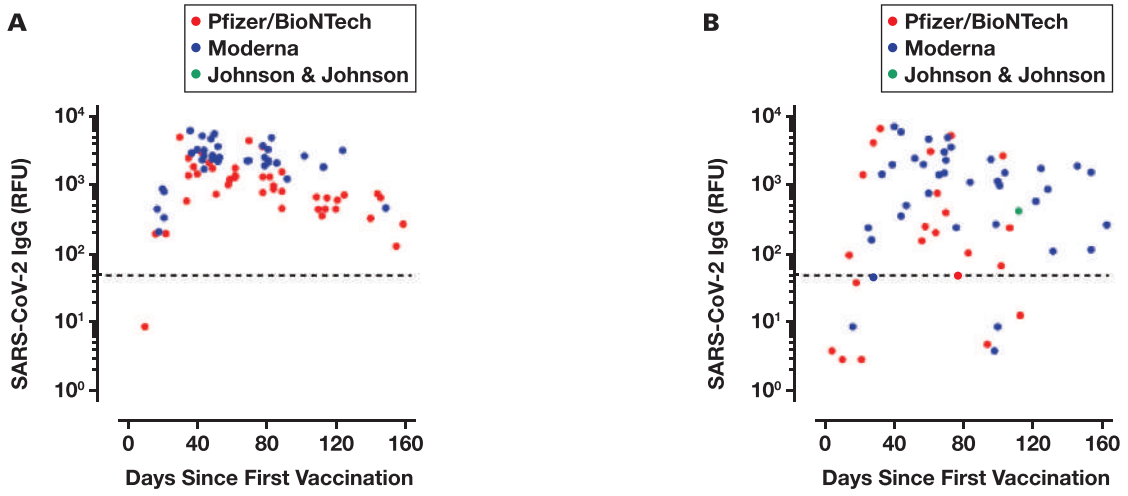

FIGURE 2. Densitometric serum protein electrophoresis scans. A, Healthy patient. B–D, Patients with no antibody production (patients 41, 12, and 13, respectively, from TABLE 1) after a COVID-19 vaccine.

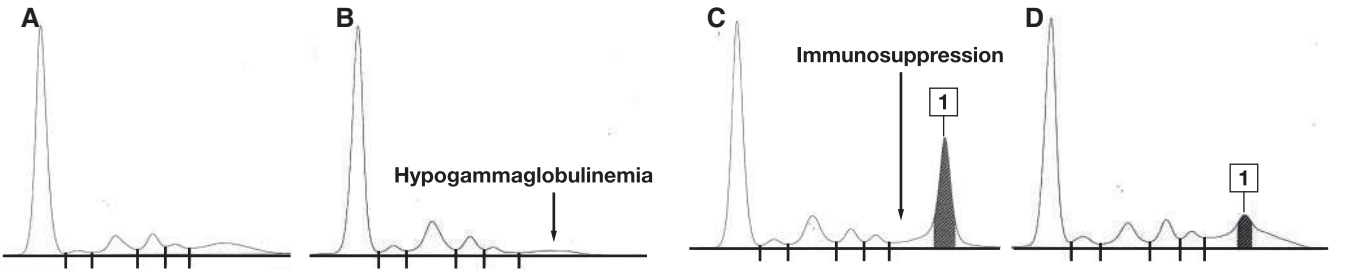

returned for a repeat blood draw (between 14 and 84 days), all but 1 had seroconverted to produce positive IgG antibodies.

Discussion

Research has shown that MGUS, which is a benign condition, has an incidence of 1.5% among individuals older than age 50 years and 3% for those older than age 70 years.[6] Although these patients are not immune suppressed because of the presence of polyclonal antibodies, they nevertheless have a higher risk of developing infections. In a study by Kristinsson et al,[7] patients with MGUS had a 2.7-fold higher risk for developing an influenza infection at a 5- and 10-year follow-up. Patients with SMM are characterized by a more advance premalignant phase than patients with MGUS, with 3 g/dL of monoclonal proteins and >10% of plasma cells in the bone marrow but no end-organ damage.[8] Our studies showed that for MGUS and SMM, SARS-CoV-2 antibodies are routinely detected in the serum after vaccination.

A more interesting question is whether antibodies are produced in patients with myeloma who exhibit immune suppression. A hallmark of this disease is the inability of patients to produce a polyclonal antibody response against common antigens, in favor of the malignant proliferation of a single B-cell clone (**FIGURE 2C**). In contrast to patients with MGUS, patients with myeloma have a 10-fold higher risk for an influenza infection.[9] This has led the European Myeloma Network to make a recommendation for influenza vaccinations for patients with MGUS, SMM, and MM.[10] Existing data are currently insufficient to inform on the optimal timing of COVID-19 vaccination among people who are planning to receive or who are receiving immunosuppressive therapies. In our study, regardless of the subtype, antibodies were produced in nearly all the patients with MM studied. As shown in **TABLE 1**, patients 36 through 42 had low gammaglobulin levels (reference range, 0.6–1.60 g/dL). This finding is relevant because the COVID-19 vaccine produces IgG antibodies that migrate within this electrophoretic region.

There have been a few recent reports of COVID-19 antibody response in patients with MM. In the United Kingdom, Bird et al[11] tested blood 21 days after vaccine administration (Pfizer-BioNTech and AstraZeneca) and reported an antibody positivity rate of 56%. There was no difference in the efficacy of the 2 vaccines used. In Italy, Pimpinelli et al[12] tested blood 5 weeks after administration of the Pfizer-BioNTech vaccine and reported that 78.6% of 42 patients with MM had antibodies. In perhaps the largest study of patients with MM to date, Van Oekelen et al[13] tested 260 patients with MM who received either the Pfizer-BioNTech (69%) or Moderna (27.2%) vaccine in the United States and reported an antibody positivity rate of 84.2%. The positivity rate found in this study (93%) is not significantly different from Pimpinelli et al[12] and Van Oekelen et al[13] but statistically higher than what was found in Bird et al.[11] The number of enrollments between this and the previous studies was too small to make any general conclusions as to why the antibody incidence rate was different. Laboratory tests for neutralizing antibody response may provide more information regarding humoral immune status. Terpos et al[14] showed that 22 days after patients were given the Pfizer-BioNTech vaccine, patients with MG had lower neutralizing antibody titers than healthy control patients (25% vs 55%). This study was limited in that only 1 dose of the vaccine had been given at the time of blood collection. We did not perform testing of serum antibodies using a surrogate virus neutralization test for our specimens.

In addition to patients with immune suppression due to their MG disease, treatment of patients using immunomodulatory drugs such as daratumumab lowers monoclonal antibody concentrations, leading to disease remission. This drug binds to CD38, a type II transmembrane glycoprotein that is expressed on plasma cells from patients with MM, resulting in cell death through complement-dependent, antibody-dependent cytotoxicity, phagocytosis, and apoptosis.[15] Daratumumab is also being used to treat AL amyloidosis. Very low gammaglobulin bands from SPE testing can be observed after treatment using this biologic agent.[16]

After administration of a COVID-19 vaccine, antibodies are consistently produced within 120 days after the first injection[17] and gradually decline over the ensuing months.[18] Our study showed that 93% of patients with MG had an adequate antibody response to a COVID-19 vaccine and were likely protected against SARS-CoV-2 infection. For the 3 patients with MG who exhibited no IgG response at or after 98 days, it is not known if their initial response declined to baseline levels or if they never had an antibody response. Nevertheless, these individuals may be at increased risk.

These results are significantly different from those of patients who have received a solid organ transplant and have been treated with immunosuppressive drugs. In a study of 658 patients who had received transplant, Boyarsky et al[19] showed a response rate of 15% after the first dose and 54% after the second dose of either the Pfizer-BioNTech or Moderna 2-dose vaccine. A different antibody assay than in the current work was used for that study, but this is not likely the reason for the differences in the incidence of antibody production. In contrast, Al-Janabi et al[20] showed that 92% of patients treated with immunomodulators for immune-mediated inflammatory disease produced antibodies after receiving a Pfizer-BioNTech vaccine. Immunomodulators are more selective than immunosuppressants and enable more retention of the host's immune response.

Study Limitations

This was an observational study using remnant blood specimens from routine clinical evaluations. For those patients who had repeat visits, the appointment schedule was fixed by the attending physicians and therefore was not controlled. As such, there may have been a selection bias. Another limitation is the higher proportion of patients with MG than HCW participants receiving the Moderna vaccine. We have previously shown that relative to the date of the second vaccine dose, individuals receiving the Moderna vaccine have higher antibody levels, and these declined at a slower rate than levels in those receiving the Pfizer-BioNTech vaccine.[18] However, this situation should not affect the overall rate of seroconversion. This study was further limited by the small numbers of patients enrolled with MG, which prohibited an analysis of subgroups (eg, disease status or therapy). We also do not have data on breakthrough infections or the role that T-cells have on immunity. Research has shown that B-cell function as determined by antibody production is only part of a patient's immune response to a SARS-CoV-2 infection. Exposure to viral proteins also produces a T-cell response. Although we are not able to assess T-cell function after administration of a COVID-19 vaccine, we expect that patients with MG should be capable of producing a cellular response because this disease disrupts humoral immunity to a greater extent than cellular immunity.

Conclusion

We found that 93% of patients with MG were able to produce an antibody response to a COVID-19 vaccine. Of the 3 patients with negative antibodies, 1 had hypogammaglobulinemia, 1 had immunosuppression because of the monoclonal band, and 1 had an adequate gammaglobulin response. Because the incidence of MM is low, it may be cost-effective to measure serum antibody levels after administration of a COVID-19 vaccine to find those few individuals who have a COVID-19 vaccine failure. Our study was insufficiently powered to determine whether immunosuppression was associated with a poor antibody response, and we have no data on breakthrough infections. Recently, a fully vaccinated former US Secretary of State with a history of MM died of complications from a COVID-19 infection. It is unknown whether the Secretary exhibited a low COVID-19 serum antibody response or hypogammaglobulinemia at the time of death. If both were present, then his case could illustrate how SPE could be a screening tool to justify COVID-19 antibody testing to assess B-cell immunity against a breakthrough infection. Detection of low total serum IgG could be a more cost-effective alternative than SPE testing. A study of antibody levels of patients with MG who become infected with SARS-CoV-2 after being fully vaccinated will be necessary to document the utility of this strategy.

REFERENCES

1. Vaxman I, Gertz M. Recent advances in the diagnosis, risk stratification, and management of systemic light-chain amyloidosis. *Acta Haematol.* 2019;141(2):93–106.
2. Chari A, Samur MK, Martinez-Lopez J, et al. Clinical features associated with COVID-19 outcome in multiple myeloma: first results from the International Myeloma Society data set. *Blood.* 2020;136(26):3033–3040.
3. Gavriatopoulou M, Ntanasis-Stathopoulos I, Korompoki E, Terpos E, Dimopoulos MA. SARS-CoV-2 vaccines in patients with multiple myeloma. *Hemasphere.* 2021;5(3):e547.
4. Branagan AR, Duffy E, Albrecht RA, et al. Clinical and serologic responses after a two-dose series of high-dose influenza vaccine in plasma cell disorders: a prospective, single-arm trial. *Clin Lymphoma Myeloma Leuk.* 2017;17(5):296–304.
5. Lynch KL, Whitman JD, Lacanienta NP, et al. Magnitude and kinetics of anti-SARS-CoV-2 antibody responses and their relationship to disease severity. *Clin Infect Dis.* 2021;72(2):301–308.
6. Kyle RA, Rajkumar SV. Monoclonal gammopathy of undetermined significance and smoldering multiple myeloma. *Curr Hematol Malig Rep.* 2010;5(2):62–69.
7. Kristinsson SY, Tang M, Pfeiffer RM, et al. Monoclonal gammopathy of undetermined significance and risk of infections: a population-based study. *Haematologica.* 2012;97(6):854–858.
8. Rajkumar SV, Landgren O, Mateos MV. Smoldering multiple myeloma. *Blood.* 2015;125(20):3069–3075.
9. Blimark C, Holmberg E, Mellqvist UH, et al. Multiple myeloma and infections: a population-based study on 9253 multiple myeloma patients. *Haematologica.* 2015;100(1):107–113.
10. Ludwig H, Boccadoro M, Moreau P, et al. Recommendations for vaccination in multiple myeloma: a consensus of the European Myeloma Network. *Leukemia.* 2021;35(1):31–44.
11. Bird S, Panopoulou A, Shea RL, et al. Response to first vaccination against SARS-CoV-2 in patients with multiple myeloma. *Lancet Haematol.* 2021;8(6):e389–e392.
12. Pimpinelli F, Marchesi F, Piaggio G, et al. Fifth-week immunogenicity and safety of anti-SARS-CoV-2 BNT162b2 vaccine in patients with multiple myeloma and myeloproliferative malignancies on active treatment: preliminary data from a single institution. *J Hematol Oncol.* 2021;14(1):81.
13. Van Oekelen O, Gleason CR, Agte S, et al; PVI/Seronet Team. Highly variable SARS-CoV-2 spike antibody responses to two doses of COVID-19 RNA vaccination in patients with multiple myeloma. *Cancer Cell.* 2021;39(8):1028–1030.
14. Terpos E, Trougakos IP, Gavriatopoulou M, et al. Low neutralizing antibody responses against SARS-CoV-2 in older patients with myeloma after the first BNT162b2 vaccine dose. *Blood.* 2021;137(26):3674–3676.
15. Touzeau C, Moreau P. Daratumumab for the treatment of multiple myeloma. *Expert Opin Biol Ther.* 2017;17(7):887–893.
16. Paul Y, Aguirre LE, Basher F, Miao F, Our-Sengul T, Hoffman JE. Hypogammaglobulinemia and its implications in patients treated with daratumumab: a single institution experience. *Blood.* 2019;134(suppl 1):131.
17. Widge AT, Rouphael NG, Jackson LA, et al.; mRNA-1273 Study Group. Durability of responses after SARS-CoV-2 mRNA-1273 vaccination. *N Engl J Med.* 2021;384(1):80–82.
18. Wu AHB, Nguyen E, Ong CM, Yun C, Lynch KL. Rate of serum SARS-CoV-2 antibody decline for two mRNA vaccines. Published online October 14, 2021. *J Appl Lab Med.* doi: 10.1093/jalm/jfab137.
19. Boyarsky JF, Werbel WA, Avery RK, et al. Antibody response to 2-dose SARS-CoV-2 mRNA vaccine series in solid organ transplant recipients. *JAMA* 2021;325(21):2204–2206.
20. Al-Janabi A, Littlewood Z, Griffiths CEM, et al. Antibody responses to single-dose SARS-CoV-2 vaccination in patients receiving immunomodulators for immune-mediated inflammatory disease. *Br J Dermatol.* 2021;185(3):646–648.

Elevated Serum HE4 Concentrations and Risk of Cardiac Complications among Hospitalized Patients with Burns

Yangyang Wu, MD[1,#], Ling Cao, MD[1,#], Jun Qi, MD[1,]*

[1]Department of Burns and Plastic Surgery, Affiliated Hospital of Nantong University, Nantong City, China; *To whom correspondence should be addressed. junqi123123123@163.com; #Contributed equally to this work.

Keywords: burn, cardiac complications, sepsis, sensitivity analysis, ROC curve, CVD

Abbreviations: SIRS, systemic inflammatory response syndrome; CVDs, cardiovascular diseases; MODS, multiple organ dysfunction syndrome; HE4, human epididymis protein 4; CAD, coronary-artery disease; DM, diabetes mellitus; EMRs, electronic medical records; BP, blood pressure; EIA, enzyme immunoassay; Hb, hemoglobin; FBG, fasting blood glucose; hs-CRP, hs–C-reactive protein; HbA1c, glycosylated hemoglobin; ALB, albumin; eGFR, estimated glomerular filtration rate; MDRD, Modification of Diet in Renal Disease; SOFA, sequential organ failure assessment; HR, heart rate; IL, interleukin; TNF-α, tumor necrosis factor alpha; HF, heart failure; CKD, chronic kidney disease; ALB, albumin; FBG, fasting blood glucose

Laboratory Medicine 2022;53:320–325; https://doi.org/10.1093/labmed/lmab110

ABSTRACT

Background: The decrease in effective blood volume after burns is closely related to abnormal heart function.

Objective: To investigate whether serum human epididymis protein 4 (HE4), an indicator of early renal injury, contributes to increased risk of cardiac complications in patients with burns.

Methods: Within 24 hours after hospital admission, clinical condition assessment and biochemical testing in patients with burns were performed. Multivariate analysis was performed by evaluating the relationship between serum HE4 levels and risk of cardiac complications (cardiac insufficiency, arrhythmia, and myocardial infarction) during hospitalization.

Results: The number (percentage) of cardiac complications in all included patients with burns was 80 (15.6%). The results of sensitivity analysis suggest that elevated serum HE4 levels were related to higher risk of cardiac complications in patients with sepsis (OR = 2.1; 95% CI, 1.19–3.17; P <.001) and in patients without sepsis (OR = 2.29; 95% CI, 1.33–4.71l; P = .005), respectively, after adjustments for clinical confounding factors were made. Sepsis did not have a modification effect on the association between serum and cardiac complications among these patients. Also, the results of ROC curve analysis showed that serum HE4 levels have good predictive value for predicting cardiac complications in patients with burns (AUC = 0.708; 95% CI, 0.61–0.81; P <.001).

Conclusions: In the current study, we identified that elevated HE4 levels contributed to increased risk of cardiac complications in the hospital in patients with burns. This novel finding suggests that burn patients with serum HE4 may provide the opportunity to predict cardiac complications before hospital admission.

Systemic inflammatory response syndrome (SIRS) often occurs in patients with severe burns, which limits the definition of sepsis among those patients.[1–3] Development of SIRS by severely burn-injured patients can easily lead to sepsis events,[3–5] especially in patients with underlying diseases that can lead to lowered immunity, such as cardiovascular diseases (CVDs). Also, although burn care has greatly improved in the past decade, a major complication, such as multiple organ dysfunction syndrome (MODS), is still the main cause of in-hospital death in patients who have initially survived their burn injuries.[6]

SIRS results in hemodynamic and cardiovascular complications in patients with severe burn injuries. For instance, cardiac complications, including cardiac insufficiency, arrhythmia, and myocardial infarction after burns, are related to shock, stress, electrolyte disturbance, and invasive infection in patients with burns.[7] However, adverse cardiovascular outcomes in these patients with burns are not well described in the literature.

Human epididymis protein 4 (HE4) is a secretory protein with a 20–25 kDa, which is expressed in the human epididymis.[8,9] Existing evidence has suggested that HE4 is overexpressed in malignant tumors in the ovaries, uterus, lungs, breasts, stomach, and other organs.[10–13] Some study findings[10,14–16] also showed that HE4 has a significant role in that it is linked to immune inflammatory responses in organs or tissues, such as upper respiratory tract and lung tissue. As an acute inflammatory complication, sepsis results from SIRS and/or bacterial infections, which may be associated with changed levels of serum HE4. Although previous study findings[17–20] have shown that elevated serum levels of HE4 were associated with higher risk of CVDs in different populations, the association of HE4 with cardiac complications in patients with burns has not been explored, to our knowledge.

Considering the previous research background, we explored whether HE4 is related to high risk of cardiac complications in hospitalized patients with burns. Also, we explored whether sepsis has a modifying effect on the association between serum HE4 and cardiac complications in patients with burns.

Methods

Study Specimens

We studied a total of 514 patients with burns who were hospitalized at the Affiliated Hospital of Nantong University, Nantong City, China, between February 2018 and October 2020. We included patients with burns who had had stable health for 3 months without a history of acute serious diseases before hospital admission. All included patients with burns had been treated within 12 hours after burn injury and underwent standardized hospital treatment during hospitalization.

The identification of sepsis was performed by 2 burn specialists.[21] The diagnostic criteria of sepsis events were as follows: patients with acute onset, chills, high fever, temperature fluctuations, increased sweating, or general progressive organ failure or large-joint pain; patients with severe poisoning symptoms who may have delirium, coma, or shock; patients with enlargement of the liver and spleen, congestion of the skin and mucous membranes, jaundice, and anemia; patients with migratory lesions (mostly seen in pyogenic cocci, especially *Staphylococcus aureus* infection); patients with an increased number of leukocytes and neutrophils; and patients with positive blood or bone marrow culture results, excluding contamination.

Sepsis was consistently identified based on clinical diagnostic guidelines by the burn specialists, who have decades of clinical experience. Of these patients with burns, 126 patients had sepsis events. In our study, classification of burn severity was assigned according to the criteria proposed by the International Burn Conference[21]: mild, second-degree burns with less than 9% of the total area burned; moderate, the total area of the burns is 10%–29%, or the area of the third-degree burns is less than 10%; severe, the total area of severe burns is 30%–49%, the area of third-degree burns is 10%–19%, or the total burn area is less than 30% but the general condition is serious, with shock and combined injury, moderate or severe inhalation injury having been found; most severe, the total burn area is greater than 50%, and the third-degree burn area is greater than 20%.

For the purposes of this study, we defined cardiac complications as cardiac insufficiency, arrhythmia, myocardial infarction, or aggravations of these previous cardiac complications during hospitalization. Also, patients with a history of cancer were excluded (n = 11).

The data regarding comorbid conditions, such as coronary artery disease (CAD), hypertension, stroke, and diabetes mellitus (DM), were based on electronic medical records (EMRs). Other clinical characteristics, including BMI and blood pressure (BP), were obtained from EMRs or telephone interviews. The Ethics Committee of the Affiliated Hospital of Nantong University approved this study; all patients gave written informed consent, according to the Declaration of Helsinki guidelines.

Laboratory Measurements

Blood specimens were obtained from the patients with burns on the first morning after hospital admission; serum was separated and stored at –80°C for HE4 testing via the commercial enzyme immunoassay (EIA) method (Fujirebio Diagnostics). The blood specimens were also tested for leukocyte count, hemoglobin (Hb), fasting blood glucose (FBG), hs–C-reactive protein (hs-CRP), LDL, HDL, glycosylated hemoglobin (HbA1c), and albumin (ALB) using an automatic biochemistry analyzer (ADVIA 2400; Siemens AG). The estimated glomerular filtration rate (eGFR) was calculated via the Modification of Diet in Renal Disease (MDRD) formula.[22]

Statistical Analyses

Multivariable logistic regression models were performed to identify the association of serum HE4 with cardiac complications in patients with burns after adjusting for age, sex, BMI, smoking status, drinking status, sequential organ failure assessment (SOFA) score, length of stay in the hospital, causes of burns (flame, chemical, scalding, electrical, and other) and admission vitals (systolic BP, diastolic BP, and heart rate [HR]).

To investigate whether sepsis has the modification effect on association between serum HE4 and cardiac complications in patients with burns, we performed stratification analysis by adding "sepsis" as the stratification variable. Also, sensitivity analyses were performed to evaluate the independent association between serum HE4 and cardiac complications by adding "comorbid conditions" (CAD, hypertension, stroke, and DM) and "eGFR", respectively, as the covariate. All of these variables were analyzed by using SPSS software, version 25.0 (IBM).

Results

Clinical Characteristics of Patients with Burns

The number (percentage) of cardiac complications in all included patients with burns was 80 (15.6%). All patients with burns were divided into 2 groups according to the presence or absence of sepsis. As shown in **TABLE 1**, the patients with burns and sepsis tended to be older; current smokers; and more likely to have higher BMI, SOFA score, length of hospital stay, and higher rates of DM and cardiac complications than the patients without sepsis (all $P < .05$). There were no significant difference regarding sex, drinking status, comorbid conditions, causes of burns, admission vitals, and burn severity between the 2 groups (all $P > .05$).

For laboratory measurements, the patients with sepsis had lower levels of eGFR and ALB, and higher levels of leukocyte count, Hs-CRP, FBG, and HbA1c. There were significant differences in other laboratory indices, namely, Hb, LDL, and HDL, between the 2 groups. Patients with sepsis had significantly higher serum HE4 levels than those without sepsis.

Logistic Regression Analysis for the Association of Serum HE4 with Cardiac Complications in Patients with Burns

To investigate whether serum HE4 may contribute to increased risk of cardiac complications in patients with burns, we used multivariable logistic regression models (**TABLE 2**). Model 1 demonstrated that elevated serum HE4 levels were linked with a higher risk of cardiac complications when adjustment was made for age and sex in patients with sepsis (OR = 2.96; 95% CI, 1.53–4.53; $P < .001$) and without sepsis (OR = 2.74; 95% CI, 1.44–3.93; $P < .001$), respectively.

After adjustment for clinical confounding factors including age, sex, BMI, smoking, drinking, SOFA score, length of stay in hospital, causes of burns (flame, chemical, scalding, electrical, and others), the results of

TABLE 1. Clinical Characteristics in 514 Patients with Burns within 24 Hours after Hospital Admission[a]

Variable	No Sepsis (n = 388)	Sepsis (n = 126)	*P* Value
Age (y), No. (range)	67.7 (61.5–72.6)	69.9 (63.8–76.4)	.03
Sex (male), No. (%)	170 (43.8)	52 (41.3)	.31
BMI (kg/m^2), No. (range)	25.3 (23.4–27.4)	27.0 (23.2–29.1)	.03
Current smoking, No. (%)	80 (20.6)	32 (25.4)	.53
Current drinking, No. (%)	134 (34.5)	66 (52.4)	.01
SOFA score, No. (range)	0 (0–2)	6 (1–5)	<.001
Cardiac complications, No. (%)	38 (9.8)	42 (33.3)	<.001
Length of stay in the hospital (d), No. (range)	28 (8–16)	70 (23–51)	<.001
Comorbid conditions, No. (%)			
Coronary artery disease	24 (6.2)	16 (12.7)	.02
Hypertension	130 (33.5)	46 (36.5)	.19
Stroke	20 (5.1)	94 (74.6)	.39
Diabetes mellitus	28 (7.2)	64 (50.8)	<.001
Causes of burns, No. (%)			
Flame	266 (68.6)	84 (66.7)	.36
Chemical	28 (7.2)	8 (6.3)	.28
Scalding	76 (19.6)	26 (20.6)	.54
Electrical	6 (1.5)	2 (1.6)	.58
Other	12 (3.1)	6 (4.8)	.29
Admission vitals, No. (range)			
Systolic BP (mm Hg)	144 (122–163)	145 (124–157)	.09
Diastolic BP (mm Hg)	80 (73–92)	81 (73–94)	.25
HR (bpm)	95 (88–100)	96 (89–101)	.17
Respiratory rate (No./min)	23 (15–25)	24 (16–27)	.10
Burn severity, No. (%)			
Moderate	102 (26.3)	40 (31.7)	.14
Severe	196 (50.5)	62 (49.2)	
Extremely severe	90 (23.2)	24 (19.0)	
Laboratory measurement			
eGFR (mL/min/1.73 m^2), No. (range)	47.3 (43.5–56.8)	44.5 (41.2–52.1)	.01
Leukocyte count (10^9/L), No. (range)	9.4 (8.0–14.6)	15.5 (12.8–21.7)	<.001
Hs-CRP (pg/mL), No. (range)	6.4 (3.5–10.4)	12.5 (5.5–19.1)	<.001
Hb (g/L), No. (range)	114 (102–124)	113 (100–123)	.11
ALB (g/L), No. (range)	36.5 (33.6–38.7)	32.9 (29.2–34.5)	<.001
FBG (mmol/L) on hospital admission, mean (SD)	5.8 (1.1)	10.2 (2.2)	.002
HbA1c (%), No. (range)	4.7 (3.3–7.3)	6.5 (6.8–8.2)	.001
HDL (mmol/L), mean (SD)	1.2 (0.15)	1.0 (0.13)	.12
LDL (mmol/L), mean (SD)	2.4 (1.2)	2.5 (1.4)	.13
HE4 (pmol/L), mean (SD)	153.5 (46.4)	369.6 (82.3)	<.001

Abbreviations: SOFA, sequential organ failure assessment; BP, blood pressure; HR, heart rate; eGFR, estimated glomerular filtration rate; hs-CRP, hs–C-reactive protein; Hb, hemoglobin; ALB, albumin; FBG, fasting blood glucose; HbA1c, glycosylated hemoglobin; HE4, human epididymis protein 4.
[a]Percentages may not total 100 because of rounding.

model 2 were consistent with those of model 1 in patients with sepsis (OR = 2.91; 95% CI, 1.51–4.93; *P* <.001) and without sepsis (OR = 2.72; 95% CI, 1.42–3.71; *P* <.001), respectively. This relationship remained minimally changed after continuing to add admission vitals (systolic BP, diastolic BP, HR, and respiratory rate) to model 2 in patients with sepsis (OR = 2.88; 95% CI, 1.47–4.87; *P* <.001) and without sepsis (OR = 2.71; 95% CI, 1.40–3.68; *P* <.001). These results suggested that sepsis did not have a modifying effect on the association between serum and cardiac complications among the patients with burns.

Sensitivity Analysis for the Association of Serum HE4 with Cardiac Complications in Patients with Burns

To further investigate whether sepsis has the modification effect on association between serum HE4 and cardiac complications in patients with

burns, sensitivity analysis was used by adding "comorbid conditions" as the covariate (**TABLE 3**). Model 1 suggested that elevated serum HE4 levels were associated with higher risk of cardiac complications when adjustment was made for age, sex, and comorbid conditions (CAD, hypertension, stroke, and DM) in patients with sepsis (OR = 2.26; 95% CI, 1.34–3.76; *P* <.001) and in patients without sepsis (OR = 2.19; 95% CI, 1.30–3.76; *P* <.001), respectively. However, after adjustment for clinical confounding factors, including age, sex, BMI, smoking status, drinking status, SOFA score, length of stay in the hospital, causes of burns (flame, chemical, scalding, electrical, and other), admission vitals (systolic BP, diastolic BP, HR, and respiratory rate), and comorbid conditions (CAD, hypertension, stroke, and DM), the results of model 3 suggested that serum HE4 still contributed to increased risk of cardiac complications in patients with sepsis (OR = 2.23; 95% CI, 1.31–3.50; *P* <.001) and in patients without sepsis (OR = 2.12; 95% CI, 1.21–3.41; *P* = .005), respectively.

TABLE 2. Logistic Regression Analysis for the Association between Serum HE4 Levels and Cardiac Complications in Patients with Burns during Hospitalization

Variable	Model 1[a]	Model 2[b]	Model 3[c]
Sepsis	2.96 (1.53–4.53)	2.91 (1.51–4.93)	2.88 (1.47–4.87)
P value	<.001		
No sepsis	2.74 (1.44–3.93)	2.72 (1.42–3.71)	2.71 (1.40–3.68)
P value	<.001		

Abbreviations: HE4, human epididymis protein 4; SOFA, sequential organ failure assessment; BP, blood pressure; HR, heart rate.
[a]Adjusted for age and sex.
[b]Adjusted for age, sex, BMI, smoking status, drinking status, SOFA score, length of stay in the hospital, and causes of burns (flame, chemical, scalding, electrical, and other).
[c]Adjusted for age, sex, BMI, smoking status, drinking status, SOFA score, length of stay in the hospital, causes of burns (flame, chemical, scalding, electrical, and other), and admission vitals (systolic BP, diastolic BP, HR, and respiratory rate).

TABLE 3. Sensitivity Analysis for the Association between Serum HE4 and Cardiac Complications in Patients with Burns during Hospitalization by Adding "Comorbid Conditions" as the Covariate

Variable	Model 1[a]	Model 2[b]	Model 3[c]
Sepsis	2.26 (1.34–3.76)	2.24 (1.32–3.52)	2.23 (1.31–3.50)
P value	<.001		
No sepsis	2.19 (1.30–3.76)	2.15 (1.26–3.64)	2.12 (1.21–3.41)
P value	<.001	.003	.005

Abbreviations: HE4, human epididymis protein 4; CAD, coronary artery disease; DM, diabetes mellitus; SOFA, sequential organ failure assessment; BP, blood pressure; HR, heart rate.
[a]Adjusted for age, sex, and comorbid conditions (CAD, hypertension, stroke, and DM).
[b]Adjusted for age, sex, BMI, smoking status, drinking status, SOFA score, length of stay in the hospital, causes of burns (flame, chemical, scalding, electrical, and other), and comorbid conditions (CAD, hypertension, stroke, and DM).
[c]Adjusted for age, sex, BMI, smoking status, drinking status, SOFA score, length of stay in the hospital, causes of burns (flame, chemical, scalding, electrical, and other), admission vitals (systolic BP, diastolic BP, HR, and respiratory rate) and comorbid conditions (CAD, hypertension, stroke, and DM).

Also, sensitivity analysis was used by adding "eGFR" as the covariate (**TABLE 4**). Similarly, our results continued to suggest that that serum HE4 levels still contributed to increased risk of cardiac complications in patients with sepsis (OR = 2.10; 95% CI, 1.19–3.17; *P* = .009) and in patients without sepsis (OR = 2.29; 95% CI, 1.33–4.71; *P* < .001), respectively, after adjustment for these clinical confounding factors were made in model 3. Sepsis did not also have a modification effect on the association between serum and cardiac complications among these patients with burns.

Predictive Value of Serum HE4 Levels on Cardiac Complications in Patients with Burns

As shown in **FIGURE 1**, the results of ROC curve analysis showed that serum HE4 levels affect the detection of cardiac complications with high AUC value (AUC = 0.708; 95% CI, 0.608–0.807; *P* < .001). This result suggests that serum HE4 levels have good predictive value for cardiac complications in patients with burns.

Discussion

Our study findings suggest that elevated serum levels of HE4 were significantly and independently associated with cardiac complications in patients with burns, as determined via multivariable logistic regression analysis. We discovered that sepsis has no modification effect on the association between serum HE4 and risk of cardiac complications among patients with burns.

The cardiovascular system is significantly affected after the body is severely injured. For example, burns can lead to microcirculatory disruption, causing extravasation of protein and fluid in burned tissues.[23] The acute inflammatory response plays an critical role on cardiovascular dysfunction.[23–25] All of these factors contribute to abnormal heart function, which increases morbidity and mortality in patients with burns.[26] The results of previous studies[27–29] have also suggested that burns can induce cardiac dysfunction. Extensive burns lead to inflammatory responses, which in turn contribute to the development of sepsis.[28,29] The findings of some studies[30–33] have shown that elevated levels of inflammatory cytokines such as interleukin (IL)–1β, tumor necrosis factor

TABLE 4. Sensitivity Analysis for the Association between Serum HE4 Levels and Cardiac Complications during Hospitalization in Patients with Burns by Adding "eGFR" as the Covariate

Variable	Model 1[a]	Model 2[b]	Model 3[c]
Sepsis	2.14 (1.26–3.32)	2.12 (1.22–3.21)	2.1 (1.19–3.17)
P value	.002	.008	.009
No sepsis	2.32 (1.37–4.84)	2.30 (1.35–4.78)	2.29 (1.33–4.71)
P value	<.001		

Abbreviations: HE4, human epididymis protein 4; eGFR, estimated glomerular filtration rate; SOFA, sequential organ failure assessment; BP, blood pressure; HR, heart rate.
[a]Adjusted for age, sex, and eGFR.
[b]Model 2: Adjusted for age, sex, BMI, smoking status, drinking status, SOFA score, length of stay in the hospital, causes of burns (flame, chemical, scalding, electrical, and other), and eGFR.
[c]Model 3: Adjusted for age, sex, BMI, smoking status, drinking status, SOFA score, length of stay in the hospital, causes of burns (flame, chemical, scalding, electrical, and other), admission vitals (systolic BP, diastolic BP, HR, and respiratory rate), and eGFR.

FIGURE 1. **ROC curve analysis of serum human epididymis protein 4 (HE4) levels effect to detect cardiac complications.**

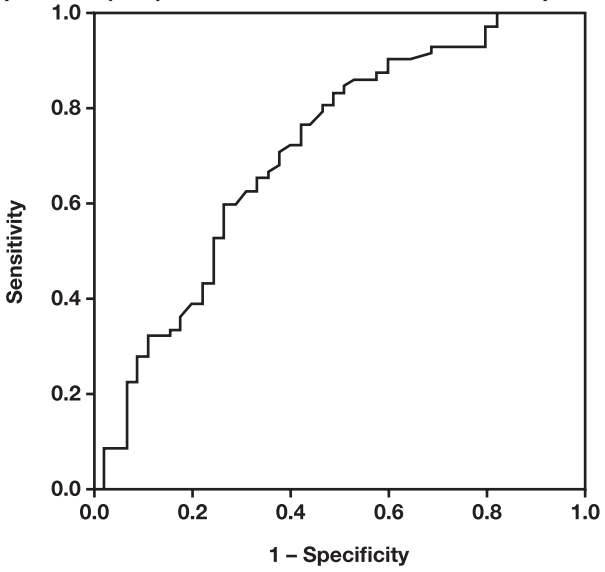

alpha (TNF-α), and IL-6 can depress intracellular calcium currents and cardiac contractility, and promote cardiomyocytes apoptosis.

Our study findings suggest that elevated serum HE4 levels were associated with higher risk of cardiac complications in patients with burns, after confounding factors were corrected. This conclusion is consistent with the findings of previous research on the association between burns and cardiac function.

Although HE4 is a tumor biomarker, its anti-inflammatory properties have been reported in the literature. For instance, serum HE4 levels were elevated in patients with CVDs, and high levels of this analyte contributed to higher risk of acute and chronic heart failure (HF), myocardial infarction, stroke, and other cardiovascular events.[17–20] These study reports infer that HE4, as an index of fibroinflammatory response, promotes the occurrence and development of cardiovascular events.[17–20]

Further, HE4 has also been to be found to be associated with renal function and is regarded as a biomarker of acute kidney injury or chronic kidney disease (CKD).[34–36] Abnormal renal function is closely related to increased risk of cardiovascular events, which may provide another explanation of why serum HE4 levels were associated with higher risk of cardiac complications. We note that some included patients with burns and mild renal dysfunction, in our study, might contribute partly to the elevated serum levels of HE4. However, although renal dysfunction was also corrected in our regression model, the independent association did exist.

Our study has several strengths. First, we identified that serum HE4 is associated with cardiac complications in hospitalized patients with burns and that sepsis has no modification effect on the association between burns and cardiac complications. Second, EMRs enable us to accurately record the occurrence time of cardiac complications during hospitalization, which can help us to determine and analyze the relationship between HE4 level and risk of cardiac complications. Third, the included study specimens had a broad spectrum of risk factors; sufficient clinical confounding variables were corrected to ensure the reliability of this study.

Our study also has several limitations. First, adequate correction of confounding factors may lead to overfitting of multivariate correction models, which could lead to our results (serum HE4 and risk of cardiac complications in the hospital) being lower than the actual value. Second, our results were from a single center and had a small sample size. In the future, further studies are necessary to verify the association of serum HE4 with cardiac complications in the hospital in patients with burns.

Conclusion

In the current study, we identified that increased serum HE4 levels contributed to increased risk of in-hospital cardiac complications in patients with burns. This finding suggests that monitoring the serum HE4 levels in patients with burns may provide the opportunity for prediction of cardiac complications before hospital admission.

REFERENCES

1. Margraf A, Ludwig N, Zarbock A, Rossaint J. Systemic inflammatory response syndrome after surgery: mechanisms and protection. *Anesth Analg.* 2020;131(6):1693–1707.
2. Churpek MM, Snyder A, Han X, et al. Quick sepsis-related organ failure assessment, systemic inflammatory response syndrome, and early warning scores for detecting clinical deterioration in infected patients outside the intensive care unit. *Am J Respir Crit Care Med.* 2017;195(7):906–911.
3. Taeb AM, Hooper MH, Marik PE. Sepsis: current definition, pathophysiology, diagnosis, and management. *Nutr Clin Pract.* 2017;32(3):296–308.
4. Dokumcu Z, Ergun O, Ak Celik H, et al. Clostridial collagenase aggravates the systemic inflammatory response in rats with partial-thickness burns. *Burns*. 2008;34(7):935–941.
5. Marsden NJ, Lawrence M, Davies N, et al. The effect of the acute inflammatory response of burns and its treatment on clot characteristics and quality: a prospective case controlled study. *Burns*. 2020;46(5):1051–1059.
6. Safiri S, Ashrafi-Asgarabad A. Platelet count: a predictor of sepsis and mortality in severe burns; methodological issues. *Burns*. 2018;44(3):728–729.
7. Niederbichler AD, Hoesel LM, Ipaktchi K, et al. Burn-induced heart failure: lipopolysaccharide binding protein improves burn and endotoxin-induced cardiac contractility deficits. *J Surg Res.* 2011;165(1):128–135.
8. Kirchhoff C, Habben I, Ivell R, Krull N. A major human epididymis-specific cDNA encodes a protein with sequence homology to extracellular proteinase inhibitors. *Biol Reprod.* 1991;45(2):350–357.
9. Kirchhoff C. Molecular characterization of epididymal proteins. *Rev Reprod.* 1998;3(2):86–95.
10. Hellström I, Raycraft J, Hayden-Ledbetter M, et al. The HE4 (WFDC2) protein is a biomarker for ovarian carcinoma. *Cancer Res.* 2003;63(13):3695–3700.
11. Plebani M; HE4 Study Group. HE4 in gynecological cancers: report of a European investigators and experts meeting. *Clin Chem Lab Med.* 2012;50(12):2127–2136.
12. Hertlein L, Stieber P, Kirschenhofer A, et al. Human epididymis protein 4 (HE4) in benign and malignant diseases. *Clin Chem Lab Med.* 2012;50(12):2181–2188.
13. Galgano MT, Hampton GM, Frierson HF Jr. Comprehensive analysis of HE4 expression in normal and malignant human tissues. *Mod Pathol.* 2006;19(6):847–853.

14. Bingle CD, Vyakarnam A. Novel innate immune functions of the whey acidic protein family. *Trends Immunol.* 2008;29(9):444–453.
15. Escudero JM, Auge JM, Filella X, Torne A, Pahisa J, Molina R. Comparison of serum human epididymis protein 4 with cancer antigen 125 as a tumor marker in patients with malignant and nonmalignant diseases. *Clin Chem.* 2011;57(11):1534–1544.
16. Drapkin R, von Horsten HH, Lin Y, et al. Human epididymis protein 4 (HE4) is a secreted glycoprotein that is overexpressed by serous and endometrioid ovarian carcinomas. *Cancer Res.* 2005;65(6):2162–2169.
17. Huang Y, Jiang H, Zhu L. Human epididymis protein 4 as an indicator of acute heart failure in patients with chronic kidney disease. *Lab Med.* 2020;51(2):169–175.
18. Piek A, Meijers WC, Schroten NF, Gansevoort RT, de Boer RA, Silljé HH. HE4 serum levels are associated with heart failure severity in patients with chronic heart failure. *J Card Fail.* 2017;23(1):12–19.
19. Jin Q, Tang Y, Liu Z, et al. Serum human epididymis protein 4 level as a predictor of clinical worsening in idiopathic pulmonary arterial hypertension: a pilot study. *BMC Cardiovasc Disord.* 2020;20(1):175.
20. Lin H, Xiao J, Su X, Song B. The association between serum human epididymis protein 4 level and cardiovascular events in patients with chronic obstructive pulmonary disease. *Lab Med.* 2021;52(3):260–266.
21. Rhodes A, Evans LE, Alhazzani W, et al. Surviving Sepsis campaign: International Guidelines for Management of Sepsis and Septic Shock: 2016. *Intensive Care Med.* 2017;43(3):304–377.
22. Levey AS, Stevens LA, Schmid CH, et al; CKD-EPI (Chronic Kidney Disease Epidemiology Collaboration). A new equation to estimate glomerular filtration rate. *Ann Intern Med.* 2009;150(9):604–612.
23. Paratz JD, Stockton K, Paratz ED, et al. Burn resuscitation–hourly urine output versus alternative endpoints: a systematic review. *Shock.* 2014;42(4):295–306.
24. Wolfe RR, Miller HI. Cardiovascular and metabolic responses during burn shock in the guinea pig. *Am J Physiol.* 1976;231(3):892–897.
25. Ganrot K, Jacobsson S, Rothman U. Transcapillary passage of plasma proteins in experimental burns. *Acta Physiol Scand.* 1974;91(4):497–501.
26. Williams FN, Herndon DN, Suman OE, et al. Changes in cardiac physiology after severe burn injury. *J Burn Care Res.* 2011;32(2):269–274.
27. Baxter CR, Cook WA, Shires GT. Serum myocardial depressant factor of burn shock. *Surg Forum.* 1966;17:1–2.
28. Abu-Sittah GS, Sarhane KA, Dibo SA, Ibrahim A. Cardiovascular dysfunction in burns: review of the literature. *Ann Burns Fire Disasters.* 2012;25(1):26–37.
29. Alexander W, Schneider HG, Smith C, Cleland H. The incidence and significance of raised troponin levels in acute burns. *J Burn Care Res.* 2018;39(5):729–735.
30. Maass DL, White J, Horton JW. IL-1β and IL-6 act synergistically with TNF-α to alter cardiac contractile function after burn trauma. *Shock.* 2002;18(4):360–366.
31. Bryant D, Becker L, Richardson J, et al. Cardiac failure in transgenic mice with myocardial expression of tumor necrosis factor-α. *Circulation.* 1998;97(14):1375–1381.
32. Pruitt BA Jr, Mason AD Jr, Moncrief JA. Hemodynamic changes in the early postburn patient: the influence of fluid administration and of a vasodilator (hydralazine). *J Trauma.* 1971;11(1):36–46.
33. Papp A, Uusaro A, Parviainen I, Hartikainen J, Ruokonen E. Myocardial function and haemodynamics in extensive burn trauma: evaluation by clinical signs, invasive monitoring, echocardiography and cytokine concentrations. A prospective clinical study. *Acta Anaesthesiol Scand.* 2003;47(10):1257–1263.
34. Yuan T, Li Y. Human epididymis protein 4 as a potential biomarker of chronic kidney disease in female patients with normal ovarian function. *Lab Med.* 2017;48(3):238–243.
35. Nagy B Jr, Krasznai ZT, Balla H, et al. Elevated human epididymis protein 4 concentrations in chronic kidney disease. *Ann Clin Biochem.* 2012;49(Pt 4):377–380.
36. Zhang M, Zhao B, Xie J, Liang Y, Yang Z. Serum human epididymis protein 4 is associated with renal function and diabetic kidney disease in patients with type 2 diabetes mellitus. *Biomed Res Int.* 2019;2019:4831459.

AQ26
AQ33
AQ36

CASE STUDY

Acute Promyelocytic Leukemia with a *BCR-ABL1* Rearrangement in a Minor Clone

Yonggeun Cho, MD, PhD,[1] Jungwon Hyun, MD,[2] Miyoung Kim, MD, PhD,[3,] Boram Han, MD,[4] Young Kyung Lee, MD, PhD[1]*

[1]Department of Laboratory Medicine, Hallym University Sacred Heart Hospital, Hallym University College of Medicine, Anyang, Republic of Korea, [2]Department of Laboratory Medicine, Dongtan Sacred Heart Hospital, Hallym University College of Medicine, Hwaseong, Republic of Korea, [3]Department of Laboratory Medicine, Asan Medical Center, University of Ulsan College of Medicine, Seoul, Republic of Korea, [4]Department of Internal Medicine, Hallym University Sacred Heart Hospital, Hallym University College of Medicine, Anyang, Republic of Korea; *To whom correspondence should be addressed. miyoungkim@amc.seoul.kr

Keywords: acute promyelocytic leukemia, *BCR-ABL1*, *PML-RARA*, concurrent, minor clone, treatment

Abbreviations: APL, acute promyelocytic leukemia; WBC, white blood cell; BM, bone marrow; PCR, polymerase chain reaction; FISH, fluorescence in situ hybridization; ATRA, all-trans retinoic acid; AML, acute myeloid leukemia; ALL, acute lymphoblastic leukemia; CML, chronic myeloid leukemia; TKI, tyrosine kinase inhibitor; SCT, stem cell transplantation.

Laboratory Medicine 2022;53:326–329; https://doi.org/10.1093/labmed/lmab097

ABSTRACT

Acute promyelocytic leukemia (APL) is a type of acute myeloid leukemia characterized by predominating abnormal promyelocytes with a *PML-RARA* rearrangement or a variant thereof. *BCR-ABL1* rearrangement is an oncogenic event that is usually associated with chronic myeloid leukemia but also occurs in both acute lymphoblastic and acute myeloid leukemias and in healthy individuals. However, APL with concurrent *PML-RARA* and *BCR-ABL1* rearrangements has rarely been reported. Herein, we describe a patient with APL exhibiting a *BCR-ABL1* rearrangement in a minor clone and discuss the importance of evaluating this genetic alteration in terms of pathogenesis and treatment.

Clinical History

A 49-year-old woman was referred to our hospital because of leukocytosis and disseminated intravascular coagulopathy. Her complete blood count on admission revealed a white blood cell (WBC) count of 6.48 × 10^9/L, hemoglobin of 6.9 g/dL, and platelet count of 27 × 10^9/L. Circulating blasts and abnormal promyelocytes (10% and 80% of WBCs, respectively) were observed on her peripheral blood smear. A coagulation test showed a prothrombin time-international normalized ratio of 1.79 (reference range: 0.88–1.13), D-dimer >20 μg/mL (reference range: <0.5 μg/mL), and fibrin degradation products >120 μg/mL (reference range: <5 μg/mL). Bone marrow (BM) examination showed hypercellular marrow with 10% blasts and 80% abnormal promyelocytes (**FIGURE 1A**); both were positive for myeloperoxidase, CD13, CD33, CD117, CD34, CD2, and CD56 but negative for human leukocyte antigen (HLA)-DR on flow cytometric analysis. Conventional karyotyping revealed 46,XX,der(6)t(6;8)(p23;q13),t(15;17)(q24;q21)[20] (**FIGURE 1B**).

Multiplex reverse-transcriptase polymerase chain reaction (PCR) for recurrent leukemic rearrangements performed using a HemaVision (DNA diagnostic A/S, Risskov, Denmark) showed the presence of concurrent *PML-RARA* and *BCR-ABL1* (b3a2 type) rearrangements in the BM; this finding was confirmed when using another specimen from the patient's BM. Quantitative reverse-transcriptase PCR of fusion genes performed using a Real-Q BCR-ABL Quantification kit (Biosewoom, Seoul, Republic of Korea) showed a *PML-RARA* fusion gene with a *PML-RARA/ABL1* ratio of 1.06 and a *BCR-ABL1* fusion gene with a *BCR-ABL1/ABL1* ratio of 0.0131 (**FIGURE 2A**). Sanger sequencing showed the fusion of *BCR* exon 14 to *ABL1* exon 2 (**FIGURE 2B**). Fluorescence in situ hybridization (FISH) using the Cytocell *BCR/ABL* (*ABL1*) Translocation, Dual Fusion (Oxford Gene Technology, Cambridge, UK) probe revealed that 5 of 500 interphase cells had a *BCR-ABL1* rearrangement of nuc ish (*ASS1* × 2, *ABL1* × 3, *BCR* × 3) (*ABL1* con *BCR* × 2) [5/500] (**FIGURE 1C**). Next-generation sequencing of 54 genes using an Illumina TruSight Myeloid Panel (Illumina, San Diego, CA) found no oncogenic mutations.

The patient was diagnosed with acute promyelocytic leukemia (APL) and treated using all-trans retinoic acid (ATRA) combined with idarubicin. She achieved complete hematologic remission 38 days after commencing induction treatment. Postinduction BM examination indicated a normal karyotype of 46,XX[20], a reduced *PML-RARA* load with a *PML-RARA/ABL1* ratio of 0.00322, and no detectable *BCR-ABL1*. After consolidation therapies, molecular remission of *PML-RARA* was also achieved. The patient has been tolerating maintenance therapy well to date (10 months since her initial diagnosis). Informed consent was not required owing to the patient's complete anonymity.

Discussion

Gene rearrangements are of pathogenic significance in hematologic malignancies; some (particularly *BCR/ABL1* and other recurrent genetic

FIGURE 1. Abnormal promyelocytes in a peripheral blood specimen and conventional karyotyping and interphase fluorescence in situ hybridization (FISH) of a bone marrow specimen from our patient obtained at initial diagnosis. A, Abnormal promyelocytes with folded nuclei and azurophilic granules visualized with Wright-Giemsa staining (×1000). B, Conventional karyotyping showing 46,XX,der(6)t(6;8)(p23;q13),t(15;17)(q24;q21)[20]. C, FISH with probes targeting *BCR* (green) and *ABL1* (red) loci showing 2 yellow fusion signals in 5 of 500 interphase cells.

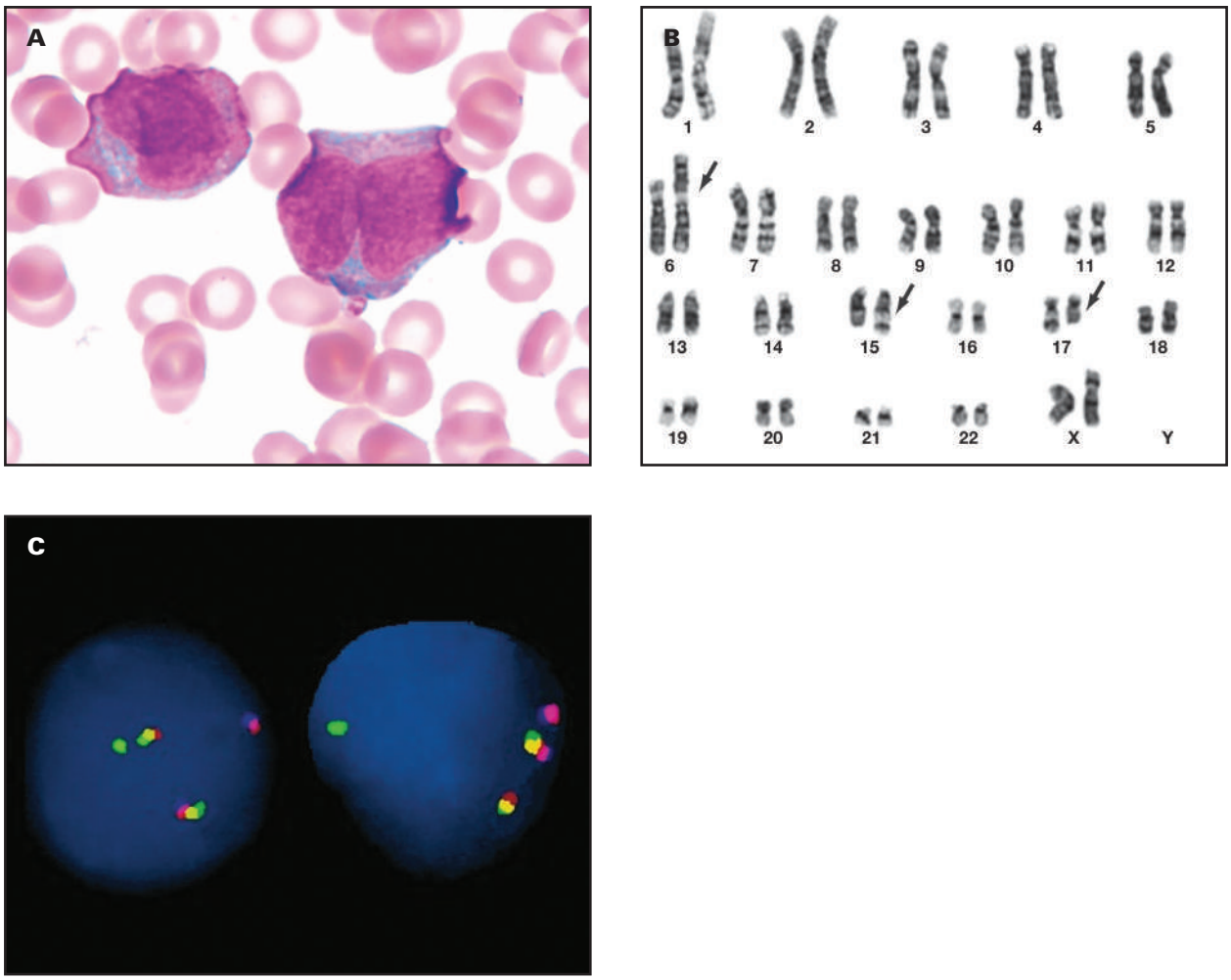

rearrangements in acute leukemias) tend to be mutually exclusive.[1,2] In a large study on concurrent pathogenic rearrangements by Chen et al,[2] 11 patients (0.15%) of 7495 with acute leukemia (including 4036 with acute myeloid leukemia [AML], 3367 with acute lymphoblastic leukemia [ALL], and 92 with mixed-phenotype acute leukemia) showed concurrent rearrangements. Among 731 patients with chronic myeloid leukemia (CML), 14 (1.92%) showed concurrent fusion genes including *CBFB/MYH11* and *RUNX1/RUNX1T1*.[2] Among the 11 patients with acute leukemia, only 2 with AML and 1 each with B-acute lymphoblastic leukemia (B-ALL) and T-acute lymphoblastic leukemia (T-ALL) had concurrent *BCR/ABL1* and other rearrangements. One of the patients with AML had *CBFB/MYH11* with no karyotype information provided, whereas the other had *DEK/NUP214* with both rearrangements present in the same major clone. The patients with B-ALL and T-ALL had *FUS/ERG* and *SIL/TAL1* rearrangements, respectively, even though neither alteration is subcategorized as a recurrent genetic change in acute leukemias per the World Health Organization classification.[1] The patient with AML who had concurrent *BCR/ABL1* and *DEK/NUP214* received chemotherapy and tyrosine kinase inhibitors (TKIs) and ultimately underwent allogeneic stem cell transplantation (SCT) and survived for 72 months. The authors concluded that the prognoses of patients with CML and acute leukemias with concurrent gene rearrangements are relatively poor and that SCT should therefore be performed as soon as possible.

Salem et al[3] reported 3 patients with AML and 7 with CML who had concurrent *BCR/ABL1* and *CBFB/MYH11* rearrangements. Among the 3 patients with AML, 1 had a *CBFB/MYH11* rearrangement in the major clone and a concurrent *BCR/ABL1* rearrangement in a subclone. The second patient with AML had a *CBFB/MYH11* rearrangement only at the time of initial diagnosis but acquired a *BCR/ABL1* rearrangement during treatment, and the third had both rearrangements in the same clone at the time of diagnosis. Most patients with CML acquired *CBFB/MYH11* rearrangements during blast crisis. All 3 patients with AML received TKIs along with chemotherapy, but their disease persisted or relapsed.

Dun et al[4] reported a patient with B-ALL with an *ETV6/RUNX1* rearrangement who acquired a *BCR/ABL1* rearrangement as a subclonal change during treatment. The patient received both chemotherapy and a TKI. Musani et al[5] reported a patient with concurrent *RUNX1/RUNX1T1*

FIGURE 2. The *BCR-ABL1* gene fusion in a bone marrow specimen from our patient. A, Amplification curve of the *BCR-ABL1* gene fusion transcript in a real-time quantitative polymerase chain reaction. B, Chromatogram of the Sanger sequencing for *BCR-ABL1* gene fusion, showing the fusion of *BCR* exon 14 to *ABL1* exon 2. RFU, relative fluorescence units.

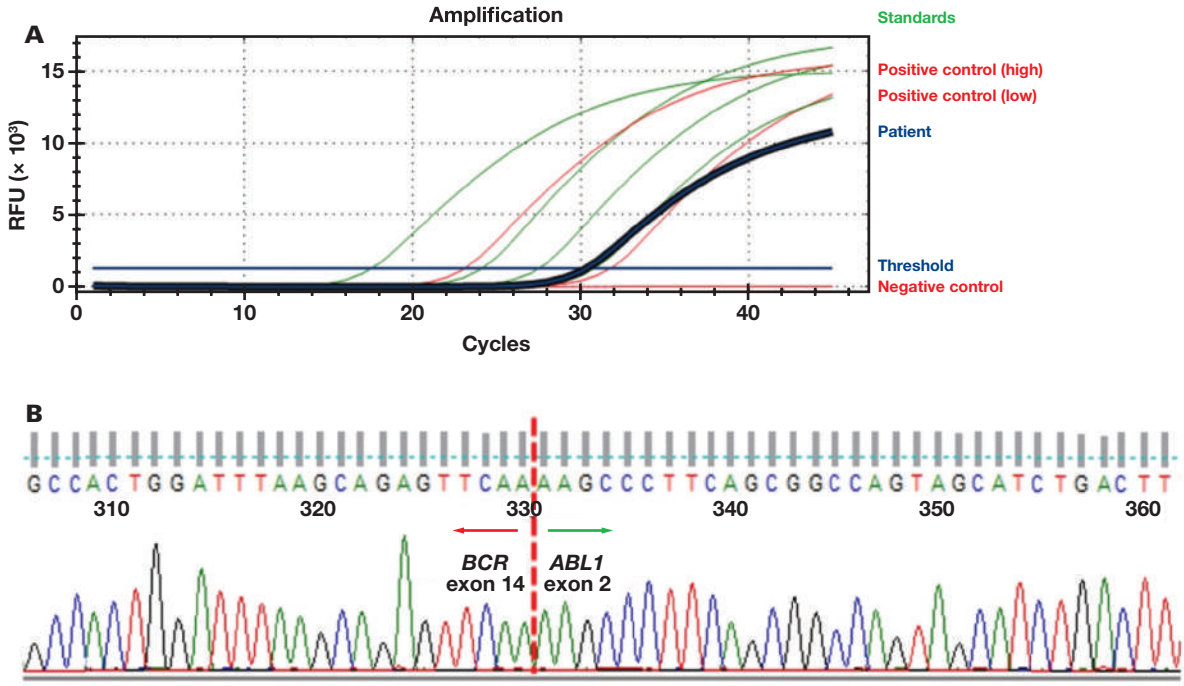

and *BCR/ABL1* rearrangements in the major clone who died within 1 month of the initial diagnosis. Behrens et al[6] reported a patient with concurrent *BCR/ABL1* and *GATA2/MECOM* rearrangements in whom it was unclear whether the underlying disease was CML in blast phase or de novo AML. The patient received both chemotherapy and a TKI and ultimately underwent allogeneic SCT that led to complete remission of the disease up to 21 months postdiagnosis.

To date, only 5 individuals with concurrent *BCR-ABL1* and *PML-RARA* rearrangements have been reported[7-11]; only 2 plus our patient had a *BCR-ABL1* rearrangement in a minor clone.[7,8] The patient in the Takahashi et al study[7] had a *BCR-ABL1* rearrangement in a minor clone independent of a major clone that exhibited a *PML-RARA* rearrangement as determined using conventional karyotyping, FISH, and PCR. An et al[8] detected a *BCR-ABL1* rearrangement in their patient only when using PCR; it was not detected by conventional karyotyping or FISH. Our patient's *BCR-ABL1* rearrangement was detected only by FISH and PCR but not by conventional karyotyping; this was similar to the An et al patient in that the clone size was too small to be detected by conventional karyotyping. Thus, it remains unknown whether the clone with the *BCR-ABL1* rearrangement existed independently of the major clone with the *PML-RARA* rearrangement or whether the clone with the *BCR-ABL1* rearrangement was part of the major clone with the *PML-RARA* rearrangement, as in the An et al patient.[8]

As for the other 3 reported co-occurrences of *BCR-ABL1* and *PML-RARA* rearrangements in the same leukemic clone, Mao et al[9] detected *BCR-ABL1* and *PML-RARA* rearrangements using a chromosome study and FISH, whereas Sun et al[10] and Zhang et al[11] detected such rearrangements using chromosome studies, FISH, and PCR. Although Mao et al[9] did not report their treatment regimen, Sun et al[10] treated their patients using ATRA and imatinib and Zhang et al[11] treated their patients using ATRA alone.

Our patient's presentation could be interpreted in 2 different ways: (1) her leukemic cells had both *BCR-ABL1* and *PML-RARA* rearrangements, although the *BCR-ABL1* rearrangements were in an independent minor clone or on top of the major clone with *PML-RARA* rearrangements; or (2) she had a *BCR-ABL1* rearrangement in a minor portion of her hematopoietic cells while she was healthy but acquired an additional *PML-RARA* rearrangement when she developed APL. These interpretations could also be applicable to the other 2 reported patients with *BCR-ABL1* rearrangements in a minor clone.[7,8] We favor the former assumption that the *BCR-ABL1* rearrangement was part of a leukemic process regardless of whether it existed independent of or together with the clone with the *PML-RARA* rearrangements. Indeed, concurrent *BCR-ABL1* and *PML-RARA* rearrangements are rarely reported, although it is already known that *BCR-ABL1* rearrangements exist in healthy individuals.[1] Given that the multiplex PCR approach is commonly used to screen for recurrent genetic abnormalities in patients with acute leukemias, it is less likely that the *BCR-ABL1* rearrangement was missed, even if it did exist. Additional, thorough investigations of the frequency and quantity of *BCR-ABL1* rearrangements in APL may clarify this issue.

Conclusion

The benefit of additional TKI therapy against AMLs with *BCR-ABL1* rearrangements other than those categorized as AML with a *BCR-ABL1* rearrangement, such as in our patient and 5 of the previously reported individuals, is not well established. Currently, the most reasonable approach would be to categorize patients with APL who are *BCR-ABL1*–positive based on the size of the *BCR-ABL1* clone to determine whether a TKI should be added to the standard APL treatment regimen. Among the 5 aforementioned patients (including ours) whose treatment regimens were reported,[7,8,10,11] only 1 received concurrent TKI therapy along with

ATRA-based APL treatment.[10] Almost all the patients achieved complete remission after induction therapy regardless of whether the ATRA-based APL regimen was combined with a TKI[7,10,11]; only 1 died of an infection after ATRA-based induction therapy.[8] The characterization of additional patients with APL who carry *BCR-ABL1* rearrangements ought to help establish a therapeutic guideline for individuals with this disease.

REFERENCES

1. Swerdlow SH, Campo E, Harris NL, et al. (eds). *WHO Classification of Tumours of Haematopoietic and Lymphoid Tissues.* Rev 4th ed. Lyon, France: IARC; 2017:30–36.
2. Chen X, Wang F, Wang T, et al. The incidence, genetic characteristics, and prognosis of leukemia with concurrent pathogenic fusion genes: a series of 25 cases from a large cohort of leukemia patients. *Cancer Gene Ther.* 2020;27(1–2):89–97.
3. Salem A, Loghavi S, Tang G, et al. Myeloid neoplasms with concurrent BCR-ABL1 and CBFB rearrangements: a series of 10 cases of a clinically aggressive neoplasm. *Am J Hematol.* 2017;92(6):520–528.
4. Dun KA, Vanhaeften R, Batt TJ, Riley LA, Diano G, Williamson J. BCR-ABL1 gene rearrangement as a subclonal change in ETV6-RUNX1-positive B-cell acute lymphoblastic leukemia. *Blood Adv.* 2016;1(2):132–138.
5. Musani R, Chang H. Coexistence of BCR-ABL1 and RUNX1-RUNX1T1 in a de novo AML. *Blood.* 2021;137(20):2853.
6. Behrens YL, Schienke A, Davenport C, et al. BCR-ABL1 positive AML or CML in blast crisis? A pediatric case report with inv(3) and t(9;22) in the initial clone. *Cancer Genet.* 2021;254–255:70–74.
7. Takahashi H, Sakai R, Hattori Y, et al. Biclonal co-existence of t(15;17) and t(9;22) chromosomal abnormalities in acute promyelocytic leukemia [in Japanese]. *Rinsho Ketsueki.* 2011;52(1):37–40.
8. An GD, Lim HH, Woo KS, et al. A case of acute promyelocytic leukemia with co-existence of BCR-ABL1 and PML-RARA rearrangements detected by PCR. *Lab Med Online.* 2017;7:196–200.
9. Mao L, Wang H, Cheng Y, Wang Y, Chen Z, Jie J. Occurrence of t(15;17)(q22;q21) and t(9;22)(q34;q11) in a patient with acute promyelocytic leukemia. *Leuk Lymphoma.* 2009;50(3):466–470.
10. Sun X, He Y, Mao C, Zhu L, Qin X, Huang S. BCR/ABL fusion gene detected in acute promyelocytic leukemia: a case study of clinical and laboratory results. *Leuk Lymphoma.* 2014;55(2):435–438.
11. Zhang LJ, Gan YM, Yu L. Occurrence of BCR/ABL fusion gene in a patient with acute promyelocytic leukemia. *Med Oncol.* 2015;32(1):382.

CASE STUDY

Urine Organic Acid Analysis: Key Diagnostic Test for Fumaric Aciduria in a Sri Lankan Child

Eresha Jasinge, MD,[1,] Mihika Fernando, MD,[1] Neluwa-Liyanage R. Indika, MBBS,[2] Roberta Trunzo, PhD,[3] Sabine Schröder, PhD,[3] Dinesha Maduri Vidanapathirana, MD,[4] Patricia M. Jones, PhD,[5] Subashini Jayasena, MBBS,[1] Anusha Varuni Gunarathne, BMLS,[1] Pyara Ratnayake, MD[6]*

[1]Department of Chemical Pathology, Lady Ridgeway Hospital for Children, Colombo, Sri Lanka; [2]Department of Biochemistry, Faculty of Medical Sciences, University of Sri Jayewardenepura, Nugegoda, Sri Lanka; [3]CENTOGENE AG, Rostock, Germany; [4]Department of Pathology, Faculty of Medical Sciences, University of Sri Jayewardenepura, Nugegoda, Sri Lanka; [5]Department of Pathology, University of Texas Southwestern Medical Center and Children's Medical Center, Dallas, Texas, US; [6]Neurology Unit, Lady Ridgeway Hospital for Children, Colombo, Sri Lanka; *To whom correspondence should be addressed. eresha.jasinge@gmail.com

Keywords: fumaric aciduria, fumarate hydratase deficiency, neutropenia, tricarboxylic acid cycle, urine organic acids, encephalopathy

Abbreviations: CSF, cerebrospinal fluid; FH, fumarate hydratase.

Laboratory Medicine 2022;53:e48–e50; https://doi.org/10.1093/labmed/lmab083

ABSTRACT

Fumaric aciduria resulting from fumarate hydratase deficiency is a rare inherited disorder of the Krebs tricarboxylic acid cycle that is characterized by neurologic manifestations, a spectrum of brain abnormalities, and the excretion of fumaric acid in urine. We describe a 3 year old Sri Lankan boy who was referred at age 10 months with poor weight gain and hypotonia for further laboratory investigations. In addition to global developmental delay, there were noticeable dysmorphic features with a prominent forehead, low-set ears, micrognathia, and hypertelorism with persistent neutropenia. Urine organic acid assay revealed a massive elevation of fumaric acid on 2 occasions. Molecular analysis revealed a homozygous likely pathogenic missense variant, NM000143.3:c.1048C>T p. (Arg350Trp), in the *FH* gene, confirming the biochemical diagnosis. Our patient was the first patient in Sri Lanka molecularly diagnosed with fumaric aciduria. This case study highlights the importance of performing organic acid assays in children presenting with neurologic manifestations especially when these are suspected to have a metabolic basis.

Clinical History

A 10 month old baby boy was referred to the department of chemical pathology at Lady Ridgeway Hospital for Children (Colombo, Sri Lanka) for further investigation for a regressive disorder. He is the second child of nonrelated Sri Lankan parents, born at term after an uneventful antenatal period. His birth weight was 4.2 kg (97th centile), his length was 52 cm (85th–97th centile), and his head circumference was 36 cm (85th centile). Neither leiomyomatosis nor renal cancers were known in the family. His 7-year-old older sibling remained unaffected and appeared healthy.

By age 6 months, the patient had poor weight gain (weight 6.8 kg [< 15th centile]), his length was 69 cm (50th–85th centile), and he had an acquired microcephaly (head circumference 42 cm; 15th centile). These characteristics were accompanied by prominent hypotonia and developmental delay with poor head control and failure to reach out for objects but with a preserved social smile. The patient was also found to have significant swallowing problems. There were noticeable dysmorphic features with a prominent forehead, low-set ears, micrognathia, and hypertelorism. He presented with further regression of motor milestones with drowsiness during a febrile illness at age 10 months.

Laboratory Information

The patient's plasma lactate level was 2.88 mmol/L (0.5–2.30) while the cerebrospinal fluid (CSF) lactate level was 3.8 mmol/L (1.11–2.44). Repeat analysis 2 weeks later showed elevation in both plasma and CSF lactate (3.26 and 4.72 mmol/L, respectively). Hematologic parameters showed persistent neutropenia ranging from 0.3 to 1.8 × 10^3 µL (6.4%–26.7 % of total white blood cell count) on several occasions. The rest of his biochemical testing, including liver and renal functions, was normal.

The magnetic resonance imaging of the brain, performed at age 11 months, showed mild atrophy of the bifrontal lobes and hypoplasia of the corpus callosum. Renal ultrasound imaging in the parents and siblings was normal.

Qualitative analysis of organic acids in urine by gas chromatography-mass spectrometry (Agilent) revealed a massive excretion of fumaric acid and moderate amounts of succinic acid (**FIGURE 1**). Repeat analysis 2 weeks later showed the same result, indicating a biochemical diagnosis of fumaric aciduria. Plasma amino acids were normal.

Given the strong biochemical suspicion of fumaric aciduria, genetic analysis of the *FH* gene was requested at CENTOGENE AG. Bidirectional Sanger sequencing of the entire coding region and the highly conserved exon-intron splice junctions was performed. A homozygous missense variant, NM000143.3:c.1048C>T p.(Arg350Trp), was detected. The variant is extremely rare and has been reported in 4 het-

FIGURE 1. Gas chromatography-mass spectrometry total ion chromatogram of urine organic acids showing massive excretion of fumaric acid and moderate amounts of succinic acid. Letters indicate the following metabolites, and the respective retention time (minutes) is given in parentheses. A, lactic acid (7.635); B, 2-hydroxyisobutyric acid (7.730); C, 4-cresol (10.446); D, 3-hydroxyisobutyric acid (11.062); E, methylmalonic acid (13.036); F, urea (14.122); G, ethylmalonic acid (15.374); H, succinic acid (16.510); I, fumaric acid (17.664); J, 4-deoxytetronic acid (18.219); K, internal standard (20.644); L, 3-methylglutaconic acid (20.849); M, citramalic acid (22.101); N, adipic acid (23.038); O, 3-methyladipic acid (24.085); P, 3-hydroxyphenylacetic acid (26.709); Q, 4-hydroxyphenylacetic acid (27.854); R, suberic acid (30.231); S, homovanillic acid (33.186); X, unknown.

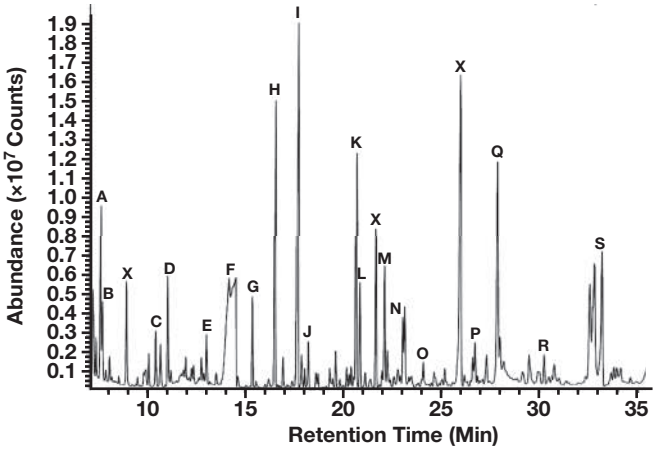

erozygous adult individuals (out of 251.258 alleles) in gnomAD (accession date February 14, 2020). In silico tools have predicted that this amino acid substitution is likely damaging to the protein structure/function. Other variants located in the same region have been reported as being causative for fumarate deficiency (p.GLy346Asp) and multiple leiomyomatosis (p.Glu355Lys). The variant detected in our patient, NM000143.3:c.1048C>T p.(Arg350Trp), has been classified as likely pathogenic based on the American College of Medical Genetics and Genomic guidelines. The following criteria for variant classification were applied: PS3 (well-established in vitro studies), PM2 (absent or very rare in control patients, ie, gnomAD), and PP3 (multiple lines of computational evidence support a deleterious effect on the gene).

Patient Follow-Up

Supportive management for the patient was instituted together with dietary modification in the form of a high-fat/low-carbohydrate diet at approximately age 11 months. With the initiation of the diet, the parents reported an improvement in well-being although his developmental delay was persistent.

At age 2 years, the patient was unable to sit unsupported, speech was limited to babbling, but hearing and vision appeared normal. He continued to have feeding difficulties. Dystonia and further regression of feeding and motor abilities occurred subsequent to a diarrheal illness.

By age 3 years, the patient continued to exhibit slow developmental gains and was able to reach and mouth objects and say 2 clear meaningful words. Some improvement was noted in the gross motor aspect, with better head control and ability to turn to one side. He had reliable response to visual and auditory stimuli and was able to respond to the environment with his limited expressive abilities; for instance, he was able to help with dressing by raising his arms. No seizures were reported. His respiratory, cardiovascular, and abdominal examinations remained unremarkable.

Discussion

Fumaric aciduria, a rare autosomal recessive disorder of the Krebs cycle, is caused by a deficiency of fumarate hydratase (FH), also known as fumarase (EC 4.2.1.2). Fumaric aciduria was first described by Whelan et al in 1983 in 2 adult siblings with speech impairment and intellectual disability.[1] Three years later, Zinn et al discovered the enzyme defect in a patient with early-onset severe encephalopathy.[2] The first molecular characterization of the *FH* gene was by Bourgeron et al in 1994.[3] In 2002, the Multiple Leiomyoma Consortium identified the *FH* gene as the tumor suppressor gene responsible for multiple cutaneous and uterine leiomyomatosis/hereditary leiomyomatosis with renal cell cancer.[4] Therefore, pathogenic variants in the *FH* gene are causative of fumaric aciduria (autosomal recessive, OMIM 606812) and leiomyomatosis and renal cell cancer (autosomal dominant, OMIM 150800).

Fumaric aciduria resulting from a deficiency of FH is characterized by developmental delay, encephalopathy, seizures, facial dysmorphism, and a spectrum of brain abnormalities.[5] The finding of very high fumaric acid in urine organic acid analysis is strongly suggestive of FH deficiency. The diagnosis is confirmed by identification of deficient FH activity and/or by molecular genetic testing of the *FH* gene.[4,6]

Our patient presented with typical clinical features of fumarase deficiency such as poor weight gain, developmental delay, hypotonia, and dysmorphic facial features described in the literature[7] at age 6 months. His presentation with severe encephalopathy in late infancy is another characteristic feature.

Neutropenia and high plasma lactate seen in our patient have also been noted in patients with FH deficiency.[6] In addition to high plasma lactate, our patient also had high CSF lactate.

Elevated fumaric acid is easily detected by analysis of urine using gas chromatography-mass spectrometry. In 1 study, the clinical and biochemical data of 36 patients showed that a massive excretion of fumaric acid in urine was common to all patients with an elevation of 15- to 1000-fold when compared to the normal range.[6] In our patient, massive amounts of fumaric acid were detected in urine twice. The peak abundance of fumaric acid was almost 1.5 times that of the internal standard. In addition to fumaric acid, succinic acid and α-ketoglutaric acids are the most relevant organic acids in urine that have been described.[6] Our patient also excreted moderate amounts of succinic acid on both occasions. **FIGURE 2** illustrates the metabolic effects of FH deficiency.

Radiologic findings of hypoplasia of the corpus callosum, cerebral atrophy, and ventriculomegaly as seen in our patient have been previously reported.[6-8]

The clinical management of fumaric aciduria is based on symptoms because there is no recommended disease-modifying treatment. Our patient was put on a high-fat/low-carbohydrate diet for 6 months based on a publication reporting clinical improvement and possible disease-modifying effects resulting from this diet[9] and showed stabilization and minimal improvement after adoption of the diet.

Conclusion

In summary, we describe a Sri Lankan child with hypotonic encephalopathy with molecularly diagnosed fumaric aciduria . Massive amounts of fumaric acid in urine oriented the clinical and molecular diagnosis. This

FIGURE 2. **Schematic representation of the consequences of FH deficiency, discussed in this case study. Solid arrows indicate direct conversion whereas dotted arrows indicate a general pathway. Downward blue arrows indicate decreased level/concentration whereas upward red arrows indicate increased levels. ADP, adenosine diphosphate; ATP, adenosine triphosphate; Co A, co-enzyme A; FH, fumarate hydratase.**

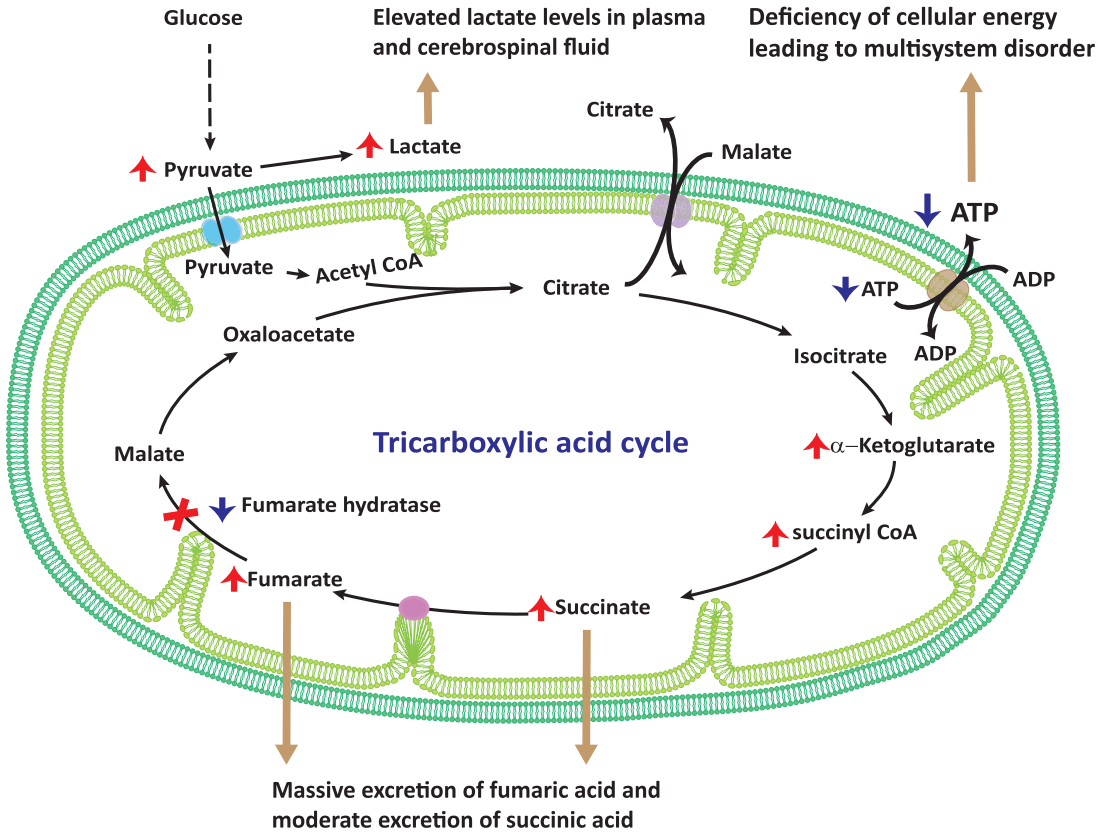

case study highlights the importance of performing organic acid assays in children presenting with neurologic manifestations, especially when these are suspected to have a metabolic basis.

Acknowledgments

The authors thank the parents of the patient for giving consent to publish the details regarding their child. We acknowledge Dr. Apsara Epa, consultant radiologist of Teaching Hospital Colombo South, Sri Lanka, for performing an ultrasound scan of the abdomen on all family members. In addition, the authors thank Ms. W.A. Irosha for providing the image file of the total ion chromatogram. Roberta Trunzo and Sabine Schröder are former or current employees of CENTOGENE GmbH (Rostock, Germany).

An ethics approval is not applicable because this is a case report written retrospectively regarding a patient investigated for the purposes of diagnosis. Informed written consent for genetic testing and for the publication of this case study was obtained from the patient's parents.

The first draft of the manuscript was written by Eresha Jasinge, graphical illustrations were created by Neluwa-Liyanage R. Indika, and all the authors revised the previous versions of the manuscript critically for important intellectual content. All authors read and approved the final manuscript.

Conflict of interest

Roberta Trunzo and Sabine Schröder are former or current employees of CENTOGENE GmbH (Rostock, Germany). All other authors have no conflicts of interest to declare that are relevant to the content of this article.

REFERENCES

1. Whelan DT, Hill RE, McClorry S. Fumaric aciduria: a new organic aciduria, associated with mental retardation and speech impairment. *Clin Chim Acta.* 1983;132(3):301–308.
2. Zinn AB, Kerr DS, Hoppel CL. Fumarase deficiency: a new cause of mitochondrial encephalomyopathy. *N Engl J Med.* 1986;315(8):469–475.
3. Bourgeron T, Chretien D, Poggi-Bach J, et al. Mutation of the fumarase gene in two siblings with progressive encephalopathy and fumarase deficiency. *J Clin Invest.* 1994;93(6):2514–2518.
4. Tomlinson IPM, Alam NA, Rowan AJ, et al. Germline mutations in FH predispose to dominantly inherited uterine fibroids, skin leiomyomata and papillary renal cell cancer. *Nat Genet.* 2002; 30(4):406–410.
5. Morava E, Carrozzo R. Disorders of the Krebs cycle. In: Blau N, Duran M, Gibson KM,Dionisi-Vici (eds). *Physician's Guide to the Diagnosis, Treatment and Follow-Up of Inherited Metabolic Diseases*. Berlin, Germany: Springer-Verlag; 2014: 313–322.
6. Allegri G, Fernandes MJ, Scalco FB et al. Fumaric aciduria: an overview and the first Brazilian case report. *J Inherit Metab Dis.* 2010;33(4):411–419.
7. Kerrigan JF, Aleck KA, Tarby TJ, Bird CR, Heidenreich RA. Fumaric aciduria: clinical and imaging features. *Ann Neurol.* 2000;47(5):583–588.
8. Maradin M, Fumić K, Hansikova H, et al. Fumaric aciduria: mild phenotype in a 8-year-old girl with novel mutations. *J Inherit Metab Dis.* 2006;29(5):683.
9. Ryder B, Moore F, Mitchell A, Thompson S, Christodoulou J, Balasubramaniam S. Fumarase deficiency: a safe and potentially disease modifying effect of high fat/low carbohydrate diet. *JIMD Rep.* 2018;40:77–83.

A Scoping Review of Medical Laboratory Science and Simulation: Promoting a Path Forward with Best Practices

Tera L. Webb, MS, MLS(ASCP)CM, CPHQ,[1,] Jarkeshia McGahee, MS, CT(ASCP)CM,[2] Michelle R. Brown, PhD, MS, MLS(ASCP)CMSBBCM, CHSE[2,3]*

[1]Department of Clinical and Diagnostic Sciences, School of Health Professions, University of Alabama at Birmingham, Birmingham, Alabama, USA; [2]Department of Health Services Administration, School of Health Professions, University of Alabama at Birmingham, Birmingham, Alabama, USA; [3]Office of Interprofessional Simulation for Innovative Clinical Practice, University of Alabama at Birmingham, Birmingham, Alabama, USA; *To whom correspondence should be addressed. teralw@uab.edu

Keywords: simulation, interprofessional, teamwork, communication, medical laboratory science, collaboration

Abbreviations: MLS, medical laboratory science; SoBP, Standard of Best Practice; INACSL, International Nursing Association for Clinical Simulation and Learning.

Laboratory Medicine 2022;53:e51–e58; https://doi.org/10.1093/labmed/lmab087

ABSTRACT

Objective: In medical laboratory science, there is a need to enhance the clinical learning curriculum beyond laboratory skill and diagnostic interpretation competency. Incorporating simulation presents an opportunity to train and produce medical laboratory scientists with the skills to communicate and work effectively in an interprofessional healthcare team.

Methods: A scoping review was performed to (i) understand the landscape of research literature on medical laboratory science and simulation and (ii) provide a path for future research directions. The International Nursing Association for Clinical Simulation and Learning Standards of Best Practice: Simulation were used as a guiding framework for literature that described simulation activities.

Results: Out of 439 articles from multiple databases, 32 were eligible for inclusion into this review. Of the 14 articles that described a simulation activity, only 3 described or partially described each component of the best practice criteria for simulation. Articles that did not describe the design and implementation of simulation (n = 18) consisted of 7 opinion-based papers, 4 narrative reviews, 5 case reports, and 2 empirical papers.

Conclusion: Despite increases in medical laboratory science with simulation, there is a need for more detailed empirical studies, more studies with an interprofessional context, and more methodological rigor.

Simulation has established itself as an effective teaching methodology in aviation, the military, and healthcare.[1,2] Likewise, simulation has grown rapidly as an evidence-based methodology in health professions education.[3,4] Within health professions education, the benefits of simulation include increased confidence, improved teamwork and communication, and increased patient safety.[5] This evidence has driven some professions to incorporate simulation into their curricula and accreditation requirements.[6] Teamwork in the care of patients is dynamic, with changes in personnel, discordant mental models, lack of shared vocabulary, and competing priorities.[7] In medical laboratory science (MLS), there is an appropriate emphasis on laboratory skills and diagnostic interpretation; however, this must be balanced with teaching communication and teamwork.[8] Clinical laboratories and MLS programs should have a commitment to the growth and development of a comprehensive laboratory profession.

As faculty look at opportunities to apply knowledge, skills, and abilities, simulation is one option that provides a space for learners to practice without risk to patients. Simulation can serve as a bridge between classroom learning or continuing education and application in clinical practice. In simulation, true-to-life situations can be used to practice new skills and apply new knowledge. To take this a step further, it is vital that laboratory students and personnel practice communication and teamwork skills with professions outside the laboratory. Recent publications have shared individual experiences with the laboratory and simulation; however, there remains a need to assess the landscape of simulation and MLS.

A synthesis of the literature does not exist. The purpose of this study is to (i) conduct a scoping review of the literature on MLS and simulation and (ii) identify manuscripts that describe the design and implementation of simulation and assess the use of evidence-based practices.

For this review, we define simulation as an opportunity for a person or people to experience a representation of a real event for the purpose of practicing, learning, evaluating, testing, or gaining understanding of procedures, systems, and/or human interaction.[9] In addition, we want to distinguish interprofessional simulation as that in which learners from 2 or more professions learn about, from, and with each other to enable effective collaboration.[10]

The Standards of Best Practice: Simulation (SoBP)[11] were used as a guiding framework for the analysis of review findings. The SoBP were

developed in 2011 by members of the International Nursing Association for Clinical Simulation and Learning (INACSL) and evolved from an initial 7 standards to 9 standards in 2015. The SoBP unite the field of simulation and share best practices in the design, implementation, and evaluation of simulation activities. With the 2015 revisions and additions, INACSL adopted a strong interprofessional approach to the SoBP, allowing them to serve as a foundation for simulations involving a broad spectrum of disciplines and professions in academic and practice settings. There is a standard for each aspect of simulation (**TABLE 1**). For the current analysis, all standards associated with the design, implementation, and evaluation of simulation were used to analyze the simulations identified through the review of the literature; however, professional integrity and operations are not readily assessable in a manuscript and were therefore not included in the evaluation.

Methods

This paper utilized a scoping review methodology to gather and examine the nature of the research centered around MLS and simulation. Scoping review methodology is considered the best method for exploring and mapping the boundaries of research.[12] The systematic approach for this scoping review was performed by applying the framework of Arksey and O'Malley.[13] The methods employed involved 5 steps of the framework: identifying the research question, identifying the relevant studies, selecting the studies, charting the data, and collating the results.

Identifying the Research Question

The research questions identified are as follows:

- What is known about simulation in MLS?
- What are the gaps and future directions for research with simulation and MLS?

Identifying Relevant Studies

In consultation with a health professions librarian, the research team developed a search strategy. An initial electronic database search was conducted in January 2020 and included the CINAHL, Embase, PubMed, and Scopus databases. The terms for the search strategy included *medical laboratory science, clinical laboratory science and simulation, clinical laboratory practice and simulation, medical laboratory personnel and simulation, medical laboratory technician and simulation,* and other strategies that can be observed in the Appendix Section. The search was limited to the English language and peer-reviewed articles that were published between 2000 and 2020.

Studies that were included met the following criteria: peer-reviewed, healthcare education, clinical laboratory science, medical laboratory science, simulation, and studies that were empirical, case studies, narrative reviews, and opinion pieces. Articles were excluded if they were not related to healthcare simulation or medical laboratory science, mentioned MLS or procedures, but lacked simulation.

Selection of Studies

Two researchers independently performed level 1 (titles and abstract) screening, then level 2 (full-text article) screening using Covidence, which detailed the inclusion criteria and exclusion criteria, allowed each reviewer to record his or her decisions, and blinded the results. A third reviewer was available to resolve any discrepancies.

Charting the Data and Collating Results

Qualtrics was used to extract study characteristics from 32 articles that were included in this scoping review. Each author completed a survey that included the journal name, title of article, article first author, publication date, data extractor's name, and the following questions: What country is this article from? Does this paper describe an interprofessional simulation? What health professions programs are included? What laboratory disciplines were involved? Where did this simulation take place? and What level of evidence is presented in the article?. After completion of the survey for each article, all data were exported to an Excel spreadsheet where authors addressed and resolved any discrepancies.

A second spreadsheet was used to collect INACSL SoBP criteria for each article that described a simulation activity. Items analyzed in each of these articles were outcomes and objectives, facilitation, debriefing, participant evaluation, simulation-enhanced interprofessional education, and simulation design.

Descriptive statistics were calculated to summarize article and study characteristics. Pivot charts in Excel were used to report frequencies and percentages to describe nominal data.

Results

Search Findings

The search of the literature yielded 439 articles across databases. After we excluded 18 duplicates, there were 421 articles remaining. The abstracts of these articles were reviewed, and 349 articles were excluded through this screening. A full-text review was performed on the remaining 72 articles. After full-text review, 40 articles were excluded for the

TABLE 1. Healthcare Simulation Standards of Best Practice

	Standard Description
Simulation Design	Simulation-based experiences are purposefully designed to meet identified objectives and optimize achievement of expected outcomes.
Outcomes and Objectives	All simulation-based experiences begin with the development of measurable objectives designed to achieve expected outcomes.
Facilitation	Facilitation methods are varied and use of a specific method is dependent on the learning needs of the participants and the expected outcomes. A facilitator assumes responsibility and oversight for managing the entire simulation-based experience.
Debriefing	All simulation-based experiences include a planned debriefing session aimed at improving future performance.
Participant Evaluation	All simulation-based experiences require participant evaluation.
Simulation-Enhanced IPE	Simulation-enhanced IPE enables participants from different professions to engage in a simulation-based experience to achieve shared or linked objectives and outcomes.
Professional Integrity	Professional integrity is demonstrated and upheld by all involved in simulation-based experiences.
Operations	All simulation-based education programs require systems and infrastructure to support and maintain operations.

INACSL, International Nursing Association for Clinical Simulation and Learning; IPE, interprofessional education; SoBP, Standard of Best Practice.

following reasons: non-full-text article (abstract only/poster), publication year outside of inclusion criteria, duplicates, newsletter/news article/book, wrong setting/student population, or not in English. Therefore, after screening abstracts and full-text articles, we found that 32 articles met all requirements for inclusion into this review (**FIGURE 1**).

Article and Study Characteristics

Thirty-two articles published between 2006 and 2020 were included in the final synthesis (**TABLE 2**). Of these, 15 were from Canada, 15 were from the United States, 1 was from Denmark, and 1 was from Norway. The majority of the studies were published in the *Canadian Journal of Medical Laboratory Science* (n = 13) and *Clinical Laboratory Science* (n = 12). There were 2 MLS scholars driving research dissemination with MLS and simulation: Brown (5 articles) and Van Der Like (3 articles). With regard to level of evidence, 7 papers were opinion-based or editorial, 4 were narrative, 8 were case reports, and 13 were empirical studies. Fourteen of the articles were within the context of uniprofessional simulations (pertaining to MLS students only), 13 articles were interprofessional in nature, and 1 was multiprofessional.

Articles Describing a Simulation Activity

Fourteen articles were based on the execution of a simulation activity. Laboratory disciplines represented in the simulations were blood bank, microbiology, histology, phlebotomy, chemistry, hematology, laboratory information systems, molecular diagnostics, coagulation, and urinalysis. The locations for these simulations varied. Three simulations occurred in a dedicated simulation center, 2 were in an MLS student laboratory, 5 took place in a simulation center and an MLS student laboratory simultaneously, and 4 were online and/or computer-based. Beyond the logistics, the design and implementation of the simulation activity within each article wwereas evaluated for their use of evidence-based standards using the SoBP as a framework (**TABLE 3**).

Outcomes and Objectives

Of the 14 studies, 5 specified that they determined expected outcomes for the simulation and included measurable objectives based on the expected outcomes. Three partially described the criteria necessary to meet this standard, and 6 did not describe outcomes and objectives.

FIGURE 1. Flow diagram of search strategy.

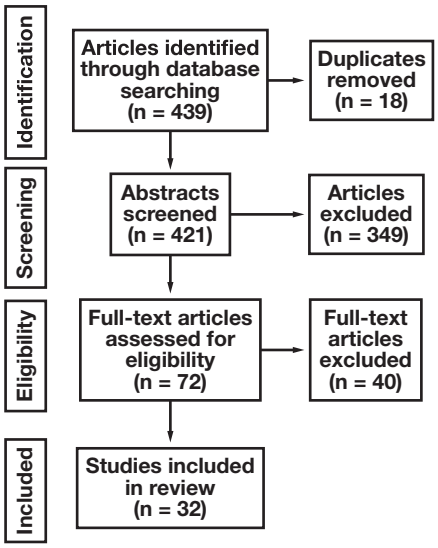

Facilitation

Three of the 14 studies fully met the criteria for the facilitation standard by describing the facilitator's knowledge and skills in simulation pedagogy, tailoring the approach to the competency level of the learners, briefing the learners adequately, cuing during the simulation to assist in achieving outcomes, and supporting participants after the simulation. Ten partially described these criteria, and 1 did not describe the facilitation of the simulation.

Debriefing

Only 2 of the 14 interprofessional articles fully met the criteria for the debriefing standard through detailing the competency of the debriefer, describing the physical environment, providing opportunity for reflection, allowing time for effective debriefing, and grounding the debriefing in a framework that explored the objectives of the simulation. Four studies partially described the criteria necessary to meet this standard and 8 did not describe debriefing.

Participant Evaluation

Twelve of the 14 articles determined evaluation methods before the simulation and described them as either formative, summative, or high-stakes evaluation. Two articles did not describe participant evaluation.

Simulation-Enhanced Interprofessional Education

The interprofessional simulations included students in a range of fields from nursing and medicine to a variety of health professions (respiratory therapy, pharmacy, health administration, physician assistant, physical therapy, and nuclear medicine). Two articles fully described using a theoretical framework, incorporating best practices (eg, mutual goals, authentic reality-based activities), overcoming barriers, and devising an evaluation plan for elevating simulation toward an interprofessional initiative. Seven articles partially described interprofessional education criteria, and 2 of the articles were based on uniprofessional simulation and could not be evaluated for this standard.

Simulation Design

Only 1 of the 14 articles was comprehensive in describing the design of the simulation, including needs assessment—creating SMART objectives, aligning theory purpose, and modality (ie, mannequin-based, virtual reality); providing context for the experience with a scenario, including the appropriate level of realism; maintaining a learner-centered approach; prebriefing; debriefing; evaluating the simulation experience; providing prelearning materials; and piloting the simulation before deployment with learners. Eleven articles partially described these criteria and 2 did not describe the design of the simulation.

Articles Not Describing a Simulation Activity

Articles that did not describe the design and implementation of simulation (n = 18) consisted of 7 opinion-based papers, 4 narrative reviews, 5 case reports, and 2 empirical papers. Themes for the opinion papers were using simulation to address challenges in clinical placement, increasing the quality of graduates, and utilizing simulation to bridge didactic and clinical practice. One opinion piece emphasized that there remains a need to assess the utility of simulation in MLS curricula. The narrative reviews focused on increasing the quality of graduates using simulation; describing the advantages and challenges associated with simulation in MLS; providing MLS programs with fundamental

TABLE 2. Articles Included in Final Synthesis

Journal Name	Title of Article	First Author	Year	Country	Participants	Level of Evidence
Canadian Journal of Medical Laboratory Science	Student Perspective on Uniting Simulation Education	Alano[17]	2019	Canada	Laboratory only	Opinion
Nordic Journal of Nursing Research	Health and Social Care Students Pursuing Different Studies, and Their Written Assignments From Workshop and Online Interprofessional Education	Almås[18]	2016	Norway	Interprofessional	Empirical study
Clinical Laboratory Science	A Study of Interprofessional Collaboration in Undergraduate Medical Laboratory Science and Nursing Education	Beard[19]	2015	US	Interprofessional	Empirical study
Clinical Laboratory Science	Introducing Interprofessional Education to BSN and CLS Students Using a Simulated Healthcare Setting	Behan[20]	2017	US	Interprofessional	Case report
Clinical Laboratory Science	Pride and Prejudice and Learning: An Interprofessional Experience with CLS and Nursing Students	Behan[21]	2017	US	Interprofessional	Empirical study
Clinical Laboratory Science	Primer on Interprofessional Simulation for Clinical Laboratory Science Programs: A Practical Guide to Structure and Terminology	Brown[22]	2016	US	Interprofessional	Opinion
Clinical Laboratory Science	Strengthening the Clinical Laboratory with Simulation-Enhanced Interprofessional Education	Brown[8]	2016	US	Interprofessional	Opinion
Clinical Laboratory Science	Incorporating Clinical Laboratory Science Students into Interprofessional Simulation	Brown[23]	2016	US	Interprofessional	Case report
Clinical Laboratory Science	Small Scale, Low Resource Options for Introducing Clinical Laboratory Science Students to Interprofessional Simulation	Brown[24]	2016	US	Interprofessional	Case report
Clinical Laboratory Science	Promoting Patient Safety Through Interprofessional Education Simulation	Cavnar[25]	2017	US	Interprofessional	Empirical study
Canadian Journal of Medical Laboratory Science	Simulations in Medical Laboratory Education: Voices of Experience	Chamberlin[26]	2007	Canada	Laboratory only	Case report
Biochemistry and Molecular Biology Education	Virtual Laboratory Simulation in the Education of Laboratory Technicians—Motivation and Study Intensity	de Vries[27]	2019	Denmark	Laboratory only	Empirical study
Canadian Journal of Medical Laboratory Science	Student Confidence in Performing Transfusion Science Competencies Following Participation in a Simulated Clinical Laboratory	Emes[28]	2015	Canada	Laboratory only	Empirical study
Canadian Journal of Medical Laboratory Science	The Use of Interprofessional Simulation to Improve Collaboration and Problem Solving Among Undergraduate BHSc Medical Laboratory Science and BScN Nursing Students	Goulding[29]	2020	Canada	Interprofessional	Empirical study
Canadian Journal of Medical Laboratory Science	Simulation-Based Learning in Medical Laboratory Education: A Critique of the Literature	Grant[30]	2007	Canada	Multiprofessional	Opinion
Canadian Journal of Medical Laboratory Science	Simulation-Based Learning in Medical Laboratory Education: Current Perspectives and Practices	Grant[31]	2007	Canada	Laboratory only	Opinion
Canadian Journal of Medical Laboratory Science	Fast-Track Models for Delivery of MLT Programming: A Perspective on the CSMLS Call to Action	Hardy[32]	2017	Canada	Laboratory only	Opinion
Clinical Laboratory Science	Development and Feasibility of an Electronic White Blood Cell Identification Trainer	Haun[33]	2013	US	Laboratory only	Empirical study
Journal of Interprofessional Education and Practice	A Case of Anaphylaxis: IPE Simulation as a Tool to Enhance Communication and Collaboration	Hodgkins[34]	2020	US	Interprofessional	Empirical study
Journal of Allied Health	Assessing the Impact of a Virtual Lab in an Allied Health Program	Kay[35]	2018	Canada	Laboratory only	Empirical study
Canadian Journal of Medical Laboratory Science	CSMLS Call to Action: A Medical Laboratory Science Educator's Perspective	Khan[36]	2019	Canada	Laboratory only	Opinion
Canadian Journal of Medical Laboratory Science	Simulation Education—Building a Better Bridge Between Theory and Reality	Kiely[37]	2012	Canada	Laboratory only	Opinion
Canadian Journal of Medical Laboratory Science	No Harm, No Foul: Putting Theory into Practice with High-Fidelity Simulation	Langille[38]	2014	Canada	Interprofessional	Case report
Canadian Journal of Medical Laboratory Science	The Impact of Simulation-Based Education	Mok[39]	2011	Canada	Laboratory only	Opinion

TABLE 2. Continued

Journal Name	Title of Article	First Author	Year	Country	Participants	Level of Evidence
Postgraduate Medical Journal	Going Glass to Digital: Virtual Microscopy as a Simulation-Based Revolution in Pathology and Laboratory Science	Nelson[40]	2013	Canada	Laboratory only	Case report
Clinical Laboratory Science	Teaching and Assessing New Method Verification Skills Using Interactive Simulations	Nielsen[41]	2006	US	Laboratory only	Case report
Journal of Interprofessional Education and Practice	The Syphilis Testing Result Interprofessional Counseling and Education (STRICE) simulation	Nunez-Argote[42]	2019	US	Interprofessional	Empirical study
Clinical Laboratory Science	Simulated STAT Laboratory in a University Based Medical Laboratory Science Program	Oja[43]	2016	US	Laboratory only	Empirical study
Canadian Journal of Medical Laboratory Science	Complementary Article to the Position Statement: The Use of Simulation to Reduce Clinical Hours	Anonymous[44]	2018	Canada	Laboratory only	Opinion
Clinical Laboratory Science	Implementation of a Laboratory Information System in a Simulated Laboratory	Thomas[45]	2017	US	Laboratory only	Empirical study
Clinical Simulation in Nursing	Interprofessional Education: A Multi-Patient, Team-Based Intensive Care Unit Simulation	Watts [46]	2014	US	Interprofessional	Case report
Canadian Journal of Medical Laboratory Science	Little Evidence to Support Simulation-Based Training for Medical Laboratory Technology Students, Research Study Concludes	Canadian Society for Medical Laboratory Science[47]	2008	Canada	Laboratory only	Opinion

TABLE 3. Standards of Best Practice Applied to Articles Describing Simulation Activity

Article	Outcomes and Objectives	Facilitation	Debriefing	Participant Evaluation	Simulation-Enhanced Interprofessional Education	Simulation Design
A Case of Anaphylaxis: IPE Simulation as a Tool to Enhance Communication and Collaboration	Described	Described	Partially described	Described	Described	Described
A Study of Interprofessional Collaboration in Undergraduate Medical Laboratory Science and Nursing Education	Not described	Partially described	Partially described	Described	Partially described	Partially described
Assessing the Impact of a Virtual Lab in an Allied Health Program	Not described	Partially described	Not described	Described	NA	Not described
Development and Feasibility of an Electronic White Blood Cell Identification Trainer	Not described	Partially described	Not described	Described	NA	Partially described
Health and Social Care Students Pursuing Different Studies, and Their Written Assignments From Workshop and Online Interprofessional Education	Not described	Partially described	Not described	Described	Partially described	Partially described
Incorporating Clinical Laboratory Science Students into Interprofessional Simulation	Described	Partially described	Described	Not described	Partially described	Partially described
Interprofessional Education: A Multi-Patient, Team-Based Intensive Care Unit Simulation	Partially described	Described	Described	Not described	Partially described	Partially described
Pride and Prejudice and Learning: An Interprofessional Experience with CLS and Nursing Students	Not described	Not described	Not described	Described	Partially described	Partially described
Promoting Patient Safety Through Interprofessional Education Simulation	Described	Partially described	Not described	Described	Partially described	Partially described
Simulated STAT Laboratory in a University Based Medical Laboratory Science Program	Described	Partially described	Not described	Described	Not described	Partially described
Teaching and Assessing New Method Verification Skills Using Interactive Simulations	Partially described	Partially described	Not described	Described	Not described	Not described
The Syphilis Testing Result Interprofessional Counseling and Education (STRICE) Simulation	Described	Partially described	Partially described	Described	Partially described	Partially described
The Use of Interprofessional Simulation to Improve Collaboration and Problem Solving Among Undergraduate BHSc Medical Laboratory Science and BScN Nursing Students	Partially described	Described	Partially described	Described	Described	Partially described
Virtual Laboratory Simulation in the Education of Laboratory Technicians—Motivation and Study Intensity	Not described	Partially described	Not described	Described	Not described	Partially described

terminology, theory, and structure to implement evidence-based simulation; and the need for additional data on the impact of simulation on MLS education. Case reports described aspects of simulation and how it can be incorporated into academic curricula and clinical practice. The empirical studies described incorporating simulation into the student laboratory.

Discussion

The use and impact of simulation in fields such as nursing and medicine are well-documented; however, the scope of simulation literature with MLS is unknown. Therefore, this scoping review identified and synthesized literature on simulation and MLS over the past 20 years. Through analysis, findings revealed 2 clusters of literature: articles that described simulation activities and those that did not. Articles that did not describe simulation activities focused on student, faculty, and professional society perspectives on the use of simulation.

Although there is a vast amount of literature within healthcare simulation, only 32 articles mentioned simulation and MLS. Even fewer specified the use of best practices in simulation activities designed for or with MLS students. The paucity of literature and the lack of SoBP application raise concern regarding both the quantity and quality of literature in this realm.

Synthesis of Major Findings

For the analysis of articles that described a simulation, the INACSL SoBP were used as a framework to assess the evidence-based design and implementation of simulation activities. Only 3 articles described or partially described the simulation in enough detail to assess its congruence with best practices. To increase the use of simulation and improve current design, studies must provide enough detail to assess the quality of the implementation and evaluation. Without a complete published description of simulation activities, other researchers and educators cannot replicate or build upon existing curricula. Another finding among these articles is that the most frequently represented expertise was phlebotomy. The scope of practice for medical laboratory professionals exceeds the ability to draw blood. Placing emphasis on a single preanalytical skill undermines the specialized knowledge and capabilities of the profession.

The articles that did not describe a simulation were primarily case reports and opinion-based pieces. Within the hierarchy of evidence, these articles are generally considered to add little to no value to the body of knowledge.

Gaps and Future Directions

Through the synthesis of the literature, several gaps were identified. There is concern over the conceptualization of simulation, particularly with simulations that only include the medical laboratory. There are inconsistencies in structure (prebriefing, scenario, debriefing), creation of a strong learning environment, and use of best practices.

Standardized structure in simulation is grounded in best practices in adult learning, instructional design, and simulation pedagogy. A prebriefing at the beginning of a simulation is important to set the stage for learning. This includes defining whether the simulation will be used for formative or summative assessment, describing the goals of the scenario, discussing the concept of a fiction contract, and, if the situation is formative, communicating that it is a place to practice, to take risks, and to try new things. Essential learning occurs during debriefing. Debriefing provides an opportunity to promote reflection on decisions and interactions during a scenario, which in turn supports the transfer of new knowledge, skills, and attitudes to future practice.

Creating a strong learning environment begins with adequate prelearning so that students are prepared to apply the material they have learned in a simulation. Faculty need to ensure that students are not asked to apply knowledge they have not yet been exposed to. They can create an environment in which students feel inadequate, overwhelmed, or tricked. Ensuring confidentiality fosters risk-taking and practicing at the edge of their ability. It is important to hold students in high regard. Faculty should communicate this level of respect to their students. Often, a phrase such as "We believe you are intelligent and capable and care about doing your best" is used. Cumulatively, these items help foster a psychologically safe environment. However, psychological safety is a perception. Faculty cannot simply tell students they are safe; they have to implement certain practices and strive toward this level of safety. Ideally, this effort would be measured with each simulation.

Faculty can familiarize themselves with best practices in simulation through a review of the literature and utilizing the INACSL SoBP. Updates to existing SoBP standards and the creation of new standards are forthcoming.

Simulation provides an opportunity to promote the value of the laboratory on an interprofessional team. Interprofessional simulation can be used to define professional roles and responsibilities, practice teamwork and communication, and instill interprofessional values and ethics.[8] Programs should use the Interprofessional Education Collaborative competency statements as a guide when collaborating with other professions in designing simulation objectives.[14] Faculty should strive to create authentic opportunities for interprofessional interaction that indicate the breadth of the laboratory's impact on patient care. This enterprise can be accomplished through creating scenarios that represent multiple areas of the laboratory (ie, blood bank, microbiology, chemistry). Likewise, faculty need to create opportunities for interprofessional interactions that are realistic. This can be face to face, over the phone, or through the computer information system.

To change practice, studies must move beyond descriptive data collection and analysis to higher levels of evaluation. Several articles included reactions to a simulation that was level 1 on Kirkpatrick's Model of Learning Evaluation[15] (**FIGURE 2**). There were no studies that analyzed data beyond learning (Kirkpatrick's level 2). Program researchers in MLS need to move up the hierarchy toward assessing behavior (level 3) and results (level 4).

The MLS and simulation literature needs more robust discussion and detailed outcomes so that program administrators can learn from the successes, challenges, enablers, and barriers of other programs with a goal of creating transferable knowledge that influences practice. In addition, the disclosure of limitations needs to be provided to understand potential biases, generalizability, and elements that were beyond the control of the researchers. With a higher level of scholarly discourse,

FIGURE 2. Kirkpatrick's model of learner evaluation.

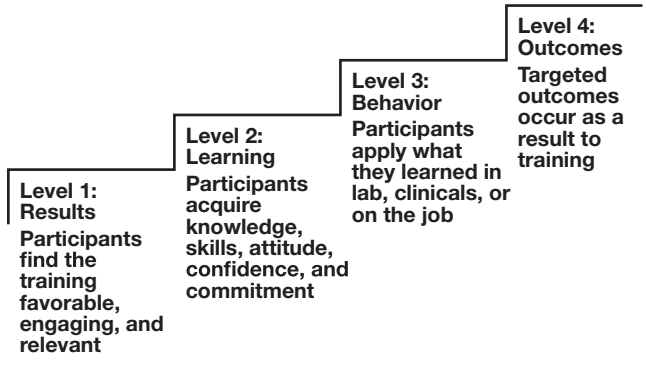

the medical laboratory profession can eliminate stereotypes and elevate perceptions of the laboratory on the interprofessional team.

Strengths and Limitations

A strength of this study is that it is the first to use the INACSL SoBP as a framework to evaluate the literature. This framework can be utilized for simulation design and as a guide for publishing empirical studies. We identified the gaps and provided a road map for future studies in MLS and simulation.

This review used the PRISMA guidelines to identify the literature to be reviewed.[16] Consequently, literature that did not provide details for which professions were included in the simulation in the abstract would have been excluded during the abstract review phase. In addition, we noted that the journal *Clinical Laboratory Science,* which contains articles on the scholarship of education, has not been indexed since 2018, so those articles would not be included in this review.

Conclusion

Despite considerable growth in simulation over the last 20 years, the inclusion of simulation in MLS curricula remains a nascent area of study. Interprofessional simulation incorporating the medical laboratory in an authentic capacity is vital to role development because it removes professional ambiguity and assumptions. To move forward and grow the body of evidence, more empirical studies are needed that incorporate evidence-based practices and methodological rigor with advanced statistical analysis and in-depth reporting of results, implications, and limitations.

REFERENCES

1. Salas E, Bowers CA, Rhodenizer L. It is not how much you have but how you use it: toward a rational use of simulation to support aviation training. *Int J Aviat Psychol.* 1998;8(3):197–208.
2. Nestel D. Ten years of simulation in healthcare: a thematic analysis of editorials. *Simul Healthc.* 2017;12(5):326–331.
3. Cook DA, Hatala R, Brydges R, et al. Technology-enhanced simulation for health professions education: a systematic review and meta-analysis. *JAMA.* 2011;306(9):978–988.
4. Cheng A, Duff J, Grant E, Kissoon N, Grant VJ. Simulation in paediatrics: an educational revolution. *Paediatr Child Health.* 2007;12(6):465–468.
5. Peterson DT, Brown M, Wingo N, Watts P. Exploring hidden curricula in an interprofessional intensive care unit simulation. *Clin Simul Nurs*. 2018;22:22–25.
6. Isaak RS, Chen F, Martinelli SM, et al. Validity of simulation-based assessment for Accreditation Council for Graduate Medical Education milestone achievement. *Simul Healthc.* 2018;13(3):201–210.
7. Okuyama A, Wagner C, Bijnen B. Speaking up for patient safety by hospital-based health care professionals: a literature review. *BMC Health Serv Res.* 2014;14:61.
8. Brown MR, Bostic D. Strengthening the clinical laboratory with simulation-enhanced interprofessional education. *Clin Lab Sci*. 2016;29(4):237–240.
9. Eppich W, Howard V, Vozenilek J, Curran I. Simulation-based team training in healthcare. *Simul Healthc.* 2011;6 Suppl:S14–S19.
10. World Health Organization. Framework for action on interprofessional education and collaborative practice. September 1, 2010. https://www.who.int/publications/i/item/framework-for-action-on-interprofessional-education-collaborative-practice. Accessed September 8, 2021.
11. Sittner BJ, Aebersold ML, Paige JB, et al. INACSL Standards of Best Practice for Simulation: past, present, and future. *Nurs Educ Perspect.* 2015;36(5):294–298.
12. Pham MT, Rajić A, Greig JD, Sargeant JM, Papadopoulos A, McEwen SA. A scoping review of scoping reviews: advancing the approach and enhancing the consistency. *Res Synth Methods.* 2014;5(4):371–385.
13. Arksey H, O'Malley L. Scoping studies: towards a methodological framework. *Int J Soc Res Methodol*. 2005;8(1):19–32.
14. Interprofessional Education Collaborative. *Core Competencies for Interprofessional Collaborative Practice*. Washington, DC: Interprofessional Education Collaborative; 2016.
15. Kvan T. Evaluating learning environments for interprofessional care. *J Interprof Care.* 2013;27(Suppl 2):31–36.
16. Moher D, Liberati A, Tetzlaff J, Altman DG, Group P. Preferred reporting items for systematic reviews and meta-analyses: the PRISMA statement. *PLoS Med.* 2009;6(7):e1000097.
17. Alano D. Student perspective on uniting simulation education. *Can J Med Lab Sci*. 2019;81(1):6.
18. Almås SH, Vasset F. Health and social care students pursuing different studies, and their written assignments from workshop and online interprofessional education. *Nord J Nurs Res*. 2016;36(3):116–121.
19. Beard TS, Robertson TM, Semler JR, Cude CJ. A study of interprofessional collaboration in undergraduate medical laboratory science and nursing education. *Clin Lab Sci*. 2015;28(2):83–90.
20. Behan KJ, Van Der Like J. Introducing interprofessional education to BSN and CLS students using a simulated healthcare setting. *Clin Lab Sci*. 2017;30(4):224–227.
21. Behan KJ, Coffey K, Promo M, Brooks T, Van Der Like J. Pride and prejudice and learning: an interprofessional experience with CLS and nursing students. *Clin Lab Sci*. 2017;30(4):233–239.
22. Brown MR, Watts P. Primer on interprofessional simulation for clinical laboratory science programs: a practical guide to structure and terminology. *Clin Lab Sci*. 2016;29(4):241–246.
23. Brown MR, Miller BV. Incorporating clinical laboratory science students into interprofessional simulation. *Clin Lab Sci*. 2016;29(4):247–251.
24. Brown MR, Maday K, Hurt J. Small scale, low resource options for introducing clinical laboratory science students to interprofessional simulation. *Clin Lab Sci*. 2016;29(4):252–256.
25. Cavnar K, Van Der Like J, Hobby-Burns L. Promoting patient safety through interprofessional education simulation. *Clin Lab Sci*. 2017;30(4):228–232.
26. Chamberlin S, Gray H, Keeping D. Simulations in medical laboratory education: voices of experience. *Can J Med Lab Sci*. 2007;69(6):246–250.
27. de Vries LE, May M. Virtual laboratory simulation in the education of laboratory technicians—motivation and study intensity. *Biochem Mol Biol Educ.* 2019;47(3):257–262.
28. Emes MT. Student confidence in performing transfusion science competencies following participation in a simulated clinical laboratory. *Can J Med Lab Sci*. 2015;77(3):21–27.
29. Goulding MH, Graham L. The use of interprofessional simulation to improve collaboration and problem solving among undergraduate BHSc medical laboratory science and BScN nursing students. *Can J Med Lab Sci*. 2020;82(2):25–33.
30. Grant MM. Simulation-based learning in medical laboratory education: a critique of the literature. *Can J Med Lab Sci*. 2009;71(3):107–116.
31. Grant MM, Davis KH. Simulation-based learning in medical laboratory education: current perspectives and practices. *Can J Med Lab Sci*. 2008;70(1):17–18.
32. Hardy G. Fast-track models for delivery of MLT programming: a perspective on the CSMLS call to action. *Can J Med Lab Sci*. 2019;81(3):11–13.

33. Haun DE, Foley AB, Jarreau PC. Development and feasibility of an electronic white blood cell identification trainer. *Clin Lab Sci.* 2013;26(1):23–29.
34. Hodgkins SR, Marian KM, Shrader S, et al. A case of anaphylaxis: IPE simulation as a tool to enhance communication and collaboration. *J Interprof Educ Pract*. 2020;18:100303.
35. Kay R, Goulding H, Li J. Assessing the impact of a virtual lab in an allied health program. *J Allied Health.* 2018;47(1):45–50.
36. Khan M, Talbot AMY. CSMLS call to action: a medical laboratory science educator's perspective. *Can J Med Lab Sci*. 2019;76(4):27–29.
37. Kiely P, Rosenberg L, Bridge P. Simulation education—building a better bridge between theory and reality. *Can J Med Lab Sci*. 2012;74(3):14.
38. Langille J. No harm, no foul: putting theory into practice with high-fidelity simulation. *Can J Med Lab Sci*. 2011;76(2):24–26.
39. Mok A. The impact of simulation-based education. *Can J Med Lab Sci*. 2011;73(1):9.
40. Nelson D, Ziv A, Bandali KS. Republished: going glass to digital: virtual microscopy as a simulation-based revolution in pathology and laboratory science. *Postgrad Med J.* 2013;89(1056):599–603.
41. Nielsen LG. Teaching and assessing new method verification skills using interactive simulations. *Clin Lab Sci.* 2006;19(3):188.
42. Nunez-Argote L, Robertson C, Teigen A, et al. The Syphilis Testing Result Interprofessional Counseling and Education (STRICE) simulation. *J Interprof Educ Pract*. 2019;17:1–5
43. Oja J, Thomas J, Nicholaou M. Simulated STAT laboratory in a university based medical laboratory science program. *Clin Lab Sci*. 2016;29(2):59–65.
44. Anonymous. Complementary article to the position statement: the use of simulation to reduce clinical hours. *Can J Med Lab Sci*. 2018;80(2):34–35.
45. Thomas J. Implementation of a laboratory information system in a simulated laboratory. *Clin Lab Sci*. 2017;30(2):65–71.
46. Watts P, Langston SB, Brown M, et al. Interprofessional education: a multi-patient, team-based intensive care unit simulation. *Clin Simul Nurs*. 2014;10(10):521–528.
47. Canadian Society for Medical Laboratory Science. Little evidence to support simulation-based training for medical laboratory technology students, research study concludes. January 2, 2008. https://www.csmls.org/About-Us/Society-News/Media-Releases/Little-Evidence-to-Support-Simulation-Based-Traini.aspx. Accessed September 8, 2021.

CASE STUDY

Gas Chromatography Mass Spectrometry Aided Diagnosis of Glutathione Synthetase Deficiency

*Parminder Kaur, MD, Chakshu Chaudhry, DM, Inusha Panigrahi, DM, Priyanka Srivastava, PhD, Anupriya Kaur, DM**

Genetic Metabolic Unit, Department of Pediatrics, Advanced Pediatrics Centre, Post Graduate Institute of Medical Education and Research (PGIMER), Chandigarh, India; *To whom correspondence should be addressed. anukaur.genetics@gmail.com

Keywords: glutathione synthetase, 5-oxoproline, metabolic acidosis, hemolyticanemia, high anion gap, GCMS

Abbreviations: NICU, neonatal intensive care unit; TMS, tandem mass spectrometry; GCMS, gas chromatography mass spectrometry; GSS, glutathione synthetase; HAGMA, high anion-gap metabolic acidosis; GSH, glutathione synthetase; RBC, red-blood-cell; pCO2, partial pressure of carbon dioxide; G6PD, glucose-6-phosphate dehydrogenase; DCT, direct Coombs test

Laboratory Medicine 2022;53:e59–e61; https://doi.org/10.1093/labmed/lmab084

ABSTRACT

Glutathione synthetase (GSS) deficiency is a rare disorder, occurring with a frequency of less than 1 in 100,000 individuals worldwide. The clinical presentation may vary from mild to severe, and manifestations include hemolytic anemia, hyperbilirubinemia, metabolic acidosis, neurological problems, and sepsis. Herein, we present a case of a newborn boy with the most severe phenotype of GSS deficiency, diagnosed based on clinical features and increased urinary 5-oxoproline levels determined via gas chromatography mass spectrometry (GCMS) testing.

Clinical History

A full-term (born at 37 weeks) baby boy was admitted to our neonatal intensive care unit (NICU) with jaundice and intractable metabolic acidosis. He was the fourth child born to a nonconsanguineously married couple. This couple had a history of 2 previous second-trimester fetal losses. Their 3rd pregnancy had been with a preterm (born at 35 weeks) baby boy who had died 3 days after birth and had had similar health complications as those of the proband. The baby whose case we present herein had been born via emergency caesarean section due to maternal preeclampsia. His birth weight was 2480 grams, and his APGAR scores were 9 and 10 at 1 and 5 minutes after birth, respectively.

The physical examination results for the baby were normal. Breast feeding was initiated immediately after birth, and the baby accepted it well. However, jaundice was observed within 24 hours after birth, for which phototherapy had to be started. The bilirubin level reached a peak of 12 mg/dL at 48 hours after birth and declined thereafter. The baby developed tachyponea on day 3 after birth. His sepsis screening and chest radiography results were normal. Further investigations revealed high anion-gap metabolic acidosis with normal blood sugar, lactate, ketones, and ammonia levels. The peripheral blood picture showed evidence of hemolysis (**TABLE 1**). Glucose-6-phosphate dehydrogenase (G6PD) levels were found to be normal, and direct Coombs test (DCT) results were documented as being negative. The results of the investigations we performed are summarized in **TABLE 1**. This clinical scenario suggested an inborn error of metabolism.

The health of the baby was managed with oxygen support, glucose and bicarbonate infusion, and empirical multiple-cofactor supplementation. We collected a dried blood spot for tandem mass spectrometry (TMS) and a urine specimen for gas chromatography mass spectrometry (GCMS) for analysis. On day 5 after birth, the baby experienced

TABLE 1. Summary of Laboratory Investigations

Investigation	Result (Reference Value)
Hemoglobin	12 g/dL (14–24 g/dL)
Peripheral blood picture	Reticulocytosis with evidence of hemolysis
Blood pH	7.10 (7.35–7.45)
Blood pCO_2	36 mm Hg (35–45 mm Hg)
Serum bicarbonate	10.8 mEq/L (23.0–30.0 mEq/L)
Serum lactate	1.9 mmol/L (0.5–1.0 mmol/L)
Anion gap	16.9 mEq/L (<10 mEq/L)
Ammonia	50 µmol/L (<50 µmol/L)
Liver transaminases (SAST/ALT)	46/42 U/L (5–40 U/L)
Total serum bilirubin	12 mg/dL (0.1–1.2 mg/dL)
G6PD	Normal
DCT	Negative
Blood glutamine	260 µmol/L (48.24–1309.25 µmol/L)
Urine 5-oxoproline	17,191.60 mmol/mol creatinine (<704.71 mmol/mol creatinine)

Abbreviations: *pCO2, partial pressure of carbon dioxide; G6PD, glucose-6-phosphate dehydrogenase; DCT, direct Coombs test.*

worsening of respiratory distress requiring ventilatory support. The results of GCMS testing revealed increased excretion of 5-oxoproline, which is suggestive of glutathione synthetase (GSS) deficiency. Supplementation with vitamin C and vitamin E was started. However, the baby had worsening encephalopathy and circulatory-respiratory failure requiring intubation and ionotropic support. Despite all of these supportive measures, the baby died on the sixth day after birth.

Discussion

GSS deficiency is a rare disorder resulting from an inborn error of glutathione metabolism caused by mutations in the *GSS* gene (OMIM 601002).[1] As of the year 2018, approximately 80 cases of GSS deficiency have been reported worldwide.[2] The presentation of this condition includes metabolic acidosis, hemolytic anemia, hyperbilirubinemia, neurological manifestations, and susceptibility to sepsis.[3,4] The diagnosis is made based on clinical presentation and increased 5-oxoproline levels in urine, detected by GCMS, and low GSS activity in the erythrocytes or fibroblasts. The definitive diagnosis can be established by sequencing *GSS*. Management is supportive with sodium bicarbonate for acidosis and antioxidant agents such as N-acetyl cysteine, vitamin C, and vitamin E.[3,4]

Glutathione is a ubiquitously present tripeptide molecule consisting of glutamate, cysteine, and glycine.[5] It is a strong antioxidant with several important biological functions, including prevention of free-radical injury and maintaining cell-membrane integrity. GSS deficiency can present with 3 clinical phenotypes. In its mildest form, there can be isolated episode or recurrent episodes of mild hemolytic anemia with or without oxoprolinuria. In its moderate form, mild/moderate hemolytic anemia is accompanied by metabolic acidosis, and constant oxoprolinuria occurs. In the most severe form, hemolytic anemia, jaundice, and high anion-gap metabolic acidosis (HAGMA) are accompanied by acute, then chronic, progressive neurological symptoms.[4]

High levels of oxoprolinuria occur in severe GSS deficiency, as we observed in our case individual. The baby demonstrated the most severe form of the disease, as evident by HAGMA (arterial blood gas analysis) and hemolysis (**TABLE 1**). He showed neurological involvement in the form of encephalopathy towards the terminal part of his illness. Children with such severe illness are prone to oxidative damage and neurological injury due to the accumulation of free radicals and peroxides in the brain. In such patients, there is also an increased risk of bacterial infections due to neutrophil granulation defect.[6]

Supportive treatment includes correcting the metabolic acidosis, administering antibiotics for sepsis, and addressing hyperbilirubinemia. Anemia often needs to be treated with blood transfusion. Antioxidative agents such as vitamin E, vitamin C, and N-acetylcysteine are often used. Vitamins C and E are recommended in all forms of GSS deficiency because they have a neuroprotective role. Vitamin C acts as an antioxidant, and vitamin E improves the polymorphonuclear leukocyte function and normalizes the microtubule assembly during phagocytic challenge in patients with GSS deficiency.[6] Drugs that are contraindicated in G6PD deficiency should also be avoided in patients with GSS deficiency. The prognosis depends on the type of mutation, severity of acidosis, associated bacterial infections, and quality of supportive therapy.

Laboratory testing plays a crucial role in determining the correct diagnosis, as does understanding the details of the metabolism of glutathione. Gluthianone is metabolized by the gamma-glutamyl cycle.[7] As seen in **FIGURE 1**, glutathione is synthesized from glutamate, cysteine, and glycine in 2 steps by gamma-glutamyl-cysteine synthetase and glutathione synthetase (GSH); in the absence of glutathione synthesis, the levels of 5-oxoproline will be raised.

The various de-ranged laboratory parameters we observed in our case individual were uncompensated metabolic acidosis with raised lactate levels, hyperbilirubinemia, and hemolytic anemia, along with GCMS showing very high levels of 5-oxoproline in urine. Because glutathione is required for cell-membrane integrity,its absence precipitates red-blood-cell (RBC) lysis and subsequent anemia and hyperbilirubinemia. Accumulation of oxoproline occurs due to subsequent metabolic block in the gamma-glutamyl cycle, causing a high level of oxoprolinuria in severe GSS deficiency, as observed in our case individual. The normal levels of 5-oxoproline in a freshly voided urine specimen range from 55-440 μmol/day.[7] Raised levels of 5-oxoproline can also be found in deficiency of 5-oxoprolinase, an enzyme required in the metabolism of glutathione. Oxoprolinase deficiency is characterized by neonatal hypoglycemia; microcytic anemia; and gastrointestinal symptoms, in the form of vomiting, diarrhea, and renal-stone formation. It can be easily differentiated from GSS deficiency because the patients with 5-oxoprolinase deficiency do not have metabolic acidosis and hemolytic anemia.[5]

GCMS combines the principles of gas chromatography and mass spectrometry to identify different molecules present in a test specimen. Different molecules in a test mixture get separated in the capillary column of the gas chromatograph, depending on their chemical properties and their relative affinity for the stationary phase of the capillary column. The molecules elute out of the column after different retention times, which allows the downstream mass spectrometer to detect the ionized molecules separately, based on their mass-to-charge ratio. This test is now being widely to diagnose several inborn errors of metabolism.[8]

Besides the gamma-glutamyl cycle, other inborn errors of metabolism leading to deficiency of ATP, particularly in the liver and kidneys (such as urea-cycle defect and tyrosinemia), may show oxoprolinuria, although not at as high levels as in the glutamyl-cycle defect.[9] Besides, drugs such as paracetamol as the precipitating trigger for the manifestations of glutathione deficiency should be ruled out.[10] Certain infant-formula diets and juices may also cause increased levels of urinary oxoproline.[11] None of the aforementioned factors were present in our case individual, and his levels of amino acids and ammonia were documented to be normal. It would have been ideal to demonstrate the underlying *GSS* gene mutation; however, we could not do so in this case study due to financial constraints.

Conclusion

GSS deficiency should be suspected in any newborn presenting with hemolytic anemia that cannot be explained by an alternative diagnosis. Urinary GCMS should be performed in such cases to detect oxoprolinuria, to aid in provisional diagnosis and subsequent therapy.

FIGURE 1. The γ-glutamyl cycle.

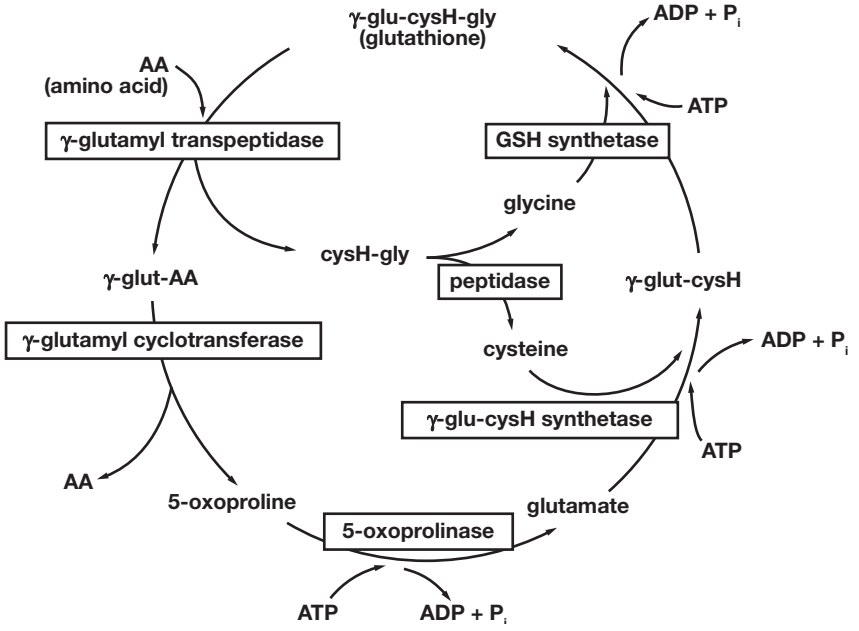

Acknowledgments: We are thankful to the family of this case for permitting us to publish clinical details regarding their child.

Personal and Professional Conflicts of Interest

None reported.

REFERENCES

1. Glutathionesynthetase. OMIM (Online Mendelian Inheritance in Man): An Online Catalog of Human Genes and Genetic Disorders. Accessed October 20, 2021. https://www.omim.org/entry/601002?search=gss&highlight=gss
2. Xia H, Ye J, Wang L, Zhu J, He Z. A case of severe glutathione synthetase deficiency with novel GSS mutations. *Braz J Med Biol Res.* 2018;51(3):e6853.
3. Li X, Ding Y, Liu Y, et al. Five Chinese patients with 5-oxoprolinuria due to glutathione synthetase and 5-oxoprolinase deficiencies. *Brain Dev.* 2015;37(10):952–959.
4. Njålsson R. Glutathione synthetase deficiency. *Cell Mol Life Sci.* 2005;62(17):1938–1945.
5. Ristoff E, Larsson A. Inborn errors in the metabolism of glutathione. *Orphanet J Rare Dis.* 2007;2:16.
6. Ristoff E, Mayatepek E, Larsson A. Long-term clinical outcome in patients with glutathione synthetase deficiency. *J Pediatr.* 2001;139(1):79–84.
7. Wellner VP, Sekura R, Meister A, Larsson A. Glutathione synthetase deficiency, an inborn error of metabolism involving the gamma-glutamyl cycle in patients with 5- oxoprolinuria (pyroglutamicaciduria). *Proc Natl Acad Sci U S A*. 1974;71(6):2505–2509.
8. Sparkman DO, Penton Z, Kitson FG. *Gas Chromatography and Mass Spectrometry: A Practical Guide*. Academic Press; 2011.
9. Larsson A, Ristoff E, Anderson ME. Glutathione synthetase deficiency and other disorders of the gamma-glutamyl cycle. In: Scriver CR, Beaudet AL, Sly WS, et al, eds. *The Metabolic and Molecular Bases of Inherited Disease.* McGraw-Hill; 2005.
10. Ghauri FY, McLean AE, Beales D, Wilson ID, Nicholson JK. Induction of 5-oxoprolinuria in the rat following chronic feeding with N-acetyl 4-aminophenol (paracetamol). *Biochem Pharmacol*. 1993;46(5):953–957.
11. Oberholzer VG, Wood CB, Palmer T, Harrison BM. Increased pyroglutamic acid levels in patients on artificial diets. *Clin Chim Acta.* 1975;62(2):299–304.

CORRIGENDUM

Corrigendum to: Urine Organic Acid Analysis: Key Diagnostic Test for Fumaric Aciduria in a Sri Lankan Child

Eresha Jasinge,[1,] Mihika Fernando,[1] Neluwa-Liyanage Ruwan Indika,[2] Roberta Trunzo,[3] Sabine Schröder,[3] Dinesha Maduri Vidanapathirana,[4] Patricia M. Jones,[5] Subashini Jayasena,[1] Anusha Varuni Gunarathne,[1] Pyara Ratnayake[6]*

[1]Department of Chemical Pathology, Lady Ridgeway Hospital for Children, Colombo, Sri Lanka, [2]Department of Biochemistry, Faculty of Medical Sciences, University of Sri Jayewardenepura, Sri Lanka, [3]CENTOGENE AG, Rostock, Germany, [4]Department of Pathology, Faculty of Medical Sciences, University of Sri Jayewardenepura, Sri Lanka, [5]Department of Pathology, University of Texas Southwestern Medical Center and Children's Medical Center, Dallas, Texas, US, [6]Neurology Unit, Lady Ridgeway Hospital for Children, Colombo, Sri Lanka; *To whom correspondence should be addressed. eresha.jasinge@gmail.com

In "Urine Organic Analysis: Key Diagnostic Test for Fumaric Aciduria in a Sri Lankan Child" (https://doi.org/10.1093/labmed/lmab083), there was an error in the title. This should read "Urine Organic Acid Analysis: Key Diagnostic Test for Fumaric Aciduria in a Sri Lankan Child" instead of "Urine Organic Analysis: Key Diagnostic Test for Fumaric Aciduria in a Sri Lankan Child". This error has now been corrected online.

OVERVIEW

Protocols to Dissolve Amorphous Urate Crystals in Urine

Kristina Jackson Behan, PhD, MLS(ASCP)[CM,1,*] *Michael A. Johnston, MS*[2]

[1]Medical Laboratory Sciences Department, University of West Florida, Pensacola, Florida, USA; [2]Pensacola State College, Pensacola, Florida, and Health and Hope Clinic, Pensacola, Florida, USA; *To whom correspondence should be addressed: kbehan@uwf.edu

Keywords: amorphous urates, urinalysis, microscopy, urine sediment, urine crystals, crystal solubility

Abbreviations: RBC, red blood cell; WBC, white blood cell; NaOH, sodium hydroxide; SE, standard error.

Laboratory Medicine 2022;53:e63–e68; https://doi.org/10.1093/labmed/lmab088

Objective: Amorphous urate crystals can obscure significant findings during a routine urinalysis. There is no standardized protocol to minimize their effect.

Materials and Methods: We tested 210 urine specimens. Three specimens had high red blood cell (RBC) or white blood cell (WBC) counts. Fifty-six specimens formed amorphous urates. Sediment from these specimens was treated with 50 mM sodium hydroxide (NaOH) at a 1:2 and/or 1:4 dilution. We warmed 22 specimens with crystals at various temperatures.

Results: Amorphous urate crystals formed in concentrated urine with an acidic pH. Adding 50 mM NaOH dissolved amorphous urates, revealing the presence of underlying bacteria and yeast, but WBC and RBC counts were grossly decreased. Prewarming unspun specimens to 60°C for 90 seconds dissolved most amorphous urates.

Conclusion: The protocol to eliminate amorphous urate crystals is to prewarm the specimen before testing. Adding 50 mM NaOH to sediment dissolves amorphous urates to enhance the visibility of bacteria and yeast but has a deleterious effect on WBC and RBC.

The microscopic analysis of urine is performed to identify the presence of significant elements associated with disease, such as red blood cells (RBCs), white blood cells (WBCs), casts, yeast, and bacteria. The presence of crystals in urine can be pathologic or benign. Many crystals form specific identifiable shapes, eg, calcium oxalate and triple phosphate. Small, shapeless crystals can form in concentrated urine, especially when specimens are refrigerated.[1] In acid urine, these crystals are called amorphous urates, urate salts of sodium, potassium, magnesium, or calcium.[2-5] In alkaline urine, they are called amorphous phosphates. Although amorphous crystals are nonpathologic, they can resemble bacteria and can obscure significant findings (**FIGURE 1A** and **1C**). Macroscopically they make the urine appear hazy or turbid.

Amorphous phosphates can be rapidly dissolved with 2% acetic acid but not with heat. Acid treatment destroys RBCs but enhances the appearance of WBCs and epithelial cells. Amorphous urates are insoluble in acetic acid but are reported to be soluble in alkali. We searched several urinalysis textbooks and the Clinical and Laboratory Standards Institute urinalysis approved guidelines and found no reference with specific instructions on which alkaline solution to use or its effect on other formed elements in urine.[1-9] The goal of the project was to produce a protocol that safely and rapidly dissolves amorphous urates in urine sediment and to determine its limitations.

Materials and Methods

We collected a total of 207 random urine specimens from healthy adults at a university and from volunteers at a walk-in clinic. Specimens were refrigerated for between 20 and 48 hours. They were allowed to reach ambient temperature before testing. Biochemical analysis was performed using a Multistix 10SG (Siemens) read on a Uritrak analyzer. Next, 12 mL of each specimens was centrifuged at 400 RCF for 5 minutes. The supernatant was discarded, and the remaining 0.5 mL of sediment was available for analysis. For the WBC and RBC evaluation, 3 urine specimens were collected from inpatients at a hospital and transferred into UA Preservative tubes (BD Vacutainer). Specimens were tested within 3 days of collection.

Sodium hydroxide (NaOH) is a common base used in the laboratory, typically available in varying concentrations. We selected 50 mM NaOH (0.2% NaOH) because it is a weak base that does not present a significant health hazard and requires only the use of routine laboratory personal protective equipment.[10] It can be stored at ambient temperature on the benchtop, making it a convenient microscopy tool.

Microscopic analysis of the sediment was performed by adding 10 µL of well-mixed urine sediment to 10 µL of 0.9% saline, making a 1:2 dilution. The presence of amorphous urates was graded as 0, 1+, or 2+ as shown in **FIGURE 2**. We treated 10 µL of urine sediment with 10 µL of 50 mM NaOH for a 1:2 dilution; 5 µL of urine sediment was treated with 15 µL of 50 mM NaOH for a 1:4 dilution. The presence of amorphous urates in each dilution was graded as 0, 1+, or 2+. In rare cases, a 1:5 dilution was used. To examine the effect of NaOH on formed elements, specimens with amorphous urates were spiked with bacteria and yeast. Patient specimens with hematuria and leukocyturia were used to evaluate RBC and WBC counts. Statistical analysis was performed using IBM SPSS version 28.

FIGURE 1. **Amorphous urate crystals obscure significant findings in microscopic analysis. A. Urine sediment from specimen 12. B. Specimen 12 after treatment with 50 mM NaOH revealed the presence of bacteria. C. Urine sediment containing amorphous crystals, yeast, and bacteria. D. After treatment with 50 mM NaOH, bacteria and yeast cells were easily seen. Photomicrographs taken at 400× magnification, bright field microscopy, no stain. NaOH, sodium hydroxide.**

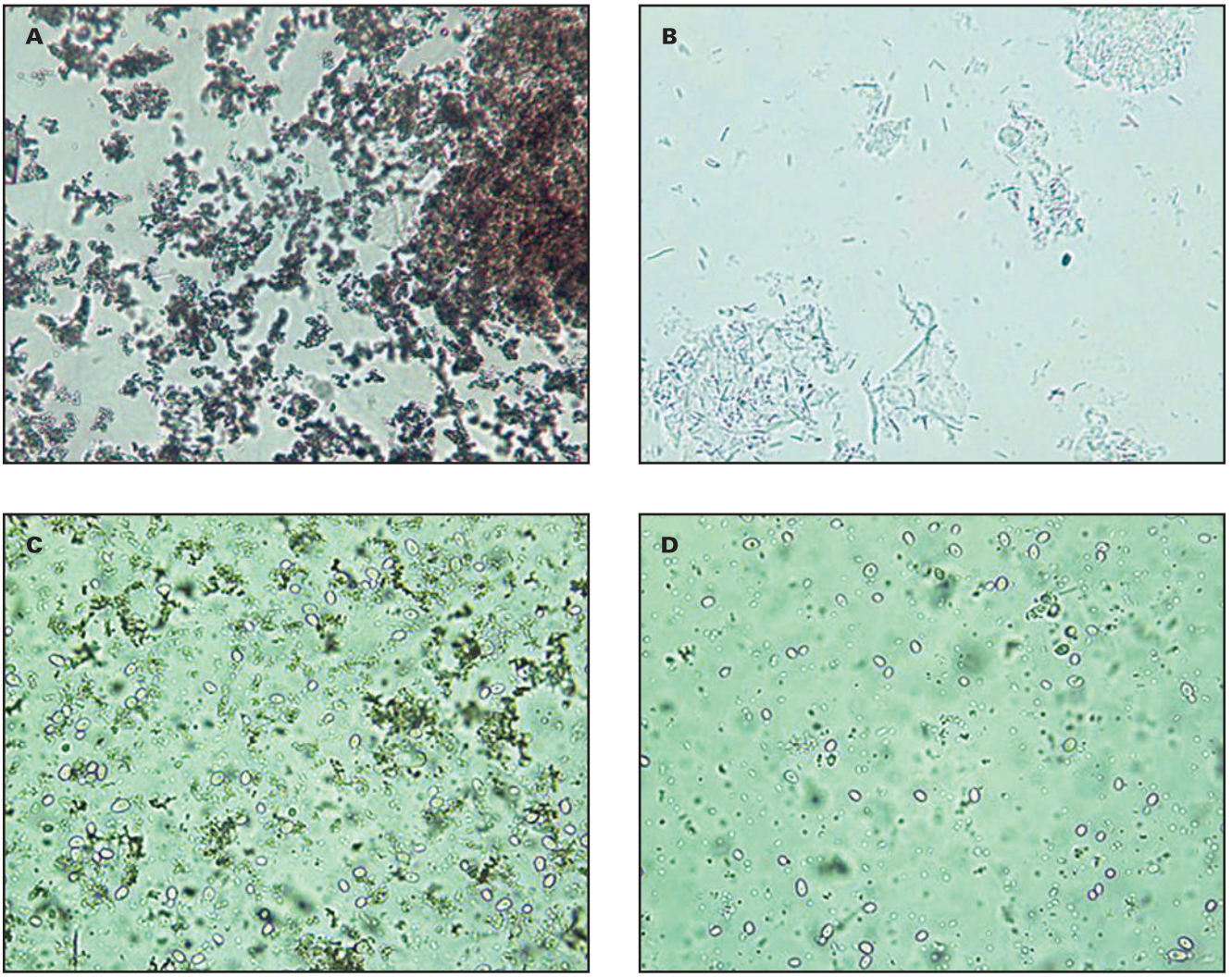

The effect of NaOH on RBC was evaluated using a specific preserved specimen identified as SH-20. The biochemical strip showed 3+ blood, pH 6.0, and specific gravity 1.015. There were no amorphous urates in the specimen. The 7 mL specimen was allowed to sediment using gravity, and 3.4 mL of supernatant was removed. The remaining sediment suspension was vortexed on high speed for 10 seconds and charged to a hemacytometer, and the cells were counted in the 5 RBC squares. To test the impact of 50 mM NaOH on the RBC, 100 µL of the sediment suspension was added to 100 µL of 50 mM NaOH. The solution was vortexed for 5 seconds and charged to a hemacytometer, and the cells were counted in the 5 RBC squares. The number of cells treated with NaOH was multiplied by 2 to correct for the dilution and was compared to the control.

The effect of NaOH on WBC was evaluated using a specific preserved specimen identified as SH-9. The biochemical strip showed 3+ leukocytes, 2+ blood, pH 6.0, specific gravity 1.025, protein 2+, and glucose 1+. There were no amorphous urates in the specimen. The 8.5 mL specimen was centrifuged at 400 RCF for 5 minutes, and the supernatant was decanted to retain 1.2 mL of sediment. The sediment was vortexed for 10 seconds. One small white clump of cells was removed, the specimen was vortexed again for 10 seconds and charged to a hemacytometer, and the cells were counted in the 5 RBC squares. To test the impact of 50 mM NaOH on the WBC, 100 µL of the sediment suspension was added to 100 µL of 50 mM NaOH. The solution was vortexed for 5 seconds and charged to a hemacytometer, and the cells were counted in the 5 RBC squares. The number of cells treated with NaOH was multiplied by 2 to correct for the dilution and was compared to the control. The analysis was repeated on a second preserved urine specimen, identified as SH-3. Biochemical strip analysis showed 3+ leukocytes, 1+ blood, pH 6.0, specific gravity 1.025, and protein 1+. There were no amorphous urates. The 7.7 mL specimen was sedimented using gravity, and the 6.6 mL of supernatant was removed to create the sediment suspension. The sediment suspension was treated as described above, and the cells were counted in the 5 RBC squares.

Statistical analysis was performed using SAS 9.4. A paired *t*-test (dependent *t*-test) was used to determine whether a difference existed

FIGURE 2. Microscopic evaluation of amorphous urate crystals quantitative grading schema. A. Grade of 0. B. Grade of 1+. C. Grade of 2+. Photomicrographs taken at 400× magnification, bright field microscopy, no stain.

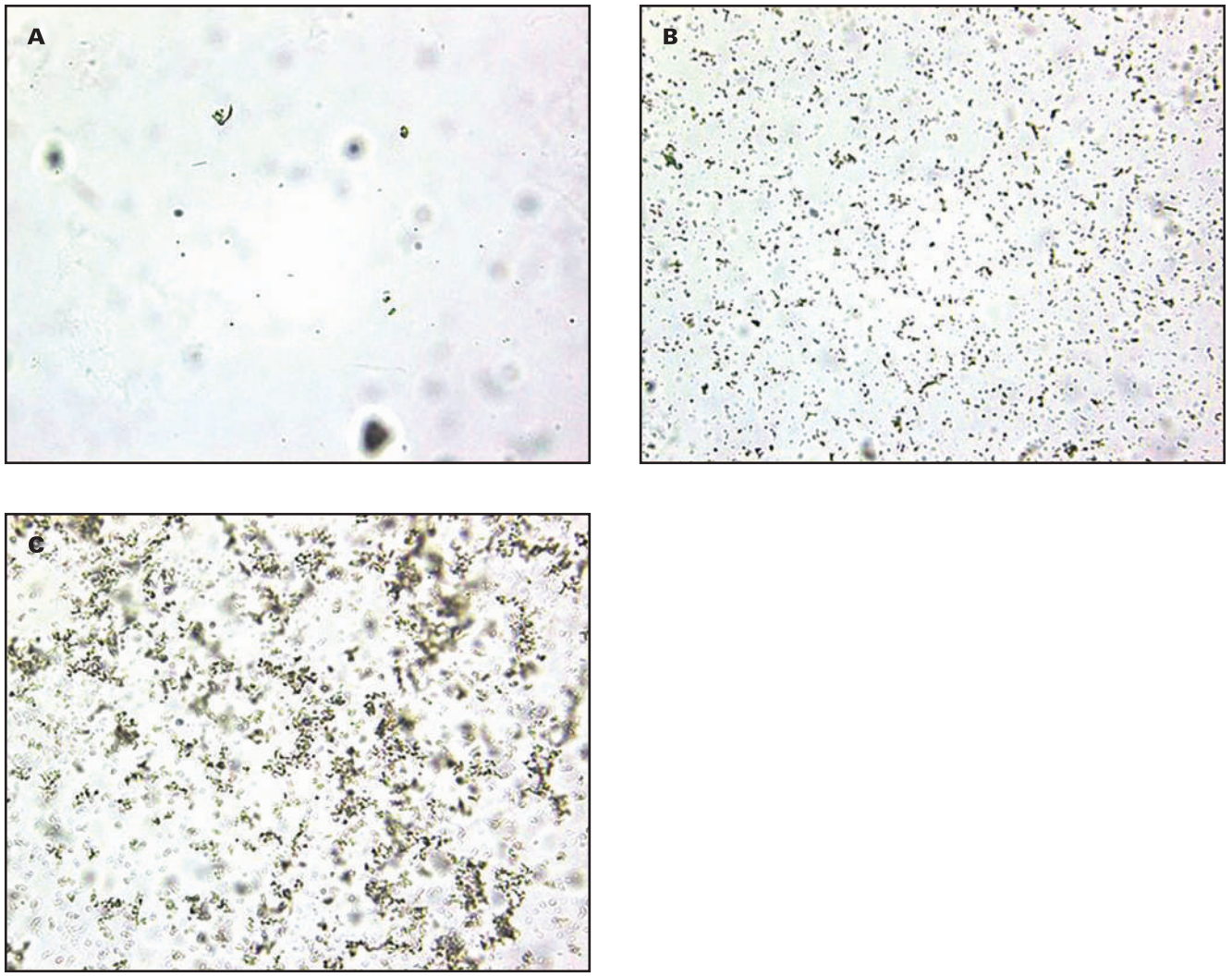

FIGURE 3. Macroscopic evaluation of amorphous urate crystals quantitative grading schema. 0 = clear, 1+ = easy to read print behind the specimen, 2+ = unable to read print, 3+ = opaque.

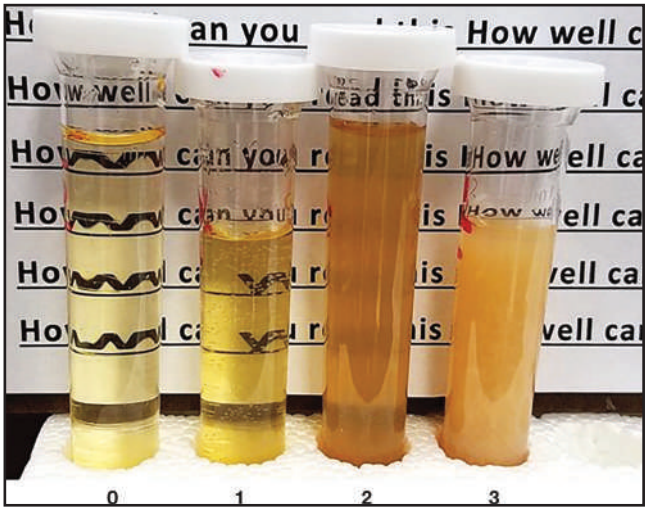

between the specimen means before and after the application of the NaOH. A goodness-of-fit test for normal distribution was used to analyze the differences between the specimens.

The effect of temperature on macroscopic turbidity was tested by refrigerating 6 to 10 mL of urine overnight at 4°C. Specimens that formed amorphous urates were graded as having 1 to 3+ turbidity based on the ability to read print through them, shown in **FIGURE 3**. Specimens were incubated for 90 seconds at 55°C, 60°C, and 65°C, and the change in their turbidity grade was evaluated.

The project was approved by the institutional review board in accord with the ethical standards established by the institution in which the experiments were performed.

Results

Specific Gravity and pH of Specimens

We collected a total of 207 urine specimens from 178 ambulatory adults at random times during the day. Fifty-six specimens formed amorphous urate crystals after refrigeration. Specimens that formed amorphous

urate crystals had an average pH of 6.0 and an average specific gravity of 1.029 (**TABLE 1**). An independent-sample *t*-test was performed to determine whether there was a difference in means between the pH and the specific gravity of the specimens that did and did not produce crystals. On average, the pH of the specimens in which urate crystals formed (mean = 6.009, SE = 0.0201) was statistically lower than the pH of the specimens in which urate crystals did not form (mean = 6.510, SE = 0.0549). This difference was significant at t (184) = −8.57, P <.001; moreover, it represented a large-sized effect, r = .53. The specific gravity analysis proved an opposite trend: The specific gravity of the specimens in which urate crystals formed (mean = 1.029, SE = 0.0002) was statistically higher than the specific gravity of the specimens in which urate crystals did not form (mean = 1.019, SE = 1.0004). This difference was significant at t (200) = 17.84, P <.001; moreover, it represented a large-sized effect, r = .78. The pH was lower in the specimens that formed crystals, and the specific gravity was higher.

Effect of 50 mM NaOH on Amorphous Urate Crystals, Bacteria, and Yeast

FIGURE 1 compares urine sediment photographs from 2 samples before and after the addition of an equal amount of 50 mM NaOH. The NaOH dissolved the amorphous urates and allowed for better visibility of bacteria and yeast.

We quantified the amount of 50 mM NaOH necessary to completely dissolve the crystals. **FIGURE 2** shows the grading scale that was used. Amorphous crystals in 23% of the specimens dissolved completely after the addition of an equal amount of 50 mM NaOH (×2 treatment); this result increased to 98% with a ×4 treatment. Only 1 of the specimens tested required a 1:5 treatment to completely dissolve the amorphous crystals.

A repeated-measures ANOVA was performed to determine whether there was a difference in grades across the standard treatments. The descriptive statistics of the crystal grade results are shown in **TABLE 2**. Mauchly's test indicated that the assumption of sphericity had been violated, χ^2 (2) = 34.02, P <.05, for the main effect of the NaOH treatment. Therefore, degrees of freedom were corrected using the Greenhouse-Geisser estimate of sphericity (ε = 0.68). The results show that the quantity of amorphous crystals statistically differed between treatments, F (1.4, 75.0) = 288, P <.01, ω^2 = 0.97. Posthoc analysis of pairwise comparisons between all 3 treatments indicated a statistically significant result as well. This finding verified that treatment with 50 mM NaOH produced a significant decrease in the quantity of crystals.

Effect of 50 mM NaOH on WBC and RBC

Urine specimens from 2 individuals with a urinary tract infection were used to evaluate the effect of 50 mM NaOH on WBC. On average, the SH-9 aliquots post NaOH treatment had a much lower WBC content (mean = 1.8, SE = 0.38) compared to the untreated aliquots (mean = 54.4, SE = 2.13; t [29] = 25.19, P <.0001, r = .98). A goodness-of-fit test for normal distribution was used to analyze the differences between aliquots, and the assumption of normality was not violated, P >.250. The NaOH had a deleterious effect on the quantity of WBC as shown in **FIGURE 4**.

The same analysis was performed on the SH-3 aliquots. On average, the SH-3 aliquots post NaOH treatment had a much lower WBC content (mean = 48.2, SE = 3.24) compared to the untreated aliquots (mean = 126.7, SE = 3.44; t [29] = 14.30, P <.0001, r = .94). A goodness-of-fit test for normal distribution was used to analyze the differences between aliquots, and the assumption of normality was not violated, P >.164. The NaOH had a deleterious effect on the quantity of WBC.

A urine specimen from a patient with hematuria was used to evaluate the effect of 50 mM NaOH on RBC. On average, the SH-20 aliquots post NaOH treatment had a much lower RBC content (mean = 8.3, SE = 0.73) compared to the untreated aliquots (mean = 276.3, SE = 12.58; t [29] = 21.5, P <.0001, r = .94). A goodness-of-fit test for normal distribution was used to analyze the differences between aliquots, and the assumption of normality was not violated, P >.250. The NaOH had a deleterious effect on the quantity of RBC as shown in **FIGURE 4**.

Effect of Temperature on Amorphous Crystals

Amorphous urates are expected to dissolve when heated to approximately 60°C.[5] We tested temperature and timing on the specimens that formed amorphous urates, using the grading schema shown in **FIGURE 3**. Twenty-two urine specimens that had a macroscopic turbidity grade of 2 or 3 were incubated in a water bath for 90 seconds at various temperatures. All of the specimens showed a decrease of at least 1 unit of turbidity when incubated at 60°C; 19 of the specimens showed a decrease of at least 2 units. Eighteen of the specimens showed a decrease of at least 2 units of macroscopic turbidity when incubated at 55°C. **FIGURE 5** shows the effect of warming the specimens macroscopically (**FIGURE 5A**) and microscopically (**FIGURE 5B** and **5C**).

Conclusion

Amorphous crystals have no clinical significance; however, they resemble bacteria and can obscure key findings in a urine microscopic examination. Urinalysis textbooks state that amorphous urates can be dissolved in weak alkali and heat, but they do not provide protocols for doing so. Here, we have provided those protocols and safety precautions[10,11] (**FIGURE 6**).

Amorphous urate crystals should be suspected when a turbid urine has a slightly pink appearance, a high specific gravity, and an acid pH. The sediment is pink because of the adherence of uroerythrin. The color is often

TABLE 1. Characteristics of Urine Specimens Associated with Amorphous Urate Crystal Formation

Were amorphous urate crystals present?		n	Mean	Standard Deviation	Standard Error Mean
pH	Yes	56	6.009	0.1505	0.0201
	No	151	6.510	0.6745	0.0549
Specific gravity	Yes	56	1.02920	0.001853	0.000248
	No	151	1.01927	0.116121	1.000498

TABLE 2. Descriptive Statistics of Crystal Grade Before and After Treatment with 50 mM NaOH

	Mean	Standard Deviation	n
Initial crystal grade	1.89	0.312	56
Crystal grade after ×2 treatment	1.00	0.714	56
Crystal grade after ×4 treatment	0.02	0.134	56

NaOH, sodium hydroxide.

FIGURE 4. Paired profiles (n = 30) of WBCs in SH-9 (A) and RBCs in SH-20 (B) content before and after NaOH treatment. Red line indicates the mean cell count. NaOH, sodium hydroxide; RBCs, red blood cells; WBCs, white blood cells.

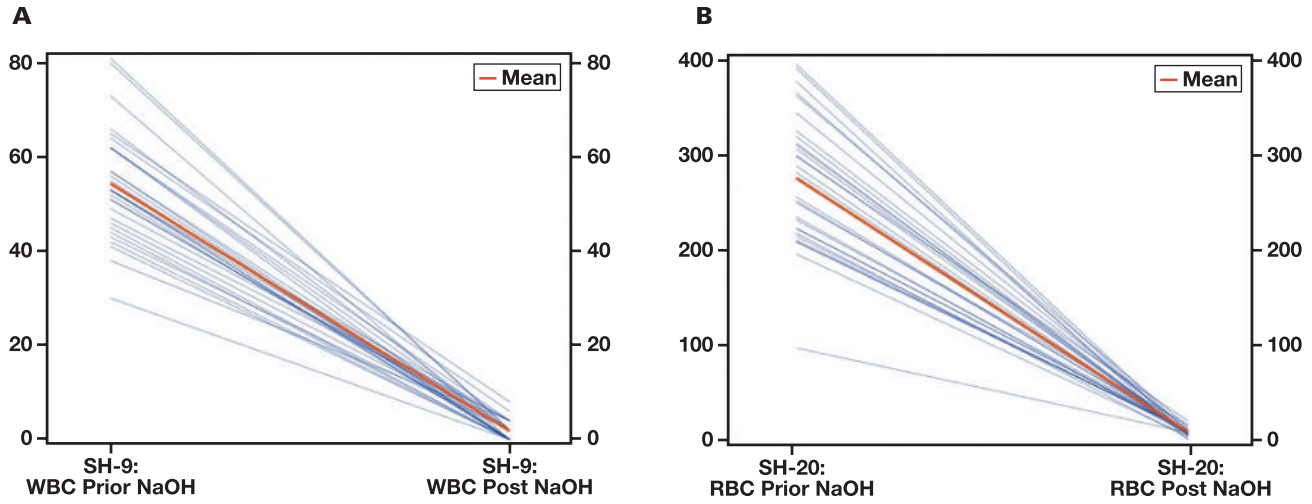

FIGURE 5. Temperature effect on amorphous urates. A. Specimen 23 before and after warming. B. Microscopically, the amorphous crystals obscured visibility in the untreated specimen. C. Microscopic view of the sediment when the specimen was prewarmed before centrifugation. Photomicrographs taken at 400× magnification, bright field microscopy, no stain.

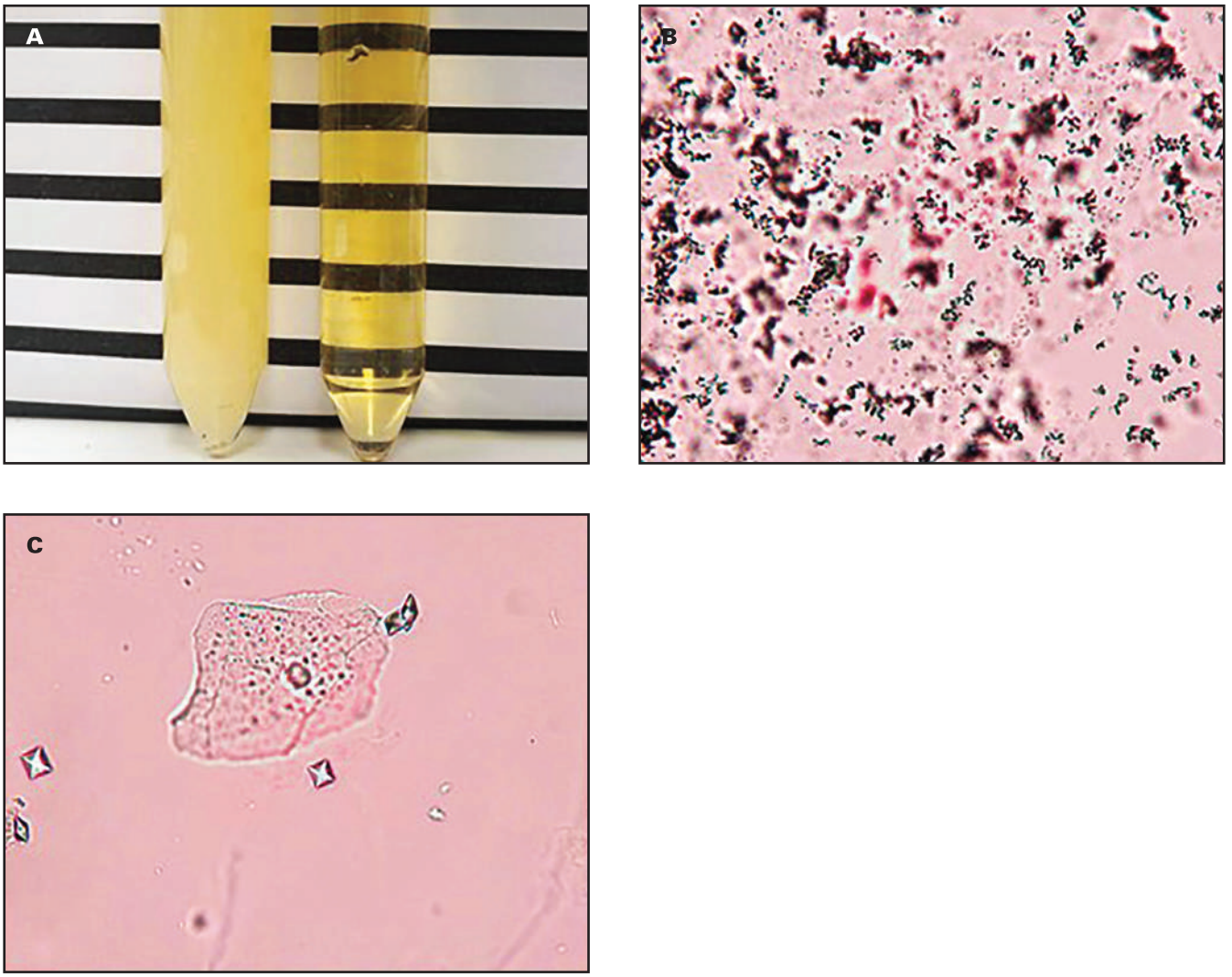

FIGURE 6. Protocols to dissolve amorphous urate crystals.

Amorphous urate crystals should be suspected when a turbid urine has a slightly pink appearance, a high specific gravity and an acid pH. Prewarm the specimen prior to testing. Transfer 10-12 mL of a well-mixed sample to a urinalysis test tube and cap it. Place the tube into a waterbath held at 60°C for 90 seconds. Invert the tube. Allow it to return to room temperature before proceeding with the routine urinalysis.

To eliminate and/or verify the presence of amorphous urates in the sediment: Transfer 10 µL of well suspended urine sediment to a microscope slide. Add 10 µL of 50 mM NaOH, and stir with the pipet tip. Coverslip and examine under the microscope. If the crystals do not dissolve, repeat the procedure using 5 µL of urine sediment and 15 µL of NaOH. Take into account the dilution factor when semi-quantitating bacteria and yeast. Do not quantitate casts, RBC, or WBC when using this method.

Caution: 50 mM NaOH (0.2%) is a weak base. It has a NFPA health rating of 1, which is considered a low hazard risk.[10] It can be purchased in this concentration. A laboratory may opt to prepare it from a 10% NaOH stock reagent solution. 10% NaOH is 2.5 M. It is a strong base with a pH ≥ 14. It has a NFPA health rating of 3 (serious hazard). It can cause severe burns and eye damage. Eye protection and face protection should be used when working with it.[11] Always read the safety data sheets when storing and preparing reagents.

referred to as "brick-dust."[1,2,5] Amorphous urates will rapidly dissolve when urine specimens are warmed to 60°C. This treatment is not deleterious to the formed elements in the urine. From a procedural standpoint, note that warming must be done before centrifugation because the sediment is too concentrated to be dissolved solely by heat. The addition of 50 mM NaOH to urine sediment is a safe and effective method to rapidly dissolve amorphous urates. It facilitates the identification of bacteria and yeast; however, it is deleterious to RBCs and WBCs.

One limitation of this study is that there is no information regarding the effect of 50 mM NaOH on casts. The number of specimens used to evaluate RBCs and WBCs was limited but conclusively indicates that the cell counts will not be accurate when a specimen is treated with NaOH.

The best specimen for a routine urinalysis microscopic examination is a fresh one, but this is not always feasible. Refrigeration is a common method for storage before analysis, and it promotes crystal formation. The analyst should suspect turbid specimens with a high specific gravity and an acid pH as having amorphous urates and prewarm them to dissolve the crystals before centrifugation. We found that 50 mM NaOH is a weak base that can be added safely to urine sediment to rapidly confirm the presence of underlying bacteria and yeast. This measure is an additional tool for the medical laboratory scientist performing urine microscopic analysis.

Acknowledgments

The authors thank Grace Mills, Parisa Taghi, and Anna Freeman from the University of West Florida for technical assistance; Gabriel Moreno-Fergusson for data support; and Dr. Carol Cox from the Health and Hope Clinic in Pensacola, Florida.

Kristina Behan, PhD, MLS(ASCP)^{CM}, designed and performed experiments, did the photography, performed microscopics, and wrote the manuscript. Michael Johnston, MS, designed experiments, recruited volunteers, and performed the statistical analysis.

This work was supported by the Medical Laboratory Sciences Department at the University of West Florida. The authors do not report any financial conflicts of interest.

REFERENCES

1. Strasinger SK, DiLorenzo MS. Microscopic examination of urine. In: Strasinger SK, DiLorenzo MS. *Urinalysis and Body Fluids.* 6th ed. Philadelphia, PA: F.A. Davis; 2014: 99–146.
2. Graff L. Microscopic examination of the urinary sediment. In: *A Handbook of Routine Urinalysis*. Philadelphia, PA: Lippincott, Williams & Wilkins; 1983:chap 3.
3. McBride LJ. Microscopic examination of urine sediment. In: McBride, LJ. *Textbook of Urinalysis and Body Fluids: A Clinical Approach*. Philadephia, PA: Lippincott-Raven Publishers; 1998.
4. Brunzel NA. Microscopic examination of urine sediment. In: *Fundamentals of Urine and Body Fluid Analysis*. 2nd ed. Philadephia, PA: Saunders; 2004:chap 8.
5. Brunzel NA. Microscopic examination of urine sediment. In: *Fundamentals of Urine and Body Fluid Analysis.* 3rd ed. St. Louis, MO: Elsevier Saunders; 2013:chap 8.
6. Mundt LA, Shanahan K. Microscopic examination of urinary sediment. *Graff's Textbook of Urinalysis and Body Fluids.* 3rd ed. Burlington, MA: Jones & Bartlett Learning; 2016.
7. Sunheimer R, Graves L, Stockwin W. Urinalysis: microscopic urine sediment examination. In: Sunheimer R, Graves L, Stockwin W, Gockel-Blessing E. *Clinical Laboratory Urinalysis and Body Fluids*. New York, NY: Pearson; 2015.
8. Clinical and Laboratory Standards Institute. *GP16-A3 Urinalysis.* 3rd ed. Wayne, PA: Clinical and Laboratory Standards Institute; 2009.
9. Clinical and Laboratory Standards Institute. *Physician and Nonphysician Provider Performed Microscopy Testing: Approved Guideline.* 2nd ed. Wayne, PA: Clinical and Laboratory Standards Institute; 2011.
10. Sodium hydroxide, 0.05N (0.05M). Safety Data Sheet. https://www.labchem.com/tools/msds/msds/LC24250.pdf. Accessed September 8, 2021.
11. Sodium hydroxide, 10% w/v. Safety Data Sheet. https://www.labchem.com/tools/msds/msds/LC24070.pdf. Accessed September 8, 2021.

SCIENCE

Kanamycin Supplement for the Disaggregation of Platelet Clumps in EDTA-Dependent Pseudothrombocytopenia Specimens

Chaicharoen Tantanate, MD,[1,*] *Supavat Talabthong, MT(ASCP),*[1] *Phenluck Lamyai, MT(ASCP)*[1]

[1]Department of Clinical Pathology, Faculty of Medicine Siriraj Hospital, Mahidol University, Bangkoknoi, Bangkok, Thailand; *To whom correspondence should be addressed. cpdoctor@hotmail.co.th

Keywords: automated analyzer, EDTA-dependent pseudothrombocytopenia, kanamycin, platelet count, platelet clumps, vortex mixing

Abbreviations: EDTA-PTCP, EDTA-dependent pseudothrombocytopenia; CBC, complete blood count; H, hemolysis; MPV, mean platelet volume; PDW, platelet distribution width; P-LCR, platelet-large cell ratio; RBC, red blood cell; WBC, white blood cell; MCV, mean corpuscular volume; RDW, red cell distribution width; FRC, fragmented red blood cell count.

Laboratory Medicine 2022;53:e69–e73; https://doi.org/10.1093/labmed/lmab090

ABSTRACT

Objective: To indicate the ability to disaggregate platelet clumps by vortex mixing and kanamycin supplementation in EDTA-dependent pseudothrombocytopenia (EDTA-PTCP) specimens.

Materials and Methods: For patients with EDTA-PTCP, citrate-anticoagulated, primary EDTA-anticoagulated, vortex-mixed, and kanamycin-treated specimens were tested for complete blood count and platelet-related parameters.

Results: Forty-eight specimens were included. Nineteen (39.6%) of the vortex-mixed specimens and 42 (87.5%) of the kanamycin-treated specimens revealed platelet counts more than those of the primary EDTA specimens, with levels exceeding 100 × 10^9/L. The platelet count and platelet recovery of the kanamycin-treated specimens were higher than those of the vortex-mixed specimens.

Conclusion: Kanamycin supplementation to EDTA-PTCP blood may be considered as an alternative approach when the recollection of specimens is impractical. Only platelet-related parameters from kanamycin treatment were suitable for guiding patient management. Further studies about the impact of these methods in patients with various conditions, such as in patients with advanced kidney disease, should be conducted.

EDTA is the anticoagulant of choice for a complete blood count (CBC) because of its ability to preserve blood cells.[1,2] However, there have been incidents of falsely low platelet counts with various hematology analyzers because of platelet clumping when EDTA is used as the anticoagulant for blood collection. The clumping disappears when an anticoagulant other than EDTA is used. Because this result implies that the phenomenon relates directly to EDTA, it is referred to as EDTA-dependent pseudothrombocytopenia (EDTA-PTCP).[3] The falsely low platelet counts result from the platelet aggregation activated by EDTA-dependent antiplatelet autoantibodies. The phenomenon only occurs in vitro. Although patients with EDTA-PTCP have neither a hemostatic defect nor clinical bleeding, EDTA-PTCP may lead to unnecessary further investigations and delays in patient management. When EDTA-PTCP is suspected, patients are requested to undergo blood resampling using a non-EDTA anticoagulant for the blood collection. With EDTA-PTCP specimens, the platelet clumps usually disappear in the non-EDTA blood, and the platelet count recovers to the normal range.

To date, there is no consensus on the anticoagulant of choice for an EDTA-PTCP solution. Apart from using a non-EDTA anticoagulant, it has been proposed that adding various additives, including aminoglycoside antibiotics, to blood specimens would act as a preventive measure before a blood cell count.[4] Various aminoglycosides, including kanamycin, have been reported to be effective additive substances to prevent EDTA-PTCP.[5-7] Although collecting new blood specimens using non-EDTA anticoagulants or additive substances is recommended, it is sometimes impractical, especially when blood resampling is hard to perform. Vibrating specimens in which platelets have clumped with a vortex mixer machine have been reported to disaggregate platelet clumps.[8-10] However, there are no data on the effects of vortex mixing specific to EDTA-PTCP specimens in which platelet clumps have already formed. The aim of this study was to indicate the ability to disaggregate platelet clumps using a kanamycin supplement and vortex mixing in EDTA-PTCP specimens.

Materials and Methods

Blood Specimens

Leftover specimens of primary blood specimens collected in collection tubes containing dipotassium EDTA anticoagulant (Vacuette; Greiner Bio-One, Frickenhausen, Germany) from June 2019 to December 2020 were investigated. When EDTA-PTCP was suspected, a request was

promptly made for a new blood specimen to be collected in a 0.109 mol/L (3.2%) sodium citrate tube (Vacuette; Greiner Bio-One, Frickenhausen, Germany). The inclusion criteria were (i) both the primary EDTA and citrated blood specimens were sent to the laboratory and tested within 4 hours of blood collection; (ii) the platelet count from the primary EDTA blood was ≤ 100×10^9/L; (iii) the platelet count from the citrated blood was ≥ 100×10^9/L and exceeded that of the EDTA tube, without platelet-related flag alerts; and (iv) the platelet clumps were only found in a blood smear of the EDTA specimen. The protocol for further investigations is summarized in **FIGURE 1**.

Three aliquots of primary EDTA blood were prepared; each aliquot contained 1 mL EDTA whole blood. The first aliquot was the blood from the primary EDTA and was designated as "E." The E aliquot was initially tested for CBC; it was then centrifuged at 1500 g for 15 minutes before its plasma was collected and analyzed for the baseline hemolysis (H) index. The second aliquot was designated as "V." The V aliquot was vibrated by a vortex mixer (Vortex-Genie 2; Scientific Industries, Bohemia, NY) at 1500 rpm for 2 minutes. This protocol was adapted from the study of Gulati et al.[8] The third aliquot was designated as "K." Blood from the K aliquot was transferred into the tube with 15 mg kanamycin acid sulfate (Kangen; General Drugs House Co. Ltd., Bangkok, Thailand). The mixture was subsequently mixed gently.

The concentration of 15 mg kanamycin per 1.5 mg potassium EDTA and 1 mL blood used in this study derived from the study of Ahn et al.[6] Both the V and K specimens were reanalyzed for CBC; upon completing that analysis, we centrifuged these 2 aliquots for plasma collection to analyze the H index. In addition, the demographic data and underlying diseases of the study population were reviewed.

Analytical Methods

All specimens were analyzed using a Sysmex XN-3000 hematology analyzer (Sysmex Corporation, Kobe, Japan) using the routine whole-blood analysis mode for CBC testing. Blood smears were also prepared and reviewed for platelet clumping and platelet satellitism. An analysis was made of the platelet-related parameters of all specimens: the impedance platelet count, mean platelet volume (MPV), platelet distribution width (PDW), and platelet-large cell ratio (P-LCR), along with the presence of platelet flags from the analyzer. The frequencies of platelet-related flag alerts, including "thrombocytopenia," "PLT Abn distribution" (for abnormal platelet distribution), and "PLT clumps?" (for platelet clumps), were also calculated. Because platelet analysis in citrated specimens was the most reliable method shown by the normal platelet counts without platelet-related flag alerts, the platelet-related parameters of citrated specimens were considered as reference values in this study.

The platelet counts from citrated specimens were multiplied by 1.1 to correct for the dilution effect of the anticoagulant. Red blood cell (RBC) parameters, white blood cell (WBC) count, and the H index were analyzed in the E, V, and K aliquots. The H index was analyzed using the Roche Cobas 8000 (Roche Diagnostics, Mannheim, Germany). The RBC count, mean corpuscular volume (MCV), red cell distribution width (RDW), fragmented red blood cell count (FRC), and H index of the V and K aliquots were compared to those of the E aliquot to determine the deteriorating effect of the investigational methods. The results from the E aliquot were considered as the baseline results for the RBC-related parameters, WBC counts, and H index. The quality of all analytical methods was assured by regular quality control checks and analyzer maintenance in accordance with the manufacturer's recommendations.

FIGURE 1. Summary of study protocol. E, primary EDTA-anticoagulated specimens; EDTA-PTCP, EDTA-dependent pseudothrombocytopenia; K, kanamycin-treated specimens; V, vortex-mixed specimens.

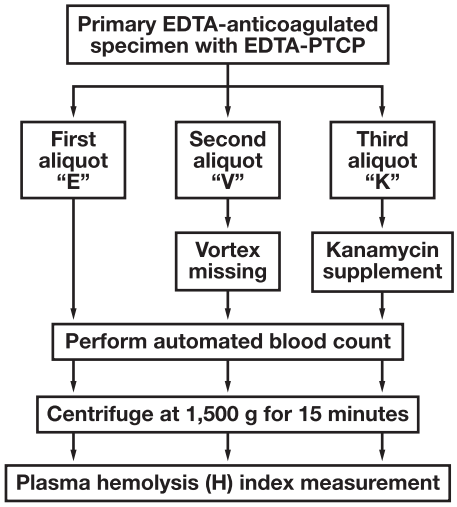

Ethical Consideration

The protocol for this study was approved by the Siriraj Institutional Review Board of the Faculty of Medicine Siriraj Hospital, Mahidol University, Bangkok, Thailand (COA number Si366/2019).

Statistical Analysis

PASW Statistics for Windows (version 18.0; SPSS Inc., Chicago, IL) was used to analyze data and prepare box and whisker plots. Continuous variables were tested for normal distribution using the Shapiro-Wilk test. Normally distributed data were analyzed and compared to each other using a 1-way repeated measures analysis of variance and the Bonferroni posthoc test. The nonnormally distributed data were analyzed using the Friedman test and the Dunn-Bonferroni posthoc test. McNemar's test was used to compare the frequencies of platelet-related flags of specimens. A 2-sided test was used for all comparisons, and a P value <.05 was deemed statistically significant. Platelet recovery of the investigational method was calculated from the difference between the platelet count from the investigational method and the E specimen, divided by the platelet count of the E specimen.

Results

Blood specimens from 48 patients with EDTA-PTCP were examined. The ages of the study population ranged from 20 to 101 years, with the median age (± standard deviation) being 51 (± 19.3) years. Thirty-nine (81.3%) patients were female. The underlying conditions of the patients at the onset of EDTA-PTCP detection were malignancies (n = 17, 35.4%), autoimmune diseases (n = 8, 16.7%), infectious diseases (n = 7, 14.6%), healthy (n = 3, 6.3%), and other conditions (n = 13, 27%) including hypertension (n = 5, 10.4%), dyslipidemia (n = 7, 14.6%), and glaucoma (n = 1, 2.1%). Only 4 (8.3%) of the cohort patients were receiving antibiotic therapy during their blood collection, and none of these 4 were being administered aminoglycoside antibiotics. From the blood smear review, platelet satellitism was not observed in the primary EDTA

specimens. Laboratory data from the automated hematology analyzer for all of the specimens are detailed in **TABLE 1**. The data are presented as medians because of the nonnormal distributed data. Details about demographic data, underlying conditions, and platelet recoveries from citrated blood collection, vortex mixing, and kanamycin supplementation of all patients are shown in Supplemental Table 1.

The platelet counts and platelet recovery of the kanamycin-treated specimens were higher than those of the vortex-mixed specimens and comparable to those of the citrated specimens. Nineteen (39.6%) vortex-mixed specimens and 42 (87.5%) kanamycin-treated specimens revealed platelet counts greater than those of the primary EDTA specimens, with levels >100 × 10^9/L. For the specimens with platelet count higher than 100 × 10^9/L, the platelet clumps were decreasing or disappeared. Twenty-three (48%) patients had platelet counts for their vortex-mixed specimens of <100 × 10^9/L, but had platelet counts for their kanamycin-treated specimens of >100 × 10^9/L. No vortex-mixed specimen had a higher platelet count than that obtained with the kanamycin-treated aliquot. The MPV, PDW, and P-LCR of 14 (29.2%) primary EDTA, 10 (21.8%) vortex-mixed, and 3 (6.2%) kanamycin-treated specimens could not be analyzed because of a significantly abnormal platelet histogram; they were therefore excluded from the data analysis. A comparison of the platelet counts, MPV, PDW, and P-LCR of the investigational methods is illustrated in **FIGURE 2**. Although the platelet counts of the vortex-mixed specimens were higher than those of the primary EDTA specimens, they were still lower than those of the kanamycin-treated specimens. The MPV, PDW, and P-LCR of the primary EDTA, vortex-mixed, and kanamycin-treated specimens were significantly higher than those of the citrated specimens.

The frequencies of occurrence of the platelet-related flags of the primary EDTA, vortex-mixed, and kanamycin-treated specimens were 95.8%, 65.2%, and 10.4%, respectively. The differences in the flag occurrences of the specimens were statistically significant (P <.001). There were no significant differences in the RBC counts, hemoglobin levels, and FRC among the specimen types. The MCV, RDW, and H indexes of the kanamycin-treated specimens were higher than those of the primary EDTA specimens (P <.001). The H index of the vortex-mixed specimens was higher than that of the primary EDTA specimens (P = .002). The WBC counts of the specimen types were not statistically significantly different.

Discussion

EDTA-PTCP is a rare phenomenon, and the epidemiologic data of patients have varied with the study population. Previous reports have shown that EDTA-PTCP is not an age- or sex-dependent phenomenon, and it can be found in individuals with various conditions, ranging from healthy individuals to patients with associated pathologic conditions.[11] The underlying conditions of the study population also included healthy individuals, patients with malignancies, and patients with infectious and autoimmune diseases, which is consistent with previous reports.[11,12] In the present study, kanamycin supplementation recovered a significant quantity of platelet counts, with a negligible effect on the blood cell morphology and histograms. Abnormal platelet flag alerts were significantly reduced. It has been shown that aminoglycosides can reduce platelet aggregation via fibrinogen-receptor activation-inhibition in a dose-dependent manner.[7,13] For vortex mixing, approximately 40% of the specimens indicated a significant platelet recovery. This result confirms the work of Gulati et al,[8] who showed that vortex mixing completely disaggregated platelet clumping in 44% of general EDTA blood specimens. The RBC indices and the H index of the kanamycin supplement and vortex mixing differed from those of the EDTA-anticoagulated specimens. This finding represents a deterioration effect on the specimens and implies that blood cell parameters other than the platelet count should not be reported from kanamycin-treated or vortex-mixed specimens.

For clinical application, vortex mixing and kanamycin supplementation can be implemented before requesting another non-EDTA specimen when a laboratory suspects EDTA-PTCP. Applicable situations may include >1 occasion of platelet clumps in the same patient and the phlebotomist has excluded any preanalytical errors. Kanamycin supplementation should be used as the first step because of the higher rate of success in platelet disaggregation. However, vortex mixing may be used in patients in whom kanamycin supplementation is not feasible. If platelet clumps are reduced in blood smear and the platelet count

TABLE 1. Laboratory Data for Citrated, Primary EDTA, Vortex-Mixed, and Kanamycin-Treated Specimens

Parameters	Citrated Specimens	Primary EDTA Specimens	Vortex-Mixed Specimens	Kanamycin-Treated Specimens
Platelet count, × 10^9/L	176 (88.4)	32 (32.7)	96 (85.6)	192 (107.7)
Platelet recovery from EDTA specimens, %	454 (417)	0 (0)	143 (206.9)	444 (497.3)
MPV, fL	9.5 (1.2)	11.7 (1.4)	11.6 (1.1)	10.5 (1.3)
PDW, fL	10.1 (2.2)	15 (3.6)	14.6 (3.6)	12.4 (3.7)
P-LCR, %	22.8 (8.4)	38.2 (9.8)	37.1 (8)	30 (10.6)
RBC count, × 10^9/L	4.1 (0.7)	4.1 (0.8)	4.1 (0.7)	4.1 (0.7)
Hb, g/L	119 (22)	119 (22)	120 (22)	118 (22)
MCV, fL	88 (8.5)	88 (8.7)	85.9 (8.5)	90.2 (8.7)
RDW, %	15.1 (3.1)	15.2 (3.2)	15.1 (3)	15.4 (3.1)
FRC, × 10^9/L	0.03 (0.03)	0.03 (0.03)	0.03 (0.04)	0.03 (0.04)
H index	NA	28.9 (20.8)	72.5 (115.9)	151.3 (149.1)
WBC count, × 10^9/L	6.4 (3.3)	6.5 (3.4)	6.4 (3.2)	6.4 (3.2)

All values are presented as median and SD in parentheses.
FRC, fragmented red blood cell; Hb, hemoglobin; H index, hemolysis index; MCV; mean corpuscular volume; MPV, mean platelet volume; NA, not applicable; PDW, platelet distribution width; P-LCR, platelet-large cell ratio; RBC, red blood cell; RDW, red cell distribution width; SD, standard deviation; WBC, white blood cell.

FIGURE 2. Differences in platelet counts (A), MPV (B), PDW (C), and P-LCR (D) of the specimen types. C, citrate-anticoagulated specimens; E, primary EDTA-anticoagulated specimens; K, kanamycin-treated specimens; MPV, mean platelet volume; PDW, platelet distribution width; P-LCR, platelet-large cell ratio; V, vortex-mixed specimens.

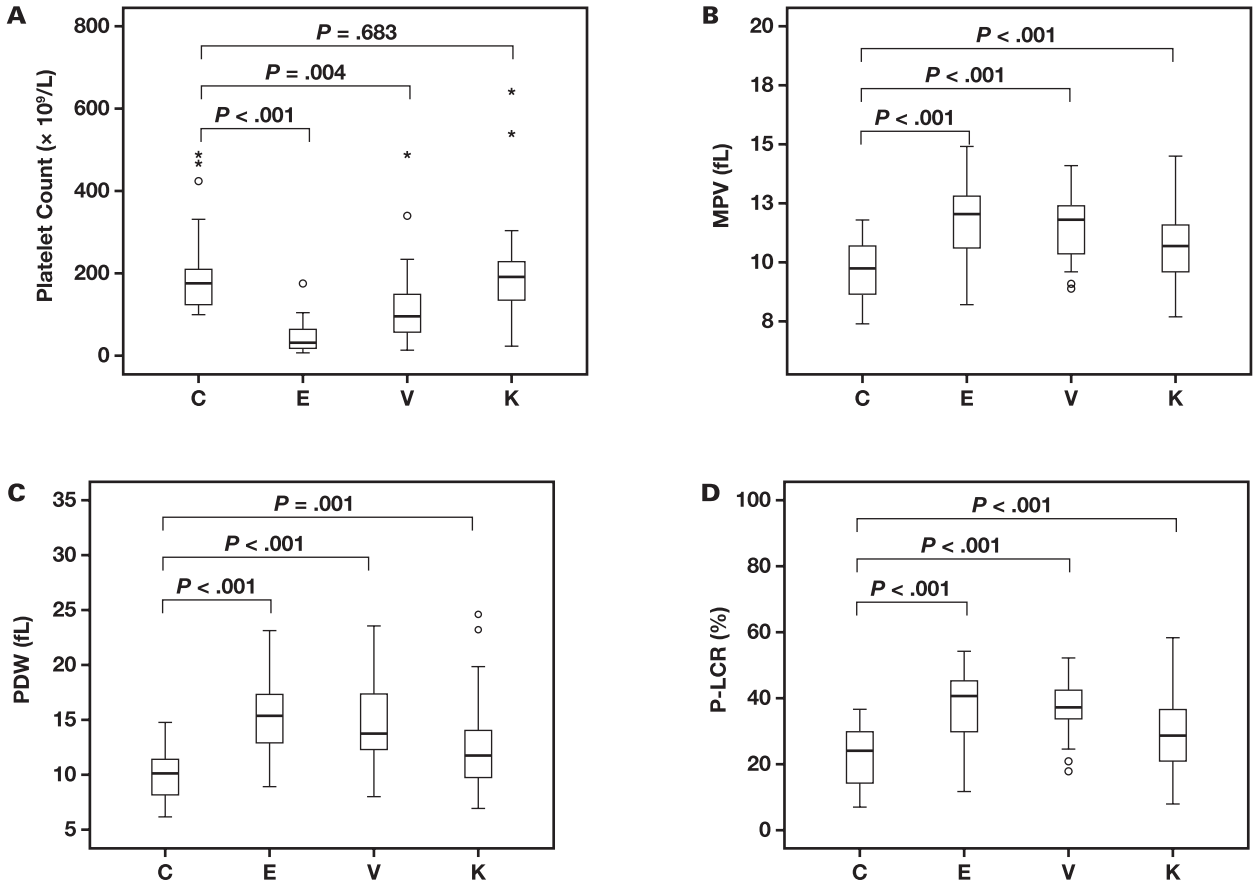

exceeds 100 × 10^9/L without any platelet-related flag alert, then the platelet count can be reliably reported to the physician. The RBC and WBC parameters can be reported according to those of the primary EDTA specimens because those parameters are similar to those of citrated blood in the experiment. This approach avoids a second blood collection for CBC testing, delays in patient management, and misdiagnoses of thrombocytopenia. The local price of kanamycin is approximately $0.5 USD per 1000 mg kanamycin acid sulfate; thus the cost per case of kanamycin supplement is less than that of using a commercially prepared sodium citrate tube. However, the total costs of kanamycin preparation and quality management must be taken into consideration to compare cost-effectiveness between the methods. Further studies aimed to answer this question are warranted.

Conclusion

This study included a large number of EDTA-PTCP specimens and reduced biases of experiment by using objective measurement by employing flagging of the automated analyzer instead of the platelet clumping estimation in the blood smear. However, there were some limitations of the study. The chief limitation was that the criteria for EDTA-PTCP diagnosis commenced from the normal platelet count in the citrated specimens. This meant that the results of this study cannot be applied in patients with EDTA-PTCP with platelet clumping in citrated specimens. Another limitation is the lack of data related to the warming of specimens because there was a limited number of specimens. From our experience, the success rate of platelet disaggregation and recovery after warming specimens is low, and this process delays the turnaround time. The last limitation is that kanamycin supplementation or vortex mixing may not be practical in all patients with EDTA-PTCP. Further studies about the impact of these methods in patients with various conditions, such as in patients with advanced kidney disease, should be performed to validate the usefulness of the measurements.

Supplementary Data

The supplemental table can be found in the online version of this article at www.labmedicine.com.

Acknowledgments

The authors gratefully acknowledge Dr. Sasima Tongsai for statistical guidance. CT was supported by a Chalermphrakiat Grant from the Faculty of Medicine Siriraj Hospital, Mahidol University, Bangkok, Thailand. CT designed the study, performed laboratory testing, analyzed data, and wrote the manuscript. ST and PL performed laboratory testing. All authors have read and approved the final manuscript. The authors have

no personal, financial, or institutional conflict of interest in any of the materials or devices described in this article.

REFERENCES

1. International Council for Standardization in Haematology: Expert Panel on Cytometry. Recommendations of the International Council for Standardization in Haematology for ethylenediaminetetraacetic acid anticoagulation of blood for blood cell counting and sizing. *Am J Clin Pathol*. 1993;100(4):371–372.
2. Clinical and Laboratory Standards Iinstitute. *Tubes and Additives for Venous and Capillary Blood Specimen Collection: Approved Standard, 6th ed.* Wayne, PA: Clinical and Laboratory Standards Institute; 2010.
3. Lippi G, Plebani M. EDTA-dependent pseudothrombocytopenia: further insights and recommendations for prevention of a clinically threatening artifact. *Clin Chem Lab Med.* 2012;50(8):1281–1285.
4. Baccini V, Geneviève F, Jacqmin H, et al. Platelet counting: ugly traps and good advice. Proposals from the French-speaking Cellular Hematology Group (GFHC). *J Clin Med*. 2020;9(3):808.
5. Sakurai S, Shiojima I, Tanigawa T, Nakahara K. Aminoglycosides prevent and dissociate the aggregation of platelets in patients with EDTA-dependent pseudothrombocytopenia. *Br J Haematol.* 1997;99(4):817–823.
6. Ahn HL, Jo YI, Choi YS, et al. EDTA-dependent pseudothrombocytopenia confirmed by supplementation of kanamycin: a case report. *Korean J Intern Med.* 2002;17(1):65–68.
7. Chen G, Fei X, Ling J. The effects of aminoglycoside antibiotics on platelet aggregation and blood coagulation. *Clin Appl Thromb Hemost.* 2012;18(5):538–541.
8. Gulati GL, Asselta A, Chen C. Using a vortex to disaggregate platelet clumps. *Lab Med*. 1997;28(10):665–667.
9. Cho D, Oh BJ, Kim IH, et al. Correction of platelet count using a vortex in pseudothrombocytopenia. *Korean J Lab Med*. 2003; 23(3):151–156.
10. Tantanate C. Vortex mixing to alleviate pseudothrombocytopenia in a blood specimen with platelet satellitism and platelet clumps. *Clin Chem Lab Med.* 2021;59(5):e189–e191.
11. Bizzaro N. EDTA-dependent pseudothrombocytopenia: a clinical and epidemiological study of 112 cases, with 10-year follow-up. *Am J Hematol.* 1995;50(2):103–109.
12. Berkman N, Michaeli Y, Or R, Eldor A. EDTA-dependent pseudothrombocytopenia: a clinical study of 18 patients and a review of the literature. *Am J Hematol.* 1991;36(3):195–201.
13. Chae H, Kim M, Lim J, Oh EJ, Kim Y, Han K. Novel method to dissociate platelet clumps in EDTA-dependent pseudothrombocytopenia based on the pathophysiological mechanism. *Clin Chem Lab Med.* 2012;50(8):1387–1391.